EPA/635/R-09/005
www.epa.gov/iris

TOXICOLOGICAL REVIEW

OF

1,4-Dioxane

(CAS No. 123-91-1)

In Support of Summary Information on the Integrated Risk Information System (IRIS)

May 2009

NOTICE

This document is an ***External Review*** **draft**. This information is distributed solely for the purpose of pre-dissemination peer review under applicable information quality guidelines. It has not been formally disseminated by EPA. It does not represent and should not be construed to represent any Agency determination or policy. It is being circulated for review of its technical accuracy and science policy implications.

U.S. Environmental Protection Agency
Washington, DC

DISCLAIMER

This document is a preliminary draft for review purposes only. This information is distributed solely for the purpose of pre-dissemination peer review under applicable information quality guidelines. It has not been formally disseminated by EPA. It does not represent and should not be construed to represent any Agency determination or policy. Mention of trade names or commercial products does not constitute endorsement or recommendation for use.

TABLE OF CONTENTS

LIST OF TABLES vii

LIST OF FIGURES x

LIST OF ABBREVIATIONS AND ACRONYMS xiv

FOREWORD xvi

AUTHORS, CONTRIBUTORS, AND REVIEWERS xvii

1. INTRODUCTION 1

2. CHEMICAL AND PHYSICAL INFORMATION 3

3. TOXICOKINETICS 6
3.1. ABSORPTION 6
3.2. DISTRIBUTION 7
3.3. METABOLISM 8
3.4. ELIMINATION 11
3.5. PHYSIOLOGICALLY BASED TOXICOKINETIC MODELS 12
3.5.1. Available Pharmacokinetic Data 13
3.5.2. Published PBPK Models for 1,4-Dioxane 15
3.5.2.1. Leung and Paustenbach (1990) 15
3.5.2.2. Reitz et al. (1990) 16
3.5.2.3. Fisher et al. (1997) 17
3.5.3. Implementation of Published PBPK Models for 1,4-Dioxane 17
3.6. Rat Nasal Exposure via Drinking Water 20

4. HAZARD IDENTIFICATION 22
4.1. STUDIES IN HUMANS – EPIDEMIOLOGY, CASE REPORTS, CLINICAL CONTROLS 22
4.1.1. Thiess et al. (1976) 24
4.1.2. Buffler et al. (1978) 25
4.2. SUBCHRONIC AND CHRONIC STUDIES AND CANCER BIOASSAYS IN ANIMALS - ORAL AND INHALATION 26
4.2.1. Oral Toxicity 26
4.2.1.1. Subchronic Oral Toxicity 26
4.2.1.1.1. Stoner et al. (1986) 26
4.2.1.1.2. Stott et al. (1981) 27
4.2.1.1.3. Kano et al. (2008). 27
4.2.1.1.4. Yamamoto et al. (1998a, b) 31
4.2.1.2. Chronic Oral Toxicity and Carcinogenicity 32
4.2.1.2.1. Argus et al. (1965). 32
4.2.1.2.2. Argus et al. (1973); Hoch-Ligeti et al. (1970). 32
4.2.1.2.3. Hoch-Ligeti and Argus (1970). 34
4.2.1.2.4. Kociba et al. (1974) 35

4.2.1.2.5. National Cancer Institute (NCI) (1978). 37
4.2.1.2.6. Japan Bioassay Research Center (JBRC) (1998a); Yamazaki et al. (1994). 41
4.2.2. Inhalation Toxicity 50
4.2.2.1. Subchronic Inhalation Toxicity 50
4.2.2.1.1. Fairley et al. (1934). 50
4.2.2.2. Chronic Inhalation Toxicity and Carcinogenicity 51
4.2.2.2.1. Torkelson et al. (1974). 51
4.2.3. Initiation/Promotion Studies 52
4.2.3.1. Bull et al. (1986) 52
4.2.3.2. King et al. (1973) 53
4.2.3.3. Lundberg et al. (1987) 54
4.3. REPRODUCTIVE/DEVELOPMENTAL STUDIES—ORAL AND INHALATION 54
4.3.1. Giavini et al. (1985) 54
4.4. OTHER DURATION OR ENDPOINT-SPECIFIC STUDIES 55
4.4.1. Acute and Short-term Toxicity 55
4.4.1.1. Oral Toxicity 55
4.4.1.2. Inhalation Toxicity 55
4.4.2. Neurotoxicity 58
4.4.2.1. Frantik et al. (1994) 58
4.4.2.2. Goldberg et al. (1964) 59
4.4.2.3. Kanada et al. (1994) 59
4.4.2.4. Knoefel (1935) 60
4.5. MECHANISTIC DATA AND OTHER STUDIES IN SUPPORT OF THE MODE OF ACTION 60
4.5.1. Genotoxicity 60
4.5.2. Mechanistic Studies 69
4.5.2.1. Free Radical Generation 69
4.5.2.2. Induction of Metabolism 69
4.5.2.3. Mechanisms of Tumor Induction 69
4.6. SYNTHESIS OF MAJOR NONCANCER EFFECTS 71
4.6.1. Oral 72
4.6.2. Inhalation 75
4.6.3. Mode of Action Information 75
4.7. EVALUATION OF CARCINOGENICITY 77
4.7.1. Summary of Overall Weight of Evidence 77
4.7.2. Synthesis of Human, Animal, and Other Supporting Evidence 77
4.7.3. Mode of Action Information 79
4.7.3.1. Identification of Key Events for Carcinogenicity 79
4.7.3.1.1. Liver. 79
4.7.3.1.2. Nasal cavity 80
4.7.3.2. Strength, Consistency, Specificity of Association 81
4.7.3.2.1. Liver. 81
4.7.3.2.2. Nasal cavity 82
4.7.3.3. Dose-Response Relationship 82
4.7.3.3.1. Liver. 82
4.7.3.3.2. Nasal cavity 84
4.7.3.4. Temporal Relationship 84
4.7.3.4.1. Liver. 84
4.7.3.4.2. Nasal cavity 84

4.7.3.5. Biological Plausibility and Coherence 85
4.7.3.5.1. Liver. 85
4.7.3.5.2. Nasal cavity 85
4.7.3.6. Other Possible Modes of Action 85
4.7.3.7. Conclusions About the Hypothesized Mode of Action 86
4.7.3.7.1. Liver. 86
4.7.3.7.2. Nasal cavity 86
4.7.3.8. Relevance of the Mode of Action to Humans 86
4.8. SUSCEPTIBLE POPULATIONS AND LIFE STAGES 87

5. DOSE-RESPONSE ASSESSMENTS 88
5.1. ORAL REFERENCE DOSE (RfD) 88
5.1.1. Choice of Principal Studies and Critical Effect with Rationale and Justification 88
5.1.2. Methods of Analysis—Including Models (PBPK, BMD, etc.) 89
5.1.3. RfD Derivation - Including Application of Uncertainty Factors (UFs) 91
5.1.4. RfD Comparison Information 92
5.1.5. Previous RfD Assessment 97
5.2. INHALATION REFERENCE CONCENTRATION (RfC) 97
5.3. UNCERTAINTIES IN THE ORAL REFERENCE DOSE (RfD) 98
5.4. CANCER ASSESSMENT 100
5.4.1. Choice of Study/Data - with Rationale and Justification 100
5.4.2. Dose-Response Data 101
5.4.3. Dose Adjustments and Extrapolation Method(s) 102
5.4.3.1. Dose Adjustments 102
5.4.3.2. Extrapolation Method(s) 104
5.4.4. Oral Slope Factor and Inhalation Unit Risk 104
5.4.5. Previous Cancer Assessment 106
5.5. UNCERTAINTIES IN CANCER RISK VALUES 106
5.5.1. Sources of Uncertainty 106
5.5.1.1. Choice of Low-Dose Extrapolation Approach 106
5.5.1.2. Dose Metric 108
5.5.1.3. Cross-Species Scaling 108
5.5.1.4. Statistical Uncertainty at the POD 108
5.5.1.5. Bioassay Selection 108
5.5.1.6. Choice of Species/Gender 108
5.5.1.7. Relevance to Humans 109
5.5.1.8. Human Population Variability 109

6. MAJOR CONCLUSIONS IN THE CHARACTERIZATION OF HAZARD AND DOSE RESPONSE 111
6.1. HUMAN HAZARD POTENTIAL 111
6.2. DOSE RESPONSE 112
6.2.1. Noncancer/Oral 112
6.2.2. Noncancer/Inhalation 113
6.2.3. Cancer/Oral 113
6.2.3.1. Choice of Low-Dose Extrapolation Approach 113
6.2.3.2. Dose Metric 114
6.2.3.3. Cross-Species Scaling 115
6.2.3.4. Statistical Uncertainty at the POD 115

6.2.3.5. Bioassay Selection 115
6.2.3.6. Choice of Species/Gender 115
6.2.3.7. Relevance to Humans 115
6.2.3.8. Human Population Variability 116
6.2.4. Cancer/Inhalation 116

7. REFERENCES 117

APPENDIX A. EXTERNAL REVIEW COMMENTS AND DISPOSITION A-1

APPENDIX B. EVALUATION OF EXISTING PBPK MODELS FOR 1,4-dioxane B-1

APPENDIX C. DETAILS OF BMD ANALYSIS FOR ORAL RfD FOR 1,4-dioxane C-1

APPENDIX D. DETAILS OF BMD ANALYSIS FOR ORAL CSF FOR 1,4-dioxane D-1

LIST OF TABLES

Table 2-1. Physical properties and chemical identity of 1,4-dioxane 3
Table 4-1. Incidence of histopathological lesions in F344/DuCrj rats exposed to 1,4-dioxane in drinking water for 13 weeks 29
Table 4-2. Incidence of histopathological lesions in Crj:BDF_1 mice exposed to 1,4-dioxane in drinking water for 13 weeks 31
Table 4-3. Number of incipient liver tumors and hepatomas in male Sprague- Dawley rats exposed to 1,4-dioxane in drinking water for 13 months 34
Table 4-4. Incidence of liver and nasal tumors in male and female Sherman rats (combined) treated with 1,4-dioxane in the drinking water for 2 years 37
Table 4-5. Incidence of nonneoplastic lesions in Osborne-Mendel rats exposed to 1,4-dioxane in drinking water 38
Table 4-6. Incidence of nasal cavity squamous cell carcinoma and liver hepatocellular adenoma in Osborne-Mendel rats exposed to 1,4-dioxane in drinking water 39
Table 4-7. Incidence of hepatocellular adenoma or carcinoma in $B6C3F_1$ mice exposed to 1,4-dioxane in drinking water 41
Table 4-8. Incidence of histopathological lesions in male F344/DuCrj rats exposed to 1,4-dioxane in drinking water for 2 years 44
Table 4-9. Incidence of histopathological lesions in female F344/DuCrj rats exposed to 1,4-dioxane in drinking water for 2 years 45
Table 4-10. Incidence of nasal cavity, peritoneum, and mammary gland tumors in F344/DuCrj rats exposed to 1,4-dioxane in drinking water for 2 years 47
Table 4-11. Incidence of liver tumors in F344/DuCrj rats exposed to 1,4-dioxane in drinking water for 2 years 47
Table 4-12. Incidence of histopathological lesions in male Crj:BDF_1 mice exposed to 1,4-dioxane in drinking water for 2 years 49
Table 4-13. Incidence of histopathological lesions in female Crj:BDF_1 mice exposed to 1,4-dioxane in drinking water for 2 years 49
Table 4-14. Incidence of liver tumors in Crj:BDF_1 mice exposed to 1,4-dioxane in drinking water for 2 years 50
Table 4-15. Acute and short-term toxicity studies of 1,4-dioxane 56
Table 4-16a. Genotoxicity studies of 1,4-dioxane 63
Table 4-16b. Genotoxicity studies of 1,4-dioxane; mammalian in vivo 66
Table 4-17. Oral toxicity studies (noncancer effects) for 1,4-dioxane 72
Table 4-18. Temporal sequence and dose-response relationship for possible key events and liver tumors in rats and mice 82
Table 5-1. Incidence of cortical tubule degeneration in Osborne-Mendel rats exposed to1,4-dioxane in drinking water for 2 years 90
Table 5-2. BMD and BMDL values derived from BMD modeling of cortical tubule degeneration in male and female Osborne-Mendel rats exposed to 1,4-dioxane in drinking water for 2 years 91
Table 5-3. Incidence of liver hyperplasia in F344/DuCrj rats exposed to 1,4-dioxane in drinking water for 2 years 91
Table 5-4. BMD and BMDL values derived from BMD modeling of liver hyperplasia in male and female F344/DuCrj rats exposed to 1,4-dioxane in drinking water for 2 years .. 91

Table 5-5. Incidence of liver, nasal cavity, peritoneal, and mammary gland tumors in rats and mice exposed to 1,4-dioxane in drinking water for 2 years (based on survival to 12 months) 100
Table 5-6. Incidence of hepatocellular adenoma or carcinoma in rats and mice exposed to 1,4-dioxane in drinking water for 2 years 102
Table 5-7. Calculated HEDs for the tumor incidence data used for dose-response modeling .. 103
Table 5-8. $BMD_{10\ HED}$ and $BMDL_{10\ HED}$ values from models fit to tumor incidence data for rats and mice exposed to 1,4-dioxane in drinking water for 2 years and corresponding oral CSFs 105
Table 5-9. Summary of uncertainty in the 1,4-dioxane cancer risk assessment 109
Table B-1. Human PBPK model parameter values for 1,4-dioxane B-9
Table B-2. PBPK metabolic and elimination parameter values resulting from re-calibration of the human model using alternative values for physiological flow rates[a] and tissue:air partition coefficients B-11
Table B-3. PBPK metabolic and elimination parameter values resulting from recalibration of the human model using biologically plausible values for physiological flow rates[a] and selected upper and lower boundary values for tissue:air partition coefficients B-18
Table C-1. Incidence of cortical tubule degeneration in Osborne-Mendel rats exposed to 1,4-dioxane in drinking water for 2 years C-1
Table C-2. Goodness-of-fit statistics and BMD_{10} and $BMDL_{10}$ values from models fit to incidence data for cortical tubule degeneration in male and female Osborne-Mendel rats exposed to 1,4-dioxane in drinking water C-2
Table C-3. Incidence of liver hyperplasia in F344/DuCrj rats exposed to 1,4-dioxane in drinking water C-5
Table C-4. Benchmark dose modeling results based on the incidence of liver hyperplasias in F344 male rats exposed to 1,4-dioxane in drinking water for 2 years C-5
Table C-5. Benchmark dose modeling results based on the incidence of liver hyperplasias in F344 female rats exposed to 1,4-dioxane in drinking water for 2 years C-22
Table D-1. Recommended models for rodents exposed to 1,4-dioxane in drinking water (JBRC, 1998a) D-6
Table D-2. Data for hepatic adenomas and carcinomas in female F344 rats (JBRC, 1998a) ... D-7
Table D-3. Summary of BMDS dose-response modeling results for the combined incidence of hepatic adenomas and carcinomas in female F344 rats D-8
Table D-4. Data for hepatic adenomas and carcinomas in male F344 rats (JBRC, 1998a) D-15
Table D-5. Summary of BMDS dose-response modeling results for the combined incidence of adenomas and carcinomas in livers of male F344 rats D-15
Table D-6. Data for significant tumors at other sites in male and female F344 rats D-20
Table D-7. Summary of BMDS dose-response modeling results for the incidence of nasal cavity tumors in female F344 rats [e] D-21
Table D-8. Summary of BMDS dose-response modeling results for the incidence of nasal cavity tumors in male F344 rats D-26
Table D-9. Summary of BMDS dose-response modeling results for the incidence of mammary gland adenomas in female F344 rats D-27
Table D-10. Summary of BMDS dose-response modeling results for the incidence of peritoneal mesotheliomas in male F344 rats D-32
Table D-11. Data for hepatic adenomas and carcinomas in female BDF_1 mice D-35
Table D-12. Summary of BMDS dose-response modeling results for the combined incidence of hepatic adenomas and carcinomas in female BDF_1 mice D-36
Table D-13. Data for hepatic adenomas and carcinomas in male BDF_1 mice D-38

Table D-14. Summary of BMDS dose-response modeling results for the combined incidence of hepatic adenomas and carcinomas in male BDF_1 mice D-39
Table D-15. Statistically significant MS dose-response models for F344 rats D-42
Table D-16. MS-combo analysis of excess risks for liver adenomas/ carcinomas, mammary gland adenomas, or nasal cavity tumors in female F344 rats using MS models ... D-43
Table D-17. MS-combo analysis of excess risks for liver adenomas, liver carcinomas, nasal cavity tumors, or peritoneal mesotheliomas in male F344 rats using MS models D-48
Table D-18. Calculation of HED values for additional studies reporting the incidence of liver and nasal cavity tumors in rats and mice exposed to 1,4-dioxane in the drinking water for 2 years D-53
Table D-19. Summary of BMD modeling estimates and CSF values associated with liver and nasal tumor incidence data resulting from chronic oral exposure to 1,4-dioxane in rats and mice D-53
Table D-20. Incidence of hepatocellular carcinoma and nasal squamous cell carcinoma in male and female Sherman rats (combined) treated with 1,4-dioxane in the drinking water for 2 years D-54
Table D-21. Goodness-of-fit statistics and $BMD_{10\ HED}$ and $BMDL_{10\ HED}$ from multistage models fit to incidence data for hepatocellular carcinoma and nasal tumors in male and female Sherman rats (combined) exposed to 1,4-dioxane in the drinking water for 2 years D-55
Table D-22. Incidence of nasal cavity squamous cell carcinoma and liver hepatocellular adenoma in Osborne-Mendel rats exposed to 1,4-dioxane in the drinking water . D-57
Table D-23. Goodness-of-fit statistics and $BMD_{10\ HED}$ and $BMDL_{10\ HED}$ from multistage models fit to incidence data for hepatocellular adenoma and nasal tumors in male and female Osborne-Mendel rats exposed to 1,4-dioxane in the drinking water for 2 years ... D-57
Table D-24. Incidence of hepatocellular adenoma or carcinoma in $B6C3F_1$ mice exposed to 1,4-dioxane in drinking water D-61
Table D-25. Goodness-of-fit statistics and $BMD_{10\ HED}$ and $BMDL_{10\ HED}$ values from multistage models fit to incidence data for hepatocellular adenoma or carcinoma in male and female $B6C3F_1$ mice exposed to 1,4-dioxane in the drinking water for 2 years ... D-61

LIST OF FIGURES

Figure 2-1. 1,4-Dioxane chemical structure. 3
Figure 3-1. Suggested metabolic pathways of 1,4-dioxane in the rat. 9
Figure 3-2. Plasma 1,4-dioxane levels in rats following i.v. doses of 3-5,600 mg/kg. 10
Figure 3-3. General PBPK model structure consisting of blood-flow limited tissue compartments connected via arterial and venous blood flows. 13
Figure 4-1. A schematic representation of the possible key events in the delivery of 1,4-dioxane to the liver and the hypothesized MOA(s) for liver carcinogenicity. 80
Figure 4-2. A schematic representation of the possible key events in the delivery of 1,4-dioxane to the nasal cavity and the hypothesized MOA(s) for nasal cavity carcinogenicity.. 81
Figure 5-1. Points of departure (POD) for liver toxicity endpoints with corresponding applied uncertainty factors and derived RfDs following oral exposure to 1,4-dioxane. 94
Figure 5-2. Points of departure (POD) for kidney toxicity endpoints with corresponding applied uncertainty factors and derived RfDs following oral exposure to 1,4-dioxane. 95
Figure 5-3. Points of departure (POD) for nasal inflammation with corresponding applied uncertainty factors and derived RfDs following oral expsorue to 1,4-dioxane. 96
Figure 5-4. Points of departure (POD) for organ specific toxicity endpoints with corresponding applied uncertainty factors and derived RfDs following oral exposure to 1,4-dioxane. 97
Figure B-1. Schematic representation of empirical model for 1,4-dioxane in rats. B-3
Figure B-2. Schematic representation of empirical model for 1,4-dioxane in humans. B-3
Figure B-3. Output of 1,4-dioxane blood level data from the acslXtreme implementation (left) and published (right) empirical rat model simulations of i.v. administration experiments. B-5
Figure B-4. Output of HEAA urine level data from acslXtreme implementation (left) and published (right) empirical rat model simulations of i.v. administration experiments. B-5
Figure B-5. acslXtreme predictions of blood 1,4-dioxane and urine HEAA levels from the empirical rat model simulations of a 6-hour, 50-ppm inhalation exposure. B-6
Figure B-6. Output of 1,4-dioxane blood level data from the acslXtreme implementation (left) and published (right) empirical human model simulations of a 6-hour, 50-ppm inhalation exposure. B-7
Figure B-7. Observations and acslXtreme predictions of cumulative HEAA in human urine following a 6-hour, 50-ppm inhalation exposure. B-8
Figure B-8. Predicted and observed blood 1,4-dioxane concentrations (left) and urinary HEAA levels (right) following re-calibration of the human PBPK model with tissue:air partition coefficient values. B-12
Figure B-9. Predicted and observed blood 1,4-dioxane concentrations (left) and urinary HEAA levels (right) following re-calibration of the human PBPK model with tissue:air partition coefficient values. B-12
Figure B-10. Predicted and observed blood 1,4-dioxane concentrations (left) and urinary HEAA levels (right) using EPA estimated biologically plausible parameters (see Table B-1). B-13
Figure B-11. The highest seven sensitivity coefficients (and associated parameters) for blood 1,4-dioxane concentrations (CV) at 1 (left) and 4 (right) hours of a 50-ppm inhalation exposure. B-15

Figure B-12. Comparisons of the range of PBPK model predictions from upper and lower boundaries on partition coefficients with empirical model predictions and experimental observations for blood 1,4-dioxane concentrations (left) and urinary HEAA levels (right) from a 6-hour, 50-ppm inhalation exposure..... B-17
Figure B-13. Comparisons of the range of PBPK model predictions from upper and lower boundaries on partition coefficients with empirical model predictions and experimental observations for blood 1,4-dioxane concentrations (left) and urinary HEAA levels (right) from a 6-hour, 50-ppm inhalation exposure..... B-17
Figure B-14. Predictions of blood 1,4-dioxane concentration following calibration of a first-order metabolism rate constant, k_{LC}, to the experimental data. B-19
Figure B-15. Predictions of blood 1,4-dioxane concentration following calibration of a first-order metabolism rate constant, k_{LC}, to only the exposure phase of the experimental data..... B-20
Figure B-16. Predictions of blood 1,4-dioxane concentration following simultaneous calibration of a first-order metabolism rate constant, k_{LC}, and slowly perfused tissue:air partition coefficient to the experimental data..... B-21
Figure C-1. BMD log probit model of cortical tubule degeneration incidence data for male rats exposed to 1,4-dioxane in drinking water for 2 years to support the results in Table C-2. ..... C-3
Figure C-2. BMD log-logistic model of cortical tubule degeneration incidence data for female rats exposed to 1,4-dioxane in drinking water for 2 years to support results Table C-2. ..... C-3
Figure C-3. BMD Weibull model of cortical tubule degeneration incidence data for female rats exposed to 1,4-dioxane in drinking water for 2 years to support the results in Table C-2. ..... C-4
Figure C-4. BMD gamma model of liver hyperplasia incidence data for F344 male rats exposed to 1,4-dioxane in drinking water for 2 years to support results Table C-4. ..... C-6
Figure C-5. BMD logistic model of liver hyperplasia incidence data for F344 male rats exposed to 1,4-dioxane in drinking water for 2 years to support results Table C-4. ..... C-8
Figure C-6. BMD log-logistic model of liver hyperplasia incidence data for F344 male rats exposed to 1,4-dioxane in drinking water for 2 years to support the results in Table C-4. ..... C-10
Figure C-7. BMD multistage model of liver hyperplasia incidence data for F344 male rats exposed to 1,4-dioxane in drinking water for 2 years to support the results in Table C-4. ..... C-12
Figure C-8. BMD probit model of liver hyperplasia incidence data for F344 male rats exposed to 1,4-dioxane in drinking water for 2 years to support results Table C-4. ..... C-14
Figure C-9. BMD probit model of liver hyperplasia incidence data for F344 male rats exposed to 1,4-dioxane in drinking water for 2 years, accounting for background incidence. C-16
Figure C-10. BMD quantal linear model of liver hyperplasia incidence data for F344 male rats exposed to 1,4-dioxane in drinking water for 2 years to support the results in Table C-4. ..... C-18
Figure C-11. BMD Weibull model of liver hyperplasia incidence data for F344 male rats exposed to 1,4-dioxane in drinking water for 2 years to support the results in Table C-4. ..... C-20
Figure C-12. BMD gamma model of liver hyperplasia incidence data for F344 female rats exposed to 1,4-dioxane in drinking water for 2 years to support the results in Table C-5. ..... C-22

Figure C-13. BMD logistic model of liver hyperplasia incidence data for F344 female rats exposed to 1,4-dioxane in drinking water for 2 years to support the results in Table C-5. ..... C-24
Figure C-14. BMD log-logistic model of liver hyperplasia incidence data for F344 female rats exposed to 1,4-dioxane in drinking water for 2 years to support the results in Table C-5. ..... C-26
Figure C-15. BMD multistage model of liver hyperplasia incidence data for F344 female rats exposed to 1,4-dioxane in drinking water for 2 years to support the results in Table C-5. ..... C-28
Figure C-16. BMD probit model of liver hyperplasia incidence data for F344 female rats exposed to 1,4-dioxane in drinking water for 2 years to support the results in Table C-5. ..... C-30
Figure C-17. BMD log-probit model of liver hyperplasia incidence data for F344 female rats exposed to 1,4-dioxane in drinking water for 2 years to support the results in Table C-5. ..... C-32
Figure C-18. BMD quantal linear model of liver hyperplasia incidence data for F344 female rats exposed to 1,4-dioxane in drinking water for 2 years to support the results in Table C-5. ..... C-34
Figure C-19. BMD Weibull model of liver hyperplasia incidence data for F344 female rats exposed to 1,4-dioxane in drinking water for 2 years to support the results in Table C-5. ..... C-36
Figure D-1. Multistage BMD model (2 degree) for the combined incidence of hepatic adenomas and carcinomas in female F344 rats. D-9
Figure D-2. Multistage BMD model (1 & 2 degree) for the combined incidence of hepatic adenomas and carcinomas in female F344 rats. D-11
Figure D-3. Log-logistic BMD model for the combined incidence of hepatic adenomas and carcinomas in female F344 rats. D-13
Figure D-4. Multistage BMD model (1 & 2 degree) for the combined incidence of hepatic adenomas and carcinomas in male F344 rats. D-16
Figure D-5. Multistage BMD model (1 & 8 degree) for the combined incidence of hepatic adenomas and carcinomas in male F344 rats. D-18
Figure D-6. Multistage BMD model (2 degree) for the nasal cavity tumors in female F344 rats. D-22
Figure D-7. Multistage BMD model (8 degree) for the nasal cavity tumors in female F344 rats. D-24
Figure D-8. Multistage BMD model (1 degree) for mammary gland adenomas in female F344 rats..... D-28
Figure D-9. Multistage BMD model (2 degree) for mammary gland adenomas in female F344 rats..... D-30
Figure D-10. Multistage BMD model (2 degree) for peritoneal mesotheliomas in male F344 rats. D-33
Figure D-11. Log-logistic BMD model (Fixed power=1) for the combined incidence of hepatic adenomas and carcinomas in female BDF_1 mice. D-36
Figure D-12. Log-logistic BMD model (Fixed power=1) for the combined incidence of hepatic adenomas and carcinomas in male BDF_1 mice..... D-40
Figure D-13. BMD multistage model (1-degree polynomial) of the incidence of hepatocellular carcinoma in male and female Sherman rats exposed to 1,4-dioxane in drinking water. D-55

Figure D-14. BMD multistage model (1-degree polynomial) of the incidence of nasal squamous cell carcinoma in male and female Sherman rats exposed to 1,4-dioxane in drinking water. D-56
Figure D-15. BMD multistage model (1-degree polynomial) of the incidence of nasal squamous cell carcinoma in male Osborne-Mendel rats exposed to 1,4-dioxane in drinking water. D-58
Figure D-16. BMD multistage model (1-degree polynomial) of the incidence of nasal squamous cell carcinoma in female Osborne-Mendel rats exposed to 1,4-dioxane in drinking water. D-59
Figure D-17. BMD multistage model (1-degree polynomial) of the incidence of hepatocellular adenoma in female Osborne-Mendel rats exposed to 1,4-dioxane in drinking water. D-60
Figure D-18. BMD multistage model (2-degree polynomial) of the incidence of hepatocellular adenoma in male $B6C3F_1$ mice exposed to 1,4-dioxane in drinking water..... D-62
Figure D-19. BMD multistage model (2-degree polynomial) of the incidence of hepatocellular adenoma in female $B6C3F_1$ mice exposed to 1,4-dioxane in drinking water. D-63

LIST OF ABBREVIATIONS AND ACRONYMS

AIC	Akaike's Information Criterion
ALP	alkaline phosphatase
ALT	alanine aminotransferase
AST	aspartate aminotransferase
ATSDR	Agency for Toxic Substances and Disease Registry
BMD	benchmark dose
BMD_{10}	benchmark dose at 10% extra risk
BMDL	benchmark dose, lower 95% confidence limit
$BMDL_{10}$	benchmark dose, lower 95% confidence limit at 10% extra risk
BMDS	Benchmark Dose Software
BMR	benchmark response
BrdU	5-bromo-2'-deoxyuridine
BUN	blood urea nitrogen
BW(s)	body weight(s)
CASE	computer automated structure evaluator
CASRN	Chemical Abstracts Service Registry Number
CHO	Chinese hamster ovary (cells)
CI	confidence interval(s)
CNS	central nervous system
CPK	creatinine phosphokinase
CREST	antikinetochore
CSF	cancer slope factor
CV	concentration in venous blood
CYP450	cytochrome P450
DEN	diethylnitrosamine
FISH	fluorescence in situ hybridization
G-6-Pase	glucose-6-phosphatase
GC	gas chromatography
GGT	γ-glutamyl transpeptidase
HEAA	β-hydroxyethoxy acetic acid
HED(s)	human equivalent dose(s)
HPLC	high-performance liquid chromatography
HSDB	Hazardous Substances Data Bank
Hz	Hertz
IARC	International Agency for Research on Cancer
i.p.	intraperitoneal
i.v.	intravenous
IRIS	Integrated Risk Information System
JBRC	Japan Bioassay Research Center
k_e	1st order elimination rate of 1,4-dioxane
k_{INH}	1st order 1,4-dioxane inhalation rate constant
k_{LC}	1st order, non-saturable metabolism rate constant for 1,4-dioxane in the liver
K_m	Michaelis constant for metabolism of 1,4-dioxane in the liver
k_{me}	1st order elimination rate of HEAA (1,4-dioxane metabolite)
LAP	leucine aminopeptidase
LD_{50}	median lethal dose

LDH	lactate dehydrogenase
LOAEL	lowest-observed-adverse-effect-level
MCV	mean corpuscular volume
MOA	mode of action
MS	mass spectrometry, multi-stage
MTD	maximum tolerated dose
MVK	Moolgavkar-Venzon-Knudsen (model)
NCE	normochromatic erythrocyte
NCI	National Cancer Institute
ND	no data, not detected
NE	not estimated
NOAEL	no-observed-adverse-effect-level
NRC	National Research Council
NTP	National Toxicology Program
OCT	ornithine carbamyl transferase
ODC	ornithine decarboxylase
PB	blood:air partition coefficient
PBPK	physiologically based pharmacokinetic
PC	partition coefficient
PCB	polychlorinated biphenyl
PCE	polychromatic erthyrocyte
PFA	fat:air partition coefficient
PLA	liver:air partition coefficient
POD	point of departure
ppm	parts per million
PRA	rapidly perfused tissue:air partition coefficient
PSA	slowy perfused tissue:air partition coefficient
QCC	normalized cardiac output
QPC	normalized alveolar ventilation rate
RBC	red blood cell
RfC	inhalation reference concentration
RfD	oral reference dose
SCE	sister chromatid exchange
SDH	sorbitol dehydrogenase
SMR	standardized mortality ratio
SRC	Syracuse Research Corporation
TPA	12-O-tetradecanoylphorbol-13-acetate
TWA	time-weighted average
UF	uncertainty factor
UNEP	United Nations Environment Programme
U.S. EPA	U.S. Environmental Protection Agency
V	volts
VAS	visual analogue scale
$\mathbf{V_d}$	volume of distribution
$\mathbf{V_{max}}$	maximal rate of metabolism
$\mathbf{V_{maxC}}$	normalized maximal rate of metabolism of 1,4-dioxane in liver
VOC(s)	volatile organic compound(s)
WBC	white blood cell
χ^2	Chi-squared

FOREWORD

The purpose of this Toxicological Review is to provide scientific support and rationale for the hazard and dose-response assessment in IRIS pertaining to chronic exposure to 1,4-dioxane. It is not intended to be a comprehensive treatise on the chemical or toxicological nature of 1,4-dioxane.

The intent of Section 6, Major Conclusions in the Characterization of Hazard and Dose Response, is to present the major conclusions reached in the derivation of the reference dose, reference concentration, and cancer assessment, where applicable, and to characterize the overall confidence in the quantitative and qualitative aspects of hazard and dose response by addressing the quality of the data and related uncertainties. The discussion is intended to convey the limitations of the assessment and to aid and guide the risk assessor in the ensuing steps of the risk assessment process.

For other general information about this assessment or other questions relating to IRIS, the reader is referred to EPA's IRIS Hotline at (202) 566-1676 (phone), (202) 566-1749 (fax), or hotline.iris@epa.gov (email address).

AUTHORS, CONTRIBUTORS, AND REVIEWERS

CHEMICAL MANAGERS

Eva D. McLanahan
National Center for Environmental Assessment
U.S. Environmental Protection Agency
Research Triangle Park, NC

Reeder Sams, II
National Center for Environmental Assessment
U.S. Environmental Protection Agency
Research Triangle Park, NC

AUTHORS AND CONTRIBUTORS

Hisham El-Masri
National Health and Environmental Effects Research Laboratory
U.S. Environmental Protection Agency
Research Triangle Park, NC

Karen Hogan
National Center for Environmental Assessment
U.S. Environmental Protection Agency
Washington, DC

Fernando Llados
Environmental Science Center
Syracuse Research Corporation
Syracuse, NY

Michael Lumpkin
Environmental Science Center
Syracuse Research Corporation
Syracuse, NY

Allan Marcus
National Center for Environmental Assessment
U.S. Environmental Protection Agency
Research Triangle Park, NC

Eva D. McLanahan
National Center for Environmental Assessment
U.S. Environmental Protection Agency
Research Triangle Park, NC

Marc Odin
Environmental Science Center
Syracuse Research Corporation
Syracuse, NY

Susan Rieth
National Center for Environmental Assessment
U.S. Environmental Protection Agency
Washington, DC

Andrew Rooney
National Center for Environmental Assessment
U.S. Environmental Protection Agency
Research Triangle Park, NC

Reeder Sams, II
National Center for Environmental Assessment
U.S. Environmental Protection Agency
Research Triangle Park, NC

Paul Schlosser
National Center for Environmental Assessment
U.S. Environmental Protection Agency
Research Triangle Park, NC

Julie Stickney
Environmental Science Center
Syracuse Research Corporation
Syracuse, NY

John Vandenberg
National Center for Environmental Assessment
U.S. Environmental Protection Agency
Research Triangle Park, NC

REVIEWERS

This document has been peer reviewed by EPA scientists, interagency reviewers from other federal agencies, and the public, and peer reviewed by and independent scientists external to EPA. Comments from all peer reviewers were evaluated carefully and considered by the Agency during the finalization of this assessment. A summary and EPA's disposition of the comments received from the independent external peer reviewers and from the public is included in Appendix A of the Toxicological Review of 1,4-dioxane.

INTERNAL EPA REVIEWERS

Anthony DeAngelo
National Health and Environmental Effects Research Laboratory
Office of Research and Development

Hisham El-Masri
National Health and Environmental Effects Research Laboratory
Office of Research and Development

Nagu Keshava
National Center for Environmental Assessment
Office of Research and Development

Jason Lambert
National Center for Environmental Assessment
Office of Research and Development

Connie Meacham
National Center for Environmental Assessment
U.S. Environmental Protection Agency
Research Triangle Park, NC

Paul Schlosser
National Center for Environmental Assessment
Office of Research and Development

Debra Walsh
National Center for Environmental Assessment
U.S. Environmental Protection Agency
Research Triangle Park, NC

Douglas Wolf
National Health and Environmental Effects Research Laboratory
Office of Research and Development

1. INTRODUCTION

This document presents background information and justification for the Integrated Risk Information System (IRIS) Summary of the hazard and dose-response assessment of 1,4-dioxane. IRIS Summaries may include oral reference dose (RfD) and inhalation reference concentration (RfC) values for chronic and subchronic exposure durations, and a carcinogenicity assessment.

The RfD and RfC, if derived, provide quantitative information for use in risk assessments for health effects known or assumed to be produced through a nonlinear (presumed threshold) mode of action. The RfD (expressed in units of mg/kg-day) is defined as an estimate (with uncertainty spanning perhaps an order of magnitude) of a daily exposure to the human population (including sensitive subgroups) that is likely to be without an appreciable risk of deleterious effects during a lifetime. The inhalation RfC (expressed in units of mg/m^3) is analogous to the oral RfD, but provides a continuous inhalation exposure estimate. The inhalation RfC considers toxic effects for both the respiratory system (portal-of-entry) and for effects peripheral to the respiratory system (extrarespiratory or systemic effects). Reference values are generally derived for chronic exposures (up to a lifetime), but may also be derived for acute (≤ 24 hours), short-term (>24 hours up to 30 days), and subchronic (>30 days up to 10% of lifetime) exposure durations, all of which are derived based on an assumption of continuous exposure throughout the duration specified. Unless specified otherwise, the RfD and RfC are derived for chronic exposure durations.

The carcinogenicity assessment provides information on the carcinogenic hazard potential of the substance in question and quantitative estimates of risk from oral and inhalation exposure may be derived. The information includes a weight-of-evidence judgment of the likelihood that the agent is a human carcinogen and the conditions under which the carcinogenic effects may be expressed. Quantitative risk estimates may be derived from the application of a low-dose extrapolation procedure. If derived, the oral slope factor is a plausible upper bound on the estimate of risk per mg/kg-day of oral exposure. Similarly, an inhalation unit risk is a plausible upper bound on the estimate of risk per $\mu g/m^3$ air breathed.

Development of these hazard identification and dose-response assessments for 1,4-dioxane has followed the general guidelines for risk assessment as set forth by the National Research Council (NRC, 1983). EPA guidelines and Risk Assessment Forum Technical Panel Reports that may have been used in the development of this assessment include the following: *Guidelines for the Health Risk Assessment of Chemical Mixtures* (U.S. EPA, 1986a), *Guidelines for Mutagenicity Risk Assessment* (U.S. EPA, 1986b), *Recommendations for and Documentation of Biological Values for Use in Risk Assessment* (U.S. EPA, 1988), *Guidelines for Developmental Toxicity Risk Assessment* (U.S. EPA, 1991), *Interim Policy for Particle Size and Limit Concentration Issues in Inhalation Toxicity* (U.S. EPA, 1994a), *Methods for Derivation of*

Inhalation Reference Concentrations and Application of Inhalation Dosimetry (U.S. EPA, 1994b), *Use of the Benchmark Dose Approach in Health Risk Assessment* (U.S. EPA, 1995), *Guidelines for Reproductive Toxicity Risk Assessment* (U.S. EPA, 1996), *Guidelines for Neurotoxicity Risk Assessment* (U.S. EPA, 1998), *Science Policy Council Handbook*: *Risk Characterization* (U.S. EPA, 2000a), *Benchmark Dose Technical Guidance Document* (U.S. EPA, 2000b), *Supplementary Guidance for Conducting Health Risk Assessment of Chemical Mixtures* (U.S. EPA, 2000c), *A Review of the Reference Dose and Reference Concentration Processes* (U.S. EPA, 2002a), *Guidelines for Carcinogen Risk Assessment* (U.S. EPA, 2005a), *Supplemental Guidance for Assessing Susceptibility from Early-Life Exposure to Carcinogens* (U.S. EPA, 2005b), *Science Policy Council Handbook*: *Peer Review* (U.S. EPA, 2006a), and *A Framework for Assessing Health Risks of Environmental Exposures to Children* (U.S. EPA, 2006b).

The literature search strategy employed for this compound was based on the Chemical Abstracts Service Registry Number (CASRN) and at least one common name. Any pertinent scientific information submitted by the public to the IRIS Submission Desk was also considered in the development of this document. The relevant literature was reviewed through August 2008.

2. CHEMICAL AND PHYSICAL INFORMATION

1,4-Dioxane, a volatile organic compound (VOC), is a colorless liquid with a pleasant odor (Lewis, 2001, 2000). Synonyms include diethylene ether, 1,4-diethylene dioxide, diethylene oxide, dioxyethylene ether, and dioxane (Lewis, 2001). The chemical structure of 1,4-dioxane is shown in Figure 2-1. Selected chemical and physical properties of this substance are listed below:

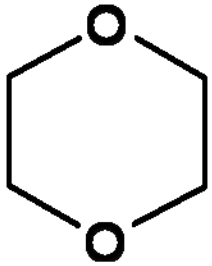

Figure 2-1. 1,4-Dioxane chemical structure.

Table 2-1. Physical properties and chemical identity of 1,4-dioxane

CASRN:	123-91-1 (Lide, 2000)
Molecular weight:	88.10 (O'Neil, 2001)
Chemical formula:	$C_4H_8O_2$ (O'Neil, 2001)
Boiling point:	101.1°C (O'Neil, 2001)
Melting point:	11.8°C (Lide, 2000)
Vapor pressure:	40 mmHg at 25°C (Lewis, 2000)
Density:	1.0337 g/mL at 20°C (Lide, 2000)
Vapor density:	3.03 (air = 1) (Lewis, 2000)
Water solubility:	Miscible with water (Lewis, 2001)
Other solubilities:	Miscible with ethanol, ether, and acetone (Lide, 2000)
Log K_{ow}:	–0.27 (Hansch et al., 1995)
Henry's Law constant:	4.80×10^{-6} atm-m^3/molecule at 25°C (Park et al., 1987)
OH reaction rate constant:	1.09×10^{-11} cm^3/molecule sec at 25°C (Atkinson, 1989)
K_{oc}:	17 (estimated using log K_{ow}) (Lyman et al., 1990)
Bioconcentration factor:	0.4 (estimated using log K_{ow}) (Meylan et al., 1999)
Conversion factors (in air):	1 ppm = 3.6 mg/m^3; 1 mg/m^3 = 0.278 ppm (25^oC and 1 atm) (HSDB, 2007)

1,4-Dioxane is produced commercially through the dehydration and ring closure of diethylene glycol (Surprenant, 2002). Concentrated sulfuric acid is used as a catalyst (Surprenant, 2002). This is a continuous distillation process with operating temperatures and pressures of 130–200°C and 188–825 mmHg, respectively (Surprenant, 2002). During the years 1986 and 1990, the U.S. production of 1,4-dioxane reported by manufacturers was within the range of 10–50 million pounds (U.S. EPA, 2002b). The production volume reported during the years 1994, 1998, and 2002 was within the range of 1–10 million pounds (U.S. EPA, 2002b).

Historically, 1,4-dioxane has been used as a stabilizer for the solvent 1,1,1-trichloroethane (Suprenant, 2002). However, this use is no longer expected to be important due to the 1990 Amendments to the Clean Air Act and the Montreal Protocol, which mandate the eventual phase-out of 1,1,1-trichloroethane production in the U.S. (ATSDR, 2007; 2006; UNEP, 2000; U.S. EPA, 1990). 1,4-Dioxane is also used as a solvent for cellulosics, organic products, lacquers, paints, varnishes, paint and varnish removers, resins, oils, waxes, dyes, cements, cosmetics, deodorants, fumigants, emulsions, and polishing compositions (Lewis, 2001; O'Neil, 2001; IARC, 1999). 1,4-Dioxane has been used as a solvent in the formulation of inks, coatings, and adhesives and in the extraction of animal and vegetable oil (Suprenant, 2002). Reaction products of 1,4-dioxane are used in the manufacture of insecticides, herbicides, plasticizers, and monomers (Suprenant, 2002).

When 1,4-dioxane enters the air, it will exist as a vapor, as indicated by its vapor pressure (HSDB, 2007). It is expected to be degraded in the atmosphere through photooxidation with hydroxyl radicals (HSDB, 2007; Suprenant, 2002). The estimated half-life for this reaction is 6.7 hours (HSDB, 2007). It may also be broken down by reaction with nitrate radicals, although this removal process is not expected to compete with hydroxyl radical photooxidation (Grosjean, 1990). 1,4-Dioxane is not expected to undergo direct photolysis (Wolfe and Jeffers, 2000). 1,4-Dioxane is primarily photooxidized to 2-oxodioxane and through reactions with nitrogen oxides (NO_x) results in the formation of ethylene glycol diformate (Platz et al., 1997). 1,4-Dioxane is expected to be highly mobile in soil based on its estimated K_{oc} and is expected to leach to lower soil horizons and groundwater (ATSDR, 2007; Lyman et al., 1990). This substance may volatilize from dry soil surfaces based on its vapor pressure (HSDB, 2007). The estimated bioconcentration factor value indicates that 1,4-dioxane will not bioconcentrate in aquatic or marine organisms (Meylan et al., 1999; Franke et al., 1994). 1,4-Dioxane is not expected to undergo hydrolysis or to biodegrade readily in the environment (HSDB, 2007; ATSDR, 2007). Therefore, volatilization is expected to be the dominant removal process for moist soil and surface water. Based on a Henry's Law constant of 4.8×10^{-6} atm-m^3/mole, the half-life for volatilization of 1,4-dioxane from a model river is 5 days and that from a model lake is 56 days (HSDB, 2007; Lyman et al., 1990; Park et al., 1987). 1,4-Dioxane may be more persistent in groundwater where volatilization is hindered.

Recent environmental monitoring data for 1,4-dioxane are lacking. Existing data indicate that 1,4-dioxane may leach from hazardous waste sites into drinking water sources located nearby (Yasuhara et al., 2003, 1997; Lesage et al., 1990). 1,4-Dioxane has been detected in contaminated surface and groundwater samples collected near hazardous waste sites and industrial facilities (DeRosa et al., 1996).

3. TOXICOKINETICS

Data for the toxicokinetics of 1,4-dioxane in humans are very limited. However, absorption, distribution, metabolism, and elimination of 1,4-dioxane are well described in rats exposed via the oral, inhalation, or intravenous (i.v.) routes. 1,4-Dioxane is extensively absorbed and metabolized in humans and rats to β-hydroxyethoxy acetic acid (HEAA), which is predominantly excreted in the urine. Saturation of 1,4-dioxane metabolism has been observed in rats and would be expected in humans; however, human exposure levels associated with nonlinear toxicokinetics are not known.

Important data elements that have contributed to our current understanding of the toxicokinetics of 1,4-dioxane are summarized in the following sections.

3.1. ABSORPTION

Absorption of 1,4-dioxane following inhalation exposure has been qualitatively demonstrated in workers and volunteers. Workers exposed to a time-weighted average (TWA) of 1.6 parts per million (ppm) of 1,4-dioxane in air for 7.5 hours showed a HEAA/1,4-dioxane ratio of 118:1 in urine (Young et al., 1976). The authors assumed lung absorption to be 100% and calculated an average absorbed dose of 0.37 mg/kg, although no exhaled breath measurements were taken. In a study with four healthy male volunteers, Young et al. (1977) reported 6-hour inhalation exposures of adult volunteers to 50 ppm of 1,4-dioxane in a chamber, followed by blood and urine analysis for 1,4-dioxane and HEAA. The study protocol was approved by a seven-member Human Research Review Committee of the Dow Chemical Company, and written informed consent of study participants was obtained. At a concentration of 50 ppm, uptake of 1,4-dioxane into plasma was rapid and approached steady-state conditions by 6 hours. The authors reported a calculated absorbed dose of 5.4 mg/kg. However, the exposure chamber atmosphere was kept at a constant concentration of 50 ppm and exhaled breath was not analyzed. Accordingly, gas uptake could not be measured. As a result, the absorbed fraction of inhaled 1,4-dioxane could not be accurately determined in humans. Rats inhaling 50 ppm for 6 hours exhibited 1,4-dioxane and HEAA in urine with an HEAA to 1,4-dioxane ratio of over 3,100:1 (Young et al., 1978a, b). Plasma concentrations at the end of the 6-hour exposure period averaged 7.3 μg/mL. The authors calculated an absorbed 1,4-dioxane dose of 71.9 mg/kg; however, the lack of exhaled breath data and dynamic exposure chamber precluded the accurate determination of the inhaled fraction of 1,4-dioxane.

No human data are available to evaluate the oral absorption of 1,4-dioxane. Gastrointestinal absorption was nearly complete in male Sprague Dawley rats orally dosed with 10–1,000 mg/kg of [^{14}C]-1,4-dioxane given as a single dose or as 17 consecutive daily doses

(Young et al., 1978a, b). Cumulative recovery of radiolabel in the feces was <1–2% of administered dose regardless of dose level or frequency.

No human data are available to evaluate the dermal absorption of 1,4-dioxane; however, Bronaugh (1982) reported an in vitro study in which 1,4-dioxane penetrated excised human skin 10 times more under occulded conditions (3.2% of applied dose) than unocculded conditions (0.3% of applied dose). [^{14}C]-1,4-dioxane was dissolved in lotion, applied to the excised skin in occluded and unoccluded diffusion cells, and absorption of the dose was recorded 205 minutes after application. Bronaugh (1982) also reported observing rapid evaporation, which further decreased the small amount available for skin absorption.

Dermal absorption data in animals are also limited. Dermal absorption in animals was reported to be low following exposure of forearm skin of monkeys (Marzulli, 1981). In this study, Rhesus monkeys were exposed to [^{14}C]-1,4-dioxane in methanol or skin lotion vehicle for 24 hours (skin was uncovered/unoccluded). Only 2–3% of the original radiolabel was cumulatively recovered in urine over a 5-day period.

3.2. DISTRIBUTION

No data are available for the distribution of 1,4-dioxane in human tissues. No data are available for the distribution of 1,4-dioxane in animals following oral or inhalation exposures.

Mikheev et al. (1990) studied the distribution of [^{14}C]-1,4-dioxane in the blood, liver, kidney, brain, and testes of rats (strain not reported) for up to 6 hours following intraperitoneal (i.p.) injection of approximately one-tenth the median lethanl dose (LD_{50}) (actual dose not reported). While actual tissue concentrations were not reported, tissue:blood ratios were given for each tissue at six time points ranging from 5 minutes to 6 hours. The time to reach maximum accumulation of radiolabel was shorter for liver and kidney than for blood or the other tissues, which the authors suggested was indicative of selective membrane transport. Tissue:blood ratios were less than one for all tissues except testes, which had a ratio greater than one at the 6-hour time point. The significance of these findings is questionable since the contribution of residual blood in the tissues was unknown (though saline perfusion may serve to clear tissues of highly water-soluble 1,4-dioxane), the tissue concentrations of radiolabel were not reported, and data were collected from so few time points.

Woo et al. (1977b) administered i.p. doses of [^{3}H]-1,4-dioxane (5 mCi/kg body weight [BW]) to male Sprague Dawley rats with and without pretreatment using mixed-function oxidase inducers (phenobarbital, 3-methylcholanthrene, or polychlorinated biphenyls [PCBs]). Liver, kidney, spleen, lung, colon, and skeletal muscle tissues were collected from 1, 2, 6, and 12 hours after dosing. Distribution was generally uniform across tissues, with blood concentrations higher than tissues at all times except for 1 hour post dosing, when kidney levels were approximately 20% higher than blood. Since tissues were not perfused prior to analysis, the contribution of residual blood to radiolabel measurements is unknown, though loss of 1,4-dioxane from tissues

would be unknown had saline perfusion been performed. Covalent binding reached peak percentages at 6 hours after dosing in liver (18.5%), spleen (22.6%), and colon (19.5%). At 16 hours after dosing, peak covalent binding percentages were observed in whole blood (3.1%), kidney (9.5%), lung (11.2%), and skeletal muscle (11.2%). Within hepatocytes, radiolabel distribution at 6 hours after dosing was greatest in the cytosolic fraction (43.8%) followed by the microsomal (27.9%), mitochondrial (16.6%), and nuclear (11.7%) fractions. While little covalent binding of radiolabel was measured in the hepatic cytosol (4.6%), greater binding was observed at 16 hours after dosing in the nuclear (64.8%), mitochondrial (45.7%), and microsomal (33.4%) fractions. Pretreatment with inducers of mixed-function oxidase activity did not significantly change the extent of covalent binding in subcellular fractions.

3.3. METABOLISM

The major product of 1,4-dioxane metabolism appears to be HEAA, although there is one report that identified 1,4-dioxane-2-one as a major metabolite (Woo et al., 1977b). However, the presence of this compound in the sample was believed to result from the acidic conditions (pH of 4.0–4.5) of the analytical procedures. The reversible conversion of HEAA and p-1,4-dioxane-2-one is pH-dependent (Braun and Young, 1977). Braun and Young (1977) identified HEAA (85%) as the major metabolite, with most of the remaining dose excreted as unchanged 1,4-dioxane in the urine of Sprague Dawley rats dosed with 1,000 mg/kg of uniformly labeled 1,4-[^{14}C]dioxane. In fact, toxicokinetic studies of 1,4-dioxane in humans and rats (Young et al., 1978a, b, 1977) employed an analytical technique that converted HEAA to the more volatile dioxanone prior to gas chromatography (GC).

A proposed metabolic scheme for 1,4-dioxane metabolism (Woo et al., 1977b) in Sprague Dawley rats is shown in Figure 3-1. Oxidation of 1,4-dioxane to diethylene glycol (pathway a), 1,4-dioxane-2-ol (pathway c), or directly to 1,4-dioxane-2-one (pathway b) could result in the production of HEAA. 1,4-Dioxane oxidation appears to be cytochrome P450 (CYP450)-mediated, as CYP450 induction with phenobarbital or Aroclor 1254 (a commercial PCB mixture) and suppression with 2,4-dichloro-6-phenylphenoxy ethylamine or cobaltous chloride were effective in significantly increasing and decreasing, respectively, the appearance of HEAA in the urine of Sprague Dawley rats (Woo et al., 1978, 1977c). 1,4-Dioxane itself induced CYP450-mediated metabolism of several barbiturates in Hindustan mice given i.p. injections of 25 and 50 mg/kg 1,4-dioxane (Mungikar and Pawar, 1978). Of the three possible pathways proposed in this scheme, oxidation to diethylene glycol and HEAA appears to be the most likely, because diethylene glycol was found as a minor metabolite in Sprague Dawley rat urine following a single 1,000 mg/kg gavage dose of 1,4-dioxane (Braun and Young, 1977). Additionally, i.p. injection of 100–400 mg/kg diethylene glycol in Sprague Dawley rats resulted in urinary elimination of HEAA (Woo et al., 1977a).

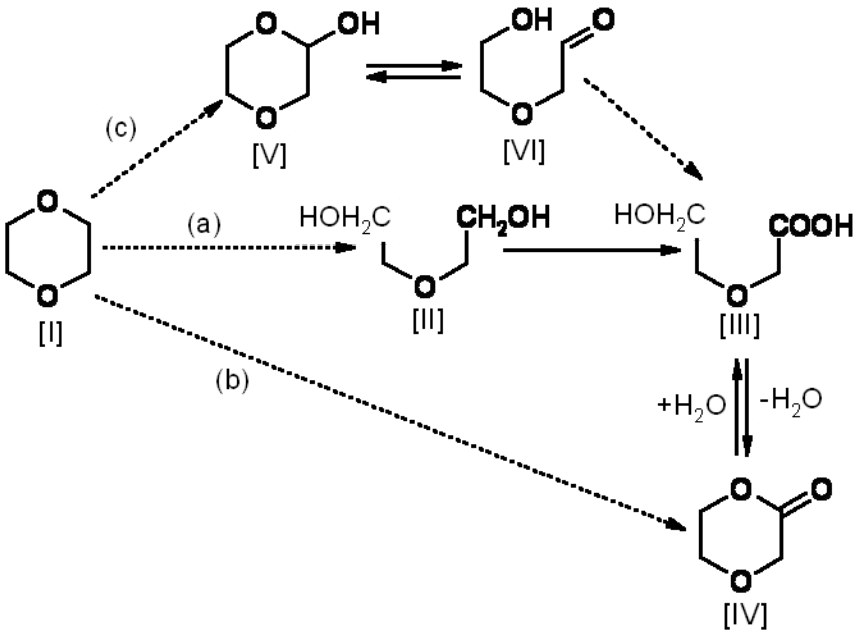

Source: Adapted from Woo et al. (1977b, c).

Figure 3-1. Suggested metabolic pathways of 1,4-dioxane in the rat. I = 1,4-dioxane; II = diethylene glycol; III = β-hydroxyethoxy acetic acid (HEAA); IV = 1,4-dioxane-2-one; V = 1,4-dioxane-2-ol; VI = β-hydroxyethoxy acetaldehyde. Note: Metabolite [V] is a likely intermediate in pathway b as well as pathway c. The proposed pathways are based on the metabolites identified; the enzymes responsible for each reaction have not been determined. The proposed pathways do not account for metabolite degradation to the labeled carbon dioxide (CO_2) identified in expired air after labeled 1,4-dioxane exposure.

Metabolism of 1,4-dioxane in humans is extensive. In a survey of 1,4-dioxane plant workers exposed to a TWA of 1.6 ppm of 1,4-dioxane for 7.5 hours, Young et al. (1976) found HEAA and 1,4-dioxane in the worker's urine at a ratio of 118:1. Similarly, in adult male volunteers exposed to 50 ppm for 6 hours (Young et al., 1977), over 99% of inhaled 1,4-dioxane (assuming negligible exhaled excretion) appeared in the urine as HEAA. The linear elimination of 1,4-dioxane in both plasma and urine indicated that 1,4-dioxane metabolism was a nonsaturated, first-order process at this exposure level.

Like humans, rats extensively metabolize inhaled 1,4-dioxane, as HEAA content in urine was over 3,000-fold higher than that of 1,4-dioxane following exposure to 50 ppm for 6 hours (Young et al., 1978a, b). 1,4-Dioxane metabolism in rats was a saturable process, as exhibited by oral and i.v. exposures to various doses of [^{14}C]-1,4-dioxane (Young et al., 1978a, b). Plasma

data from Sprague Dawley rats given single i.v. doses of 3, 10, 30, 100, 300, or 1,000 mg [^{14}C]-1,4-dioxane/kg demonstrated a dose-related shift from linear, first-order to nonlinear, saturable metabolism of 1,4-dioxane between plasma 1,4-dioxane levels of 30 and 100 µg/mL (Figure 3-2). Similarly, in rats given, via gavage in distilled water, 10, 100, or 1,000 mg [^{14}C]-1,4-dioxane/kg singly or 10 or 1,000 mg [^{14}C]-1,4-dioxane/kg in 17 daily doses, the percent urinary excretion of the radiolabel decreased significantly with dose while radiolabel in expired air increased. Specifically, with single [^{14}C]-1,4-dioxane/kg doses, urinary radiolabel decreased from 99 to 76% and expired 1,4-dioxane increased from <1 to 25% as dose increased from 10 to 1,000 mg/kg. Likewise, with multiple daily doses 10 or 1,000 mg [^{14}C]-1,4-dioxane/kg, urinary radiolabel decreased from 99 to 82% and expired 1,4-dioxane increased from 1 to 9% as dose increased. The differences between single and multiple doses in urinary and expired radiolabel support the notion that 1,4-dioxane may induce its own metabolism.

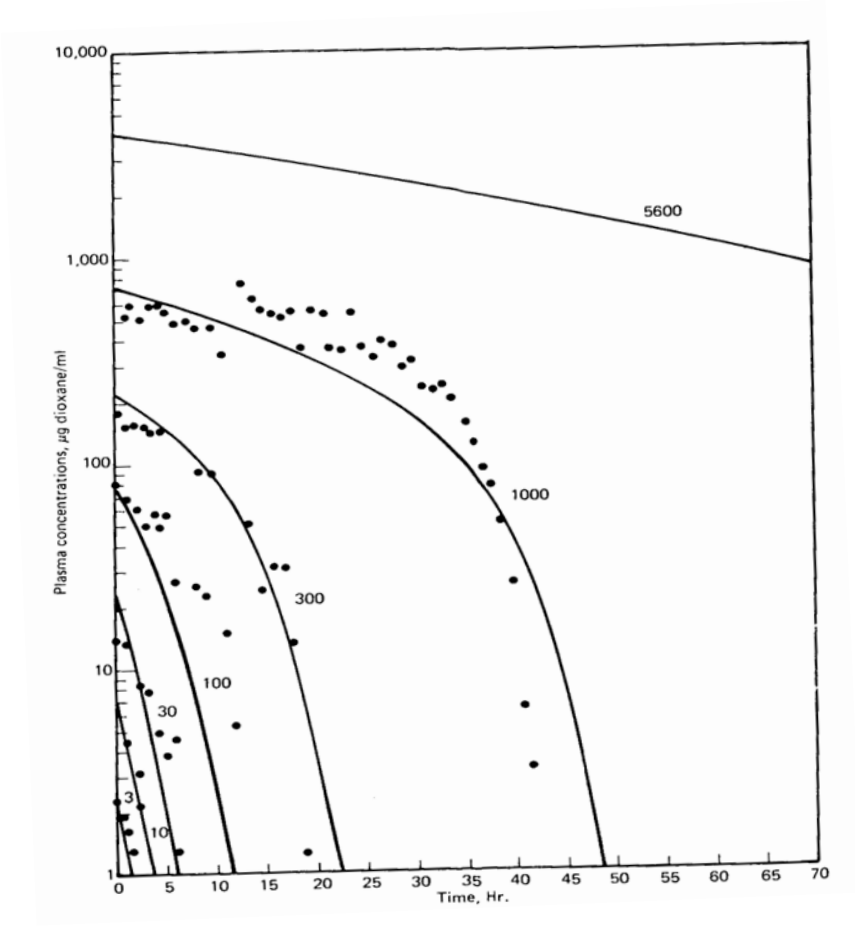

Source: Young et al. (1978a).

Figure 3-2. Plasma 1,4-dioxane levels in rats following i.v. doses of 3-5,600 mg/kg.

1,4-Dioxane has been shown to induce several isoforms of CYP450 in various tissues following acute oral administration by gavage or drinking water (Nannelli et al., 2005). Male Sprague Dawley rats were exposed to either 2,000 mg/kg 1,4-dioxane via gavage for 2 consecutive days or by ingestion of a 1.5% 1,4-dioxane drinking water solution for 10 days. Both exposures resulted in significantly increased CYP2B1/2, CYP2C11, and CYP2E1 activities in hepatic microsomes. The gavage exposure alone resulted in increased CYP3A activity. The increase in 2C11 activity was unexpected, as that isoform has been observed to be under hormonal control and was typically suppressed in the presence of 2B1/2 and 2E1 induction. In the male rat, hepatic 2C11 induction is associated with masculine pulsatile plasma profiles of growth hormone (compared to the constant plasma levels in the female), resulting in masculinization of hepatocyte function (Waxman et al., 1991). The authors postulated that 1,4-dioxane may alter plasma growth hormone levels, resulting in the observed 2C11 induction. However, growth hormone induction of 2C11 is primarily dependent on the duration between growth hormone pulses and secondarily on growth hormone plasma levels (Agrawal and Shapiro, 2000; Waxman et al., 1991). Thus, the induction of 2C11 by 1,4-dioxane may be mediated by changes in the time interval between growth hormone pulses rather than changes in growth hormone levels. This may be accomplished by 1,4-dioxane temporarily influencing the presence of growth hormone cell surface binding sites (Agrawal and Shapiro, 2000). However, no studies are available to confirm the influence of 1,4-dioxane on either growth hormone levels or changes in growth hormone pulse interval.

In nasal and renal mucosal cell microsomes, CYP2E1 activity, but not CYP2B1/2 activity, was increased. Pulmonary mucosal CYP450 activity levels were not significantly altered. Observed increases in 2E1 mRNA in rats exposed by gavage and i.p. injection suggest that 2E1 induction in kidney and nasal mucosa is controlled by a transcriptional activation of 2E1 genes. The lack of increased mRNA in hepatocytes suggests that induction is regulated via a post-transcriptional mechanism. Differences in 2E1 induction mechanisms in liver, kidney, and nasal mucosa suggest that induction is controlled in a tissue-specific manner.

3.4. ELIMINATION

In workers exposed to a TWA of 1.6 ppm for 7.5 hours, 99% of 1,4-dioxane eliminated in urine was in the form of HEAA (Young et al., 1976). The elimination half-life was 59 minutes in adult male volunteers exposed to 50 ppm 1,4-dioxane for 6 hours, with 90% of urinary 1,4-dioxane and 47% of urinary HEAA excreted within 6 hours of onset of exposure (Young et al., 1977). There are no data for 1,4-dioxane elimination in humans from oral exposures.

Elimination of 1,4-dioxane in rats (Young et al., 1978a, b) was primarily via urine. Like humans, the elimination half-life in rats exposed to 50 ppm 1,4-dioxane for 6 hours was calculated to be 1.01 hours. In Sprague Dawley rats given single daily doses of 10, 100, or 1,000 mg [^{14}C]-1,4-dioxane/kg or multiple doses of 10 or 1,000 mg [^{14}C]-1,4-dioxane/kg, urinary

radiolabel ranged from 99% down to 76% of total radiolabel. Fecal elimination was less than 2% for all doses. The effect of saturable metabolism on expired 1,4-dioxane was apparent, as expired 1,4-dioxane in singly dosed rats increased with dose from 0.4 to 25% while expired $^{14}CO_2$ changed little (between 2 and 3%) across doses. The same relationship was seen in Sprague Dawley rats dosed i.v. with 10 or 1,000 mg [^{14}C]-1,4-dioxane/kg. Higher levels of $^{14}CO_2$ relative to 1,4-dioxane were measured in expired air of the 10 mg/kg group, while higher levels of expired 1,4-dioxane relative to $^{14}CO_2$ were measured in the 1,000 mg/kg group.

3.5. PHYSIOLOGICALLY BASED TOXICOKINETIC MODELS

PBPK models have been developed for 1,4-dioxane in rats and humans (Leung and Paustenbach, 1990; Reitz et al., 1990) and lactating humans (Fisher et al., 1997). Each of the models simulates the body as a series of compartments representing tissues or tissue groups that receive blood from the central vascular compartment (Figure 3-3). Modeling was conducting under the premise that transfers of 1,4-dioxane between blood and tissues occur sufficiently fast to be effectively blood flow-limited, which is consistent with the available data (Ramsey and Andersen, 1984). Blood time course and metabolite production data in rats and humans suggest that absorption and metabolism are accomplished through common mechanisms in both species (Young et al., 1978a, b, 1977), allowing identical model structures to be used for both species (and by extension, for mice as well). In all three models, physiologically relevant, species-specific parameter values for tissue volume, blood flow, and metabolism and elimination are used. The models and supporting data are reviewed below, from the perspective of assessing their utility for predicting internal dosimetry and for cross-species extrapolation of exposure-response relationships for critical neoplastic and non-neoplastic endpoints (also see Appendix B).

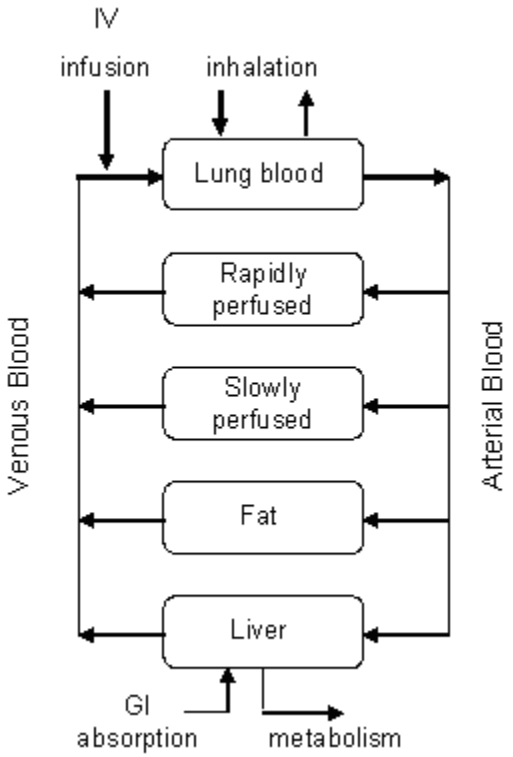

Figure 3-3. General PBPK model structure consisting of blood-flow limited tissue compartments connected via arterial and venous blood flows. Note: Orally administered chemicals are absorbed directly into the liver while inhaled and intravenously infused chemicals enter directly into the arterial and venous blood pools, respectively.

3.5.1. Available Pharmacokinetic Data

Animal and human data sets available for model calibration derive from Young et al. (1978a, b, 1977), Mikheev et al. (1990), and Woo et al. (1977a, b). Young et al. (1978a, b) studied the disposition of radiolabeled [^{14}C]-1,4-dioxane in adult male Sprague Dawley rats following i.v., inhalation, and single and multiple oral gavage exposures. Plasma concentration-time profiles were reported for i.v. doses of 3, 10, 30, 100, and 1,000 mg/kg. In addition, exhaled $^{14}CO_2$ and urinary 1,4-dioxane and HEAA profiles were reported following i.v. doses of 10 and 1,000 mg/kg. The plasma 1,4-dioxane concentration-time course, cumulative urinary 1,4-dioxane and cumulative urinary HEAA concentrations were reported following a 6-hour inhalation exposure to 50 ppm. Following oral gavage doses of 10–1,000 mg/kg, percentages of total orally administered radiolabel were measured in urine, feces, expired air, and the whole body.

Oral absorption of 1,4-dioxane was extensive, as only approximately 1% of the administered dose appeared in the feces within 72 hours of dosing (Young et al., 1978a, b). Although it may be concluded that the rate of oral absorption was high enough to ensure nearly

complete absorption by 72 hours, a more quantitative estimate of the rate of oral absorption is not possible due to the absence of plasma time course data by oral exposure.

Saturable metabolism of 1,4-dioxane was observed in rats exposed by either the i.v. or oral routes (Young et al., 1978a, b). Elimination of 1,4-dioxane from plasma appeared to be linear following i.v. doses of 3-30 mg/kg, but was nonlinear following doses of 100–1,000 mg/kg. Accordingly, 10 mg/kg i.v. doses resulted in higher concentrations of $^{14}CO_2$ (from metabolized 1,4-dioxane) in expired air relative to unchanged 1,4-dioxane, while 1,000 mg/kg i.v. doses resulted in higher concentrations of expired 1,4-dioxane relative to $^{14}CO_2$. Thus, at higher i.v. doses, a higher proportion of unmetabolized 1,4-dioxane is available for exhalation. Taken together, the i.v. plasma and expired air data from Young et al. (1978a, b) corroborate previous studies describing the saturable nature of 1,4-dioxane metabolism in rats (Woo et al. 1977a, b) and are useful for optimizing metabolic parameters (V_{max} and K_m) in a PBPK model.

Similarly, increasing single or multiple oral doses of 10–1,000 mg/kg resulted in increasing percentage of 1,4-dioxane in exhaled air and decreasing percentage of radiolabel (either as 1,4-dioxane or a metabolite) in the urine, with significant differences in both metrics being observed between doses of 10 and 100 mg/kg (Young et al., 1978a, b). These data identify the region (10–100 mg/kg) in which oral exposures will result in nonlinear metabolism of 1,4-dioxane and can be used to test whether metabolic parameter value estimates derived from i.v. dosing data are adequate for modeling oral exposures.

Post-exposure plasma data from a single 6-hour, 50 ppm inhalation exposure in rats were reported (Young et al., 1978a, b). The observed linear elimination of 1,4-dioxane after inhalation exposure suggests that, via this route, metabolism is in the linear region at this exposure level.

The only human data adequate for use in PBPK model development (Young et al., 1977) come from adult male volunteers exposed to 50 ppm 1,4-dioxane for 6 hours. Plasma 1,4-dioxane and HEAA concentrations were measured both during and after the exposure period, and urine concentrations were measured following exposure. Plasma levels of 1,4-dioxane approached steady-state at 6 hours. HEAA data were insufficient to describe the appearance or elimination of HEAA in plasma. Data on elimination of 1,4-dioxane and HEAA in the urine up to 24 hours from the beginning of exposure were reported. At 6 hours from onset of exposure, approximately 90% and 47% of the cumulative (0–24 hours) urinary 1,4-dioxane and HEAA, respectively, were measured in the urine. The ratio of HEAA to 1,4-dioxane in urine 24 hours after onset of exposure was 192:1 (similar to the ratio of 118:1 observed by Young et al. [1976] in workers exposed to 1.6 ppm for 7.5 hours), indicating extensive metabolism of 1,4-dioxane As with Sprague Dawley rats, the elimination of 1,4-dioxane from plasma was linear across all observations (6 hours following end of exposure), suggesting that human metabolism of 1,4-dioxane is linear for a 50 ppm inhalation exposure to steady-state. Thus, estimation of

human V_{max} and K_m from these data will introduce uncertainty into internal dosimetry performed in the nonlinear region of metabolism.

Further data were reported for the tissue distribution of 1,4-dioxane in rats. Mikheev et al. (1990) administered i.p. doses of [^{14}C]-1,4-dioxane to rats (strain not reported) and reported time-to-peak blood, liver, kidney, and testes concentrations. They also reported ratios of tissue to blood concentrations at various time points after dosing. Woo et al. (1977a, b) administered i.p. doses of [^{14}C]-1,4-dioxane to Sprague Dawley rats and measured radioactivity levels in urine. However, since i.p. dosing is not relevant to human exposures, these data are of limited use for PBPK model development.

3.5.2. Published PBPK Models for 1,4-Dioxane

3.5.2.1. *Leung and Paustenbach (1990)*

Leung and Paustenbach (1990) developed a PBPK model for 1,4-dioxane and its primary metabolite, HEAA, in rats and humans. The model, based on the structure of a PBPK model for styrene (Ramsey and Andersen, 1984), consists of a central blood compartment and four tissue compartments: liver, fat, slowly perfused tissues (mainly muscle and skin), and richly perfused tissues (brain, kidney, and viscera other than the liver). Tissue volumes were calculated as percentages of total BW, and blood flow rates to each compartment were calculated as percentages of cardiac output. Equivalent cardiac output and alveolar ventilation rates were allometrically scaled to a power (0.74) of BW for each species. The concentration of 1,4-dioxane in alveolar blood was assumed to be in equilibrium with alveolar air at a ratio equal to the experimentally measured blood:air partition coefficient. Transfers of 1,4-dioxane between blood and tissues were assumed to be blood flow-limited and to achieve rapid equilibrium between blood and tissue, governed by tissue:blood equilibrium partition coefficients. The latter were derived from the quotient of blood:air and tissue:air partition coefficients, which were measured in vitro (Leung and Paustenbach, 1990) for blood, liver, fat, and skeletal muscle (slowly perfused tissue). Blood:air partition coefficients were measured for both humans and rats. Rat tissue:air partition coefficients were used as surrogate values for humans, with the exception of slowly perfused tissue:blood, which was estimated by optimization to the plasma time-course data. Portals of entry included i.v. infusion (over a period of 36 seconds) into the venous blood, inhalation by diffusion from the alveolar air into the lung blood at the rate of alveolar ventilation, and oral administration via zero-order absorption from the gastrointestinal tract to the liver. Elimination of 1,4-dioxane was accomplished through pulmonary exhalation and saturable hepatic metabolism. Urinary excretion of HEAA was assumed to be instantaneous with the generation of HEAA from the hepatic metabolism of 1,4-dioxane.

The parameter values for hepatic metabolism of 1,4-dioxane, V_{max} and K_m, were optimized and validated against plasma and/or urine time course data for 1,4-dioxane and HEAA

in rats following i.v. and inhalation exposures and humans following inhalation exposure (Young et al., 1978a, b, 1977); the exact data (i.e., i.v., inhalation, or both) used for the optimization and calibration were not reported. Although the liver and fat were represented by tissue-specific compartments, no tissue-specific concentration data were available for model development, raising uncertainty as the model's ability to adequately predict exposure to these tissues. The human inhalation exposure of 50 ppm for 6 hours (Young et al., 1977) was reported to be in the linear range for metabolism; thus, uncertainty exists in the ability of the allometrically-scaled value for the human metabolic V_{max} to accurately describe 1,4-dioxane metabolism from exposures resulting in metabolic saturation. Nevertheless, these values resulted in the model producing good fits to the data. For rats, the values for V_{max} had to be adjusted upwards by a factor of 1.8 to reasonably simulate exposures greater than 300 mg/kg. The model authors attributed this to metabolic enzyme induction by high doses of 1,4-dioxane.

3.5.2.2. *Reitz et al. (1990)*

Reitz et al. (1990) developed a model for 1,4-dioxane and HEAA in the mouse, rat, and human. This model, also based on the styrene model of Ramsey and Andersen (1984), included a central blood compartment and compartments for liver, fat, and rapidly and slowly perfused tissues. Tissue volumes and blood flow rates were defined as percentages of total BW and cardiac output, respectively. Physiological parameter values were similar to those used by Andersen et al. (1987), except that flow rates for cardiac output and alveolar ventilation were doubled in order to produce a better fit of the model to human blood level data (Young et al., 1977). Portals of entry included i.v. injection into the venous blood, inhalation, oral bolus dosing, and oral dosing via drinking water. Oral absorption of 1,4-dioxane was simulated, in all three species, as a first-order transfer to liver (halftime approximately 8 minutes).

Alveolar blood levels of 1,4-dioxane were assumed to be in equilibrium with alveolar air at a ratio equal to the experimentally measured blood:air partition coefficient. Transfers of 1,4-dioxane between blood and tissues were assumed to be blood flow-limited and to achieve rapid equilibrium between blood and tissue, governed by tissue:blood equilibrium partition coefficients. These coefficients were derived by dividing experimentally measured (Leung and Paustenbach, 1990) in vitro blood:air and tissue:air partition coefficients for blood, liver, fat. Blood:air partition coefficients were measured for both humans and rats. The mouse blood:air partition coefficient was different from rat or human values; the source of the partition coefficient for blood in mice was not reported. Rat tissue:air partition coefficients were used as surrogate values for humans. Rat tissue partition coefficient values were the same values as used in the Leung and Paustenbach (1990) model (with the exception of slowly perfused tissues) and were used in the models for all three species. The liver value was used for the rapidly perfused tissues, as well as slowly perfused tissues. Although slowly perfused tissue:air partition coefficients for rats were measured, the authors suggested that 1,4-dioxane in the muscle and air

may not have reached equilibrium in the highly gelatinous tissue homogenate (Reitz et al., 1990). Substitution of the liver value provided much closer agreement to the plasma data than when the muscle value was used. Further, doubling of the measured human blood:air partition coefficient improved the fit of the model to the human blood level data compared to the fit resulting from the measured value (Reitz et al., 1990). The Reitz et al. (1990) model simulated three routes of 1,4-dioxane elimination: pulmonary exhalation, hepatic metabolism to HEAA, and urinary excretion of HEAA. The elimination of HEAA was modeled as a first-order transfer of 1,4-dioxane metabolite to urine.

Values for the metabolic rate constants, V_{max} and K_m, were optimized to achieve agreement with various observations. Reitz et al. (1990) optimized values for human V_{max} and K_m against the experimental human 1,4-dioxane inhalation data (Young et al., 1977). As noted previously, because the human exposures were below the level needed to exhibit nonlinear kinetics, uncertainty exists in the ability of the optimized value of V_{max} to simulate human 1,4-dioxane metabolism above the concentration that would result in saturation of metabolism. Rat metabolic rate constants were obtained by optimization to simulated data from a two-compartment empirical pharmacokinetic model, which was fitted to i.v. exposure data (Young et al., 1978a, b). As with the Leung and Paustenbach (1990) model, the Reitz et al. (1990) model included compartments for the liver and fat, although no tissue-specific concentration data were available to validate dosimetry for these organs. The derivations of human and rat HEAA elimination rate constants were not reported. Since no pharmacokinetics data for 1,4-dioxane in mice were available, mouse metabolic rate constants were allometrically scaled from rat and human values.

3.5.2.3. *Fisher et al. (1997)*

A PBPK model was developed by Fisher et al. (1997) to simulate a variety of volatile organic compounds (VOCs, including 1,4-dioxane) in lactating humans. This model was similar in structure to those of Leung and Paustenbach (1990) and Reitz et al. (1990) with the addition of elimination of 1,4-dioxane to breast milk. Experimental measurements were made for blood:air and milk:air partition coefficients. Other partition coefficient values were taken from Reitz et al. (1990). The model was not optimized, nor was performance tested against experimental exposure data. Thus, the ability of the model to simulate 1,4-dioxane exposure data is unknown.

3.5.3. Implementation of Published PBPK Models for 1,4-Dioxane

As previously described, several pharmacokinetic models have been developed to predict the absorption, distribution, metabolism, and elimination of 1,4-dioxane in rats and humans. Single compartment, empirical models for rats (Young et al., 1978a, b) and humans (Young et al., 1977) were developed that predict blood levels of 1,4-dioxane and urine levels of the primary metabolite, HEAA. PBPK models, which describe the kinetics of 1,4-dioxane using

biologically realistic flow rates, tissue volumes and affinities, metabolic processes, and elimination behaviors, were also developed (Fisher et al., 1997; Leung and Paustenbach, 1990; Reitz et al., 1990).

In developing updated toxicity values for 1,4-dioxane the available PBPK models were evaluated for their ability to predict observations made in experimental studies of rat and human exposures to 1,4-dioxane (Appendix B). The Reitz et al. (1990) and Leung and Paustenbach (1990) PBPK models were both developed from a PBPK model of styrene (Ramsey and Anderson, 1984), with the exception of minor differences in the use of partition coefficients and biological parameters. The model code for Leung and Paustenbach (1990) was unavailable in contrast to Reitz et al. (1990). The model of Reitz et al. (1990) was identified for further consideration to assist in the derivation of toxicity values.

Issues related to the biological plausibility of parameter values in the human model were identified. Specifically, the model is able to predict the only available human inhalation data set (50 ppm 1,4-dioxane for 6 hours; Young et al., 1977) by increasing (i.e., doubling) the parameter values for human alveolar ventilation, cardiac output, and the blood:air partition coefficient above the measured values. Furthermore, the measured value for the slowly perfused tissue:air partition coefficient (i.e., muscle) was replaced with the measured liver value to improve the fit. Analysis of the Young et al. (1977) human data suggested that the apparent volume of distribution (V_d) for 1,4-dioxane was approximately 10-fold higher in rats than humans, presumably due to species differences in tissue partitioning or other process not represented in the model. Subsequent exercising of the model demonstrated that selecting a human slowly perfused tissue:air partition coefficient much lower than the measured rat value resulted in better agreement between model predictions of 1,4-dioxane in blood and experimental observations. Based upon these observations the model (e.g., metabolism/elimination parameters) was re-calibrated using biologically plausible values for flow rates and tissue:air partition coefficients.

Appendix B describes all activities that have been conducted in the evaluation of the empirical models and re-calibration and exercising of the Reitz et al. (1990) PBPK model to determine the adequacy and preference for the potential use of the models for 1,4-dioxane

The evaluation consisted of implementation of the Young et al. (1978a, b, 1977) empirical rat and human models using the acslXtreme simulation software and re-calibration of the Reitz et al. (1990) human PBPK model. Using the model descriptions and equations given in Young et al. (1978a, b, 1977), model code was developed for the empirical models and executed, simulating the reported experimental conditions. The model output was then compared with the model output reported in Young et al. (1978a, b, 1977).

The PBPK model of Reitz et al. (1990) was re-calibrated using measured values for cardiac and alveolar flow rates and tissue:air partition coefficients. The predictions of blood and urine levels of 1,4-dioxane and HEAA, respectively, from the re-calibrated model were

compared with the empirical model predictions of the same dosimeters to determine whether the re-calibrated PBPK model could perform similarly to the empirical model. As part of the PBPK model evaluation, a sensitivity analysis was performed to identify the model parameters having the greatest influence on the primary dosimeter of interest, the blood level of 1,4-dioxane. Variability data for the experimental measurements of the tissue:air partition coefficients were incorporated to determine a range of model outputs bounded by biologically plausible values for these parameters.

The rat and human empirical models of Young et al. (1978a, b, 1977) were successfully implemented in acslXtreme and perform identically to the models reported in the published papers (Figures B-3 through B-6), with the exception of the lower predicted HEAA concentrations and early appearance of the peak HEAA levels in rat urine. The early appearance of peak HEAA levels cannot presently be explained, but may result from manipulations of k_{me} or other parameters by Young et al. (1978a, b) that were not reported. The lower predictions of HEAA levels are likely due to reliance on a standard urine volume production rate in the absence of measured (but unreported) urine volumes. While the human urinary HEAA predictions were lower than observations, this is due to parameter fitting of Young et al. (1977). No model output was published in Young et al. (1977) for comparison. The empirical models were modified to allow for user-defined inhalation exposure levels. However, no modifications were made to model oral exposures as adequate data to parameterize such modifications do not exist for rats or humans.

Several procedures were applied to the human PBPK model to determine if an adequate fit of the model to the empirical model output or experimental observations could be attained using biologically plausible values for the model parameters. The re-calibrated model predictions for blood 1,4-dioxane levels do not come within 10-fold of the experimental values using measured tissue:air partition coefficients from Leung and Paustenbach (1990) or Sweeney et al. (2008) (Figures B-8 and B-9). The utilization of a slowly perfused tissue:air partition coefficient 10-fold lower than measured values produces exposure-phase predictions that are much closer to observations, but does not replicate the elimination kinetics (Figure B-10). Recalibration of the model with upper bounds on the tissue:air partition coefficients results in predictions that are still six- to sevenfold lower than empirical model prediction or observations (Figures B-12 and B-13). Exploration of the model space using an assumption of first-order metabolism (valid for the 50 ppm inhalation exposure) showed that an adequate fit to the exposure and elimination data can be achieved only when unrealistically low values are assumed for the slowly perfused tissue:air partition coefficient (Figure B-16). Artificially low values for the other tissue:air partition coefficients are not expected to improve the model fit, as these parameters are shown in the sensitivity analysis to exert less influence on blood 1,4-dioxane than V_{maxC} and K_m. In the absence of actual measurements for the human slowly perfused tissue:air partition coefficient, high uncertainty exists for this model parameter value. Differences in the

ability of rat and human blood to bind 1,4-dioxane may contribute to the difference in V_d. However, this is expected to be evident in very different values for rat and human blood:air partition coefficients, which is not the case (Table B-1). Therefore, some other, as yet unknown, modification to model structure may be necessary.

Similarly, Sweeney et al. (2008) also evaluated the available PBPK models (Leung and Paustenbach, 1990; Reitz et al., 1990) for 1,4-dioxane. To address uncertainties and deficiencies in these models, the investigators conducted studies to fill data gaps and reduce uncertainties pertaining to the pharmacokinetics of 1,4-dioxane and HEAA in rats, mice, and humans. The following studies were performed:

Partition coefficients, including measurements for mouse blood and tissues (liver, kidney, fat, and muscle) and confirmatory measurements for human blood and rat blood and muscle.

Blood time course measurements in mice conducted for gavage administration of nominal single doses (20, 200, or 2,000 mg/kg) of 1,4-dioxane administered in water.

Metabolic rate constants for rat, mouse, and human liver based on incubations of 1,4-dioxane with rat, mouse, and human hepatocytes and measurement of HEAA.

Updated PBPK models were developed based on these new data and data from previous kinetic studies in rats, workers, and human volunteers reported by Young et al. (1978a, b, 1977, 1976). The optimized rate of metabolism for the mouse was significantly higher than the value previously estimated. The optimized rat kinetic parameters were similar to those in the 1990 models. Of the two available human studies (Young et al., 1977, 1976), model predictions were consistent with one study, but did not fit the second as well.

3.6. RAT NASAL EXPOSURE VIA DRINKING WATER

Sweeney et al. (2008) conducted a rat nasal exposure study to explore the potential for direct contact of nasal tissues with 1,4-dioxane-containing drinking water under bioassay conditions. Two groups of male Sprague Dawley rats (5/group) received drinking water in 45-mL drinking water bottles containing a fluorescent dye mixture (Cell Tracker Red/FluoSpheres). The drinking water for one of these two groups also contained 0.5% 1,4-dioxane, a concentration within the range used in chronic toxicity studies. A third group of five rats received tap water alone (controls). Water was provided to the rats overnight. The next morning, the water bottles were weighed to estimate the amounts of water consumed. Rats were sacrificed and heads were split along the midline for evaluation by fluorescence microscopy. One additional rat was dosed twice by gavage with 2 mL of drinking water containing fluorescent dye (the second dose was 30 minutes after the first dose; total of 4 mL administered) and sacrificed 5 hours later to evaluate the potential for systemic delivery of fluorescent dye to the nasal tissues.

The presence of the fluorescent dye mixture had no measurable impact on water consumption; however, 0.5% 1,4-dioxane reduced water consumption by an average of 62% of controls following a single, overnight exposure. Fluorescent dye was detected in the oral cavity and nasal airways of each animal exposed to the Cell Tracker Red/FluoSpheres mixture in their drinking water, including numerous areas of the anterior third of the nose along the nasal vestibule, maxillary turbinates, and dorsal nasoturbinates. Fluorescent dye was occasionally detected in the ethmoid turbinate region and nasopharynx. 1,4-Dioxane had no effect on the detection of the dye. Little or no fluorescence at the wavelength associated with the dye mixture was detected in control animals or in the single animal that received the dye mixture by oral gavage. The investigators concluded that the findings indicate rat nasal tissues are exposed by direct contact with drinking water under bioassay conditions.

4. HAZARD IDENTIFICATION

4.1. STUDIES IN HUMANS – EPIDEMIOLOGY, CASE REPORTS, CLINICAL CONTROLS

Case reports of acute occupational poisoning with 1,4-dioxane indicated that exposure to high concentrations resulted in liver, kidney, and central nervous system (CNS) toxicity (Johnstone, 1959; Barber, 1934). Barber (1934) described four fatal cases of hemorrhagic nephritis and centrilobular necrosis of the liver attributed to acute inhalation exposure to high (unspecified) concentrations of 1,4-dioxane. Death occurred within 5–8 days of the onset of illness. Autopsy findings suggested that the kidney toxicity may have been responsible for lethality, while the liver effects may have been compatible with recovery. Jaundice was not observed in subjects and fatty change was not apparent in the liver. Johnstone (1959) presented the fatal case of one worker exposed to high concentrations of 1,4-dioxane through both inhalation and dermal exposure for a 1 week exposure duration. Measured air concentrations in the work environment of this subject were 208–650 ppm, with a mean value of 470 ppm. Clinical signs that were observed following hospital admission included severe epigastric pain, renal failure, headache, elevation in blood pressure, agitation and restlessness, and coma. Autopsy findings revealed significant changes in the liver, kidney, and brain. These included centrilobular necrosis of the liver and hemorrhagic necrosis of the kidney cortex. Perivascular widening was observed in the brain with small foci of demyelination in several regions (e.g., cortex, basal nuclei). It was suggested that these neurological changes may have been secondary to anoxia and cerebral edema.

Several studies examined the effects of acute inhalation exposure in volunteers. In a study performed at the Pittsburgh Experimental Station of the U.S. Bureau of Mines, eye irritation and a burning sensation in the nose and throat were reported in five men exposed to 5,500 ppm of 1,4-dioxane vapor for 1 minute (Yant et al., 1930). Slight vertigo was also reported by three of these men. Exposure to 1,600 ppm of 1,4-dioxane vapor for 10 minutes resulted in similar symptoms with a reduced intensity of effect. In a study conducted by the Government Experimental Establishment at Proton, England (Fairley et al., 1934), four men were exposed to 1,000 ppm of 1,4-dioxane for 5 minutes. Odor was detected immediately and one volunteer noted a constriction in the throat. Exposure of six volunteers to 2,000 ppm for 3 minutes resulted in no symptoms of discomfort. Wirth and Klimmer (1936), of the Institute of Pharmacology, University of Wurzburg, reported slight mucous membrane irritation in the nose and throat of several human subjects exposed to concentrations greater than 280 ppm for several minutes. Exposure to approximately 1,400 ppm for several minutes caused a prickling sensation in the nose and a dry and scratchy throat. Silverman et al. (1946) exposed 12 male and 12 female subjects to varying air concentrations of 1,4-dioxane for 15 minutes. A 200 ppm

concentration was reported to be tolerable, while a concentration of 300 ppm caused irritation to the eyes, nose, and throat. The study conducted by Silverman et al. (1946) was conducted by the Department of Industrial Hygiene, Harvard School of Public Health, and was sponsored and supported by a grant from the Shell Development Company. These volunteer studies published in the 1930s and 1940s (Silverman et al., 1946; Wirth and Klimmer, 1936; Fairley et al., 1934; Yant et al., 1930) do not provide information on the human subjects research ethics procedures undertaken in these study; however, there is no evidence that the conduct of the research was fundamentally unethical or significantly deficient relative to the ethical standards prevailing at the time the research was conducted.

Young et al. (1977) exposed four healthy adult male volunteers to a 50-ppm concentration of 1,4-dioxane for 6 hours. The investigators reported that the protocol of this study was approved by a seven-member Human Research Review Committee of the Dow Chemical Company and was followed rigorously. Perception of the odor of 1,4-dioxane appeared to diminish over time, with two of the four subjects reporting inability to detect the odor at the end of the exposure period. Eye irritation was the only clinical sign reported in this study. The pharmacokinetics and metabolism of 1,4-dioxane in humans were also evaluated in this study (see Section 3.3). Clinical findings were not reported in four workers exposed in the workplace to a TWA concentration of 1.6 ppm for 7.5 hours (Young et al., 1976).

Ernstagård et al. (2006) examined the acute effects of 1,4-dioxane vapor in male and female volunteers. The study protocol was approved by the Regional Ethics Review Board in Stockholm, and performed following informed consent and according to the Helsinki declaration. In a screening study by these investigators, no self-reported symptoms (based on a visual analogue scale (VAS) that included ratings for discomfort, breathing difficulty, headache, fatigue, nausea, dizziness, or feeling of intoxication) were observed at concentrations up to 20 ppm; this concentration was selected as a tentative no-observed-adverse-effect-level (NOAEL) in the main study. In the main study, six male and six female healthy volunteers were exposed to 0 or 20 ppm 1,4-dioxane, at rest, for 2 hours. This exposure did not significantly affect symptom VAS ratings, blink frequency, pulmonary function or nasal swelling (measured before and at 0 and 3 hours after exposure), or inflammatory markers in the plasma (C-reactive protein and interleukin-6) of the volunteers. Only ratings for "solvent smell" were significantly increased during exposure.

Only two well documented epidemiology studies were available for occupational workers exposed to 1,4-dioxane (Buffler et al., 1978; Thiess et al., 1976). These studies did not provide evidence of effects in humans; however, the cohort size and number of reported cases were small.

4.1.1. Thiess et al. (1976)

A cross-sectional survey was conducted in German workers exposed to 1,4-dioxane. The study evaluated health effects in 74 workers, including 24 who were still actively employed in 1,4-dioxane production at the time of the investigation, 23 previously exposed workers who were still employed by the manufacturer, and 27 retired or deceased workers. The actively employed workers were between 32 and 62 years of age and had been employed in 1,4-dioxane production for 5–41 years. Former workers (age range not given) had been exposed to 1,4-dioxane for 3–38 years and retirees (age range not given) had been exposed for 12–41 years. Air concentrations in the plant at the time of the study were 0.06–0.69 ppm. A simulation of previous exposure conditions (prior to 1969) resulted in air measurements between 0.06 and 7.2 ppm.

Active and previously employed workers underwent a thorough clinical examination and X-ray, and hematological and serum biochemistry parameters were evaluated. The examination did not indicate pathological findings for any of the workers and no indication of malignant disease was noted. Hematology results were generally normal. Serum transaminase levels were elevated in 16 of the 47 workers studied; however, this finding was consistent with chronic consumption of more than 80 g of alcohol per day, as reported for these workers. No liver enlargement or jaundice was found. Renal function tests and urinalysis were normal in exposed workers. Medical records of the 27 retired workers (15 living at the time of the study) were reviewed. No symptoms of liver or kidney disease were reported and no cancer was detected. Medical reasons for retirement did not appear related to 1,4-dioxane exposure (e.g., emphysema, arthritis).

Chromosome analysis was performed on six actively employed workers and six control persons (not characterized). Lymphocyte cultures were prepared and chromosomal aberrations were evaluated. No differences were noted in the percent of cells with gaps or other chromosome aberrations. Mortality statistics were calculated for 74 workers of different ages and varying exposure periods. The proportional contribution of each of the exposed workers to the total time of observation was calculated as the sum of man-years per 10-year age group. Each person contributed one man-year per calendar year to the specific age group in which he was included at the time. The expected number of deaths for this population was calculated from the age-specific mortality statistics for the German Federal Republic for the years 1970–1973. From the total of 1,840.5 person-years, 14.5 deaths were expected; however, only 12 deaths were observed in exposed workers between 1964 and 1974. Two cases of cancer were reported, including one case of lamellar epithelial carcinoma and one case of myelofibrotic leukemia. These cancers were not considered to be the cause of death in these cases and other severe illnesses were present. Standardized mortality ratios (SMRs) for cancer did not significantly

differ from the control population (SMR for overall population = 0.83; SMR for 65–75-year-old men = 1.61; confidence intervals (CIs) not provided).

4.1.2. Buffler et al. (1978)

Buffler et al. (1978) conducted a mortality study on workers exposed to 1,4-dioxane at a chemical manufacturing facility in Texas. 1,4-Dioxane exposure was known to occur in a manufacturing area and in a processing unit located 5 miles from the manufacturing plant. Employees who worked between April 1, 1954, and June 30, 1975, were separated into two cohorts based on at least 1 month of exposure in either the manufacturing plant (100 workers) or the processing area (65 workers). Company records and follow-up techniques were used to compile information on name, date of birth, gender, ethnicity, job assignment and duration, and employment status at the time of the study. Date and cause of death were obtained from copies of death certificates and autopsy reports (if available). Exposure levels for each job category were estimated using the 1974 Threshold Limit Value for 1,4-dioxane (i.e., 50 ppm) and information from area and personal monitoring. Exposure levels were classified as low (<25 ppm), intermediate (50–75 ppm), and high (>75 ppm). Monitoring was not conducted prior to 1968 in the manufacturing areas or prior to 1974 in the processing area; however, the study authors assumed that exposures would be comparable, considering that little change had been made to the physical plant or the manufacturing process during that time. Exposure to 1,4-dioxane was estimated to be below 25 ppm for all individuals in both cohorts. Manufacturing area workers were exposed to several other additional chemicals and processing area workers were exposed to vinyl chloride.

Seven deaths were identified in the manufacturing cohort and five deaths were noted for the processing cohort. The average exposure duration was not greater for those workers who died, as compared to those still living at the time of the study. Cancer was the underlying cause of death for two cases from the manufacturing area (carcinoma of the stomach, alveolar cell carcinoma) and one case from the processing area (malignant mediastinal tumor). The workers from the manufacturing area were exposed for 28 or 38 months and both had a positive smoking history (>1 pack/day). Smoking history was not available for processing area workers. The single case of cancer in this area occurred in a 21-year-old worker exposed to 1,4-dioxane for 1 year. The mortality data for both industrial cohorts were compared to age-race-sex specific death rates for Texas (1960–1969). Person-years of observation contributed by workers were determined over five age ranges with each worker contributing one person-year for each year of observation in a specific age group. The expected number of deaths was determined by applying the Texas 1960–1969 death rate statistics to the number of person years calculated for each cohort. The observed and expected number of deaths for overall mortality (i.e., all causes) was comparable for both the manufacturing area (7 observed versus 4.9 expected) and the processing area (5 observed versus 4.9 expected). No significant excess in cancer-related deaths was

identified for both areas of the facility combined (3 observed versus 1.7 expected). A separate analysis was performed to evaluate mortality in manufacturing area workers exposed to 1,4-dioxane for more than 2 years. Six deaths occurred in this group as compared to 4.1 expected deaths. The use of a conditional Poisson distribution indicated no apparent excess in mortality or death due to malignant neoplasms in this study. It is important to note that the cohorts evaluated were limited in size. In addition, the mean exposure duration was less than 5 years (<2 years for 43% of workers) and the latency period for evaluation was less than 10 years for 59% of workers. The study authors recommended a follow-up investigation to allow for a longer latency period; however, no follow-up study of these workers has been published.

4.2. SUBCHRONIC AND CHRONIC STUDIES AND CANCER BIOASSAYS IN ANIMALS - ORAL AND INHALATION

The majority of the subchronic (>30 days) and chronic (>1 year) studies conducted for 1,4-dioxane were oral drinking water studies. Longer-term inhalation studies consisted of only one subchronic study (Fairley et al., 1934) and one chronic study (Torkelson et al., 1974). These studies were not sufficient to characterize the inhalation risks of 1,4-dioxane (see Section 4.2.2.).

4.2.1. Oral Toxicity

4.2.1.1. *Subchronic Oral Toxicity*

Six rats and six mice (unspecified strains) were given drinking water containing 1.25% 1,4-dioxane for up to 67 days (Fairley et al. 1934). Using reference BWs and drinking water ingestion rates for rats and mice (U.S. EPA, 1988), it can be estimated that these rats and mice received doses of approximately 1,900 and 3,300 mg/kg-day, respectively. Gross pathology and histopathology were evaluated in all animals. Five of the six rats in the study died or were sacrificed in extremis prior to day 34 of the study. Mortality was lower in mice, with five of six mice surviving up to 60 days. Kidney enlargement was noted in 5/6 rats and 2/5 mice. Renal cortical degeneration was observed in all rats and 3/6 mice. Large areas of necrosis were observed in the cortex, while cell degeneration in the medulla was slight or absent. Tubular casts were observed and vascular congestion and hemorrhage were present throughout the kidney. Hepatocellular degeneration with vascular congestion was also noted in five rats and three mice. EPA identified the tested doses of 1,900 mg/kg-day in rats and 3,300 mg/kg-day in mice as the lowest-observed-adverse-effect-levels (LOAELs) for liver and kidney degeneration in this study.

4.2.1.1.1. *Stoner et al. (1986).* 1,4-dioxane was evaluated for its ability to induce lung adenoma formation in A/J mice. Six- to 8-week-old male and female A/J mice (16/sex/group) were given 1,4-dioxane by gavage or i.p. injection, 3 times/week for 8 weeks. Total cumulative dose levels were given as 24,000 mg/kg (oral), and 4,800, 12,000, or 24,000 mg/kg (i.p.). Average daily

dose estimates were calculated to be 430 mg/kg-day (oral), and 86, 210, or 430 mg/kg-day (i.p.) by assuming an exposure duration of 56 days. The authors indicated that i.p. doses represent the maximum tolerated dose (MTD), 0.5 times the MTD, and 0.2 times the MTD. Mice were killed 24 weeks after initiation of the bioassay, and lungs, liver, kidney, spleen, intestines, stomach, thymus, salivary, and endocrine glands were examined for gross lesions. Histopathology examination was performed if gross lesions were detected. 1,4-Dioxane did not induce lung tumors in male or female A/J mice in this study.

4.2.1.1.2. ***Stott et al. (1981).*** Male Sprague Dawley rats (4–6/group) were given average doses of 0, 10, or 1,000 mg/kg-day 1,4-dioxane (>99% pure) in their drinking water, 7 days/week for 11 weeks. It should noted that the methods description in this report stated that the high dose was 100 mg/kg-day, while the abstract, results, and discussion sections indicated that the high dose was 1,000 mg/kg-day. Rats were implanted with a [$^{6\text{-}3}$H]thymidine loaded osmotic pump 7 days prior to sacrifice. Animals were sacrificed by cervical dislocation and livers were removed, weighed, and prepared for histopathology evaluation. [^{3}H]-Thymidine incorporation was measured by liquid scintillation spectroscopy.

An increase in the liver to BW ratio was observed in rats from the high dose group (assumed to be 1,000 mg/kg-day). Histopathological alterations, characterized as minimal centrilobular swelling, were also seen in rats from this dose group (incidence values were not reported). Hepatic DNA synthesis, measured by [^{3}H]-thymidine incorporation, was increased 1.5-fold in high-dose rats. No changes relative to control were observed for rats exposed to 10 mg/kg-day. EPA found a NOAEL value of 10 mg/kg-day and a LOAEL value of 1,000 mg/kg-day for this study based on histopathological changes in the liver.

Stott et al. (1981) also performed several acute experiments designed to evaluate potential mechanisms for the carcinogenicity of 1,4-dioxane. These experiments are discussed separately in Section 4.5.2 (Mechanistic Studies).

4.2.1.1.3. ***Kano et al. (2008).*** Groups of 6-week-old F344/DuCrj rats (10/sex/group) and Crj:BDF$_1$ mice (10/sex/group) were administered 1,4-dioxane (>99% pure) in the drinking water for 13 weeks. The animals were observed daily for clinical signs of toxicity. Food consumption and BWs were measured once per week and water consumption was measured twice weekly. Food and water were available ad libitum. The concentrations of 1,4-dioxane in the water for rats and mice were 0, 640, 1,600, 4,000, 10,000, or 25,000 ppm. The investigators used data from water consumption and BW changes to calculate a daily intake of 1,4-dioxane by the male and female animals. Thus, male rats received doses of approximately 0, 52, 126, 274, 657, and 1,554 mg 1,4-dioxane/kg-day and female rats received 0, 83, 185, 427, 756, and 1,614 mg/kg-day. Male mice received 0, 86, 231, 585, 882, or 1,570 mg/kg-day and female mice received 0, 170, 387, 898, 1,620, or 2,669 mg/kg-day.

No information was provided as to when the blood and urine samples were collected. Hematology analysis included red blood cell (RBC) count, hemoglobin, hematocrit, mean corpuscular volume (MCV), platelet count, white blood cell (WBC) count, and differential WBCs. Serum biochemistry included total protein, albumin, bilirubin, glucose, cholesterol, triglyceride (rat only), alanine aminotransferase (ALT), aspartate aminotransferase (AST), lactate dehydrogenase (LDH), leucine aminopeptidase (LAP), alkaline phosphatase (ALP), creatinine phosphokinase (CPK) (rat only), urea nitrogen, creatinine (rat only), sodium, potassium, chloride, calcium (rat only), and inorganic phosphorous (rat only). Urinalysis parameters were pH, protein, glucose, ketone body, bilirubin (rat only), occult blood, and urobilinogen. Organ weights (brain, lung, liver, spleen, heart, adrenal, testis, ovary, and thymus) were measured, and gross necropsy and histopathologic examination of tissues and organs were performed on all animals (skin, nasal cavity, trachea, lungs, bone marrow, lymph nodes, thymus, spleen, heart, tongue, salivary glands, esophagus, stomach, small and large intestine, liver, pancreas, kidney, urinary bladder, pituitary thyroid adrenal, testes, epididymis, seminal vesicle, prostate, ovary, uterus, vagina, mammary gland, brain, spinal cord, sciatic nerve, eye, Harderian gland, muscle, bone, and parathyroid). Dunnett's test and χ^2 test were used to assess the statistical significance of changes in continuous and discrete variables, respectively.

Clinical signs of toxicity in rats were not discussed in the study report. One female rat in the high dose group (1,614 mg/kg-day) group died, but cause and time of death were not specified. Final BWs were reduced at the two highest dose levels in females (12 and 21%) and males (7 and 21%), respectively. Food consumption was reduced 13% in females at 1,614 mg/kg-day and 8% in 1,554 mg/kg-day males. A dose-related decrease in water consumption was observed in male rats starting at 52 mg/kg-day (15%) and in females starting at 185 mg/kg-day (12%). Increases in RBCs, hemoglobin, hematocrit, and neutrophils, and a decrease in lymphocytes were observed in males at 1554 mg/kg-day. In females, MCV was decreased at doses ≥ 756 mg/kg and platelets were decreased at 1,614 mg/kg-day. With the exception of the 30% increase in neutrophils in high-dose male rats, hematological changes were within 2–15% of control values. Total serum protein and albumin were significantly decreased in males at doses ≥ 274 mg/kg-day and in females at doses ≥ 427 mg/kg-day. Additional changes in high-dose male and female rats included decreases in glucose, total cholesterol, triglycerides, and sodium (and calcium in females), and increases in ALT (males only), AST, ALP, and LAP. Serum biochemistry parameters in treated rats did not differ more than twofold from control values. Urine pH was decreased in males at ≥ 274 mg/kg-day and in females at ≥ 756 mg/kg-day.

Kidney weights were increased in females at ≥185 mg/kg-day with a maximum increase of 15% and 44% at 1,614 mg/kg-day for absolute and relative kidney weight, respectively. No organ weight changes were noted in male rats. Histopathology findings in rats that were related to exposure included nuclear enlargement of the respiratory epithelium, nuclear enlargement of

the olfactory epithelium, nuclear enlargement of the tracheal epithelium, hepatocyte swelling of the centrilobular area of the liver, vacuolar changes in the liver, granular changes in the liver, single cell necrosis in the liver, nuclear enlargement of the proximal tubule of the kidneys, hydropic changes in the proximal tubule of the kidneys, and vacuolar changes in the brain. The incidence data for histopathological lesions in rats are presented in Table 4-1. The effects that occurred at the lowest doses were nuclear enlargement of the respiratory epithelium in the nasal cavity and hepatocyte swelling in the central area of the liver in male rats. Based on these histopathological findings the study authors identified the LOAEL as 126 mg/kg-day and the NOAEL as 52 mg/kg-day.

Table 4-1. Incidence of histopathological lesions in F344/DuCrj rats exposed to 1,4-dioxane in drinking water for 13 weeks

Effect	Male dose (mg/kg-day)[a]					
	0	**52**	**126**	**274**	**657**	**1,554**
Nuclear enlargement; nasal respiratory epithelium	0/10	0/10	9/10[b]	10/10[b]	9/10[b]	10/10[b]
Nuclear enlargement; nasal olfactory epithelium	0/10	0/10	0/10	10/10[b]	9/10[b]	10/10[b]
Nuclear enlargement; tracheal epithelium	0/10	0/10	0/10	10/10[b]	10/10[b]	10/10[b]
Hepatocyte swelling	0/10	0/10	9/10[b]	10/10[b]	10/10[b]	10/10[b]
Vacuolic change; liver	0/10	0/10	0/10	0/10	10/10[b]	10/10[b]
Granular change; liver	0/10	0/10	0/10	5/10[c]	2/10	10/10[b]
Single cell necrosis; liver	0/10	0/10	0/10	5/10[c]	2/10	10/10[b]
Nuclear enlargement; renal proximal tubule	0/10	0/10	0/10	1/10	5/10[c]	9/10[b]
Hydropic change; renal proximal tubule	0/10	0/10	0/10	0/10	0/10	7/10[b]
Vacuolic change; brain	0/10	0/10	0/10	0/10	0/10	10/10[b]
	Female dose (mg/kg-day)[a]					
	0	**83**	**185**	**427**	**756**	**1,614**
Nuclear enlargement; nasal respiratory epithelium	0/10	0/10	5/10[c]	10/10[b]	10/10[b]	8/9[b]
Nuclear enlargement; nasal olfactory epithelium	0/10	0/10	0/10	9/10[b]	10/10[b]	8/9[b]
Nuclear enlargement; tracheal epithelium	0/10	0/10	0/10	9/10[b]	10/10[b]	9/9[b]
Hepatocyte swelling	0/10	0/10	0/10	0/10	9/10[b]	9/9[b]
Vacuolic change; liver	0/10	0/10	0/10	0/10	0/10	9/9[b]
Granular change; liver	2/10	0/10	1/10	5/10[c]	5/10[c]	8/9[b]
Single cell necrosis; liver	2/10	0/10	1/10	5/10	5/10	8/9[b]
Nuclear enlargement; proximal tubule	0/10	0/10	0/10	0/10	8/10[b]	9/9[b]
Hydropic change; proximal tubule	0/10	0/10	0/10	0/10	0/10	5/9[c]
Vacuolic change; brain	0/10	0/10	0/10	0/10	0/10	9/9[b]

[a]Data are presented for sacrificed animals.
[b]$p \leq 0.01$ by χ^2 test.
[c]$p \leq 0.05$.

Source: Kano et al. (2008).

Clinical signs of toxicity in mice were not discussed in the study report One male mouse in the high-dose group (1,570 mg/kg-day) died, but no information was provided regarding cause or time of death. Final BWs were decreased 29% in male mice at 1,570 mg/kg-day, but changed less than 10% relative to controls in the other male dose groups and in female mice. Food consumption was not significantly reduced in any exposure group. Water consumption was reduced 14–18% in male mice exposed to 86, 231, or 585 mg/kg-day. Water consumption was further decreased by 48 and 70% in male mice exposed to 882 and 1,570 mg/kg-day, respectively. Water consumption was also decreased 31 and 57% in female mice treated with 1,620 and 2,669 mg/kg-day, respectively. An increase in MCV was observed in the two highest dose groups in both male (882 and 1,570 mg/kg-day) and female mice (1,620 and 2,669 mg/kg-day). Increases in RBCs, hemoglobin, and hematocrit were also observed in high dose males (1570 mg/kg-day). Hematological changes were within 2–15% of control values. Serum biochemistry changes in exposed mice included decreased total protein (at 1,570 mg/kg-day in males, ≥1,620 mg/kg-day in females), decreased glucose (at 1,570 mg/kg-day in males, ≥1,620 mg/kg-day in females), decreased albumin (at 1,570 mg/kg-day in males, 2,669 mg/ kg-day in females), decreased total cholesterol (≥ 585 mg/kg-day in males, ≥1,620 mg/kg-day in females), increased serum ALT (at 1,570 mg/kg-day in males, ≥ 620 mg/kg-day in females), increased AST (at 1,570 mg/kg-day in males, 2,669 mg/kg-day in females), increased ALP (≥ 585 mg/kg-day in males, 2,669 mg/kg-day in females), and increased LDH (in females only at doses ≥ 1,620 mg/kg-day). With the exception of a threefold increase in ALT in male and female mice, serum biochemistry parameters in treated rats did not differ more than twofold from control values. Urinary pH was decreased in males at ≥ 882 mg/kg-day and in females at ≥ 1,620 mg/kg-day.

Absolute and relative lung weights were increased in males at 1,570 mg/kg-day and in females at 1,620 and 2,669 mg/kg-day. Absolute kidney weights were also increased in females at 1,620 and 2,669 mg/kg-day and relative kidney weight was elevated at 2,669 mg/kg-day. Histopathology findings in mice that were related to exposure included nuclear enlargement of the respiratory epithelium, nuclear enlargement of the olfactory epithelium, eosinophilic change in the olfactory epithelium, vacuolic change in the olfactory nerve, nuclear enlargement of the tracheal epithelium, accumulation of foamy cells in the lung and bronchi, nuclear enlargement and degeneration of the bronchial epithelium, hepatocyte swelling of the centrilobular area of the liver, and single cell necrosis in the liver. The incidence data for histopathological lesions in mice are presented in Table 4-2. Based on the changes in the bronchial epithelium in female mice, the authors identified the dose level of 387 mg/kg-day as the LOAEL for mice; the NOAEL was 170 mg/kg-day (Kano et al., 2008).

Table 4-2. Incidence of histopathological lesions in Crj:BDF$_1$ mice exposed to 1,4-dioxane in drinking water for 13 weeks

Effect	Male dose (mg/kg-day)[a]					
	0	**86**	**231**	**585**	**882**	**1,570**
Nuclear enlargement; nasal respiratory epithelium	0/10	0/10	0/10	2/10	5/10[b]	0/9
Eosinophilic change; nasal respiratory epithelium	0/10	0/10	0/10	0/10	0/10	5/9[b]
Nuclear enlargement; nasal olfactory epithelium	0/10	0/10	0/10	9/10[c]	10/10[c]	9/9[c]
Eosinophilic change; nasal olfactory epithelium	0/10	0/10	0/10	0/10	0/10	6/9[c]
Vacuolic change; olfactory nerve	0/10	0/10	0/10	0/10	0/10	9/9[c]
Nuclear enlargement; tracheal epithelium	0/10	0/10	0/10	7/10[c]	9/10[c]	9/9[c]
Accumulation of foamy cells; lung/bronchi	0/10	0/10	0/10	0/10	0/10	6/9[c]
Nuclear enlargement; bronchial epithelium	0/10	0/10	0/10	9/10[c]	9/10[c]	9/9[c]
Degeneration; bronchial epithelium	0/10	0/10	0/10	0/10	0/10	8/9[c]
Hepatocyte swelling	0/10	0/10	0/10	10/10[c]	10/10[c]	9/9[c]
Single cell necrosis; liver	0/10	0/10	0/10	5/10[b]	10/10[c]	9/9[c]
	Female dose (mg/kg-day)[a]					
	0	**170**	**387**	**898**	**1,620**	**2,669**
Nuclear enlargement; nasal respiratory epithelium	0/10	0/10	0/10	3/10	3/10	7/10[c]
Eosinophilic change; nasal respiratory epithelium	0/10	0/10	1/10	1/10	5/10[b]	9/10[c]
Nuclear enlargement; nasal olfactory epithelium	0/10	0/10	0/10	6/10[b]	10/10[c]	10/10[c]
Eosinophilic change; nasal olfactory epithelium	0/10	0/10	0/10	1/10[c]	6/10[b]	6/10[b]
Vacuolic change; olfactory nerve	0/10	0/10	0/10	0/10	2/10	8/10[c]
Nuclear enlargement; tracheal epithelium	0/10	0/10	2/10	9/10[c]	10/10[c]	10/10[c]
Accumulation of foamy cells; lung/bronchi	0/10	0/10	0/10	0/10	10/10[c]	10/10[c]
Nuclear enlargement; bronchial epithelium	0/10	0/10	10/10[c]	10/10[c]	10/10[c]	10/10[c]
Degeneration; bronchial epithelium	0/10	0/10	0/10	0/10	7/10[c]	10/10[c]
Hepatocyte swelling	0/10	1/10	1/10	10/10[c]	10/10[c]	9/10[b]
Single cell necrosis; liver	0/10	0/10	0/10	7/10[c]	10/10[c]	9/10[c]

[a]Data are presented for sacrificed animals.
[b]$p \leq 0.01$ by χ^2 test.
[c]$p \leq 0.05$.

Source: Kano et al (2008).

4.2.1.1.4. ***Yamamoto et al. (1998a, b).*** Studies in rasH2 transgenic mice carrying the human prototype c-Ha-ras gene have been investigated as a bioassay model for rapid carcinogenicity testing. As part of validation studies of this model, 1,4-dioxane was one of many chemicals that were evaluated. RasH2 transgenic mice were F1 offspring of transgenic male C57BLr6J and normal female BALBrcByJ mice. CB6F$_1$ mice were used as a nontransgenic control. Seven- to nine-week-old mice (10–15/group) were exposed to 0, 0.5, or 1% 1,4-dioxane in drinking water for 26 weeks. An increase in lung adenomas was observed in treated transgenic mice, as

compared to treated nontransgenic mice. The tumor incidence in transgenic animals, however, was not greater than that observed in vehicle-treated transgenic mouse controls. Further study details were not provided.

4.2.1.2. *Chronic Oral Toxicity and Carcinogenicity*

4.2.1.2.1. ***Argus et al. (1965).*** Twenty-six adult male Wistar rats weighing between 150 and 200 g were exposed to 1,4-dioxane (purity not reported) in the drinking water at a concentration of 1% for 64.5 weeks. A group of nine untreated rats served as control. Food and water were available ad libitum. The drinking water intake for treated animals was reported to be 30 mL/day, resulting in a dose/rat of 300 mg/day. Using a reference BW of 0.462 kg for chronic exposure to male Wistar rats (U.S. EPA, 1988), it can be estimated that these rats received daily doses of approximately 640 mg/kg-day. All animals that died or were killed during the study underwent a complete necropsy. A list of specific tissues examined microscopically was not provided; however, it is apparent that the liver, kidneys, lungs, lymphatic tissue, and spleen were examined. No statistical analysis of the results was conducted.

Six of the 26 treated rats developed hepatocellular carcinomas, and these rats had been treated for an average of 452 days (range, 448–455 days). No liver tumors were observed in control rats. In two rats that died after 21.5 weeks of treatment, histological changes appeared to involve the entire liver. Groups of cells were found that had enlarged hyperchromic nuclei. Rats that died or were killed at longer intervals showed similar changes, in addition to large cells with reduced cytoplasmic basophilia. Animals killed after 60 weeks of treatment showed small neoplastic nodules or multifocal hepatocellular carcinomas. No cirrhosis was observed in this study. Many rats had extensive changes in the kidneys often resembling glomerulonephritis, however, incidence data was not reported for these findings. This effect progressed from increased cellularity to thickening of the glomerular capsule followed by obliteration of the glomeruli. One treated rat had an early transitional cell carcinoma in the kidney's pelvis; this rat also had a large tumor in the liver. The lungs from many treated and control rats (incidence not reported) showed severe bronchitis with epithelial hyperplasia and marked peribronchial infiltration, as well as multiple abscesses. One rat treated with 1,4-dioxane developed leukemia with infiltration of all organs, particularly the liver and spleen, with large, round, isolated neoplastic cells. In the liver, the distribution of cells in the sinusoids was suggestive of myeloid leukemia. The dose of 640 mg/kg-day tested in this study was a free-standing LOAEL, identified by EPA, for glomerulonephritis in the kidney and histological changes in the liver (hepatocytes with enlarged hyperchromic nuclei, large cells with reduced cytoplasmic basophilia).

4.2.1.2.2. ***Argus et al. (1973); Hoch-Ligeti et al. (1970).*** Groups of 2–3-month-old male Sprague Dawley rats (28–32/dose group) weighing 110–230 g at the beginning of the experiment

were administered 1,4-dioxane (purity not reported) in the drinking water for up to 13 months at concentrations of 0, 0.75, 1.0, 1.4, or 1.8%. The drinking water intake was determined for each group over a 3-day measurement period conducted at the beginning of the study and twice during the study (weeks were not specified). The rats were killed with ether at 16 months or earlier if nasal tumors were clearly observable. Complete autopsies were apparently performed on all animals, but only data from the nasal cavity and liver were presented and discussed. The nasal cavity was studied histologically only from rats in which gross tumors in these locations were present; therefore, early tumors may have been missed and pre-neoplastic changes were not studied. No statistical analysis of the results was conducted. Assuming a BW of 0.523 kg for an adult male Sprague Dawley rat (U.S. EPA, 1988) and a drinking water intake of 30 mL/day as reported by the study authors, dose estimates were 0, 430, 574, 803, and 1,032 mg/kg-day. The progression of liver tumorigenesis was evaluated by an additional group of 10 male rats administered 1% 1,4-dioxane in the drinking water (574 mg/kg-day), 5 of which were sacrificed after 8 months of treatment and 5 were killed after 13 months of treatment. Liver tissue from these rats and control rats was processed for electron microscopy examination.

Nasal cavity tumors were observed upon gross examination in six rats (one rat in the 0.75% group, one in the 1.0% group, two in the 1.4% group, and two in the 1.8% group). Gross observation showed the tumors visible either at the tip of the nose, bulging out of the nasal cavity, or on the back of the nose covered by intact or later ulcerated skin. As the tumors obstructed the nasal passages, the rats had difficulty breathing and lost weight rapidly. No neurological signs or compression of the brain were observed. In all cases, the tumors were squamous cell carcinomas with marked keratinization and formation of keratin pearls. Bony structure was extensively destroyed in some animals with tumors, but there was no invasion into the brain. In addition to the squamous carcinoma, two adenocarcinomatous areas were present. One control rat had a small, firm, well-circumscribed tumor on the back of the nose, which proved to be subcutaneous fibroma. The latency period for tumor onset was 329–487 days. Evaluation of the latent periods and doses received did not suggest an inverse relationship between these two parameters.

Argus et al. (1973) studied the progression of liver tumorigenesis by electron microscopy of liver tissues obtained following interim sacrifice at 8 and 13 months of exposure (5 rats/group, 574 mg/kg-day). The first change observed in the liver was an increase in the size of the nucleus of the hepatocytes, mostly in the periportal area. Precancerous changes were characterized by disorganization of the rough endoplasmic reticulum, an increase in smooth endoplasmic reticulum, and a decrease in glycogen and increase in lipid droplets in hepatocytes. These changes increased in severity in the hepatocellular carcinomas in rats exposed to 1,4-dioxane for 13 months.

Three types of liver nodules were observed in exposed rats at 13–16 months. The first consisted of groups of cells with reduced cytoplasmic basophilia and a slightly nodular

appearance as viewed by light microscopy. The second type of circumscribed nodule was described consisting of large cells, apparently filled and distended with fat. The third type of nodule was described as finger-like strands, 2–3 cells thick, of smaller hepatocytes with large hyperchromic nuclei and dense cytoplasm. This third type of nodule was designated as an incipient hepatoma, since it showed all the histological characteristics of a fully developed hepatoma. All three types of nodules were generally present in the same liver. Cirrhosis of the liver was not observed. The numbers of incipient liver tumors and hepatomas in rats from this study (treated for 13 months and observed at 13–16 months) are presented in Table 4-3.

Table 4-3. Number of incipient liver tumors and hepatomas in male Sprague- Dawley rats exposed to 1,4-dioxane in drinking water for 13 months

Dose (mg/kg-day)[a]	Incipient tumors	Hepatomas	Total
430	4	0	4
574	9	0	9
803	13	3	16
1,032	11	12	23

[a]Precise incidences cannot be calculated since the number of rats per group was reported as 28–32; incidence in control rats was not reported; no statistical analysis of the results was conducted in the study.

Source: Argus et al. (1973).

Treatment with all dose levels of 1,4-dioxane induced marked kidney alterations, but quantitative incidence data were not provided. Qualitatively, the changes indicated glomerulonephritis and pyelonephritis, with characteristic epithelial proliferation of Bowman's capsule, periglomerular fibrosis, and distension of tubules. No kidney tumors were found. No tumors were found in the lungs. One rat at the 1.4% treatment level showed early peripheral adenomatous change of the alveolar epithelium and another rat in the same group showed papillary hyperplasia of the bronchial epithelium. The lowest dose tested (430 mg/kg-day) was considered a LOAEL by EPA for hepatic and renal effects in this study.

4.2.1.2.3. *Hoch-Ligeti and Argus (1970).* Hoch-Ligeti and Argus (1970) provided a brief account of the results of exposure of guinea pigs to 1,4-dioxane. A group of 22 male guinea pigs (neither strain nor age provided) was administered 1,4-dioxane (purity not provided) in the drinking water for at least 23 months and possibly up to 28 months. The authors stated that the concentration of 1,4-dioxane was regulated so that normal growth of the guinea pigs was maintained, and varied 0.5–2% (no further information provided). The investigators further stated that the amount of 1,4-dioxane received by the guinea pigs over a 23-month period was 588–635 g. Using a reference BW of 0.89 kg for male guinea pigs in a chronic study (U.S. EPA, 1988) and assuming an exposure period of 700 days (23 months), the guinea pigs received doses

between 944 and 1,019 mg 1,4-dioxane/kg-day. A group of ten untreated guinea pigs served as controls. All animals were sacrificed within 28 months, but the scope of the postmortem examination was not provided.

Nine treated guinea pigs showed peri- or intrabronchial epithelial hyperplasia and nodular mononuclear infiltration in the lungs. Also, two guinea pigs had carcinoma of the gallbladder, three had early hepatomas, and one had an adenoma of the kidney. Among the controls, four guinea pigs had peripheral mononuclear cell accumulation in the lungs, and only one had hyperplasia of the bronchial epithelium. One control had formation of bone in the bronchus. No further information was presented in the brief narrative of this study. Given the limited reporting of the results, a NOAEL or LOAEL value was not provided for this study.

4.2.1.2.4. ***Kociba et al. (1974).*** Groups of 6–8-week-old Sherman rats (60/sex/dose level) were administered 1,4-dioxane (purity not reported) in the drinking water at levels of 0 (controls), 0.01, 0.1, or 1.0% for up to 716 days. The drinking water was prepared twice weekly during the first year of the study and weekly during the second year of the study. Water samples were collected periodically and analyzed for 1,4-dioxane content by routine gas liquid chromatography. Food and water were available ad libitum. Rats were observed daily for clinical signs of toxicity, and BWs were measured twice weekly during the first month, weekly during months 2–7, and biweekly thereafter. Water consumption was recorded at three different time periods during the study: days 1–113, 114–198, and 446–460. Blood samples were collected from a minimum of five male and five female control and high-dose rats during the 4th, 6th, 12th, and 18th months of the study and at termination. Each sample was analyzed for packed cell volume, total erythrocyte count, hemoglobin, and total and differential WBC counts. Additional endpoints evaluated included organ weights (brain, liver, kidney, testes, spleen, and heart) and gross and microscopic examination of major tissues and organs (brain, bone and bone marrow, ovaries, pituitary, uterus, mesenteric lymph nodes, heart, liver, pancreas, spleen, stomach, prostate, colon, trachea, duodenum, kidneys, esophagus, jejunum, testes, lungs, spinal cord, adrenals, thyroid, parathyroid, nasal turbinates, and urinary bladder). The number of rats with tumors, hepatic tumors, hepatocellular carcinomas, and nasal carcinomas were analyzed for statistical significance with Fisher's Exact test (one-tailed), comparing each treatment group against the respective control group. Survival rates were compared using χ^2 Contingency Tables and Fisher's Exact test. Student's t test was used to compare hematological parameters, body and organ weights, and water consumption of each treatment group with the respective control group.

Male and female rats in the high-dose group (1% in drinking water) consumed slightly less water than controls. BW gain was depressed in the high-dose groups relative to the other groups almost from the beginning of the study (food consumption data were not provided). Based on water consumption and BW data for specific exposure groups, Kociba et al. (1974)

calculated mean daily doses of 9.6, 94, and 1,015 mg/kg-day for male rats and 19, 148, and 1,599 mg/kg-day for female rats during days 114–198 for the 0.01, 0.1, and 1.0% concentration levels, respectively. Treatment with 1,4-dioxane significantly increased mortality among high-dose males and females beginning at about 2–4 months of treatment. These rats showed degenerative changes in both the liver and kidneys. From the 5th month on, mortality rates of control and treated groups were essentially the same. There were no treatment-related alterations in hematological parameters. At termination, the only alteration in organ weights noted by the authors was a significant increase in absolute and relative liver weights in male and female high-dose rats (data not shown). Histopathological lesions were restricted to the liver and kidney from the mid- and high-dose groups and consisted of variable degrees of renal tubular epithelial and hepatocellular degeneration and necrosis (no quantitative incidence data were provided). Rats from these groups also showed evidence of hepatic regeneration, as indicated by hepatocellular hyperplastic nodule formation and evidence of renal tubular epithelial regenerative activity (observed after 2 years of exposure). These changes were not seen in controls or in low-dose rats. The authors determined a LOAEL of 94 mg/kg-day based on the liver and kidney effects in male rats. The corresponding NOAEL value was 9.6 mg/kg-day.

Histopathological examination of all the rats in the study revealed a total of 132 tumors in 114 rats. Treatment with 1% 1,4-dioxane in the drinking water resulted in a significant increase in the incidence of hepatic tumors (hepatocellular carcinomas in six males and four females). In addition, nasal carcinomas (squamous cell carcinoma of the nasal turbinates) occurred in one high-dose male and two high-dose females. Since 128 out of 132 tumors occurred in rats from the 12th to the 24th month, Kociba et al. (1974) assumed that the effective number of rats was the number surviving at 12 months, which was also when the first hepatic tumor was noticed. The incidences of liver and nasal tumors from Kociba et al. (1974) are presented in Table 4-4. Tumors in other organs were not elevated when compared to control incidence and did not appear to be related to 1,4-dioxane administration.

Table 4-4. Incidence of liver and nasal tumors in male and female Sherman rats (combined) treated with 1,4-dioxane in the drinking water for 2 years

Dose in mg/kg-day (average of male and female dose)	Effective number of animals[a]	Number of tumor-bearing animals	Number of animals		
			Hepatic tumors (all types)	Hepatocellular carcinomas	Nasal carcinomas
0	106	31	2	1	0
14	110	34	0	0	0
121	106	28	1	1	0
1307	66	21	12[b]	10[c]	3[d]

[a]Rats surviving until 12 months on study.
[b]$p = 0.00022$ by one-tailed Fisher's Exact test.
[c]$p = 0.00033$ by one-tailed Fisher's Exact test.
[d]$p = 0.05491$ by one-tailed Fisher's Exact test.

Source: Kociba et al. (1974).

The only dose level that increased the formation of liver tumors over control (average dose for male and female rats, 1,307 mg/kg-day) was also demonstrated to cause significant liver and kidney toxicity in these animals. The mid-dose group (average dose for male and female rats, 121 mg/kg-day) experienced hepatic and renal degeneration and necrosis, as well as regenerative hyperplasia in hepatocytes and renal tubule epithelial cells. No increase in tumor formation was seen in the mid-dose group. No toxicity or tumor formation was observed in the low-dose group of rats (average dose for male and female rats, 14 mg/kg-day).

4.2.1.2.5. ***National Cancer Institute (NCI) (1978).*** Groups of Osborne-Mendel rats (35/sex/dose) and B6C3F$_1$ mice (50/sex/dose) were administered 1,4-dioxane (≥ 99.95% pure) in the drinking water for 110 or 90 weeks, respectively, at levels of 0 (matched controls), 0.5, or 1%. Solutions of 1,4-dioxane were prepared with tap water. The report indicated that at 105 weeks from the earliest starting date, a new necropsy protocol was instituted. This affected the male controls and high-dose rats, which were started a year later than the original groups of rats and mice. Food and water were available ad libitum. Endpoints monitored in this bioassay included clinical signs (twice daily), BWs (once every 2 weeks for the first 12 weeks and every month during the rest of the study), food and water consumption (once per month in 20% of the animals in each group during the second year of the study), and gross and microscopic appearance of all major organs and tissues (mammary gland, trachea, lungs and bronchi, heart, bone marrow, liver, bile duct, spleen, thymus, lymph nodes, salivary gland, pancreas, kidney, esophagus, thyroid, parathyroid, adrenal, gonads, brain, spinal cord, sciatic nerve, skeletal muscle, stomach, duodenum, colon, urinary bladder, nasal septum, and skin). Based on the measurements of water consumption and BWs, the investigators calculated average daily intakes of 1,4-dioxane of 0, 240, and 530 mg/kg-day in male rats, 0, 350, and 640 mg/kg-day in female rats, 0, 720, and 830 mg/kg-day in male mice, and 0, 380, and 860 mg/kg-day in female mice.

According to the report, the doses of 1,4-dioxane in high-dose male mice were only slightly higher than those of the low-dose group due to decreased fluid consumption in high-dose male mice.

During the second year of the study, the BWs of high-dose rats were lower than controls, those of low-dose males were higher than controls, and those of low-dose females were comparable to controls. The fluctuations in the growth curves were attributed to mortality by the investigators; quantitative analysis of BW changes was not done. Mortality was significantly increased in treated rats, beginning at approximately 1 year on study. Analysis of Kaplan-Meier curves (plots of the statistical estimates of the survival probability function) revealed significant positive dose-related trends ($p < 0.001$, Tarone test). In male rats, 33/35 (94%) in the control group, 26/35 (74%) in the mid-dose group, and 33/35 (94%) in the high-dose group were alive on week 52 of the study. The corresponding numbers for females were 35/35 (100%), 30/35 (86%), and 29/35 (83%). Nonneoplastic lesions associated with treatment with 1,4-dioxane were seen in the kidneys (males and females), liver (females only), and stomach (males only). Kidney lesions consisted of vacuolar degeneration and/or focal tubular epithelial regeneration in the proximal cortical tubules and occasional hyaline casts. Elevated incidence of hepatocytomegaly also occurred in treated female rats. Gastric ulcers occurred in treated males, but none were seen in controls. The incidence of pneumonia was increased above controls in high-dose female rats. The incidence of nonneoplastic lesions in rats following drinking water exposure to 1,4-dioxane is presented in Table 4-5. EPA identified the LOAEL in rats from this study as 240 mg/kg-day for increased incidence of gastric ulcer and cortical tubular degeneration in the kidney in males; a NOAEL was not established.

Table 4-5. Incidence of nonneoplastic lesions in Osborne-Mendel rats exposed to 1,4-dioxane in drinking water

	Males (mg/kg-day)			Females (mg/kg-day)		
	0	**240**	**530**	**0**	**350**	**640**
Cortical tubule degeneration	0/31[a]	20/31[b] (65%)	27/33[b] (82%)	0/31[a]	0/34	10/32[b] (31%)
Hepatocytomegaly	5/31 (16%)	3/32 (9%)	11/33 (33%)	7/31[a] (23%)	11/33 (33%)	17/32[b] (53%)
Gastric ulcer	0/30[a]	5/28[b] (18%)	5/30[b] (17%)	0/31	1/33 (3%)	1/30 (3%)
Pneumonia	8/30 (27%)	15/31 (48%)	14/33 (42%)	6/30[a] (20%)	5/34 (15%)	25/32[b] (78%)

[a]Statistically significant trend for increased incidence by Cochran-Armitage test ($p < 0.05$) performed for this review.
[b]Incidence significantly elevated compared to control by Fisher's Exact test ($p < 0.05$) performed for this review.

Source: NCI (1978).

Neoplasms associated with 1,4-dioxane treatment were limited to the nasal cavity (squamous cell carcinomas, adenocarcinomas, and one rhabdomyoma) in both sexes, liver (hepatocellular adenomas) in females, and testis/epididymis (mesotheliomas) in males. The first tumors were seen at week 52 in males and week 66 in females. The incidence of squamous cell carcinomas in the nasal turbinates in male and female rats is presented in Table 4-6. Squamous cell carcinomas were first seen on week 66 of the study. Morphologically, these tumors varied from minimal foci of locally invasive squamous cell proliferation to advanced growths consisting of extensive columns of epithelial cells projecting either into free spaces of the nasal cavity and/or infiltrating into the submucosa. Adenocarcinomas of the nasal cavity were observed in 3 of 34 high-dose male rats, 1 of 35 low-dose female rats, and 1 of 35 high-dose female rats. The single rhabdomyoma (benign skeletal muscle tumor) was observed in the nasal cavity of a male rat from the low-dose group. A subsequent re-examination of the nasal tissue sections by Goldsworthy et al. (1991) concluded that the location of the tumors in the nasal apparatus was consistent with the possibility that the nasal tumors resulted from inhalation of water droplets by the rats (see Section 4.5.2 for more discussion of Goldsworthy et al., 1991).

Table 4-6. Incidence of nasal cavity squamous cell carcinoma and liver hepatocellular adenoma in Osborne-Mendel rats exposed to 1,4-dioxane in drinking water

Males (mg/kg-day)[a]			
	0	**240[b]**	**530**
Nasal cavity squamous cell carcinoma	0/33 (0%)	12/33 (36%)	16/34 (47%)[c]
Hepatocellular adenoma	2/31 (6%)	2/32 (6%)	1/33 (3%)
Females (mg/kg-day)[a]			
	0	**350**	**640**
Nasal cavity squamous cell carcinoma	0/34 (0%)[d]	10/35 (29%)[e]	8/35 (23%)[c]
Hepatocellular adenoma	0/31 (0%)[f]	10/33 (30%)[e]	11/32 (34%)[e]

[a]Tumor incidence values were not adjusted for mortality.
[b]Group not included in statistical analysis by NCI because the dose group was started a year earlier without appropriate controls.
[c]$p \leq 0.003$ by Fisher's Exact test pair-wise comparison with controls.
[d]$p = 0.008$ by Cochran-Armitage test.
[e]$p \leq 0.001$ by Fisher's Exact test pair-wise comparison with controls.
[f]$p = 0.001$ by Cochran-Armitage test.

Source: NCI (1978).

The incidence of hepatocellular adenomas in male and female rats is presented in Table 4-7. Hepatocellular adenomas were first observed in high-dose females in week 70 of the study. These tumors consisted of proliferating hepatic cells oriented as concentric cords. Hepatic cell size was variable; mitoses and necrosis were rare. Mesothelioma of the vaginal tunics of the testis/epididymis was seen in male rats (2/33, 4/33, and 5/34 in controls, low-, and

high-dose animals, respectively). The difference between the treated groups and controls was not statistically significant. These tumors were characterized as rounded and papillary projections of mesothelial cells, each supported by a core of fibrous tissue. Other reported neoplasms were considered spontaneous lesions not related to treatment with 1,4-dioxane.

In mice, mean BWs of high-dose female mice were lower than controls during the second year of the study, while those of low-dose females were higher than controls. In males, mean BWs of high-dose animals were higher than controls during the second year of the study. According to the investigators, these fluctuations could have been due to mortality; no quantitative analysis of BWs was done. No other clinical signs were reported. Mortality was significantly increased in female mice ($p < 0.001$, Tarone test), beginning at approximately 80 weeks on study. The numbers of female mice that survived to 91 weeks were 45/50 (90%) in the control group, 39/50 (78%) in the low-dose group, and 28/50 (56%) in the high-dose group. In males, at least 90% of the mice in each group were still alive at week 91. Nonneoplastic lesions that increased significantly due to treatment with 1,4-dioxane were pneumonia in males and females and rhinitis in females. The incidences of pneumonia were 1/49 (2%), 9/50 (18%), and 17/47 (36%) in control, low-dose, and high-dose males, respectively; the corresponding incidences in females were 2/50 (4%), 33/47 (70%), and 32/36 (89%). The incidences of rhinitis in female mice were 0/50, 7/48 (14%), and 8/39 (21%) in control, low-dose, and high-dose groups, respectively. Pair-wise comparisons of low-dose and high-dose incidences with controls for incidences of pneumonia and rhinitis in females using Fisher's Exact test (done for this review) yielded p-values < 0.001 in all cases. Incidences of other lesions were considered to be similar to those seen in aging mice. The authors stated that hepatocytomegaly was commonly found in dosed mice, but the incidences were not significantly different from controls and showed no dose-response trend. EPA concluded the LOAEL for 1,4-dioxane in mice was 380 mg/kg-day based on the increased incidence of pneumonia and rhinitis in female mice; a NOAEL was not established in this study.

As shown in Table 4-7, treatment with 1,4-dioxane significantly increased the incidence of hepatocellular carcinomas or adenomas in male and female mice in a dose-related manner. Tumors were first observed on week 81 in high-dose females and in week 58 in high-dose males. Tumors were characterized by parenchymal cells of irregular size and arrangement, and were often hypertrophic with hyperchromatic nuclei. Mitoses were seldom seen. Neoplasms were locally invasive within the liver, but metastasis to the lungs was rarely observed.

Table 4-7. Incidence of hepatocellular adenoma or carcinoma in B6C3F$_1$ mice exposed to 1,4-dioxane in drinking water

Males (mg/kg-day)[a]			
	0	**720**	**830**
Hepatocellular carcinoma	2/49 (4%)[b]	18/50 (36%)[c]	24/47 (51%)[c]
Hepatocellular adenoma or carcinoma	8/49 (16%)[b]	19/50 (38%)[d]	28/47 (60%)[c]
Females (mg/kg-day)[a]			
	0	**380**	**860**
Hepatocellular carcinoma	0/50 (0%)[b]	12/48 (25%)[c]	29/37 (78%)[c]
Hepatocellular adenoma or carcinoma	0/50 (0%)[b]	21/48 (44%)[c]	35/37 (95%)[c]

[a]Tumor incidence values were not adjusted for mortality.
[b]$p < 0.001$, positive dose-related trend (Cochran-Armitage test).
[c]$p < 0.001$ by Fisher's Exact test pair-wise comparison with controls.
[d]$p = 0.014$.

Source: NCI (1978).

In addition to liver tumors, a variety of other benign and malignant neoplasms occurred. However, the report (NCI, 1978) indicated that each type had been encountered previously as a spontaneous lesion in the B6C3F$_1$ mouse. The report further stated that the incidences of these neoplasms were unrelated by type, site, group, or sex of the animal, and hence, not attributable to exposure to 1,4-dioxane. There were a few nasal adenocarcinomas (1/48 in low-dose females and 1/49 in high-dose males) that arose from proliferating respiratory epithelium lining of the nasal turbinates. These growths extended into the nasal cavity, but there was minimal local tissue infiltration. Nasal mucosal polyps were rarely observed. The polyps were derived from mucus-secreting epithelium and were otherwise unremarkable. There was a significant negative trend for alveolar/bronchiolar adenomas or carcinomas of the lung in male mice, such that the incidence in the matched controls was higher than in the dosed groups. The report (NCI, 1978) indicated that the probable reason for this occurrence was that the dosed animals did not live as long as the controls, thus diminishing the possibility of the development of tumors in the dosed groups.

4.2.1.2.6. ***Japan Bioassay Research Center (JBRC) (1998a); Yamazaki et al. (1994).***

Groups of F344/DuCrj rats (50/sex/dose level) were exposed to 1,4-dioxane (>99% pure) in the drinking water at levels of 0, 200, 1,000, or 5,000 ppm for 2 years. Groups of Crj:BDF$_1$ mice (50/sex/dose level) were similarly exposed to 0, 500, 2,000, or 8,000 ppm of 1,4-dioxane in the drinking water. Both rats and mice were 6 weeks old at the beginning of the study. Food and water were available ad libitum. The animals were observed daily for clinical signs of toxicity, and BWs were measured once per week for 14 weeks and once every 2 weeks until the end of the study. Food consumption was measured once a week for 14 weeks and once every 4 weeks for the remainder of the study. The investigators used data from water consumption and BW

changes to calculate the daily intake of 1,4-dioxane by the male and female animals and presented these estimates as ranges. In order to simplify the summary of the results, the doses presented here represent the midpoint of the ranges calculated by JBRC (1998a). Thus, male rats received doses of approximately 0, 16, 81, or 398 mg/kg-day and female rats received 0, 21, 103, or 514 mg/kg-day. Male mice received 0, 66, 251, or 768 mg/kg-day and female mice received 0, 77, 323, or 1,066 mg/kg-day.

No information was provided as to when urine samples were collected. Blood samples were collected only at the end of the 2-year study (email from Dr. Kazunori Yamazaki, JBRC, to Dr. Julie Stickney, SRC, dated 12/18/06). Hematology analysis included RBCs, hemoglobin, hematocrit, MCV, platelets, WBCs and differential WBCs. Serum biochemistry included total protein, albumin, bilirubin, glucose, cholesterol, triglyceride (rat only), phospholipid, ALT, AST, LDH, LAP, ALP, γ-glutamyl transpeptidase (GGT), CPK, urea nitrogen, creatinine (rat only), sodium, potassium, chloride, calcium, and inorganic phosphorous. Urinalysis parameters were pH, protein, glucose, ketone body, bilirubin (rat only), occult blood, and urobilinogen. Organ weights (brain, lung, liver, spleen, heart, adrenal, testis, ovary, and thymus) were measured, and gross necropsy and histopathologic examination of tissues and organs were performed on all animals (skin, nasal cavity, trachea, lungs, bone marrow, lymph nodes, thymus, spleen, heart, tongue, salivary glands, esophagus, stomach, small and large intestine, liver, pancreas, kidney, urinary bladder, pituitary, thyroid, adrenal, testes, epididymis, seminal vesicle, prostate, ovary, uterus, vagina, mammary gland, brain, spinal cord, sciatic nerve, eye, Harderian gland, muscle, bone, and parathyroid). Dunnett's test and χ^2 test were used to assess the statistical significance of changes in continuous and discrete variables, respectively.

Survival was significantly decreased in the rat high-dose groups (80% in control males versus 44% in high-dose males; 76% in control females versus 48% in high-dose females). The effect on survival in high-dose rats occurred in the second year of the study, as all control and exposed rats lived at least 12 months following study initiation (email from Dr. Kazunori Yamazaki, JBRC, to Dr. Julie Stickney, SRC, dated 12/18/06). The extra mortality in the high-dose groups was primarily related to tumors in these groups (peritoneal mesothelioma, liver and nasal tumors) (email from Dr. Kazunori Yamazaki, JBRC, to Dr. Julie Stickney, SRC, dated 12/18/06). Neither food nor water consumption were significantly affected by treatment in males or females. Terminal BWs were reduced 10% in high-dose males and 19% in high-dose females. RBC (males only), hemoglobin, hematocrit, and MCV were decreased, and platelets were increased in high-dose groups. These changes (except for MCV) also occurred in mid-dose males. With the exception of a 23% decrease in hemoglobin in high-dose male rats and a 27% increase in platelets in high-dose female rats, hematological changes were within 15% of control values. Significant changes in serum chemistry parameters occurred only in high-dose rats (males: increased phospholipids, AST, ALT, LDH, ALP, GGT, CPK, potassium, and inorganic phosphorus and decreased total protein, albumin, and glucose; females: increased total bilirubin,

cholesterol, phospholipids, AST, ALT, LDH, GGT, ALP, CPK, and potassium, and decreased blood glucose). Increases in serum enzyme activities ranged from <2- to 17-fold above control values, with the largest increases seen for ALT, AST, and GGT. Urine pH was significantly decreased at 398 mg/kg-day in males (not tested at other dose levels) and at 103 and 514 mg/kg-day in females. Also, blood in the urine was seen in females at 103 and 514 mg/kg-day. In males, relative liver weights were increased at 81 and 398 mg/kg-day and absolute liver weights were increased at 398 mg/kg-day. In females, relative and absolute lung and liver weights and relative kidney weights were increased at 514 mg/kg-day.

Microscopic examination of the tissues showed nonneoplastic alterations in the nasal cavity, liver, and kidneys mainly in high-dose rats and, in a few cases, in mid-dose rats (Tables 4-8 and 4-9). Alterations in high-dose males consisted of nuclear enlargement and metaplasia of the olfactory and respiratory epithelia, atrophy of the olfactory epithelium, hydropic changes and sclerosis of the lamina propria, adhesion, and inflammation. In females, nuclear enlargement of the olfactory epithelium occurred at doses ≥103 mg/kg-day, and nuclear enlargement and metaplasia of the respiratory epithelium, squamous cell hyperplasia, respiratory metaplasia of the olfactory epithelium, hydropic changes and sclerosis of the lamina propria, adhesion, inflammation, and proliferation of the nasal gland occurred at 514 mg/kg-day. Alterations were seen in the liver at ≥81 mg/kg-day in males (spongiosis hepatis, hyperplasia, and clear and mixed cell foci) and at 514 mg/kg-day in females (hyperplasia, spongiosis hepatis, cyst formation, and mixed cell foci). Nuclear enlargement of the renal proximal tubule occurred in males at 398 mg/kg-day and in females at ≥ 103 mg/kg-day.

Table 4-8. Incidence of histopathological lesions in male F344/DuCrj rats exposed to 1,4-dioxane in drinking water for 2 years

	Dose (mg/kg-day)[a]			
	0	**16**	**81**	**398**
Nuclear enlargement; nasal respiratory epithelium	0/40	0/45	0/35	12/22[b]
Squamous cell metaplasia; nasal respiratory epithelium	0/40	0/45	0/35	15/22[b]
Nuclear enlargement; nasal olfactory epithelium	0/40	0/45	4/35	20/22[b]
Respiratory metaplasia; nasal olfactory epithelium	10/40	11/45	17/35	22/22[b]
Atrophy; nasal olfactory epithelium	0/40	0/45	0/35	17/22[b]
Hydropic change; lamina propria	0/40	0/45	0/35	20/22[b]
Sclerosis; lamina propria	0/40	0/45	1/35	20/22[b]
Adhesion; nasal cavity	0/40	0/45	0/35	21/22[b]
Inflammation; nasal cavity	0/40	0/45	0/35	7/22[b]
Hyperplasia; liver	3/40	2/45	9/35[c]	12/22[b]
Spongiosis hepatis; liver	12/40	20/45	21/35[c]	21/22[b]
Clear cell foci; liver	3/40	3/45	9/35[c]	7/22[c]
Basophilic cell foci; liver	7/40	11/45	6/35	8/22[c]
Mixed-cell foci; liver	2/40	8/45	14/35[b]	22/22[b]
Nuclear enlargement; kidney proximal tubule	0/40	0/45	0/35	22/22[b]

[a]Data presented for sacrificed animals.
[b]$p \leq 0.01$ by χ^2 test.
[c]$p \leq 0.05$.

Source: JBRC (1998a).

Table 4-9. Incidence of histopathological lesions in female F344/DuCrj rats exposed to 1,4-dioxane in drinking water for 2 years

	Dose (mg/kg-day)[a]			
	0	21	103	514
Nuclear enlargement; nasal respiratory epithelium	0/38	0/37	0/38	7/24[b]
Squamous cell metaplasia; nasal respiratory epithelium	0/38	0/37	0/38	18/24[b]
Squamous cell hyperplasia; nasal cavity	0/38	0/37	0/38	4/24[c]
Nuclear enlargement; nasal olfactory epithelium	0/38	0/37	24/38[b]	22/24[b]
Respiratory metaplasia; nasal olfactory epithelium	1/38	0/37	1/38	24/24[b]
Atrophy; nasal olfactory epithelium	0/38	0/37	1/38	22/24[b]
Hydropic change; lamina propria	0/38	0/37	0/38	23/24[b]
Sclerosis; lamina propria	0/38	0/37	0/38	23/24[b]
Adhesion; nasal cavity	0/38	0/37	0/38	24/24[b]
Inflammation; nasal cavity	0/38	0/37	1/38	7/24[b]
Proliferation; nasal gland	0/38	0/37	0/38	8/24[b]
Hyperplasia; liver	2/38	2/37	9/38	24/24[b]
Spongiosis hepatis; liver	0/38	0/37	1/38	14/24[b]
Cyst formation; liver	0/38	1/37	0/38	5/24[c]
Mixed-cell foci; liver	1/38	1/37	3/38	7/24[a]
Nuclear enlargement; kidney proximal tubule	0/38	0/37	6/38[b]	22/24[a]

[a]Data presented for sacrificed animals.
[b]$p \leq 0.01$ by χ^2 test.
[c]$p \leq 0.05$.

Source: JBRC (1998a).

NOAEL and LOAEL values for rats in this study were identified by EPA as 81 and 398 mg/kg-day, respectively, based on toxicity observed in nasal tissue of male rats (i.e., atrophy of olfactory epithelium, adhesion, and inflammation). Metaplasia and hyperplasia of the nasal epithelium were also observed in high-dose male and female rats. These effects are likely to be associated with the formation of nasal cavity tumors in these dose groups. Nuclear enlargement was observed in the nasal olfactory epithelium and the kidney proximal tubule at a dose of 103 mg/kg-day in female rats; however, it is unclear whether these alterations represent adverse toxicological effects. Hematological effects noted in male rats given 81 and 398 mg/kg-day (decreased RBCs, hemoglobin, hematocrit, increased platelets) were within 20% of control values. In female rats decreases in hematological effects were observed in the high dose group (514 mg/kg-day). A reference range database for hematological effects in laboratory animals (Wolford et al., 1986) indicates that a 20% change in these parameters may fall within a normal range (10th–90th percentile values) and may not represent a treatment-related effect of concern. Liver lesions were also seen at a dose of 81 mg/kg-day in male rats; these changes are likely to be associated with liver tumorigenesis. Clear and mixed-cell foci are commonly considered preneoplastic changes and would not be considered evidence of noncancer toxicity. The nature

of spongiosis hepatis as a preneoplastic change is less well understood (Bannash, 2003; Karbe and Kerlin, 2002; Stroebel et al., 1995). Spongiosis hepatis is a cyst-like lesion that arises from the perisinusoidal Ito cells of the liver. It is commonly seen in aging rats, but has been shown to increase in incidence following exposure to hepatocarcinogens. Spongiosis hepatis can be seen in combination with preneoplastic foci in the liver or with hepatocellular adenoma or carcinoma and has been considered a preneoplastic lesion (Bannash et al., 2003; Stroebel et al., 1995). This change can also be associated with hepatocellular hypertrophy and liver toxicity and has been regarded as a secondary effect of some liver carcinogens (Karbe and Kerlin, 2002). In the case of the JBRC (1998a) study, spongiosis hepatis was associated with other preneoplastic changes in the liver (clear and mixed-cell foci). No other lesions indicative of liver toxicity were seen in this study; therefore, spongiosis hepatis was not considered indicative of noncancer effects. Serum chemistry changes (increases in total protein, albumin, and glucose; decreases in AST, ALT, LDH, and ALP, potassium, and inorganic phosphorous) were observed in both male and female rats (JBRC, 1998a) in the high dose groups, 398 and 514 mg/kg-day, respectively. These serum chemistry changes seen in terminal blood samples from high-dose male and female rats are likely related to tumor formation in these dose groups.

Significantly increased incidences of liver tumors (adenomas and carcinomas) and tumors of the nasal cavity occurred in high-dose male and female rats (Tables 4-11 and 4-12) treated with 1,4-dioxane for 2 years. The first liver tumor was seen at 85 weeks in high-dose male rats and 73 weeks in high-dose female rats (vs. 101–104 weeks in lower dose groups and controls) (email from Dr. Kazunori Yamazaki, JBRC, to Dr. Julie Stickney, SRC, dated 12/18/06). In addition, a significant increase ($p \leq 0.01$, Fisher's Exact test) in mesotheliomas of the peritoneum was seen in high-dose males (28/50 versus 2/50 in controls). Mesotheliomas were the single largest cause of death among high-dose male rats, accounting for 12 of 28 pretermination deaths (email from Dr. Kazunori Yamazaki, JBRC, to Dr. Julie Stickney, SRC, dated 12/18/06). Also, in males, there were increasing trends in mammary gland fibroadenoma and fibroma of the subcutis, both statistically significant ($p < 0.01$) by the Peto test of dose-response trend. Females showed a significant increasing trend in mammary gland adenomas ($p = 0.006$ Cochran-Armitage trend test). The tumor incidence values presented in Tables 4-10 and 4-11 were not adjusted for survival because all rats lived longer than 12 months on study.

Table 4-10. Incidence of nasal cavity, peritoneum, and mammary gland tumors in F344/DuCrj rats exposed to 1,4-dioxane in drinking water for 2 years

	Males				Females			
Dose (mg/kg-day)	**0**	**16**	**81**	**398**	**0**	**21**	**103**	**514**
Nasal Cavity								
Squamous cell carcinoma	0/50	0/50	0/50	3/50	0/50[a]	0/50	0/50	7/50[b]
Sarcoma	0/50	0/50	0/50	2/50	0/50	0/50	0/50	0/50
Rhabdomyosarcoma	0/50	0/50	0/50	1/50	0/50	0/50	0/50	0/50
Esthesioneuro-epithelioma	0/50	0/50	0/50	1/50	0/50	0/50	0/50	1/50
All Nasal Cavity Tumors	0/50[a]	0/50	0/50	7/50[b]	0/50[a]	0/50	0/50	8/50[c]
Peritoneum								
Mesothelioma	2	2	5	28	1	0	0	0
Mammary Gland								
Fibroadenoma	1	1	0	4[a]	3	2	1	3
Adenoma	0	0	0	0	6	7	10	16[d]
All Mammary Gland Tumors	1	1	0	4	9	9	11	19

[a]$p < 0.01$ by Peto test for trend.
[b]$p \leq 0.05$.
[c]$p \leq 0.01$ by Fisher's Exact test.
[d]$p = 0.006$ by Cochran-Armitage trend test.

Source: JBRC (1998a).

Table 4-11. Incidence of liver tumors in F344/DuCrj rats exposed to 1,4-dioxane in drinking water for 2 years

	Males				Females			
Dose (mg/kg-day)	**0**	**16**	**81**	**398**	**0**	**21**	**103**	**514**
Hepatocellular adenoma	0/50[a]	2/50	4/49	24/50[a]	1/50[b]	0/50	5/50	38/50[a]
Hepatocellular carcinoma	0/50[a]	0/50	0/49	14/50[a]	1/50[b]	0/50	0/50	10/50[a]
Adenoma or carcinoma	0/50[a]	2/50	4/49	33/50[a]	1/50[b]	0/50	5/50	40/50[a]

[a]$p \leq 0.01$ by Fisher's Exact test.
[b]$p < 0.01$ by Peto test for trend.

Source: JBRC (1998a).

In the study in mice, survival was low in all male groups (31/50, 33/50, 25/50, and 26/50 in control, low-, mid-, and high-dose groups, respectively) and particularly low in high-dose females (29/50, 29/50, 17/50, and 5/50 in control, low-, mid-, and high-dose groups, respectively). Deaths occurred primarily during the second year of the study. Survival at 12 months in male mice was 50/50, 48/50, 50/50, and 48/50 in control, low-, mid-, and high-dose groups, respectively. Female mouse survival at 12 months was 50/50, 50/50, 48/50, and 48/50 in control, low-, mid-, and high-dose groups, respectively (email from Dr. Kazunori Yamazaki,

JBRC, to Dr. Julie Stickney, Syracuse Research Corporation (SRC), dated 12/18/06). The deaths were primarily tumor-related (e.g., liver tumors were listed as the cause of death for 31 of the 45 pretermination deaths in high-dose female rats) (email from Dr. Kazunori Yamazaki, JBRC, to Dr. Julie Stickney, SRC, dated 12/18/06). Food consumption was not significantly affected, but water consumption was reduced 26% in high-dose males and 28% in high-dose females. Final BWs were reduced 43% in high-dose males and 15 and 45% in mid- and high-dose females, respectively. Males showed increases in RBC counts, hemoglobin, and hematocrit, whereas in females, there was a decrease in platelets in mid- and high-dose rats. With the exception of a 60% decrease in platelets in high-dose female mice, hematological changes were within 15% of control values. Serum AST, ALT, LDH, and ALP activities were significantly increased in mid- and high-dose males, whereas LAP and CPK were increased only in high-dose males. AST, ALT, LDH, and ALP activities were increased in mid- and high-dose females, but CPK activity was increased only in high-dose females. Increases in serum enzyme activities ranged from less than two- to sevenfold above control values. Glucose and triglycerides were decreased in high-dose males and in mid- and high-dose females. High-dose females also showed decreases in serum phospholipid and albumin concentrations (not reported in males). Blood calcium was lower in high-dose females and was not reported in males. Urinary pH was decreased in high-dose males, whereas urinary protein, glucose, and occult blood were increased in mid- and high-dose females. Relative and absolute lung weights were increased in high-dose males and in mid- and high-dose females. Microscopic examination of the tissues for nonneoplastic lesions showed significant alterations in the epithelium of the respiratory tract, mainly in high-dose animals, although some changes occurred in mid-dose mice (Tables 4-12 and 4-13). Commonly seen alterations included nuclear enlargement, atrophy, and inflammation of the epithelium. Other notable changes observed included nuclear enlargement of the proximal tubule of the kidney and angiectasis in the liver in high-dose males.

Table 4-12. Incidence of histopathological lesions in male Crj:BDF$_1$ mice exposed to 1,4-dioxane in drinking water for 2 years

	Dose (mg/kg-day)[a]			
	0	66	251	768
Nuclear enlargement; nasal respiratory epithelium	0/31	0/33	0/25	19/26[b]
Nuclear enlargement; nasal olfactory epithelium	0/31	0/33	7/25[b]	26/26[b]
Atrophy; nasal olfactory epithelium	0/31	0/33	0/25	26/26[b]
Inflammation; nasal cavity	1/31	1/33	1/25	15/26[b]
Atrophy; tracheal epithelium	0/31	0/33	0/25	24/26[b]
Nuclear enlargement; tracheal epithelium	0/31	0/33	0/25	12/26[b]
Nuclear enlargement; bronchial epithelium	0/31	0/33	0/25	24/26[b]
Atrophy; lung/bronchial epithelium	0/31	0/33	0/25	26/26[b]
Accumulation of foamy cells; lung	1/31	0/33	0/25	22/26[b]
Angiectasis; liver	2/31	2/33	3/25	8/26[c]
Nuclear enlargement; kidney proximal tubule	0/31	0/33	0/25	22/26[b]

[a]Data presented for sacrificed animals.
[b]$p \leq 0.01$ by χ^2 test.
[c]$p \leq 0.05$.

Source: JBRC (1998a).

Table 4-13. Incidence of histopathological lesions in female Crj:BDF$_1$ mice exposed to 1,4-dioxane in drinking water for 2 years

	Dose (mg/kg-day)[a]			
	0	77	323	1,066
Nuclear enlargement; nasal respiratory epithelium	0/29	0/29	0/17	5/5[b]
Nuclear enlargement; nasal olfactory epithelium	0/29	0/29	17/17[b]	1/5
Atrophy; nasal olfactory epithelium	0/29	0/29	0/17	5/5[b]
Inflammation; nasal cavity	0/29	0/29	5/17[b]	5/5[b]
Atrophy; tracheal epithelium	0/29	0/29	1/17	5/5[b]
Nuclear enlargement; bronchial epithelium	0/29	1/29	13/17[b]	5/5[b]
Atrophy; lung/bronchial epithelium	0/29	0/29	3/17	5/5[b]
Accumulation of foamy cells; lung	0/29	1/29	3/17	5/5[b]

[a]Data presented for sacrificed animals.
[b]$p \leq 0.01$ by χ^2 test.

Source: JBRC (1998a).

NOAEL and LOAEL values for mice in this study were identified by EPA as 77 and 323 mg/kg-day, respectively, based on nasal inflammation observed in female mice. Nuclear enlargement of the nasal olfactory epithelium and bronchial epithelium was also observed at a dose of 323 mg/kg-day in female rats; however, it is unclear whether these alterations represent adverse toxicological effects. The serum chemistry changes seen in terminal blood samples from

male and female mice (mid- and high-dose groups) are likely related to tumor formation in these animals. Liver angiectasis, an abnormal dilatation and/or lengthening of a blood or lymphatic vessel, was seen in male mice given 1,4-dioxane at a dose of 768 mg/kg-day.

Treatment with 1,4-dioxane resulted in an increase in the formation of liver tumors (adenomas and carcinomas) in male and female mice. The incidence of hepatocellular adenoma was increased in male mice in the mid-dose group only. The incidence of male mice with hepatocellular carcinoma or either tumor type (adenoma or carcinoma) was increased in the low, mid, and high-dose groups. The appearance of the first liver tumor occurred in male mice at 64, 74, 63, and 59 weeks in the control, low- mid-, and high-dose groups, respectively (email from Dr. Kazunori Yamazaki, JBRC, to Dr. Julie Stickney, SRC, dated 12/18/06). In female mice, increased incidence was observed for each liver tumor type in all treatment groups (Table 4-14). The appearance of the first liver tumor in female mice occurred at 95, 79, 71, and 56 weeks in the control, low- mid-, and high-dose groups, respectively (email from Dr. Kazunori Yamazaki, JBRC, to Dr. Julie Stickney, SRC, dated 12/18/06). The tumor incidence data presented for male and female mice were based on mice that survived at least 12 months on study. Mice that died prior to 12 months were not included in Table 4-14.

Table 4-14. Incidence of liver tumors in Crj:BDF$_1$ mice exposed to 1,4-dioxane in drinking water for 2 years

	Males				Females			
Dose (mg/kg-day)	**0**	**66**	**251**	**768**	**0**	**77**	**323**	**1,066**
Hepatocellular adenoma	7/50	16/48	22/50[b]	8/48	4/50	30/50[c]	20/48[c]	2/48
Hepatocellular carcinoma	15/50[a]	20/48	23/50	36/48[b]	0/50[a]	6/50[b]	30/48[c]	45/48[c]
Adenoma or carcinoma	21/50	31/48[c]	37/50[b]	39/48[b]	4/50[a]	34/50[c]	41/48[c]	46/48[c]

[a]$p < 0.05$; positive dose-related trend (Cochran-Armitage test or Peto test)
[b]$p \leq 0.05$ by Fisher's Exact test.
[c]$p \leq 0.01$ by Fisher's Exact test.

Sources: JBRC (1998a); email from Dr. Kazunori Yamazaki, JBRC, to Dr. Julie Stickney, SRC (12/18/06).

A weight of evidence evaluation of the carcinogenicity studies presented in Section 4.2.1.2 is located in Section 4.7 and Table 4-18.

4.2.2. Inhalation Toxicity

4.2.2.1. *Subchronic Inhalation Toxicity*

4.2.2.1.1. *Fairley et al. (1934).* Rabbits, guinea pigs, rats, and mice (3–6/species/group) were exposed to 1,000, 2,000, 5,000, or 10,000 ppm of 1,4-dioxane vapor for 3 hours/day, 5 days/week and 1.5 hours on the 6th day (16.5 hours/week). Animals were exposed until death occurred or were sacrificed at varying time periods. At the 10,000 ppm concentration, only one

animal (rat) survived a 7-day exposure. The rest of the animals (six guinea pigs, three mice, and two rats) died within the first five exposures. Severe liver and kidney damage and acute vascular congestion of the lungs were observed in these animals. Kidney damage was described as patchy degeneration of cortical tubules with vascular congestion and hemorrhage. Liver lesions varied from cloudy hepatocyte swelling to large areas of necrosis. At 5,000 ppm, mortality was observed in two mice and one guinea pig following 15–34 exposures. The remaining animals were sacrificed following 49.5 hours (3 weeks) of exposure (three rabbits) or 94.5 hours (5 weeks) of exposure (three guinea pigs). Liver and kidney damage in both dead and surviving animals was similar to that described for the 10,000 ppm concentration. Animals (four rabbits, four guinea pigs, six rats, and five mice) were exposed to 2,000 ppm for 45–102 total exposure hours (approximately 2–6 weeks). Kidney and liver damage was still apparent in animals exposed to this concentration. Animals exposed to 1,000 ppm were killed at intervals with the total exposure duration ranging between 78 and 202.5 hours (approximately 4–12 weeks). Cortical kidney degeneration and hepatocyte degeneration and liver necrosis were observed in these animals (two rabbits, three guinea pigs, three rats, and four mice). The low concentration of 1,000 ppm was identified by EPA as a LOAEL for liver and kidney degeneration in rats, mice, rabbits, and guinea pigs in this study.

4.2.2.2. *Chronic Inhalation Toxicity and Carcinogenicity*

4.2.2.2.1. ***Torkelson et al. (1974).*** Whole body exposures of male and female Wistar rats (288/sex) to 1,4-dioxane vapors (99.9% pure) at a concentration of 0.4 mg/L (111 ppm), were carried out 7 hours/day, 5 days/week for 2 years. The age of the animals at the beginning of the study was not provided. The concentration of 1,4-dioxane vapor during exposures was determined with infrared analyzers. Food and water were available ad libitum except during exposures. Endpoints examined included clinical signs, eye and nasal irritation, skin condition, respiratory distress, and tumor formation. BWs were determined weekly. Standard hematological parameters were determined on all surviving animals after 16 and 23 months of exposure. Blood collected at termination was used also for determination of clinical chemistry parameters (serum AST and ALP activities, blood urea nitrogen [BUN], and total protein). Liver, kidneys, and spleen were weighed and the major tissues and organs were processed for microscopic examination (lungs, trachea, thoracic lymph nodes, heart, liver, pancreas, stomach, intestine, spleen, thyroid, mesenteric lymph nodes, kidneys, urinary bladder, pituitary, adrenals, testes, ovaries, oviduct, uterus, mammary gland, lacrimal gland, lymph nodes, brain, vagina, and bone marrow, and any abnormal growths). Nasal tissues were not obtained for histopathological evaluation. Control and experimental groups were compared statistically using Student's t test, Yates corrected χ^2 test, or Fisher's Exact test.

Exposure to 1,4-dioxane vapors had no significant effect on mortality or BW gain and induced no signs of eye or nasal irritation or respiratory distress. Slight, but statistically

significant, changes in hematological and clinical chemistry parameters were within the normal physiological limits and were considered to be of no toxicological importance by the investigators. Altered hematological parameters included decreases in packed cell volume, RBC count, and hemoglobin, and an increase in WBC count in male rats. Clinical chemistry changes consisted of a decrease in BUN (control—23 ± 9.9; 111-ppm dioxane—19.8 ± 8.8) and an increase in ALP activity (control—34.4 ± 12.1; 111-ppm dioxane—29.9 ± 9.2) and total protein (control—7.5 ± 0.37; 111-ppm dioxane—7.9 ± 0.53) in male rats (values are mean ± standard deviation). Organ weights were not significantly affected. Microscopic examination of organs and tissues did not reveal any treatment-related effects. Based of the lack of significant effects on several endpoints, EPA identified the exposure concentration of 0.4 mg/L (111 ppm) as a free standing NOAEL. The true NOAEL was likely to be higher.

Tumors, observed in all groups including controls, were characteristic of the rat strain used and were considered unrelated to 1,4-dioxane inhalation. The most common tumors were reticulum cell sarcomas and mammary tumors. Using Fisher's Exact test and a significance level of $p < 0.05$, no one type of tumor occurred more frequently in treated rats than in controls. No hepatic or nasal cavity tumors were seen in any rat.

4.2.3. Initiation/Promotion Studies

4.2.3.1. *Bull et al. (1986)*

Bull et al. (1986) tested 1,4-dioxane as a cancer initiator in mice using oral, subcutaneous, and topical routes of exposure. A group of 40 female SENCAR mice (6–8 weeks old) was administered a single dose of 1,000 mg/kg dioxane (purity >99%) by gavage, subcutaneous injection, or topical administration (vehicle was not specified). A group of rats was used as a vehicle control (number of animals not specified). Food and water were provided ad libitum. Two weeks after administration of 1,4-dioxane, 12-O-tetradecanoylphorbol-13-acetate (TPA) (1.0 µg in 0.2 mL of acetone) was applied to the shaved back of mice 3 times/week for a period of 20 weeks. The yield of papillomas at 24 weeks was selected as a potential predictor of carcinoma yields at 52 weeks following the start of the promotion schedule. Acetone was used instead of TPA in an additional group of 20 mice in order to determine whether a single dose of 1,4-dioxane could induce tumors in the absence of TPA promotion.

1,4-Dioxane did not increase the formation of papillomas compared to mice initiated with vehicle and promoted with TPA, indicating lack of initiating activity under the conditions of the study. Negative results were obtained for all three exposure routes. A single dose of 1,4-dioxane did not induce tumors in the absence of TPA promotion.

4.2.3.2. *King et al. (1973)*

1,4-Dioxane was evaluated for complete carcinogenicity and tumor promotion activity in mouse skin. In the complete carcinogenicity study, 0.2 mL of a solution of 1,4-dioxane (purity not specified) in acetone was applied to the shaved skin of the back of Swiss Webster mice (30/sex) 3 times/week for 78 weeks. Acetone was applied to the backs of control mice (30/sex) for the same time period. In the promotion study, each animal was treated with 50 μg of dimethylbenzanthracene 1 week prior to the topical application of the 1,4-dioxane solution described above (0.2 mL, 3 times/week, 78 weeks) (30 mice/sex). Acetone vehicle was used in negative control mice (30/sex). Croton oil was used as a positive control in the promotion study (30/sex). Weekly counts of papillomas and suspect carcinomas were made by gross examination. 1,4-Dioxane was also administered in the drinking water (0.5 and 1%) to groups of Osborne-Mendel rats (35/sex/group) and $B6C3F_1$ mice for 42 weeks (control findings were only reported for 34 weeks).

1,4-Dioxane was negative in the complete skin carcinogenicity test using dermal exposure. One treated female mouse had malignant lymphoma; however, no papillomas were observed in male or female mice by 60 weeks. Neoplastic lesions of the skin, lungs, and kidney were observed in mice given the promotional treatment with 1,4-dioxane. In addition, the percentage of mice with skin tumors increased sharply after approximately 10 weeks of promotion treatment. Significant mortality was observed when 1,4-dioxane was administered as a promoter (only 4 male and 5 female mice survived for 60 weeks), but not as a complete carcinogen (22 male and 25 female mice survived until 60 weeks). The survival of acetone-treated control mice in the promotion study was not affected (29 male and 26 female mice survived until 60 weeks); however, the mice treated with croton oil as a positive control experienced significant mortality (0 male and 1 female mouse survived for 60 weeks). The incidence of mice with papillomas was similar for croton oil and 1,4-dioxane; however, the tumor multiplicity (i.e., number of tumors/mouse) was higher for the croton oil treatment.

Oral administration of 1,4-dioxane in drinking water caused appreciable mortality in rats, but not mice, and increased weight gain in surviving rats and male mice. Histopathological lesions (i.e., unspecified liver and kidney effects) were also reported in exposed male and female rats; however, no histopathological changes were indicated for mice.

1,4-Dioxane was demonstrated to be a tumor promoter, but not a complete carcinogen in mouse skin, in this study. Topical administration for 78 weeks following initiation with dimethylbenzanthracene caused an increase in the incidence and multiplicity of skin tumors in mice. Tumors were also observed at remote sites (i.e., kidney and lung), and survival was affected. Topical application of 1,4-dioxane for 60 weeks in the absence of the initiating treatment produced no effects on skin tumor formation or mortality in mice.

4.2.3.3. *Lundberg et al. (1987)*

Lundberg et al. (1987) evaluated the tumor promoting activity of 1,4-dioxane in rat liver. Male Sprague Dawley rats (8/dose group, 19 for control group) weighing 200 g underwent a partial hepatectomy followed 24 hours later by an i.p. injection of 30 mg/kg diethylnitrosamine (DEN) (initiation treatment). 1,4-Dioxane (99.5% pure with 25 ppm butylated hydroxytoluene as a stabilizer) was then administered daily by gavage (in saline vehicle) at doses of 0, 100, or 1,000 mg/kg-day, 5 days/week for 7 weeks. Control rats were administered saline daily by gavage, following DEN initiation. 1,4-Dioxane was also administered to groups of rats that were not given the DEN initiating treatment (saline used instead of DEN). Ten days after the last dose, animals were sacrificed and liver sections were stained for GGT. The number and total volume of GGT-positive foci were determined.

1,4-Dioxane did not increase the number or volume of GGT-foci in rats that were not given the DEN initiation treatment. The high dose of 1,4-dioxane (1,000 mg/kg-day) given as a promoting treatment (i.e., following DEN injection) produced an increase in the number of GGT-positive foci and the total foci volume. Histopathological changes were noted in the livers of high-dose rats. Enlarged, foamy hepatocytes were observed in the midzonal region of the liver, with the foamy appearance due to the presence of numerous fat-containing cytoplasmic vacuoles. These results suggest that cytotoxic doses of 1,4-dioxane may be associated with tumor promotion of 1,4-dioxane in rat liver.

4.3. REPRODUCTIVE/DEVELOPMENTAL STUDIES—ORAL AND INHALATION

4.3.1. Giavini et al. (1985)

Pregnant female Sprague Dawley rats (18–20 per dose group) were given 1,4-dioxane (99% pure, 0.7% acetal) by gavage in water at concentrations of 0, 0.25, 0.5, or 1 mL/kg-day, corresponding to dose estimates of 0, 250, 500, or 1,000 mg/kg-day (density of 1,4-dioxane is approximately 1.03 g/mL). The chemical was administered at a constant volume of 3 mL/kg on days 6–15 of gestation. Food consumption was determined daily and BWs were measured every 3 days. The dams were sacrificed with chloroform on gestation day 21 and the numbers of corpora lutea, implantations, resorptions, and live fetuses were recorded. Fetuses were weighed and examined for external malformations prior to the evaluation of visceral and skeletal malformations (Wilson's free-hand section method and staining with Alizarin red) and a determination of the degree of ossification.

Maternal weight gain was reduced by 10% in the high-dose group (1,000 mg/kg-day). Food consumption for this group was 5% lower during the dosing period, but exceeded control levels for the remainder of the study. No change from control was observed in the number of implantations, live fetuses, or resorptions; however, fetal birth weight was 5% lower in the highest dose group ($p < 0.01$). 1,4-Dioxane exposure did not increase the frequency of major

malformations or minor anomalies and variants. Ossification of the sternebrae was reduced in the 1,000 mg/kg-day dose group ($p < 0.05$). The study authors suggested that the observed delay in sternebrae ossification combined with the decrease in fetal birth weight indicated a developmental delay related to 1,4-dioxane treatment. NOAEL and LOAEL values of 500 and 1,000 mg/kg-day were identified from this study by EPA and based on delayed ossification of the sternebrae and reduced fetal BWs.

4.4. OTHER DURATION OR ENDPOINT-SPECIFIC STUDIES

4.4.1. Acute and Short-term Toxicity

The acute (≤ 24 hours) and short-term toxicity studies (<30 days) of 1,4-dioxane in laboratory animals are summarized in Table 4-15. Several exposure routes were employed in these studies, including dermal application, drinking water exposure, gavage, vapor inhalation, and i.v. or i.p. injection.

4.4.1.1. *Oral Toxicity*

Mortality was observed in many acute high-dose studies, and LD50 values for 1,4-dioxane were calculated for rats, mice, and guinea pigs (see Table 4-15; Pozzani et al., 1959; Smyth et al., 1941; Laug et al., 1939). Clinical signs of CNS depression were observed, including staggered gait, narcosis, paralysis, coma, and death (Nelson, 1951; Laug et al., 1939; Schrenk and Yant, 1936; de Navasquez, 1935). Severe liver and kidney degeneration and necrosis were often seen in acute studies (JBRC, 1998b; David, 1964; Kesten et al., 1939; Laug et al., 1939; Schrenk and Yant, 1936; de Navasquez, 1935). JBRC (1998b) additionally reported histopathological lesions in the nasal cavity and the brain of rats following 2 weeks of exposure to 1,4-dioxane in the drinking water.

4.4.1.2. *Inhalation Toxicity*

Acute and short-term toxicity studies (all routes) are summarized in Table 4-15. Mortality occurred in many high-concentration studies (Pozzani et al., 1959; Nelson, 1951; Wirth and Klimmer, 1936). Inhalation of 1,4-dioxane caused eye and nasal irritation, altered respiration, and pulmonary edema and congestion (Yant et al., 1930). Clinical signs of CNS depression were observed, including staggered gait, narcosis, paralysis, coma, and death (Nelson, 1951; Wirth and Klimmer, 1936). Liver and kidney degeneration and necrosis were also seen in acute and short-term inhalation studies (Drew et al., 1978; Fairley et al., 1934).

Table 4-15. Acute and short-term toxicity studies of 1,4-dioxane

Animal	Exposure route	Test conditions	Results	Dose[a]	Reference
Oral studies					
Rat (inbred strain and gender unspecified)	Oral via drinking water	1–10 Days of exposure	Ultrastructural changes in the kidney, degenerative nephrosis, hyaline droplet accumulation, crystal formation in mitochondria	11,000 mg/kg-day (5%)	David, 1964
Rat (strain and gender unspecified)	Oral via drinking water	5–12 Days of exposure	Extensive degeneration of the kidney, liver damage, mortality in 8/10 animals by 12 days	11,000 mg/kg-day (5%)	Kesten et al., 1939
F344/DuCrj rat	Oral via drinking water	14-Day exposure	Mortality, decreased BWs, histopathological lesions in the nasal cavity, liver, kidney, and brain	2,500 mg/kg-day (nuclear enlargement of olfactory epithelial cells), >7,500 mg/kg-day for all other effects	JBRC, 1998b
Female Sprague Dawley rat	Gavage	0, 168, 840, 2550, or 4,200 mg/kg by gavage, 21 and 4 hours prior to sacrifice	Increased ODC activity, hepatic CYP450 content, and DNA single-strand breaks	840 mg/kg (ODC activity only)	Kitchin and Brown, 1990
Female Carworth Farms-Nelson rat	Gavage	Determination of a single dose LD_{50}	Lethality	LD_{50} = 6,400 mg/kg (14,200 ppm)	Pozzani et al., 1959
Male Wistar rat, guinea pig	Gavage	Single dose, LD_{50} determination	Lethality	LD_{50} (mg/kg): rat = 7,120 guinea pig = 3,150	Smyth et al., 1941
Rat, mouse, guinea pig	Gavage	Single dose; several dose groups	Clinical signs of CNS depression, stomach hemorrhage, kidney enlargement, and liver and kidney degeneration	LD_{50} (mg/kg): mouse = 5,900 rat = 5,400 guinea pig = 4,030	Laug et al., 1939
Rabbit	Gavage	Single gavage dose of 0, 207, 1,034, or 2,068 mg/kg-day	Clinical signs of CNS depression, mortality at 2068 mg/kg, renal toxicity (polyuria followed by anuria), histopathological changes in liver and kidneys	1,034 mg/kg-day	de Navasquez, 1935
Rat, rabbit	Gavage	Single dose; mortality after 2 weeks	Mortality and narcosis	3,160 mg/kg	Nelson, 1951

Animal	Exposure route	Test conditions	Results	Dose[a]	Reference
Crj:BDF_1 mouse	Oral via drinking water	14-Day exposure	Mortality, decreased BWs, histopathological lesions in the nasal cavity, liver, kidney, and brain	10,800 mg/kg-day; hepatocellular swelling	JBRC, 1998b
Dog	Drinking water ingestion	3–10 Days of exposure	Clinical signs of CNS depression, and liver and kidney degeneration	11,000 mg/kg-day (5%)	Schrenk and Yant, 1936
Inhalation studies					
Male CD1 rat	Vapor inhalation	Serum enzymes measured before and after a single 4 hour exposure	Increase in ALT, AST, and OCT; no change in G-6-Pase	1,000 ppm	Drew et al., 1978
Rat	Vapor inhalation	5 Hours of exposure	Mortality and narcosis	6,000 ppm	Nelson, 1951
Female Carworth Farms-Nelson rat	Vapor inhalation	Determination of a 4-hour inhalation LC_{50}	Lethality	LC_{50} = 51.3 mg/L	Pozzani et al., 1959
Mouse, cat	Vapor inhalation	8 Hours/day for 17 days	Paralysis and death	8,400 ppm	Wirth and Klimmer, 1936
Guinea pig	Vapor inhalation	8-Hour exposure to 0.1–3% by volume	Eye and nasal irritation, retching movements, altered respiration, narcosis, pulmonary edema and congestion, hyperemia of the brain	0.5% by volume	Yant et al., 1930
Rabbit, guinea pig, rat, mouse	Vapor inhalation	3 Hours exposure, for 5 days; 1.5 hour exposure for 1 day	Degeneration and necrosis in the kidney and liver, vascular congestion in the lungs	10,000 ppm	Fairley et al., 1934
Other routes					
Male COBS/Wistar rat	Dermal	Nonoccluded technique using shaved areas of the back and flank; single application, 14-day observation	Negative; no effects noted	8,300 mg/kg	Clark et al., 1984
Rabbit, cat	i.v. injection	Single injection of 0, 207, 1,034, 1,600 mg/kg-day	Clinical signs of CNS depression, narcosis at 1,034 mg/kg, mortality at 1,600 mg/kg	1,034 mg/kg-day	de Navasquez, 1935

Animal	Exposure route	Test conditions	Results	Dose[a]	Reference
Female Sprague Dawley rat	i.p. injection	Single dose; LD_{50} values determined 24 hours and 14 days after injection	Increased serum SDH activity at 1/16th of the LD_{50} dose; no change at higher or lower doses	LD_{50} (mg/kg): 24 hours = 4,848 14 days = 799	Lundberg et al., 1986
CBA/J mouse	i.p. injection	Daily injection for 7 days, 0, 0.1, 1, 5, and 10%	Slightly lower lymphocyte response to mitogens	2,000 mg/kg-day (10%)	Thurman et al., 1978

[a]Lowest effective dose for positive results/ highest dose tested for negative results.
ND = no data; OCT = ornithine carbamyl transferase; ODC = ornithine decarboxylase; SDH = sorbitol dehydrogenase

4.4.2. Neurotoxicity

Clinical signs of CNS depression have been reported in humans and laboratory animals following high dose exposure to 1,4-dioxane (see Sections 4.1 and 4.2.1.1). Neurological symptoms were reported in the fatal case of a worker exposed to high concentrations of 1,4-dioxane through both inhalation and dermal exposure (Johnstone, 1959). These symptoms included headache, elevation in blood pressure, agitation and restlessness, and coma. Autopsy findings demonstrated perivascular widening in the brain, with small foci of demyelination in several regions (e.g., cortex, basal nuclei). It was suggested that these neurological changes may have been secondary to anoxia and cerebral edema. In laboratory animals, the neurological effects of acute high-dose exposure included staggered gait, narcosis, paralysis, coma, and death (Nelson, 1951; Laug et al., 1939; Schrenk and Yant, 1936; de Navasquez, 1935; Yant et al., 1930). The neurotoxicity of 1,4-dioxane was further investigated in several studies described below (Frantik et al., 1994; Kanada et al., 1994; Goldberg et al., 1964; Knoefel, 1935).

4.4.2.1. *Frantik et al. (1994)*

The acute neurotoxicity of 1,4-dioxane was evaluated following a 4-hour inhalation exposure to male Wistar rats (four per dose group) and a 2-hour inhalation exposure to female H-strain mice (eight per dose group). Three exposure groups and a control group were used in this study. Exposure concentrations were not specified, but apparently were chosen from the linear portion of the concentration-effect curve. The neurotoxicity endpoint measured in this study was the inhibition of the propagation and maintenance of an electrically-evoked seizure discharge. This endpoint has been correlated with the behavioral effects and narcosis that occur following acute exposure to higher concentrations of organic solvents. Immediately following 1,4-dioxane exposure, a short electrical impulse was applied through ear electrodes (0.2 seconds, 50 hertz (Hz), 180 volts (V) in rats, 90 V in mice). Several time characteristics of the response were recorded; the most sensitive and reproducible measures of chemically-induced effects were

determined to be the duration of tonic hind limb extension in rats and the velocity of tonic extension in mice.

Linear regression analysis of the concentration-effect data was used to calculate an isoeffective air concentration that corresponds to the concentration producing a 30% decrease in the maximal response to an electrically-evoked seizure. The isoeffective air concentrations for 1,4-dioxane were 1,860 ± 200 ppm in rats and 2,400 ± 420 ppm in mice. A NOAEL value was not identified from this study.

4.4.2.2. *Goldberg et al. (1964)*

Goldberg et al. (1964) evaluated the effect of solvent inhalation on pole climb performance in rats. Female rats (Carworth Farms Elias strain) (eight per dose group) were exposed to 0, 1,500, 3,000, or 6,000 ppm of 1,4-dioxane in air for 4 hours/day, 5 days/weeks, for 10 exposure days. Conditioned avoidance and escape behaviors were evaluated using a pole climb methodology. Prior to exposure, rats were trained to respond to a buzzer or shock stimulus by using avoidance/escape behavior within 2 seconds. Behavioral criteria were the abolishment or significant deferment (>6 seconds) of the avoidance response (conditioned or buzzer response) or the escape response (buzzer plus shock response). Behavioral tests were administered on day 1, 2, 3, 4, 5, and 10 of the exposure period. Rat BWs were also measured on test days.

1,4-Dioxane exposure produced a dose-related effect on conditioned avoidance behavior in female rats, while escape behavior was generally not affected. In the 1,500 ppm group, only one of eight rats had a decreased avoidance response, and this only occurred on days 2 and 5 of exposure. A larger number of rats exposed to 3,000 ppm (two or three of eight) experienced a decrease in the avoidance response, and this response was observed on each day of the exposure period. The maximal decrease in the avoidance response was observed in the 6,000 ppm group during the first 2 days of exposure (75–100% of the animals were inhibited in this response). For exposure days 3–10, the percent of rats in the 6,000 ppm group with significant inhibition of the avoidance response ranged from 37–62%. At the end of the exposure period (day 10), the BWs for rats in the high exposure group were lower than controls.

4.4.2.3. *Kanada et al. (1994)*

Kanada et al. (1994) evaluated the effect of oral exposure to 1,4-dioxane on the regional neurochemistry of the rat brain. 1,4-Dioxane was administered by gavage to male Sprague Dawley rats (5/group) at a dose of 1,050 mg/kg, approximately equal to one-fourth the oral LD50. Rats were sacrificed by microwave irradiation to the head 2 hours after dosing, and brains were dissected into small brain areas. Each brain region was analyzed for the content of biogenic amine neurotransmitters and their metabolites using high-performance liquid chromatography (HPLC) or GC methods. 1,4-Dioxane exposure was shown to reduce the dopamine and serotonin content of the hypothalamus. The neurochemical profile of all other brain regions in exposed rats was similar to control rats.

4.4.2.4. *Knoefel (1935)*

The narcotic potency of 1,4-dioxane was evaluated following i.p. injection in rats and gavage administration in rabbits. Rats were given i.p. doses of 20, 30, or 50 mmol/kg. No narcotic effect was seen at the lowest dose; however, rats given 30 mmol/kg were observed to sleep approximately 8–10 minutes. Rats given the high dose of 50 mmol/kg died during the study. Rabbits were given 1,4-dioxane at oral doses of 10, 20, 50, 75, or 100 mmol/kg. No effect on the normal erect animal posture was observed in rabbits treated with less than 50 mmol/kg. At 50 and 75 mmol/kg, a semi-erect or staggering posture was observed; lethality occurred at both the 75 and 100 mmol/kg doses.

4.5. MECHANISTIC DATA AND OTHER STUDIES IN SUPPORT OF THE MODE OF ACTION

4.5.1. Genotoxicity

The genotoxicity data for 1,4-dioxane are presented in Table 4-16. 1,4-Dioxane has been tested for genotoxic potential using in vitro assay systems with prokaryotic organisms, non-mammalian eukaryotic organisms, and mammalian cells, and in vivo assay systems using several strains of rats and mice. In the large majority of in vitro systems, 1,4-dioxane was not genotoxic. Where a positive genotoxic response was observed, it was generally observed in the presence of toxicity. Similarly, in in vivo systems, 1,4-dioxane was not genotoxic in the majority of available studies. 1,4-Dioxane did not bind covalently to DNA in a single study with calf thymus DNA. Several investigators have reported that 1,4-dioxane caused increased DNA synthesis indicative of cell proliferation. Overall, the available literature indicates that 1,4-dioxane is nongenotoxic or weakly genotoxic.

Negative findings were reported for mutagenicity in in vitro assays with the prokaryotic organisms Salmonella typhimurium, Escherichia coli, and Photobacterium phosphoreum (Mutatox assay) (Morita and Hayashi, 1998; Hellmer and Bolcsfoldi, 1992; Kwan et al., 1990; Khudoley et al., 1987; Nestmann et al., 1984; Haworth et al., 1983; Stott et al., 1981). In in vitro assays with nonmammalian eukaryotic organisms, negative results were obtained for the induction of aneuploidy in yeast (Saccharomyces cerevisiae) and in the sex-linked recessive lethal test in Drosophila melanogaster (Yoon et al., 1985; Zimmerman et al., 1985). In the presence of toxicity, positive results were reported for meiotic nondisjunction in Drosophila (Munoz and Barnett, 2002).

The ability of 1,4-dioxane to induce genotoxic effects in mammalian cells in vitro has been examined in model test systems with and without exogenous metabolic activation and in hepatocytes that retain their xenobiotic-metabolizing capabilities. 1,4-Dioxane was reported as negative in the mouse lymphoma cell forward mutation assay (Morita and Hayashi, 1998; McGregor et al., 1991). 1,4-Dioxane did not produce chromosomal aberrations or micronucleus

formation in Chinese hamster ovary (CHO) cells (Morita and Hayashi, 1998; Galloway et al., 1987). Results were negative in one assay for sister chromatid exchange (SCE) in CHO (Morita and Hayashi, 1998) and were weakly positive in the absence of metabolic activation in another (Galloway et al., 1987). In rat hepatocytes, 1,4-dioxane exposure in vitro caused single-strand breaks in DNA at concentrations also toxic to the hepatocytes (Sina et al., 1983) and produced a positive genotoxic response in a cell transformation assay with BALB/3T3 cells also in the presence of toxicity (Sheu et al., 1988).

1,4-Dioxane was not genotoxic in the majority of available in vivo mammalian assays. Studies of micronucleus formation following in vivo exposure to 1,4-dioxane produced mostly negative results, including studies of bone marrow micronucleus formation in B6C3F$_1$, BALB/c, CBA, and C57BL6 mice (McFee et al., 1994; Mirkova, 1994; Tinwell and Ashby, 1994) and micronucleus formation in peripheral blood of CD1 mice (Morita and Hayashi, 1998; Morita, 1994). Mirkova (1994) reported a dose-related increase in the incidence of bone marrow micronuclei in male and female C57BL6 mice 24 or 48 hours after administration of 1,4-dioxane. At a sampling time of 24 hours, a dose of 450 mg/kg produced no change relative to control, while doses of 900, 1,800, and 3,600 mg/kg increased the incidence of bone marrow micronuclei by approximately two-, three-, and fourfold, respectively. A dose of 5,000 mg/kg also increased the incidence of micronuclei by approximately fourfold at 48 hours. This compares with the negative results for BALB/c male mice tested in the same study at a dose of 5,000 mg/kg and sampling time of 24 hours. Tinwell and Ashby (1994) could not explain the difference in response in the mouse bone marrow micronucleus assay with C57BL6 mice obtained in their laboratory (i.e., nonsignificant 1.6-fold increase over control) with the dose-related positive findings reported by Mirkova (1994) using the same mouse strain, 1,4-dioxane dose (3,600 mg/kg) and sampling time (24 hours). Morita and Hayashi (1998) demonstrated an increase in micronucleus formation in hepatocytes following 1,4-dioxane dosing and partial hepatectomy to induce cellular mitosis. DNA single-strand breaks were demonstrated in hepatocytes following gavage exposure to female rats (Kitchin and Brown, 1990).

Roy et al. (2005) examined micronucleus formation in male CD1 mice exposed to 1,4-dioxane to confirm the mixed findings from earlier mouse micronucleus studies and to identify the origin of the induced micronuclei. Mice were administered 1,4-dioxane by gavage at doses of 0, 1,500, 2,500, and 3,500 mg/kg-day for 5 days. The mice were also implanted with 5-bromo-2-deoxyuridine (BrdU)-releasing osmotic pumps to measure cell proliferation in the liver and to increase the sensitivity of the hepatocyte assay. The frequency of micronuclei in the bone marrow erythrocytes and in the proliferating BrdU-labeled hepatocytes was determined 24 hours after the final dose. Significant dose-related increases in micronuclei were seen in the bone-marrow at all the tested doses ($\geq$ 1,500 mg/kg-day). In the high-dose (3,500-mg/kg) mice, the frequency of bone marrow erythrocyte micronuclei was about 10-fold greater than the control frequency. Significant dose-related increases in micronuclei were also observed at the two

highest doses (≥ 2,500 mg/kg-day) in the liver. Antikinetochore (CREST) staining or pancentromeric fluorescence in situ hybridization (FISH) was used to determine the origin of the induced micronuclei. The investigators determined that 80–90% of the micronuclei in both tissues originated from chromosomal breakage; small increase in micronuclei originating from chromosome loss was seen in hepatocytes. Dose-related statistically significant decreases in the ratio of bone marrow polychromatic erythrocytes (PCE):normochromatic erthyrocytes (NCE), an indirect measure of bone marrow toxicity, were observed. Decreases in hepatocyte proliferation were also observed. Based on these results, the authors concluded that at high doses 1,4-dioxane exerts genotoxic effects in both the mouse bone marrow and liver; the induced micronuclei are formed primarily from chromosomal breakage; and 1,4-dioxane can interfere with cell proliferation in both the liver and bone marrow. The authors noted that reasons for the discrepant micronucleus assay results among various investigators was unclear, but could be related to the inherent variability present when detecting moderate to weak responses using small numbers of animals, as well as differences in strain, dosing regimen, or scoring criteria.

1,4-Dioxane did not affect in vitro or in vivo DNA repair in hepatocytes or in vivo DNA repair in the nasal cavity (Goldsworthy et al., 1991; Stott et al., 1981), but increased hepatocyte DNA synthesis indicative of cell proliferation in several in vivo studies (Miyagawa et al., 1999; Uno et al., 1994; Goldsworthy et al., 1991; Stott et al., 1981). 1,4-Dioxane caused a transient inhibition of RNA polymerase A and B in the rat liver (Kurl et al., 1981), indicating a negative impact on the synthesis of ribosomal and messenger RNA (DNA transcription). Intravenous administration of 1,4-dioxane at doses of 10 or 100 mg/rat produced inhibition of both polymerase enzymes, with a quicker and more complete recovery of activity for RNA polymerase A, the polymerase for ribosomal RNA synthesis.

1,4-Dioxane did not covalently bind to DNA under in vitro study conditions (Woo et al., 1977a). DNA alkylation was also not detected in the liver 4 hours following a single gavage exposure (1,000 mg/kg) in male Sprague Dawley rats (Stott et al., 1981).

Rosenkranz and Klopman (1992) analyzed 1,4-dioxane using the computer automated structure evaluator (CASE) structure activity method to predict its potential genotoxicity and carcinogenicity. The CASE analysis is based on information contained in the structures of approximately 3,000 chemicals tested for endpoints related to mutagenic/genotoxic and carcinogenic potential. CASE selects descriptors (activating [biophore] or inactivating [biophobe] structural fragments) from a learning set of active and inactive molecules. Using the CASE methodology, Rosenkranz and Klopman (1992) predicted that 1,4-dioxane would be inactive for mutagenicity in several in vitro systems, including Salmonella, induction of chromosomal aberrations in CHO cells, and unscheduled DNA synthesis in rat hepatocytes. 1,4-Dioxane was predicted to induce SCE in cultured CHO cells, micronuclei formation in rat bone marrow, and carcinogenicity in rodents.

Gene expression profiling in cultured human hepatoma HepG2 cells was performed using DNA microarrays to discriminate between genotoxic and other carcinogens (van Delft et al., 2004). Van Delft et al. (2004) examined this method using a training set of 16 treatments (nine genotoxins and seven nongenotoxins) and a validation set (three and three), with discrimination models based on Pearson correlation analyses for the 20 most discriminating genes. 1,4-Dioxane was included in the training set as a "nongenotoxic" carcinogen. The gene expression profile for 1,4-dioxane indicated a classification of this chemical as a "nongenotoxic" carcinogen. The correctness for carcinogen classification using this method ranged from 33 to 100%, depending on which chemical data sets and gene expression signals were included in the analysis.

Table 4-16a. Genotoxicity studies of 1,4-dioxane

Test system	Endpoint	Test conditions	Results[a]		Dose[b]	Source
			Without activation	With activation		
Prokaryotic organisms in vitro						
S. typhimurium strains TA98, TA100, TA1535, TA1537	Reverse mutation	Plate incorporation assay	–	–	10,000 µg/plate	Haworth et al., 1983
S. typhimurium strains TA98, TA100, TA1530, TA1535, TA1537	Reverse mutation	Plate incorporation assay	–	–	ND	Khudoley et al., 1987
S. typhimurium strains TA98, TA100, TA1535, TA1537	Reverse mutation	Plate incorporation and preincubation assays	–	–	5,000 µg/plate	Morita and Hayashi, 1998
S. typhimurium strains TA100, TA1535	Reverse mutation	Preincubation assay	–	–	103 mg	Nestmann et al., 1984
S. typhimurium strains TA98, TA100, TA1535, TA1537, TA1538	Reverse mutation	Plate incorporation assay	–	–	103 mg	Stott et al., 1981
E. coli K-12 uvrB/recA	DNA repair	Host mediated assay	–	–	1,150 mmol/L	Hellmer and Bolcsfoldi, 1992
E. coli WP2/WP2uvrA	Reverse mutation	Plate incorporation and preincubation assays	–	–	5,000 µg/plate	Morita and Hayashi, 1998
P. phosphoreum M169	Mutagenicity, DNA damage	Mutatox assay	–	ND	ND	Kwan et al., 1990

Test system	Endpoint	Test conditions	Results[a]		Dose[b]	Source
			Without activation	With activation		
Nonmammalian eukaryotic organisms in vitro						
S. cerevisiae D61.M	Aneuploidy	Standard 16-hour incubation or cold-interruption regimen	–T	ND	4.75%	Zimmerman et al., 1985
D. melanogaster	Meiotic nondisjunction	Oocytes were obtained for evaluation 24 and 48 hours after mating	+T[c]	ND[d]	2% in sucrose media	Munoz and Barnett, 2002
D. melanogaster	Sex-linked recessive lethal test	Exposure by feeding and injection	–	ND[d]	35,000 ppm in feed, 7 days or 50,000 ppm (5% in water) by injection	Yoon et al., 1985
Mammalian cells in vitro						
Rat hepatocytes	DNA damage; single-strand breaks measured by alkaline elution	3-Hour exposure to isolated primary hepatocytes	+T[e]	ND[d]	0.3 mM	Sina et al., 1983
Primary hepatocyte culture from male F344 rats	DNA repair	Autoradiography	–	ND[d]	1 mM	Goldsworthy et al., 1991
L5178Y mouse lymphoma cells	Forward mutation assay	Thymidine kinase mutagenicity assay (trifluorothymidine resistance)	–	–	5,000 µg/mL	McGregor et al., 1991
L5178Y mouse lymphoma cells	Forward mutation assay	Thymidine kinase mutagenicity assay (trifluorothymidine resistance)	–	–T	5,000 µg/mL	Morita and Hayashi, 1998
BALB/3T3 cells	Cell transformation	48-Hour exposure followed by 4 weeks incubation; 13 day exposure followed by 2.5 weeks incubation	+T[f]	ND[d]	0.5 mg/mL	Sheu et al., 1988

Test system	Endpoint	Test conditions	Results[a]		Dose[b]	Source
			Without activation	With activation		
CHO cells	SCE	BrdU was added 2 hours after 1,4-dioxane addition; chemical treatment was 2 hours with S9 and 25 hours without S9	±[g]	–	10,520 µg/mL	Galloway et al., 1987
CHO cells	Chromosomal aberration	Cells were harvested 8–12 hours or 18–26 hours after treatment (time of first mitosis)	–	–	10,520 µg/mL	Galloway et al., 1987
CHO cells	SCE	3 Hour pulse treatment; followed by continuous treatment of BrdU for 23 or 26 hours	–	–	5,000 µg/mL	Morita and Hayashi, 1998
CHO cells	Chromosomal aberration	5 Hour pulse treatment, 20 hour pulse and continuous treatments, or 44 hour continuous treatment; cells were harvested 20 or 44 hours following exposure	–	–	5,000 µg/mL	Morita and Hayashi, 1998

Test system	Endpoint	Test conditions	Results[a]		Dose[b]	Source
			Without activation	With activation		
CHO cells	Micronucleus formation	5 Hour pulse treatment or 44 hour continuous treatment; cells were harvested 42 hours following exposure	–	–	5,000 µg/mL	Morita and Hayashi, 1998
Calf thymus DNA	Covalent binding to DNA	Incubation with microsomes from 3-methylcholanthrene treated rats	–	–	0.04 pmol/mg DNA (bound)	Woo et al., 1977a

[a] + = positive, ± = equivocal or weak positive, – = negative, T = toxicity. Endogenous metabolic activation is not applicable for in vivo studies.
[b] Lowest effective dose for positive results/highest dose tested for negative results; ND = no data.
[c] A dose-related decrease in viability was observed with 0, 2.4, 8.1, 51.7, and 82.8% mortality at concentrations of 1, 1.5, 2, 3, and 3.5%, respectively. In mature oocytes, meiotic nondisjunction was decreased at 2, 3, and 3.5%; however, a dose-response trend was not evident.
[d] Exogenous metabolic activation not used for most tests of fungi and many mammalian cell types in vitro, or in vivo studies in mammals, due to endogenous metabolic ability in many of these systems.
[e] Cell viability was 98, 57, 54, 31, and 34% of control at concentrations 0, 0.03, 0.3, 10, and 30 mM. DNA damage was observed at 0.3, 3, 10, and 30 mM; however, no dose-response trend was observed for the extent of DNA damage (severity score related to the elution rate).
[f] For the 13-day exposure, relative survival was 92, 85, 92, and 61% of control for concentrations of 0.25, 0.5, 1, and 2 mg/mL, respectively. A significant increase in transformation frequency was observed at the highest dose level (2 mg/mL). Similar results were observed for the 48-hour exposure, with increased transformation frequency seen at concentrations of 2, 3, and 4 mg/mL. Concentrations >2 mg/mL also caused a significant decrease in cell survival (relative survival ranged between 6 and 52% of control).
[g] The highest concentration tested (10,520 µg/L) produced a 27% increase in the number of SCE/cell in the absence of S9 mix. No effect was seen at lower doses (1,050 and 3,500 µg/L) in the absence of S9 mix or at any concentration level (1,050, 3,500, 10,500 µg/L) tested in the presence of S9.

Table 4-16b. Genotoxicity studies of 1,4-dioxane; mammalian in vivo

Test system	Endpoint	Test Conditions	Results	Dose	Source
Female Sprague Dawley Rat	DNA damage; single-strand breaks measured by alkaline elution	Two gavage doses given 21 and 4 hours prior to sacrifice	+[h]	2,550 mg/kg	Kitchin and Brown, 1990
Male Sprague Dawley Rat	DNA alkylation in hepatocytes	Gavage; DNA isolation and HPLC analysis 4 hours after dosing	–	1,000 mg/kg	Stott et al., 1981

Test system	Endpoint	Test Conditions	Results	Dose	Source
Male $B6C3F_1$ Mouse	Micronucleus formation in bone marrow	i.p. injection; analysis of polychromatic erythrocytes 24 or 48 hours after dosing	–	Single dose of 4,000 mg/kg; 3 daily doses of 2,000	McFee et al., 1994
Male and female C57BL6 Mouse; male BALB/c Mouse	Micronucleus formation in bone marrow	Gavage; analysis of polychromatic erythrocytes 24 or 48 hours after dosing	+ (C57BL6)[i] – (BALB/c)	900 mg/kg (C57BL6); 5,000 mg/kg (BALB/c)	Mirkova, 1994
Male CD1 Mouse	Micronucleus formation in peripheral blood	Two i.p. injections (1/day); micronucleated reticulocytes measured 24, 48, and 72 hours after the 2nd dose	–	3,200 mg/kg	Morita, 1994
Male CD1 Mouse	Micronucleus formation in hepatocytes	Gavage, partial hepatectomy 24 hours after dosing, hepatocytes analyzed 5 days after hepatectomy	+[j]	2,000 mg/kg	Morita and Hayashi, 1998
Male CD1 Mouse	Micronucleus formation in peripheral blood	Gavage, partial hepatectomy 24 hours after dosing, peripheral blood obtained from tail vein 24 hours after hepatectomy	–	3,000 mg/kg	Morita and Hayashi, 1998
Male CBA and C57BL6 Mouse	Micronucleus formation in bone marrow	Gavage; analysis of polychromatic erythrocytes from specimens prepared 24 hours after dosing	–	3,600 mg/kg	Tinwell and Ashby, 1994
Male CD1 Mouse	Micronuclei formation in bone marrow	Gavage; analysis for micronucleated erythrocytes 24 hours after dosing	+[k]	1,500 mg/kg-day for 5 days	Roy et al., 2005
Male CD1 Mouse	Micronuclei formation in hepatocytes	Gavage; analysis for micronuclei 24 hours after dosing	+[l]	2,500 mg/kg-day for 5 days	Roy et al., 2005
Male Sprague Dawley Rat	DNA repair in hepatocytes	Drinking water; thymidine incorporation with hydroxyurea to repress normal DNA synthesis	–	1,000 mg/kg-day for 11 weeks	Stott et al., 1981
Male F344 Rat	DNA repair in hepatocytes (autoradiography)	Gavage and drinking water exposure; thymidine incorporation	–	1,000 mg/kg for 2 or 12 hours; 1,500 mg/kg-day for 2 weeks or 3,000 mg/kg-day for 1 week	Goldsworthy et al., 1991
Male F344 Rat	DNA repair in nasal epithelial cells from the nasoturbinate or maxilloturbinate	Gavage and drinking water exposure; thymidine incorporation	–	1,500 mg/kg-day for 8 days + 1,000 mg/kg gavage dose 12 hours prior to sacrifice	Goldsworthy et al., 1991
Male F344 Rat	Replicative DNA synthesis (i.e., cell proliferation) in hepatocytes	Gavage and drinking water exposure; thymidine incorporation	+[m] (1–2-week exposure)	1,000 mg/kg for 24 or 48 hours; 1,500 mg/kg-day for 1 or 2 weeks	Goldsworthy et al., 1991

Test system	Endpoint	Test Conditions	Results	Dose	Source
Male F344 Rat	Replicative DNA synthesis (i.e., cell proliferation) in nasal epithelial cells	Drinking water exposure; thymidine incorporation	–	1,500 mg/kg-day for 2 weeks	Goldsworthy et al., 1991
Male Sprague Dawley Rat	RNA synthesis; inhibition of RNA polymerase A and B	i.v. injection; activity measured in isolated hepatocytes	+[n]	10 mg/rat	Kurl et al., 1981
Male F344 Rat	DNA synthesis in hepatocytes	Gavage; thymidine and BrdU incorporation	+[o]	1,000 mg/kg	Miyagawa et al., 1999
Male F344 Rat	DNA synthesis in hepatocytes	Thymidine incorporation	±[p]	2,000 mg/kg	Uno et al., 1994
Male Sprague Dawley Rat	DNA synthesis in hepatocytes	Drinking water; thymidine incorporation	+[q]	1,000 mg/kg-day for 11 weeks	Stott et al., 1981

[a] + = positive, ± = equivocal or weak positive, – = negative, T = toxicity. Endogenous metabolic activation is not applicable for in vivo studies.

[b] Lowest effective dose for positive results/highest dose tested for negative results; ND = no data.

[h] Rats were given doses of 0, 168, 840, 2,550, or 4,200 mg/kg at 4 and 21 hours prior to sacrifice. A 43 and 50% increase in the fraction of DNA eluted was observed for doses of 2,550 and 4,200 mg/kg, respectively. Alkaline elution of DNA was not significantly different from control in the two lowest dose groups (168 and 840 mg/kg).

[i] A dose-related increase in the incidence of bone marrow micronuclei was observed in male and female C57BL6 mice 24 or 48 hours after administration of 1,4-dioxane. A dose of 450 mg/kg produced no change relative to control, while doses of 900, 1,800, 3,600, and 5,000 mg/kg increased the incidence of bone marrow micronuclei by approximately two-,three-, four- and fourfold, respectively.

[j] A dose-related increase in the incidence of hepatocyte micronuclei was observed in partially hepatectomized mice 6 days after administration of 1,4-dioxane. A dose of 1,000 mg/kg produced no change relative to control, while doses of 2,000 and 3,000 mg/kg increased the incidence of hepatocyte micronuclei by 2.4- and 3.4-fold, respectively.

[k] Significant increases in the frequency of micronucleated erythrocytes were observed at each test dose of 1,4-dioxane (1,500, 2,500 and 3,500 mg/kg-day, 5 days/week).

[l] A dose-related increase in the frequency of micronuclei was observed in proliferating cells with micronuclei at 2,500 and 3,500 mg/kg-day, 5 days/week. No increase in the frequency of micronuclei was seen in the non-proliferating cells.

[m] No increase in the hepatocyte labeling index was observed 24 or 48 hours following a single gavage exposure of 1,000 mg/kg. Continuous administration of 1% 1,4-dioxane in the drinking water for up to 2 weeks produced a twofold increase in the hepatocyte labeling index.

[n] A similar pattern of RNA polymerase inhibition was observed at doses of 10 and 100 mg/rat. Inhibition was more pronounced at the higher dose.

[o] Hepatocyte viability was 86, 89, 87, 88, 78, and 86% 24 hours following exposure to 0, 1,000, 1,500, 2,000, or 4,000 mg/kg. The incidence (%) of replicative DNA synthesis was increased by 2.5-fold (1,000 mg/kg) or 4.5-fold (1,500 and 2,000 mg/kg). No increase in replicative DNA synthesis was observed at the highest dose (4,000 mg/kg).

[p] Replicative DNA synthesis was measured 24, 39, and 48 hours following a single dose of 0, 1,000, or 2,000 mg/kg. Hepatocyte viability ranged from 71 to 82%. The only increase in replicative DNA synthesis was observed 24 hours after administration of 2,000 mg/kg (threefold increase). Cell viability for this group was 79%.

[q] Replicative DNA synthesis was increased 1.5-fold in rats given 1,000 mg/kg of 1,4-dioxane for 11 weeks. No change from control was observed in rats exposed to 10 mg/kg for 11 weeks or rats acutely exposed to 10, 100, or 1,000 mg/kg.

4.5.2. Mechanistic Studies

4.5.2.1. *Free Radical Generation*

Burmistrov et al. (2001) investigated the effect of 1,4-dioxane inhalation on free radical processes in the rat ovary and brain. Female rats (6–9/group, unspecified strain) were exposed to 0, 10, or 100 mg/m^3 of 1,4-dioxane vapor for 4 hours/day, 5 days/week, for 1 month. Rats were sacrificed during the morning or evening following exposure and the ovaries and brain cortex were removed and frozen. Tissue preparations were analyzed for catalase activity, glutathione peroxidase activity, and protein peroxidation. 1,4-Dioxane inhalation was shown to increase glutathione peroxidase activity at the 100 mg/m^3 exposure level only in both rat ovary and rat brain. No change in catalase activity or protein peroxidation was observed at either concentration. A circadian rhythm for glutathione peroxidase activity was absent in control rats, but occurred in rat brain and ovary following 1,4-dioxane exposure.

4.5.2.2. *Induction of Metabolism*

The metabolism of 1,4-dioxane is discussed in detail in Section 3.3. 1,4-Dioxane has been shown to induce its own metabolism (Young et al., 1978a, b). Nannelli et al. (2005) characterized the CYP450 isozymes that were induced by 1,4-dioxane in the liver, kidney, and nasal mucosa of the rat. In the liver, the activities of several CYP450 isozymes were increased (i.e., CYP2B1/2, CYP2E1, CYPC11); however, only CYP2E1 was inducible in the kidney and nasal mucosa. CYP2E1 mRNA was increased approximately two- to threefold in the kidney and nasal mucosa, but mRNA levels were not increased in the liver, suggesting that regulation of CYP2E1 is organ-specific. Induction of hepatic CYPB1/2 and CYP2E1 levels by phenobarbital or fasting did not increase the liver toxicity of 1,4-dioxane, as measured by hepatic glutathione content or serum ALT activity. This result suggested that highly reactive and toxic intermediates did not play a large role in the liver toxicity of 1,4-dioxane, even under conditions where metabolism was enhanced. This finding was supported by a previous comparison of the pharmacokinetic profile of 1,4-dioxane with the toxicology data from a chronic drinking water study (Kociba et al., 1975). This analysis indicated that liver toxicity and eventual tumor formation occurred only at doses where clearance pathways were saturated and elimination of 1,4-dioxane from the blood was reduced. Nannelli et al. (2005) further suggested that a sustained induction of CYP2E1 may lead to generation of reactive oxygen species contributing to target organ toxicity and regenerative cell proliferation; however, no data were provided to support this hypothesis.

4.5.2.3. *Mechanisms of Tumor Induction*

Several studies have been performed to evaluate potential mechanisms for the carcinogenicity of 1,4-dioxane (Goldsworthy et al., 1991; Kitchin and Brown, 1990; Stott et al., 1981). Stott et al. (1981) evaluated 1,4-dioxane in several test systems, including salmonella

mutagenicity in vitro, rat hepatocyte DNA repair activity in vitro, DNA synthesis determination in male Sprague Dawley rats following acute gavage dosing or an 11-week drinking water exposure (described in Section 4.2.1), and hepatocyte DNA alkylation and DNA repair following a single gavage dose. This study used doses of 0, 10, 100, or 1,000 mg/kg-day, with the highest dose considered to be a tumorigenic dose level. Liver histopathology and liver to BW ratios were also evaluated in rats from acute gavage or repeated dose drinking water experiments.

The histopathology evaluation indicated that liver cytotoxicity (i.e., centrilobular hepatocyte swelling) was present in rats from the 1,000 mg/kg-day dose group that received 1,4-dioxane in the drinking water for 11 weeks (Stott et al., 1981). An increase in the liver to BW ratio accompanied by an increase in hepatic DNA synthesis was also seen in this group of animals. No effect on histopathology, liver weight, or DNA synthesis was observed in acutely exposed rats or rats that were exposed to a lower dose of 10 mg/kg-day for 11 weeks. 1,4-Dioxane produced negative findings in the remaining genotoxicity assays conducted as part of this study (i.e., Salmonella mutagenicity, in vitro and in vivo rat hepatocyte DNA repair, and DNA alkylation in rat liver). The study authors suggested that the observed lack of genotoxicity at tumorigenic and cytotoxic dose levels indicates an epigenetic mechanism for 1,4-dioxane hepatocellular carcinoma in rats.

Goldsworthy et al. (1991) evaluated potential mechanisms for the nasal and liver carcinogenicity of 1,4-dioxane in the rat. DNA repair activity was evaluated as a measure of DNA reactivity and DNA synthesis was measured as an indicator of cell proliferation or promotional activity. In vitro DNA repair was evaluated in primary hepatocyte cultures from control and 1,4-dioxane-treated rats (1 or 2% in the drinking water for 1 week). DNA repair and DNA synthesis were also measured in vivo following a single gavage dose of 1,000 mg/kg, a drinking water exposure of 1% (1,500 mg/kg-day) for 1 week, or a drinking water exposure of 2% (3,000 mg/kg-day) for 2 weeks. Liver to BW ratios and palmitoyl CoA oxidase activity were measured in the rat liver to determine whether peroxisome proliferation played a role in the liver carcinogenesis of 1,4-dioxane. In vivo DNA repair was evaluated in rat nasal epithelial cells derived from either the nasoturbinate or the maxilloturbinate of 1,4-dioxane-treated rats. These rats received 1% 1,4-dioxane (1,500 mg/kg-day) in the drinking water for 8 days, followed by a single gavage dose of 10, 100, or 1,000 mg/kg 12 hours prior to sacrifice. Archived tissues from the NCI (1978) bioassay were reexamined to determine the primary sites for tumor formation in the nasal cavity following chronic exposure in rats. Histopathology and cell proliferation were determined for specific sites in the nasal cavity that were related to tumor formation. This evaluation was performed in rats that were exposed to drinking water containing 1% 1,4-dioxane (1,500 mg/kg-day) for 2 weeks.

1,4-Dioxane and its metabolite 1,4-dioxane-2-one did not affect in vitro DNA repair in primary hepatocyte cultures (Goldsworthy et al., 1991). In vivo DNA repair was also unaffected by acute gavage exposure or ingestion of 1,4-dioxane in the drinking water for a 1- or 2-week

period. Hepatocyte cell proliferation was not affected by acute gavage exposure, but was increased approximately twofold following a 1–2-week drinking water exposure. A 5-day drinking water exposure to 1% 1,4-dioxane (1,500 mg/kg-day) did not increase the activity of palmitoyl coenzyme A or the liver to BW ratio, suggesting that peroxisome proliferation did not play a role in the hepatocarcinogenesis of 1,4-dioxane. Nannelli et al. (2005) also reported a lack of hepatic palmitoyl CoA induction following 10 days of exposure to 1.5% 1,4-dioxane in the drinking water (2,100 mg/kg-day).

Treatment of rats with 1% (1,500 mg/kg-day) 1,4-dioxane for 8 days did not alter DNA repair in nasal epithelial cells (Goldsworthy et al., 1991). The addition of a single gavage dose of up to 1,000 mg/kg 12 hours prior to sacrifice also did not induce DNA repair. Reexamination of tissue sections from the NCI (1978) bioassay suggested that the majority of nasal tumors were located in the dorsal nasal septum or the nasoturbinate of the anterior portion of the dorsal meatus (Goldsworthy et al., 1991). No histopathological lesions were observed in nasal section of rats exposed to drinking water containing 1% 1,4-dioxane (1,500 mg/kg-day) for 2 weeks and no increase was observed in cell proliferation at the sites of highest tumor formation in the nasal cavity.

Female Sprague Dawley rats (three to nine per group) were given 0, 168, 840, 2,550, or 4,200 mg/kg 1,4-dioxane (99% purity) by corn oil gavage in two doses at 21 and 4 hours prior to sacrifice (Kitchin and Brown, 1990). DNA damage (single-strand breaks measured by alkaline elution), ODC activity, reduced glutathione content, and CYP450 content were measured in the liver. Serum ALT activity and liver histopathology were also evaluated. No changes were observed in hepatic reduced glutathione content or ALT activity. Light microscopy revealed minimal to mild vacuolar degeneration in the cytoplasm of hepatocytes from three of five rats from the 2,550 mg/kg dose group. No histopathological lesions were seen in any other dose group, including rats given a higher dose of 4,200 mg/kg. 1,4-Dioxane caused 43 and 50% increases in DNA single-strand breaks at dose levels of 2,550 and 4,200 mg/kg, respectively. CYP450 content was also increased at the two highest dose levels (25 and 66% respectively). ODC activity was increased approximately two-, five-, and eightfold above control values at doses of 840, 2,550, and 4,200 mg/kg, respectively. The results of this study demonstrated that hepatic DNA damage can occur in the absence of significant cytotoxicity. Parameters associated with tumor promotion (i.e., ODC activity, CYP450 content) were also elevated, suggesting that promotion may play a role in the carcinogenesis of 1,4-dioxane.

4.6. SYNTHESIS OF MAJOR NONCANCER EFFECTS

Liver and kidney toxicity were the primary noncancer health effects associated with exposure to 1,4-dioxane in humans and laboratory animals. Several fatal cases of hemorrhagic nephritis and centrilobular necrosis of the liver were related to occupational exposure (i.e., inhalation and dermal contact) to 1,4-dioxane (Johnstone, 1959; Barber, 1934). Neurological

changes were also reported in one case; including, headache, elevation in blood pressure, agitation and restlessness, and coma (Johnstone, 1959). Perivascular widening was observed in the brain of this worker, with small foci of demyelination in several regions (e.g., cortex, basal nuclei). Liver and kidney degeneration and necrosis were observed in acute oral and inhalation studies (JBRC, 1998b; Drew et al., 1978; David, 1964; Kesten et al., 1939; Laug et al., 1939; Schrenk and Yant, 1936; de Navasquez, 1935; Fairley et al., 1934). The results of subchronic and chronic studies are discussed below.

4.6.1. Oral

Table 4-17 presents a summary of the noncancer results for the subchronic and chronic oral studies of 1,4-dioxane toxicity in experimental animals. Liver and kidney toxicity were the primary noncancer health effects of oral exposure to 1,4-dioxane in animals. Kidney damage at high doses was characterized by degeneration of the cortical tubule cells, necrosis with hemorrhage, and glomerulonephritis (NCI, 1978; Kociba et al., 1974; Argus et al., 1973, 1965; Fairley et al., 1934). Renal cell degeneration generally began with cloudy swelling of cells in the cortex (Fairley et al., 1934). Nuclear enlargement of proximal tubule cells was observed at doses below those producing renal necrosis (Kano et al., 2008; JBRC, 1998a), but is of uncertain toxicological significance. The lowest dose reported to produce kidney damage was 94 mg/kg-day, which produced renal degeneration and necrosis of tubule epithelial cells in male rats in the Kociba et al. (1974) study. Cortical tubule degeneration was seen at higher doses in the NCI (1978) bioassay (240 mg/kg-day, male rats), and glomerulonephritis was reported for rats given doses of ≥ 430 mg/kg-day (Argus et al., 1965, 1973).

Table 4-17. Oral toxicity studies (noncancer effects) for 1,4-dioxane

Species	Dose/duration	NOAEL (mg/kg-day)	LOAEL (mg/kg-day)	Effect	Reference
Subchronic studies					
Rat and mouse (6/species); unknown strain	Rats 0 or 1,900 mg/kg-day; mice 0 or 3,300 mg/kg-day for 67 days	NA	1,900 rats 3,300 mice	Renal cortical degeneration and necrosis, hemorrhage; hepatocellular degeneration	Fairley et al., 1934
Male Sprague Dawley Rat (4–6/group)	0, 10, or 1,000 mg/kg-day for 11 weeks	10	1,000	Minimal centrilobular hepatocyte swelling; increased DNA synthesis	Stott et al., 1981
F344/DuCrj rat (10/sex/group)	Males 0, 52, 126, 274, 657, or 1,554 mg/kg-day; females 0, 83, 185, 427, 756, or 1,614 mg/kg-day for 13 weeks	52	126	Nuclear enlargement of nasal respiratory epithelium; hepatocyte swelling	Kano et al., 2008

Species	Dose/duration	NOAEL (mg/kg-day)	LOAEL (mg/kg-day)	Effect	Reference
Crj:BDF_1 Mouse (10/sex/group)	Males 0, 86, 231, 585, 882, or 1,570 mg/kg-day; females 0, 170, 387, 898, 1,620, or 2,669 mg/kg-day for 13 weeks	170	387	Nuclear enlargement of bronchial epithelium	Kano et al., 2008
Chronic studies					
Male Wistar Rat (26 treated, 9 controls)	0 or 640 mg/kg-day for 63 weeks	NA	640	Hepatocytes with enlarged hyperchromic nuclei; glomerulonephritis	Argus et al., 1965
Male Sprague Dawley rats (30/group)	0, 430, 574, 803, or 1,032 mg/kg-day for 13 months	NA	430	Hepatocytomegaly; glomerulonephritis	Argus et al., 1973
Sherman rat (60/sex/dose group)	Males 0, 9.6, 94, or 1,015 mg/kg-day; females 0, 19, 148, or 1,599 mg/kg-day for 2 years	9.6	94	Degeneration and necrosis of renal tubular cells and hepatocytes	Kociba et al., 1974
Osborne-Mendel rat (35/sex/dose level)	Males 0, 240, or 530 mg/kg-day; females 0, 350, or 640 mg/kg-day for 110 weeks	NA	240	Pneumonia, gastric ulcers, and cortical tubular degeneration in the kidney	NCI, 1978
B6C3F_1 mouse (50/sex/dose level)	Males 0, 720, or 830 mg/kg-day; females 0, 380, or 860 mg/kg-day for 90 weeks	NA	380	Pneumonia and rhinitis	NCI, 1978
F344/DuCrj rat (50/sex/dose level)	Males 0, 16, 81, or 398 mg/kg-day; females 0, 21, 103, or 514 mg/kg-day for 2 years	81	398	Atrophy of nasal olfactory epithelium; nasal adhesion and inflammation	JBRC, 1998a
F344/DuCrj rat (50/sex/dose level)	Males 0, 16, 81, or 398 mg/kg-day; females 0, 21, 103, or 514 mg/kg-day for 2 years	16	81	Liver hyperplasia	JBRC, 1998a
F344/DuCrj rat (50/sex/dose level)	Males 0, 16, 81, or 398 mg/kg-day; females 0, 21, 103, or 514 mg/kg-day for 2 years	81	398	Increases in serum liver enzymes (GOT, GPT, LDH, and ALP)	JBRC, 1998a
Crj:BDF_1 mouse (50/sex/dose level)	Males 0, 66, 251 or 768 mg/kg-day; females 0, 77, 323, or 1,066 mg/kg-day for 2 years	77	323	Nasal inflammation	JBRC, 1998a
Crj:BDF_1 mouse (50/sex/dose level)	Males 0, 66, 251 or 768 mg/kg-day; females 0, 77, 323, or 1,066 mg/kg-day for 2 years	66	251	Increases in serum liver enzymes (GOT, GPT, LDH, and ALP)	JBRC, 1998a
Developmental studies					
Sprague Dawley rat (18–20/group)	Pregnant dams 0, 250, 500, or 1,000 mg/kg-day on gestation days 6–15	500	1,000	Delayed ossification of the sternebrae and reduced fetal BWs	Giavini et al., 1985

Liver effects included degeneration and necrosis, hepatocyte swelling, cells with hyperchromic nuclei, spongiosis hepatis, hyperplasia, and clear and mixed cell foci of the liver (Kano et al., 2008; NCI, 1978; Kociba et al., 1974; Argus et al., 1965, 1973; Fairley et al., 1934). Hepatocellular degeneration and necrosis were seen at high doses in a subchronic study (1,900 mg/kg-day in rats) (Fairley et al., 1934) and at lower doses in a chronic study (94 mg/kg-day, male rats) (Kociba et al., 1974). Argus et al. (1973) described a progression of preneoplastic effects in the liver of rats exposed to a dose of 575 mg/kg-day. Early changes (8 months exposure) were described as an increased nuclear size of hepatocytes, disorganization of the rough endoplasmic reticulum, an increase in smooth endoplasmic reticulum, a decrease in glycogen, an increase in lipid droplets in hepatocytes, and formation of liver nodules. Spongiosis hepatis, hyperplasia, and clear and mixed-cell foci were also observed in the liver of rats (doses > 81 mg/kg-day in male rats) (JBRC, 1998a). Clear and mixed-cell foci are commonly considered preneoplastic changes and would not be considered evidence of noncancer toxicity when observed in conjunction with tumor formation. If exposure to 1,4-dioxane had not resulted in tumor formation, these lesions could represent potential noncancer toxicity. The nature of spongiosis hepatis as a preneoplastic change is less well understood (Bannash, 2003; Karbe and Kerlin, 2002; Stroebel et al., 1995). Spongiosis hepatis is a cyst-like lesion that arises from the perisinusoidal Ito cells of the liver. This change is sometimes associated with hepatocellular hypertrophy and liver toxicity (Karbe and Kerlin, 2002), but may also occur in combination with preneoplastic foci, or hepatocellular adenoma or carcinoma (Bannash et al., 2003; Stroebel et al., 1995). In the case of the JBRC (1998a) study, spongiosis hepatis was associated with other preneoplastic changes in the liver (hyperplasia, clear and mixed-cell foci). No other lesions indicative of liver toxicity were seen in this study; therefore, spongiosis hepatis was not considered indicative of noncancer effects. The activity of serum enzymes (i.e., AST, ALT, LDH, and ALP) was increased in rats and mice exposed to 1,4-dioxane, although only in groups with high incidence of liver tumors. Blood samples were collected only at the end of the 2-year study, so altered serum chemistry may be associated with the tumorigenic changes in the liver.

Hematological changes were reported in the JBRC (1998a) study only. Observed increases in RBCs, hematocrit, hemoglobin in high-dose male mice (768 mg/kg-day) may be related to lower drinking water consumption (74% of control drinking water intake). Hematological effects noted in male rats given 81 mg/kg-day (decreased RBCs, hemoglobin, hematocrit, increased platelets) were within 20% of control values. A reference range database for hematological effects in laboratory animals (Wolford et al., 1986) indicates that a 20% change in these parameters may fall within a normal range (10th–90th percentile values) and may not represent a treatment-related effect of concern.

Rhinitis and inflammation of the nasal cavity were reported in both the NCI (1978) (mice only, dose ≥380 mg/kg-day) and JBRC (1998a) studies (≥98 mg/kg-day in rats, >323 mg/kg-day in mice). The JBRC (1998a) study also demonstrates atrophy of the nasal epithelium and adhesion in rats and mice. Nasal inflammation may be a response to direct contact of the nasal mucosa with drinking water containing 1,4-dioxane (Sweeney et al., 2008; Goldsworthy et al., 1991) or could result from systemic exposure. Regardless, inflammation may indicate toxicity due to 1,4-dioxane exposure. A significant increase in the incidence of pneumonia was reported in mice from the NCI (1978) study. The significance of this effect is unclear, as it was not observed in other studies that evaluated lung histopathology (Kano et al., 2008; JBRC, 1998a; Kociba et al., 1974). No studies were available regarding the potential for 1,4-dioxane to cause immunological effects. Metaplasia and hyperplasia of the nasal epithelium were also observed in high-dose male and female rats (JBRC, 1998a); however, these effects are likely to be associated with the formation of nasal cavity tumors in these dose groups. Nuclear enlargement of the nasal olfactory epithelium was observed at a dose of 103 mg/kg-day in female rats (JBRC, 1998a); however, it is unclear whether this alteration represents an adverse toxicological effect. Nuclear enlargement of the tracheal and bronchial epithelium and an accumulation of foamy cells in the lung were also seen in male and female mice give 1,4-dioxane at doses of ≥323 mg/kg for 2 years.

4.6.2. Inhalation

Only one subchronic study (Fairley et al., 1934) and one chronic inhalation study (Torkelson et al., 1974) were identified. In the subchronic study, rabbits, guinea pigs, rats, and mice (3–6/species/group) were exposed to 1,000, 2,000, 5,000, or 10,000 ppm of 1,4-dioxane vapor for 16.5 hours/week. Animals were exposed until death occurred or were sacrificed at varying time periods. Severe liver and kidney damage and acute vascular congestion of the lungs were observed. Kidney damage was described as patchy degeneration of cortical tubules with vascular congestion and hemorrhage. Liver lesions varied from cloudy hepatocyte swelling to large areas of necrosis. Torkelson et al. (1974) performed a chronic inhalation study in which male and female Wistar rats (288/sex) were exposed to 111 ppm 1,4-dioxane vapor for 7 hours/day, 5 days/week for 2 years. Control rats (192/sex) were exposed to filtered air. No significant effects were observed on BWs, survival, organ weights, hematology, clinical chemistry, or histopathology. These studies were not sufficient to characterize the inhalation risks of 1,4-dioxane, due to the nature of the available data (i.e., free-standing LOAEL and NOAEL values).

4.6.3. Mode of Action Information

The metabolism of 1,4-dioxane in humans was extensive at low doses (<50 ppm). The linear elimination of 1,4-dioxane in both plasma and urine indicated that 1,4-dioxane metabolism

was a nonsaturated, first-order process at this exposure level (Young et al., 1977, 1976). Like humans, rats extensively metabolized inhaled 1,4-dioxane; however, plasma data from rats given single i.v. doses of 3, 10, 30, 100, or 1,000 mg [^{14}C]-1,4-dioxane/kg demonstrated a dose-related shift from linear, first-order to nonlinear, saturable metabolism of 1,4-dioxane (Young et al., 1978a, b).

1,4-Dioxane oxidation appeared to be CYP450-mediated, as CYP450 induction with phenobarbital or Aroclor 1254 and suppression with 2,4-dichloro-6-phenylphenoxy ethylamine or cobaltous chloride was effective in significantly increasing and decreasing, respectively, the appearance of HEAA in the urine of rats (Woo et al., 1978, 1977c). 1,4-Dioxane itself induced CYP450-mediated metabolism of several barbiturates in Hindustan mice given i.p. injections of 25 and 50 mg/kg of 1,4-dioxane (Mungikar and Pawar, 1978). The differences between single and multiple doses in urinary and expired radiolabel support the notion that 1,4-dioxane may induce its own metabolism. 1,4-Dioxane has been shown to induce several isoforms of CYP450 in various tissues following acute oral administration by gavage or drinking water (Nannelli et al., 2005). In the liver, the activity of several CYP450 isozymes was increased (i.e., CYP2B1/2, CYP2E1, CYPC11); however, only CYP2E1 was inducible in the kidney and nasal mucosa. CYP2E1 mRNA was increased approximately two- to threefold in the kidney and nasal mucosa, but mRNA levels were not increased in the liver, suggesting that regulation of CYP2E1 was organ-specific.

Nannelli et al. (2005) investigated the role of CYP450 isozymes in the liver toxicity of 1,4-dioxane. Hepatic CYPB1/2 and CYP2E1 levels were induced by phenobarbital or fasting and liver toxicity was measured as hepatic glutathione content or serum ALT activity. No increase in glutathione content or ALT activity was observed, suggesting that highly reactive and toxic intermediates did not play a large role in the liver toxicity of 1,4-dioxane, even under conditions where metabolism was enhanced. Pretreatment with inducers of mixed-function oxidases also did not significantly change the extent of covalent binding in subcellular fractions (Woo et al., 1977a). Covalent binding was measured in liver, kidney, spleen, lung, colon, and skeletal muscle 1–12 hours after i.p. dosing with 1,4-dioxane. Covalent binding was highest in liver, spleen, and colon. Within hepatocytes, 1,4-dioxane distribution was greatest in the cytosolic fraction, followed by the microsomal, mitochondrial, and nuclear fractions.

The absence of an increase in toxicity following an increase in metabolism suggests that accumulation of the parent compound may be related to 1,4-dioxane toxicity. This hypothesis is supported by a comparison of the pharmacokinetic profile of 1,4-dioxane with the toxicology data from a chronic drinking water study (Kociba et al., 1975). This analysis indicated that liver toxicity did not occur unless clearance pathways were saturated and elimination of 1,4-dioxane from the blood was reduced. Alternative metabolic pathways (i.e., not CYP450 mediated) may be present at high doses of 1,4-dioxane; however, the available studies have not characterized

these pathways or identified any possible reactive intermediates. The mechanism by which 1,4-dioxane induces tissue damage is not known.

4.7. EVALUATION OF CARCINOGENICITY

4.7.1. Summary of Overall Weight of Evidence

Under the Guidelines for Carcinogen Risk Assessment (U.S. EPA, 2005a), 1,4-dioxane can be described as likely to be carcinogenic to humans, based on adequate evidence of liver carcinogenicity in several 2-year bioassays conducted in three strains of rats, two strains of mice, and in guinea pigs (JBRC, 1998a; NCI, 1978; Kociba et al., 1974; Argus et al., 1973; Hoch-Ligeti and Argus, 1970; Hoch-Ligeti et al., 1970; Argus et al., 1965). Additionally, mesothiolomas of the peritoneam (JBRC, 1998a), mammary (JBRC, 1998a), and nasal tumors (JBRC, 1998a; NCI, 1978; Kociba et al., 1974; Argus et al., 1973; Hoch-Ligeti et al., 1970) have been observed in rats due to exposure to 1,4-dioxane. Studies in humans are inconclusive regarding evidence for a causal link between occupational exposure to 1,4-dioxane and increased risk for cancer; however, only two studies were available and these were limited by small cohort size and a small number of reported cancer cases (Buffler et al., 1978; Thiess et al., 1976).

The available evidence is inadequate to establish a mode of action (MOA) by which 1,4-dioxane induces liver tumors in rats and mice. A MOA hypothesis involving sustained proliferation of spontaneously transformed liver cells has some support from data indicating that 1,4-dioxane acts as a tumor promoter in mouse skin and rat liver bioassays (Lundberg et al.,1987; King et al., 1973). Dose-response and temporal data support the occurrence of cell proliferation and hyperplasia prior to the development of liver tumors (JBRC, 1998a; Kociba et al., 1974) in the rat model. However, the dose-response relationship for induction of hepatic cell proliferation has not been characterized, and it is unknown if it would reflect the dose-response relationship for liver tumors in the 2-year rat and mouse studies. Conflicting data from rat and mouse bioassays (JBRC, 1998a; Kociba et al., 1974) suggest that cytotoxicity may not be a required precursor event for 1,4-dioxane-induced cell proliferation. Data regarding a plausible dose response and temporal progression (see Table 4-18) from cytotoxicity and cell proliferation to eventual liver tumor formation are not available.

The MOA by which 1,4-dioxane produces liver, nasal, peritoneal (mesothiolomas), and mammary gland tumors is unknown, and the available data do not support any hypothesized carcinogenic MOA for 1,4-dioxane.

4.7.2. Synthesis of Human, Animal, and Other Supporting Evidence

Human studies of occupational exposure to 1,4-dioxane were inconclusive; in each case, the cohort size and number of reported cases were of limited size (Buffler et al., 1978; Thiess et al., 1976).

Several carcinogenicity bioassays have been conducted for 1,4-dioxane in mice, rats, and guinea pigs (JBRC, 1998a; NCI, 1978; Kociba et al., 1974; Torkelson et al., 1974; Argus et al., 1973; Hoch-Ligeti and Argus, 1970; Hoch-Ligeti et al., 1970; Argus et al., 1965). Liver tumors have been observed following drinking water exposure in male Wistar rats (Argus et al., 1965), male guinea pigs (Hoch-Ligeti and Argus, 1970), male Sprague Dawley rats (Argus et al., 1973; Hoch-Ligeti et al., 1970), male and female Sherman rats (Kociba et al., 1974), female Osborne-Mendel rats (NCI, 1978), male and female F344/DuCrj rats (JBRC, 1998a), male and female $B6C3F_1$ mice (NCI, 1978), and male and female Crj:BDF_1 mice (JBRC, 1998a). In the earliest cancer bioassays, the liver tumors were described as hepatomas (Argus et al., 1973; Hoch-Ligeti and Argus, 1970; Hoch-Ligeti et al., 1970; Argus et al., 1965); however, later studies made a distinction between hepatocellular carcinoma and hepatocellular adenoma (JBRC, 1998a; NCI, 1978; Kociba et al., 1974). Both tumor types have been seen in rats and mice exposed to 1,4-dioxane. Kociba et al. (1974) noted evidence of liver toxicity at or below the dose levels that produced liver tumors but did not report incidence data for these effects. Hepatocellular degeneration and necrosis were observed in the mid- and high-dose groups of male and female Sherman rats exposed to 1,4-dioxane, while tumors were only observed at the highest dose. Hepatic regeneration was indicated in the mid- and high-dose groups by the formation of hepatocellular hyperplastic nodules. Findings from JBRC (1998a) also provided evidence of liver hyperplasia in male F344/DuCrj rats at a dose level below the dose that induced a statistically significant increase in tumor formation.

Nasal cavity tumors were also observed in Sprague Dawley rats (Argus et al., 1973; Hoch-Ligeti et al., 1970), Osborne-Mendel rats (NCI, 1978), Sherman rats (Kociba et al., 1974), and F344/DuCrj rats (JBRC, 1998a). Most tumors were characterized as squamous cell carcinomas. Nasal tumors were not elevated in $B6C3F_1$ or Crj:BDF_1 mice. JBRC (1998a) was the only study that evaluated nonneoplastic changes in nasal cavity tissue following prolonged exposure to 1,4-dioxane in the drinking water. Histopathological lesions in female F344/DuCrj rats were suggestive of toxicity and regeneration in this tissue (i.e., atrophy, adhesion, inflammation, nuclear enlargement, and hyperplasia and metaplasia of respiratory and olfactory epithelium). Some of these effects occurred at a lower dose (103 mg/kg-day) than that shown to produce nasal cavity tumors (513 mg/kg-day). Reexamination of tissue sections from the NCI (1978) bioassay suggested that the majority of nasal tumors were located in the dorsal nasal septum or the nasoturbinate of the anterior portion of the dorsal meatus. Nasal tumors were not observed in an inhalation study in Wistar rats exposed to 111 ppm for 5 days/week for 2 years (Torkelson et al., 1974). It is unlikely that 1,4-dioxane in expired air following a drinking water exposure could exceed this air concentration.

Tumor initiation and promotion studies in mouse skin and rat liver suggested that 1,4-dioxane does not initiate the carcinogenic process, but instead acts as a tumor promoter (Lundberg et al., 1987; Bull et al., 1986; King et al., 1973) (see Section 4.2.3).

In addition to the liver and nasal tumors observed in several studies, a statistically significant increase in mesotheliomas of the peritoneum was seen in male rats from the JBRC (1998a) study. Female rats also showed a statistically significant increase in mammary gland adenomas. A significant increase in the incidence of these tumors was not observed in other chronic oral bioassays of 1,4-dioxane (NCI, 1978; Kociba et al., 1974).

4.7.3. Mode of Action Information

The MOA by which 1,4-dioxane produces liver, nasal, peritoneal (mesothiolomas), and mammary gland tumors is unknown, and the available data do not support any hypothesized mode of carcinogenic action for 1,4-dioxane. The hypothesized MOAs for 1,4-dioxane carcinogenicity are discussed below within the context of the modified Hill criteria of causality as recommended in the most recent Agency guidelines (U.S. EPA, 2005a). The hypothesized MOA(s) presented in the following sections were not explored for peritoneal or mammary gland tumors due to the absence of any chemical specific information for these tumor types.

4.7.3.1. *Identification of Key Events for Carcinogenicity*

4.7.3.1.1. ***Liver.*** A key event in this MOA hypothesis is sustained proliferation of spontaneously transformed liver cells, resulting in the eventual formation of liver tumors. Precursor events in which 1,4-dioxane may promote proliferation of transformed liver cells are uncertain. One study suggests that induced liver cytotoxicity may be a key precursor event to cell proliferation leading to the formation of liver tumors (Kociba et al., 1974), however, they did not report incidence data for these effects. Other studies suggest that cell proliferation can occur in the absence of liver cytotoxicity (JBRC, 1998a). Figure 4-1 presents a schematic representation of possible key events in the MOA for 1,4-dioxane liver carcinogenicity. These include: (1) oxidation by CYP2E1 and CYP2B1/2 (i.e., detoxification pathway for 1,4-dioxane), (2) saturation of metabolism/clearance leading to accumulation of the parent 1,4-dioxane, (3) liver damage followed by regenerative cell proliferation, or (4) cell proliferation in the absence of cytotoxicity (i.e., mitogenesis), (5) hyperplasia, and (6) tumor formation. It is suggested that liver toxicity is related to the accumulation of the parent compound following metabolic saturation at high doses (Kociba et al., 1975); however, no in vivo or in vitro assays have examined the toxicity of metabolites resulting from 1,4-dioxane to support this hypothesis. Nanelli et al. (2005) demonstrated that an increase in the oxidative metabolism of 1,4-dioxane via CYP450 induction using phenobarbital or fasting does not result in an increase in liver toxicity. This result suggested that highly reactive and toxic intermediates did not play a large role in the liver toxicity of 1,4-dioxane, even under conditions where metabolism was enhanced. Alternative metabolic pathways (e.g., not CYP450 mediated) may be present at high doses of 1,4-dioxane; although the available studies have not characterized these pathways nor identified any possible reactive intermediates. Tumor promotion studies in mouse skin and rat liver

suggest that 1,4-dioxane may enhance the growth of previously initiated cells (Lundberg et al.,1987; King et al., 1973). This is consistent with the increase in hepatocyte cell proliferation observed in several studies (Miyagawa et al., 1999; Uno et al., 1994; Goldsworthy et al., 1991; Stott et al., 1981). These mechanistic studies provide evidence of cell proliferation, but do not indicate whether mitogenesis or cytotoxicity is responsible for increased cell turnover.

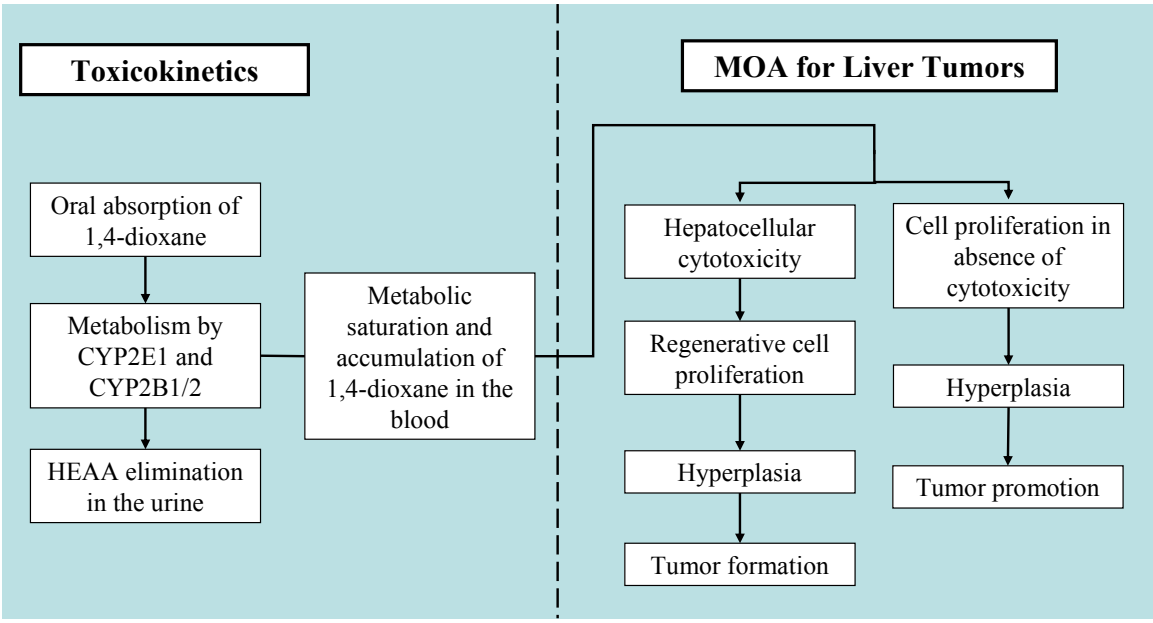

Figure 4-1. A schematic representation of the possible key events in the delivery of 1,4-dioxane to the liver and the hypothesized MOA(s) for liver carcinogenicity.

4.7.3.1.2. ***Nasal cavity.*** A possible key event in the MOA hypothesis for nasal tumors is sustained proliferation of spontaneously transformed nasal epithelial cells, resulting in the eventual formation of nasal cavity tumors. Precursor events in which 1,4-dioxane may promote proliferation of transformed nasal cells are highly uncertain. Figure 4-2 presents a schematic representation of possible key events leading to the formation of nasal cavity tumors. Histopathological lesions in female rats were suggestive of toxicity and regeneration in this tissue (i.e., atrophy, adhesion, inflammation, nuclear enlargement, and hyperplasia and metaplasia of respiratory and olfactory epithelium) (JBRC, 1998a).

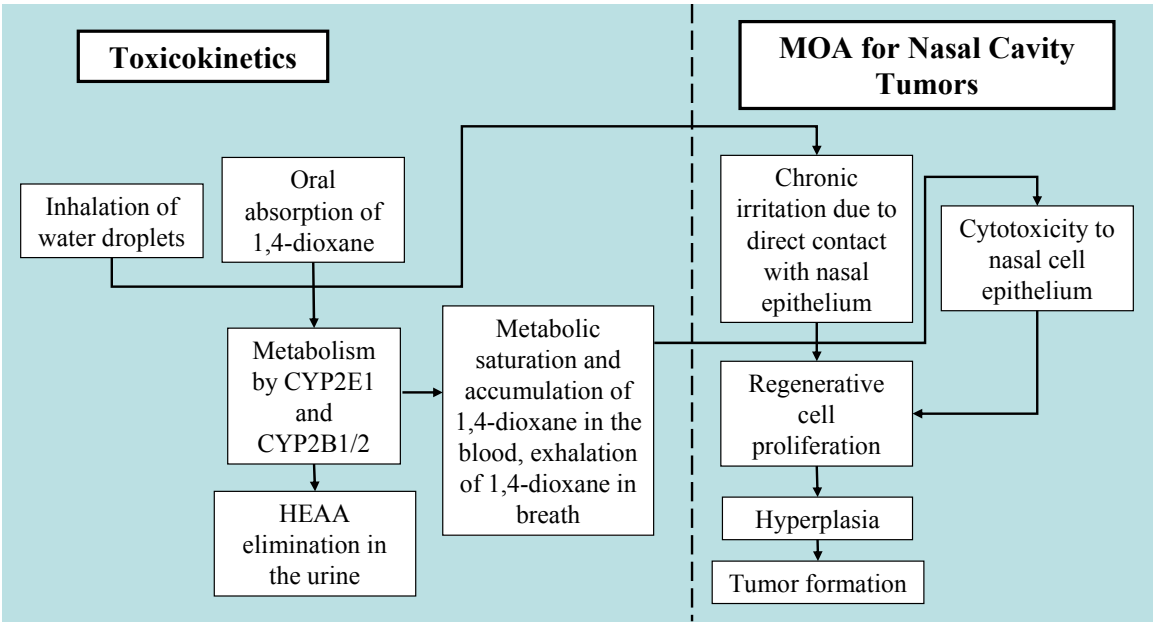

Figure 4-2. A schematic representation of the possible key events in the delivery of 1,4-dioxane to the nasal cavity and the hypothesized MOA(s) for nasal cavity carcinogenicity.

4.7.3.2. *Strength, Consistency, Specificity of Association*

4.7.3.2.1. *Liver.* The plausibility of a MOA that would include liver cytotoxicity, with subsequent reparative cell proliferation, as precursor events to liver tumor formation is minimally supported by findings that nonneoplastic liver lesions occurred at exposure levels lower than those resulting in significantly increased incidences of hepatocellular tumors (Kociba et al., 1974) and the demonstration of nonneoplastic liver lesions in subchronic (Kano et al., 2008) and acute and short-term oral studies (see Table 4-15). Because the incidence of nonneoplastic lesions was not reported by Kociba et al. (1974), it is difficult to know whether the incidence of liver lesions increased with increasing 1,4-dioxane concentration. Contradicting the observations by Kociba et al. (1974), liver tumors were observed in female rats and female mice in the absence of lesions indicative of cytotoxicity (Kano et al., 2008; JBRC, 1998a; NCI, 1978). This suggests that cytotoxicity may not be a requisite step in the MOA for liver cancer. Mechanistic and tumor promotion studies suggest that enhanced cell proliferation without cytotoxicity may be a key event; however, data showing a plausible dose response and temporal progression from cell proliferation to eventual liver tumor formation are not available (see Sections 4.7.3.3 and 4.7.3.4). Mechanistic studies that demonstrated cell proliferation after short-term exposure did not evaluate liver cytotoxicity (Miyagawa et al., 1999; Uno et al., 1994; Goldsworthy et al., 1991). Studies have not investigated possible precursor events that may lead to cell proliferation in the absence of cytotoxicity (i.e., genetic regulation of mitogenesis).

4.7.3.2.2. *Nasal cavity.* Nasal cavity tumors have been demonstrated in several rat strains (JBRC, 1998a; NCI, 1978; Kociba et al., 1974), but were not elevated in two strains of mice (JBRC, 1998a; NCI, 1978). Chronic irritation was indicated by the observation of rhinitis and inflammation of the nasal cavity in rats from the JBRC (1998a) study. This study also showed atrophy of the nasal epithelium and adhesion in rats. Regeneration of the nasal epithelium is demonstrated by metaplasia and hyperplasia observed in rats exposed to 1,4-dioxane (JBRC, 1998a).

4.7.3.3. *Dose-Response Relationship*

4.7.3.3.1. *Liver.* Table 4-18 presents the temporal sequence and dose-response relationship for possible key events in the liver carcinogenesis of 1,4-dioxane. Dose-response information provides some support for enhanced cell proliferation as a key event in the liver tumorigenesis of 1,4-dioxane; however, the role of cytotoxicity as a required precursor event is not supported by data from more than one study. Kociba et al. (1974) demonstrated that liver toxicity and hepatocellular regeneration occurred at a lower dose level than tumor formation. Hepatocellular degeneration and necrosis were observed in the mid- and high-dose groups of Sherman rats exposed to 1,4-dioxane, although it is not possible to discern whether this effect was observed in both genders due to the lack of incidence data (Kociba et al., 1974). Hepatic tumors were only observed at the highest dose (Kociba et al., 1974). Hepatic regeneration was indicated in the mid- and high-dose group by the formation of hepatocellular hyperplastic nodules. Liver hyperplasia was also seen in rats from the JBRC (1998a) study, at or below the dose level that resulted in tumor formation; however, hepatocellular degeneration and necrosis were not observed. These results suggest that hepatic cell proliferation and hyperplasia may occur in the absence of significant cytotoxicity. Liver angiectasis (i.e., dilation of blood or lymphatic vessels) was observed in male mice at the same dose that produced liver tumors; however, the relationship between this vascular abnormality and tumor formation is unclear.

Table 4-18. Temporal sequence and dose-response relationship for possible key events and liver tumors in rats and mice

Dose (mg/kg-day)	Key event (time →)				
	Metabolism 1,4-dioxane	Liver damage	Cell proliferation	Hyperplasia	Adenomas and/or carcinomas
Kociba et al., 1974—Sherman rats (male and female combined)					
0	—[a]				—[a]
14	↑[b]	—[a]	—[a]	—[a]	—[a]
121	↑[b]	↑[c]	—[a]	↑[c]	—[a]
1,307	↑[b]	↑[c]	—[a]	↑[c]	↑[c]

Dose (mg/kg-day)	Key event (time →)				
	Metabolism 1,4-dioxane	Liver damage	Cell proliferation	Hyperplasia	Adenomas and/or carcinomas
NCI, 1978—female Osborne-Mendel rats					
0	—[a]	—[a]	—[a]	—[a]	—[a]
350	[[b]	—[a]	—[a]	—[a]	[[c]
640	[[b]	—[a]	—[a]	—[a]	[[c]
NCI, 1978—male B6C3F$_1$ mice					
0	—[a]	—[a]	—[a]	—[a]	—[a]
720	[[b]	—[a]	—[a]	—[a]	[[c]
830	[[b]	—[a]	—[a]	—[a]	[[c]
NCI, 1978—female B6C3F$_1$ mice					
0	—[a]	—[a]	—[a]	—[a]	—[a]
380	[[b]	—[a]	—[a]	—[a]	[[c]
860	[[b]	—[a]	—[a]	—[a]	[[c]
JBRC, 1998a—male F344/DuCrj rats					
0	—[a]	—[a]	—[a]	—[a]	—[a]
16	[[b]	—[a]	—[a]	—[a]	—[a]
81	[[b]	—[a]	—[a]	[[c]	—[a]
398	[[b]	[[c,d]	—[a]	[[c]	[[c]
JBRC, 1998a—female F344/DuCrj rats					
0	—[a]	—[a]	—[a]	—[a]	—[a]
21	[[b]	—[a]	—[a]	—[a]	—[a]
103	[[b]	—[a]	—[a]	—[a]	—[a]
514	[[b]	—[a]	—[a]	[[c]	[[c]
JBRC, 1998a—male Crj:BDF$_1$ mice					
0	—[a]	—[a]	—[a]	—[a]	—[a]
66	[[b]	—[a]	—[a]	—[a]	[[c]
251	[[b]	—[a]	—[a]	—[a]	[[c]
768	[[b]	[[c,d]	—[a]	—[a]	[[c]
JBRC, 1998a—female Crj:BDF$_1$ mice					
0	—[a]	—[a]	—[a]	—[a]	—[a]
77	[[b]	—[a]	—[a]	—[a]	[[c]
323	[[b]	—[a]	—[a]	—[a]	[[c]
1,066	[[b]	[[c,d]	—[a]	—[a]	[[c]

[a]— No evidence demonstrating key event.

[b][1,4-dioxane metabolism was not evaluated as part of the chronic bioassays. Data from pharmacokinetic studies suggest that metabolism of 1,4-dioxane by CYP2E1 and CYP2B2 occurs immediately and continues throughout the duration of exposure at all exposure levels.

[c][Evidence demonstrating key event.

[d][Single cell necrosis was observed in a 13 week bioassay for male rats (274 mg/kg-day), male mice (585 mg/kg-day), and female mice (898 mg/kg-day) exposed to 1,4-dioxane in drinking water.

4.7.3.3.2. ***Nasal cavity.*** *T*oxicity and regeneration in nasal epithelium (i.e., atrophy, adhesion, inflammation, and hyperplasia and metaplasia of respiratory and olfactory epithelium) was evident in one study at the same dose levels that produced nasal cavity tumors (JBRC, 1998a).

4.7.3.4. *Temporal Relationship*

4.7.3.4.1. ***Liver.*** Available information regarding temporal relationships between the key event (sustained proliferation of spontaneously transformed liver cells) and the eventual formation of liver tumors is limited. A comparison of 13-week and 2-year studies conducted in F344/DuCrj rats and Crj:BDF_1 mice at the same laboratory revealed that tumorigenic doses of 1,4-dioxane produced liver toxicity by 13 weeks of exposure (Kano et al., 2008; JBRC, 1998a). Hepatocyte swelling of the centrilobular area of the liver, vacuolar changes in the liver, granular changes in the liver, and single cell necrosis in the liver were observed in mice and rats given 1,4-dioxane in the drinking water for 13 weeks. Sustained liver damage could presumably lead to regenerative hyperplasia and tumor formation following chronic exposure. As discussed above, histopathological evidence of regenerative hyperplasia has been seen following long-term exposure to 1,4-dioxane (JBRC, 1998a; Kociba et al., 1974). Tumors occurred earlier at high doses in both mice and rats from this study (email from Dr. Kazunori Yamazaki, JBRC, to Dr. Julie Stickney, SRC, dated 12/18/06); however, temporal information regarding hyperplasia or other possible key events was not available (i.e., interim blood samples not collected, interim sacrifices were not performed). Argus et al. (1973) studied the progression of tumorigenesis by electron microscopy of liver tissues obtained following interim sacrifices at 8 and 13 months of exposure (five rats/group, 574 mg/kg-day). The first change observed was an increase in the size of the nuclei of the hepatocytes, mostly in the periportal area. Precancerous changes were characterized by disorganization of the rough endoplasmic reticulum, increase in smooth endoplasmic reticulum, and decrease in glycogen and increase in lipid droplets in hepatocytes. These changes increased in severity in the hepatocellular carcinomas in rats exposed to 1,4-dioxane for 13 months.

Three types of liver nodules were observed in exposed rats at 13–16 months. The first consisted of groups of these cells with reduced cytoplasmic basophilia and a slightly nodular appearance as viewed by light microscopy. The second type of nodule was described consisting of large cells, apparently filled and distended with fat. The third type of nodule was described as finger-like strands, 2–3 cells thick, of smaller hepatocytes with large hyperchromic nuclei and dense cytoplasm. This third type of nodule was designated as an incipient hepatoma, since it showed all the histological characteristics of a fully developed hepatoma. All three types of nodules were generally present in the same liver.

4.7.3.4.2. ***Nasal cavity.*** No information was available regarding the temporal relationship between toxicity in the nasal epithelium and the formation of nasal cavity tumors.

4.7.3.5. *Biological Plausibility and Coherence*

4.7.3.5.1. *Liver.* The hypothesis that sustained proliferation of spontaneously transformed liver cells is a key event within a MOA is possible based on supporting evidence indicating that 1,4-dioxane is a tumor promoter of mouse skin and rat liver tumors (Lundberg et al., 1987; Bull et al., 1986; King et al., 1973). Further support for this hypothesis is provided by studies demonstrating that 1,4-dioxane increased hepatocyte DNA synthesis, indicative of cell proliferation (Miyagawa et al., 1999; Uno et al., 1994; Goldsworthy et al., 1991; Stott et al., 1981). In addition, the generally negative results for 1,4-dioxane in a number of genotoxicity assays indicates the carcinogenicity of 1,4-dioxane may not be mediated by a mutagenic MOA. The importance of cytotoxicity as necessary precursor to sustained cell proliferation is biologically plausible, but is not supported by the dose-response in the majority of studies of 1,4-dioxane carcinogenicity.

4.7.3.5.2. *Nasal cavity.* Sustained cell proliferation in response to cell death from toxicity may be related to the formation of nasal cavity tumors; however, this MOA is also not established . Nasal carcinogens are generally characterized as potent genotoxins (Ashby, 1994); however, other MOAs have been proposed for nasal carcinogens that induce effects through other mechanisms (Kasper et al. 2007; Green et al. 2000).

National Toxicological Program (NTP) database identified 12 chemicals from approximately 500 bioassays as nasal carcinogens and 1,4-dioxane was the only identified nasal carcinogen that showed little evidence of genotoxicity (Haseman and Hailey, 1997). Nasal tumors were not observed in an inhalation study in Wistar rats exposed to 111 ppm for 5 days/week for 2 years (Torkelson et al., 1974). It is unlikely that 1,4-dioxane in expired air following a drinking water exposure could exceed this air concentration.

4.7.3.6. *Other Possible Modes of Action*

An alternate MOA could be hypothesized that 1,4-dioxane alters DNA, either directly or indirectly, which causes mutations in critical genes for tumor initiation, such as oncogenes or tumor suppressor genes. Following these events, tumor growth may be promoted by a number of molecular processes leading to enhanced cell proliferation or inhibition of programmed cell death. The results from in vitro and in vivo assays do not provide overwhelming support for the hypothesis of a genotoxic MOA for 1,4-dioxane carcinogenicity. The genotoxicity data for 1,4-dioxane were reviewed in Section 4.5.1 and were summarized in Table 4-16. Negative findings were reported for mutagenicity in Salmonella typhimurium, Escherichia coli, and Photobacterium phosphoreum (Mutatox assay) (Morita and Hayashi, 1998; Hellmer and Bolcsfoldi, 1992; Kwan et al., 1990; Khudoley et al., 1987; Nestmann et al., 1984; Haworth et al., 1983; Stott et al., 1981). Negative results were also indicated for the induction of aneuploidy in yeast (Saccharomyces cerevisiae) and the sex-linked recessive lethal test in

Drosophila melanogaster (Zimmerman et al., 1985). In contrast, positive results were reported in assays for sister chromatid exchange (Galloway et al., 1987), DNA damage (Kitchin and Brown, 1990), and in in vivo micronucleus formation in bone marrow (Roy et al., 2005; Mirkova, 1994), and liver (Roy et al., 2005; Morita and Hayashi, 1998). Lastly, in the presence of toxicity, positive results were reported for meiotic nondisjunction in drosophila (Munoz and Barnett, 2002), DNA damage (Sina et al., 1983), and cell transformation (Sheu et al., 1988).

Additionally, 1,4-dioxane metabolism did not produce reactive intermediates that covalently bound to DNA (Stott et al., 1981; Woo et al., 1977a) and DNA repair assays were generally negative (Goldsworthy et al., 1991; Stott et al., 1981). No studies were available to assess the ability of 1,4-dioxane or its metabolites to induce oxidative damage to DNA.

4.7.3.7. *Conclusions About the Hypothesized Mode of Action*

4.7.3.7.1. ***Liver.*** The MOA by which 1,4-dioxane produces liver tumors is unknown, and available evidence in support of any hypothetical mode of carcinogenic action for 1,4-dioxane is inconclusive. A MOA hypothesis involving 1,4-dioxane induced cell proliferation is possible but data are not available to support this hypothesis. Pharmacokinetic data suggest that clearance pathways were saturable and target organ toxicity occurs after metabolic saturation. Liver toxicity preceded tumor formation in one study (Kociba et al., 1974) and a regenerative response to tissue injury was demonstrated by histopathology. Liver hyperplasia and tumor formation have also been observed in the absence of cytotoxicity (JBRC, 1998a). Cell proliferation and tumor promotion have been shown to occur after prolonged exposure to 1,4-dioxane (Miyagawa et al., 1999; Uno et al., 1994; Goldsworthy et al., 1991; Lundberg et al., 1987; Bull et al., 1986; Stott et al., 1981; King et al., 1973).

4.7.3.7.2. ***Nasal cavity.*** The MOA for the formation of nasal cavity tumors is unknown, and evidence in support of any hypothetical mode of carcinogenic action for 1,4-dioxane is inconclusive.

4.7.3.8. *Relevance of the Mode of Action to Humans*

Several hypothesized MOAs for 1,4-dioxane induced tumors in laboratory animals have been discussed along with the supporting evidence for each. As was stated, the MOA by which 1,4-dioxane produces liver, nasal, peritoneal, and mammary gland tumors is unknown. Currently there does exist some mechanistic information to present hypothesized MOAs for liver and nasal tumors but no information exists to present hypothesis for the observed peritoneal or mammary gland tumors (JBRC, 1998a). At this time there is inadequate evidence to determine the human relevance of any of the hypothesized MOAs for 1,4-dioxane-induced tumors.

4.8. SUSCEPTIBLE POPULATIONS AND LIFE STAGES

There is no direct evidence to establish that certain populations and lifestages may be potentially susceptible to 1,4-dioxane. Changes in susceptibility with lifestage as a function of the presence of microsomal enzymes that metabolize and detoxify this compound (i.e., CYP2E1 present in liver, kidney, and nasal mucosa can be hypothesized). Vieira et al. (1996) reported that large increases in hepatic CYP2E1 protein occur postnatally between 1 and 3 months in humans. Adult hepatic concentrations of CYP2E1 are achieved sometime between 1 and 10 years. To the extent that hepatic CYP2E1 levels are lower, children may be more susceptible to liver toxicity from 1,4-dioxane than adults. CYP2E1 has been shown to be inducible in the rat fetus. The level of CYP2E1 protein was increased by 1.4-fold in the maternal liver and 2.4-fold in the fetal liver following ethanol treatment, as compared to the untreated or pair-fed groups (Carpenter et al., 1996). Pre- and postnatal induction of microsomal enzymes resulting from exposure to 1,4-dioxane or other drugs or chemicals may reduce overall toxicity following sustained exposure to 1,4-dioxane.

Genetic polymorphisms have been identified for the human CYP2E1 gene (Watanabe et al., 1994; Hayashi et al., 1991) and were considered to be possible factors in the abnormal liver function seen in workers exposed to vinyl chloride (Huang et al., 1997). Individuals with a CYP2E1 genetic polymorphism resulting in increased expression of this enzyme may be less susceptible to toxicity following exposure to 1,4-dioxane.

Gender differences were noted in subchronic and chronic toxicity studies of 1,4-dioxane in mice and rats (see Sections 4.6 and 4.7). No consistent pattern of gender sensitivity was identified across studies.

5. DOSE-RESPONSE ASSESSMENTS

5.1. ORAL REFERENCE DOSE (RFD)

5.1.1. Choice of Principal Studies and Critical Effect with Rationale and Justification

Liver and kidney toxicity were the primary noncancer health effects associated with exposure to 1,4-dioxane in humans and laboratory animals. Occupational exposure to 1,4-dioxane has resulted in hemorrhagic nephritis and centrilobular necrosis of the liver (Johnstone, 1959; Barber, 1934). In animals, liver and kidney degeneration and necrosis were observed frequently in acute oral and inhalation studies (JBRC, 1998b; Drew et al., 1978; David, 1964; Kesten et al., 1939; Laug et al., 1939; Schrenk and Yant, 1936; de Navasquez, 1935; Fairley et al., 1934). Liver and kidney effects were also observed following chronic oral exposure to 1,4-dioxane in animals (JBRC, 1998a; NCI, 1978; Kociba et al., 1974; Argus et al., 1973, 1965) (see Table 4-17).

Liver toxicity in the available chronic studies was characterized by necrosis, spongiosis hepatic, hyperplasia, cyst formation, clear foci, and mixed cell foci. Kociba et al. (1974) demonstrated hepatocellular degeneration and necrosis at doses of 94 mg/kg-day (LOAEL in male rats) or greater. The NOAEL for liver toxicity was 9.6 mg/kg-day and 19 mg/kg-day in male and female rats, respectively. No quantitative incidence data were provided in this study. Argus et al. (1973) described early preneoplastic changes in the liver and JBRC (1998) demonstrated liver lesions that are primarily associated with the carcinogenic process. Clear and mixed-cell foci in the liver are commonly considered preneoplastic changes and would not be considered evidence of noncancer toxicity. In the JBRC (1998a) study, spongiosis hepatis was associated with other preneoplastic changes in the liver (clear and mixed-cell foci) and no other lesions indicative of liver toxicity were seen. Spongiosis hepatis was therefore not considered indicative of noncancer effects in this study. The activity of serum enzymes (i.e., AST, ALT, LDH, and ALP) was increased in mice and rats chronically exposed to 1,4-dioxane (JBRC, 1998a); however, these increases were seen only at tumorigenic dose levels. Blood samples were collected at study termination and elevated serum enzymes may reflect changes associated with tumor formation. Histopathological evidence of liver toxicity was not seen in rats from the JBRC (1998a) study. The highest non-tumorigenic dose levels for this study approximated the LOAEL derived from the Kociba et al. (1974) study (94 and 148 mg/kg-day for male and female rats, respectively).

Kidney damage in chronic toxicity studies was characterized by degeneration of the cortical tubule cells, necrosis with hemorrhage, and glomerulonephritis (NCI, 1978; Kociba et al., 1974; Argus et al., 1965, 1973; Fairley et al., 1934). Kociba et al. (1974) described renal

tubule epithelial cell degeneration and necrosis at doses of 94 mg/kg-day (LOAEL in male rats) or greater, with a NOAEL of 9.6 mg/kg-day. No quantitative incidence data were provided in this study. Doses of ≥ 430 mg/kg-day 1,4-dioxane induced marked kidney alterations (Argus et al., 1973). The observed changes included glomerulonephritis and pyelonephritis, with characteristic epithelial proliferation of Bowman's capsule, periglomerular fibrosis, and distension of tubules. Quantitative incidence data were not provided in this study. In the NCI (1978) study, kidney lesions in rats consisted of vacuolar degeneration and/or focal tubular epithelial regeneration in the proximal cortical tubules and occasional hyaline casts. Kidney toxicity was not seen in rats from the JBRC (1998a) study at any dose level (highest dose was 398 mg/kg-day in male rats and 514 mg/kg-day in female rats).

Kociba et al. (1974) was chosen as the principal study for derivation of the RfD because the liver and kidney effects in this study are adverse and represent the most sensitive effects identified in the database (NOAEL 9.6 mg/kg-day, LOAEL 94 mg/kg-day in male rats). Kociba et al. (1974) reported degenerative effects in the liver, while liver lesions reported in other studies (JBRC, 1998a; Argus et al., 1973) appeared to be related to the carcinogenic process. Kociba et al. (1974) also reported degenerative changes in the kidney. NCI (1978) and Argus et al. (1973) provided supporting data for this endpoint; however, kidney toxicity was observed in these studies at higher doses. JBRC (1998a) reported nasal inflammation in rats (NOAEL 81 mg/kg-day, LOAEL 398 mg/kg-day) and mice (NOAEL 77 mg/kg-day, LOAEL 323 mg/kg-day).

5.1.2. Methods of Analysis—Including Models (PBPK, BMD, etc.)

Several procedures were applied to the human PBPK model to determine if an adequate fit of the model to the empirical model output or experimental observations could be attained using biologically plausible values for the model parameters. The re-calibrated model predictions for blood 1,4-dioxane levels do not come within 10-fold of the experimental values using measured tissue:air partition coefficients of Leung and Paustenbach (1990) or Sweeney et al. (2008) (Figures B-8 and B-9). The utilization of a slowly perfused tissue:air partition coefficient 10-fold lower than measured values produces exposure-phase predictions that are much closer to observations, but does not replicate the elimination kinetics (Figure B-10). Re-calibration of the model with upper bounds on the tissue:air partition coefficients results in predictions that are still six- to sevenfold lower than empirical model prediction or observations (Figures B-12 and B-13). Exploration of the model space using an assumption of first-order metabolism (valid for the 50 ppm inhalation exposure) showed that an adequate fit to the exposure and elimination data can be achieved only when unrealistically low values are assumed for the slowly perfused tissue:air partition coefficient (Figure B-16). Artificially low values for the other tissue:air partition coefficients are not expected to improve the model fit, as these parameters are shown in the sensitivity analysis to exert less influence on blood 1,4-dioxane than

V_{maxC} and K_m. This suggests that the model structure is insufficient to capture the apparent 10-fold species difference in the blood 1,4-dioxane V_d between rats and humans. In the absence of actual measurements for the human slowly perfused tissue:air partition coefficient, high uncertainty exists for this model parameter value. Differences in the ability of rat and human blood to bind 1,4-dioxane may contribute to the difference in V_d. However, this is expected to be evident in very different values for rat and human blood:air partition coefficients, which is not the case (Table B-1). Therefore, some other, as yet unknown, modification to model structure may be necessary.

Kociba et al. (1974) did not provide quantitative incidence or severity data for liver and kidney degeneration and necrosis. Benchmark dose (BMD) modeling could not be performed for this study and the NOAEL for liver and kidney degeneration (9.6 mg/kg-day in male rats) was used as the point of departure (POD) in deriving the RfD for 1,4-dioxane.

Alternative PODs were calculated using incidence data reported for cortical tubule degeneration in male and female rats (NCI, 1978) and liver hyperplasia (JBRC, 1998a). The incidence data for cortical tubule cell degeneration in male and female rats exposed to 1,4-dioxane in the drinking water for 2 years are presented in Table 5-1. Details of the BMD analysis of these data are presented in Appendix C. Male rats were more sensitive to the kidney effects of 1,4-dioxane than females and the male rat data provided the lowest POD for cortical tubule degeneration in the NCI (1978) study ($BMDL_{10}$ of 38.5 mg/kg-day) (see Table 5-2). Incidence data for liver hyperplasia in male and female rats exposed to 1,4-dioxane in the drinking water for 2 years are presented in Table 5-3. Details of the BMD analysis of these data are presented in Appendix C. Male rats were more sensitive to developing liver hyperplasia due to exposure to 1,4-dioxane than females and the male rat data provided the lowest POD for hyperplasia in the JBRC (1998a) study ($BMDL_{10}$ of 34.7 mg/kg-day) (see Table 5-4). The $BMDL_{10}$ values of 38.5 mg/kg-day and 34.7 mg/kg-day from the NCI (1978) and JBRC (1998a) studies, respectively, supports the NOAEL of 9.6 mg/kg-day observed by Kociba et al. (1974).

Table 5-1. Incidence of cortical tubule degeneration in Osborne-Mendel rats exposed to1,4-dioxane in drinking water for 2 years

Males (mg/kg-day)			Females (mg/kg-day)		
0	**240**	**530**	**0**	**350**	**640**
0/31[a]	20/31[b]	27/33[b]	0/31[a]	0/34	10/32[b]

[a]Statistically significant trend for increased incidence by Cochran-Armitage test ($p < 0.05$) performed for this review.
[b]Incidence significantly elevated compared to control by Fisher's Exact test ($p < 0.001$) performed for this review.

Source: NCI (1978).

Table 5-2. BMD and BMDL values derived from BMD modeling of cortical tubule degeneration in male and female Osborne-Mendel rats exposed to 1,4-dioxane in drinking water for 2 years

	BMD_{10} (mg/kg-day)	$BMDL_{10}$ (mg/kg-day)
Male rats	51.4	38.5
Female rats	591.8	447.2

Source: NCI (1978).

Table 5-3. Incidence of liver hyperplasia in F344/DuCrj rats exposed to 1,4-dioxane in drinking water for 2 years

Males (mg/kg-day)				Females (mg/kg-day)			
0	**16**	**81**	**398**	**0**	**21**	**103**	**514**
3/40	2/45	9/35[a]	12/22[b]	0/38[a]	0/37	1/38	14/24[b]

[a]Statistically significant compared to controls by the Dunnett's test ($p < 0.05$).
[b]Incidence significantly elevated compared to control by Chi^2 test ($p < 0.01$).

Source: JBRC (1998a).

Table 5-4. BMD and BMDL values derived from BMD modeling of liver hyperplasia in male and female F344/DuCrj rats exposed to 1,4-dioxane in drinking water for 2 years

	BMD_{10} (mg/kg-day)	$BMDL_{10}$ (mg/kg-day)
Male rats	52.3	34.7
Female rats	69.0	38.7

Source: JBRC (1998a).

5.1.3. RfD Derivation - Including Application of Uncertainty Factors (UFs)

The RfD of 3×10^{-2} mg/kg-day is based on liver and kidney toxicity in rats exposed to 1,4-dioxane in the drinking water for 2 years (Kociba et al., 1974). The Kociba et al. (1974) study was chosen as the principal study because it provides the most sensitive measure of adverse effects by 1,4-dioxane. The incidence of liver and kidney lesions was not reported for each dose group. Therefore, BMD modeling could not be used to derive a POD. The RfD for 1,4-dioxane is derived by dividing the NOAEL of 9.6 mg/kg-day (Kociba et al.,1974) by a composite UF of 300, as follows:

$$\text{RfD} = \text{NOAEL / UF}$$
$$= 9.6 \text{ mg/kg-day} / 300$$
$$= 0.03 \text{ or } 3 \times 10^{-2} \text{ mg/kg-day}$$

The composite UF of 300 includes factors of 10 for animal-to-human extrapolation and interindividual variability, and a partial UF of 3 for database deficiencies.

A default interspecies UF of 10 was used to account for pharmacokinetic and pharmacodynamic differences across species. Existing PBPK models could not be used to derive an oral RfD for 1,4-dioxane (see Appendix B).

A default interindividual variability UF of 10 is used to account for variation in sensitivity within human populations because there is limited information on the degree to which humans of varying gender, age, health status, or genetic makeup might vary in the disposition of, or response to, 1,4-dioxane.

A default UF of 3 for database deficiencies is selected due to the lack of a multigeneration reproductive toxicity study. A single oral prenatal developmental toxicity study in rats was available for 1,4-dioxane (Giavini et al., 1985). This developmental study indicates that the developing fetus may be a target of toxicity.

An UF to extrapolate from a subchronic to a chronic exposure duration was not necessary because the RfD was derived from a study using a chronic exposure protocol.

An UF to extrapolate from a LOAEL to a NOAEL was not necessary because the RfD was based on a NOAEL. Kociba et al. (1974) was a well-conducted, chronic drinking water study with an adequate number of animals. Histopathological examination was performed for many organs and tissues, but clinical chemistry analysis was not performed. NOAEL and LOAEL values were derived from the study based on liver and kidney toxicity. Several additional oral studies (acute/short-term, subchronic, and chronic durations) were available that support liver and kidney toxicity as the critical effect (Kano et al., 2008; JBRC, 1998a; NCI, 1978; Argus et al., 1973, see Tables 4-15 and 4-17). Although degenerative liver and kidney toxicity was not observed in rats from the JBRC (1998a) study at doses at or below the LOAEL value in the Kociba et al. (1974) study, other endpoints such as metaplasia and hyperplasia of the nasal epithelium, nuclear enlargement, and hematological effects, were noted.

5.1.4. RfD Comparison Information

PODs and sample oral RfDs based on selected studies included in Table 4-17 are arrayed in Figures 5-1 to 5-3, and provide perspective on the RfD supported by Kociba et al. (1974). These figures should be interpreted with caution because the PODs across studies are not necessarily comparable, nor is the confidence in the data sets from which the PODs were derived the same. PODs in these figures may be based on a NOAEL, LOAEL, or BMDL (as indicated), and the nature, severity, and incidence of effects occurring at a LOAEL are likely to vary. To some extent, the confidence associated with the resulting sample RfD is reflected in the

magnitude of the total UF applied to the POD (i.e., the size of the bar); however, the text of Sections 5.1.1 and 5.1.2 should be consulted for a more complete understanding of the issues associated with each data set and the rationale for the selection of the critical effect and principal study used to derive the RfD.

The predominant noncancer effect of chronic oral exposure to 1,4-dioxane is degenerative effects in the liver and kidney. Figure 5-1 provides a graphical display of effects that were observed in the liver following chronic oral exposure to 1,4-dioxane. Information presented includes the PODs and UFs that could be considered in deriving the oral RfD. As discussed in Sections 5.1.1 and 5.1.2, among those studies that demonstrated liver toxicity, the study by Kociba et al. (1974) provided the data set most appropriate for deriving the RfD. For degenerative liver effects resulting from 1,4-dioxane exposure, the Kociba et al. (1974) study represents the most sensitive effect and dataset observed in a chronic bioassay (Figure 5-1).

Kidney toxicity as evidenced by glomerulonephritis (Argus et al., 1973; 1965) and degeneration of the cortical tubule (NCI, 1978; Kociba et al., 1974) has also been observed in response to chronic exposure to 1,4-dioxane. As was discussed in Sections 5.1 and 5.2, degenerative effects were observed in the kidney at the same dose level as effects in the liver (Kociba et al., 1974). A comparison of the available datasets from which an RfD could potentially be derived is presented in Figure 5-2.

Rhinitis and inflammation of the nasal cavity were reported in both the NCI (1978) (mice only, dose ≥ 380 mg/kg-day) and JBRC (1998a) studies (≥ 398 mg/kg-day in rats, >323 mg/kg-day in mice). JBRC (1998a) reported nasal inflammation in rats (NOAEL 81 mg/kg-day, LOAEL 398 mg/kg-day) and mice (NOAEL 77 mg/kg-day, LOAEL 323 mg/kg-day). A comparison of the available datasets from which an RfD could potentially be derived is presented in Figure 5-3.

Figure 5-4 displays PODs for the major targets of toxicity associated with oral exposure to 1,4-dioxane. Studies in experimental animals have also found that relatively high doses of 1,4-dioxane (1,000 mg/kg-day) during gestation can produce delayed ossification of the sternebrae and reduced fetal BWs (Giavini et al., 1985). This graphical display (Figure 5-4) compares organ specific toxicity for 1,4-dioxane, including a single developmental study. The most sensitive measures of degenerative liver are and kidney effects. The sample RfDs for degenerative liver and kidney effects are identical since they were derived from the same study and dataset (Kociba et al., 1974) and are presented for completeness.

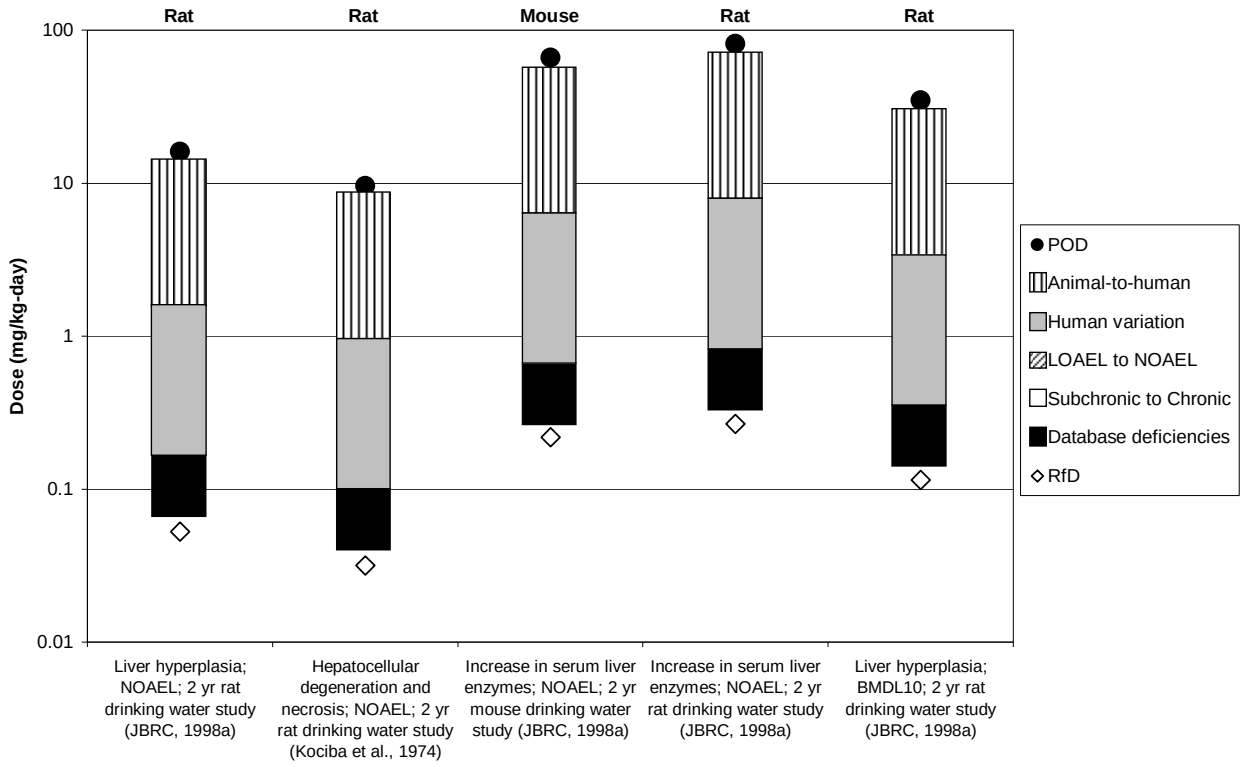

Figure 5-1. Points of departure (POD) for liver toxicity endpoints with corresponding applied uncertainty factors and derived RfDs following oral exposure to 1,4-dioxane.

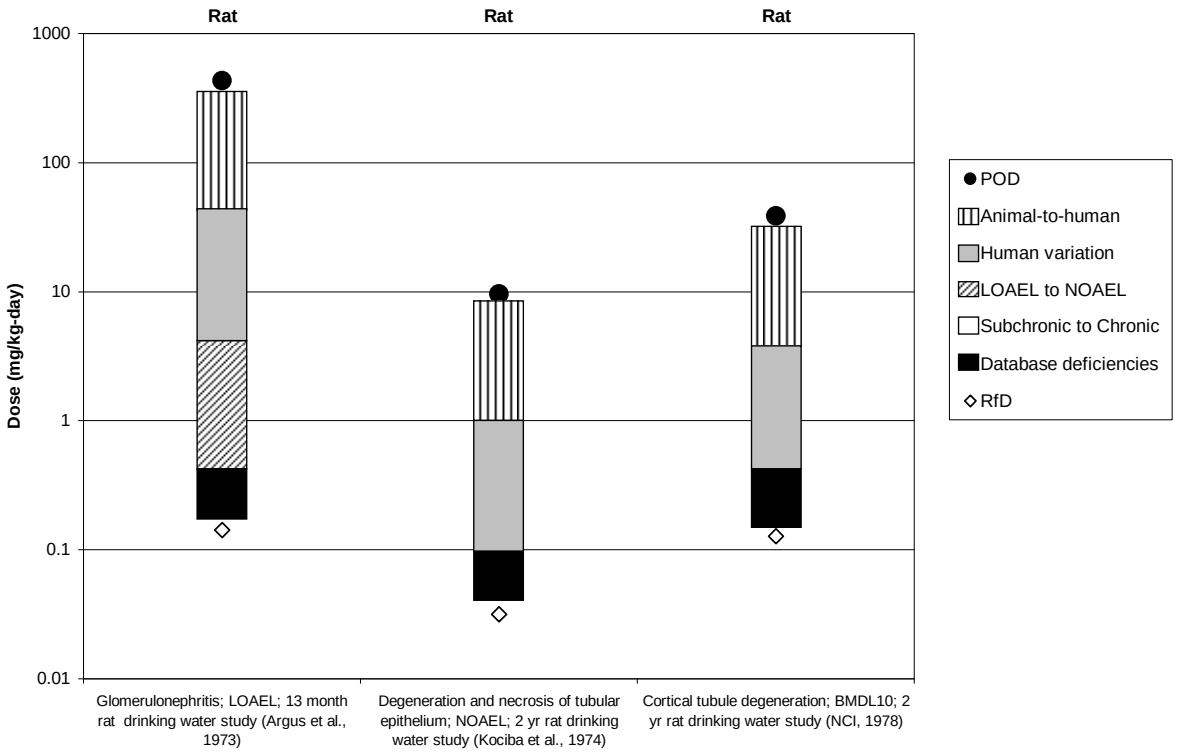

Figure 5-2. Points of departure (POD) for kidney toxicity endpoints with corresponding applied uncertainty factors and derived RfDs following oral exposure to 1,4-dioxane.

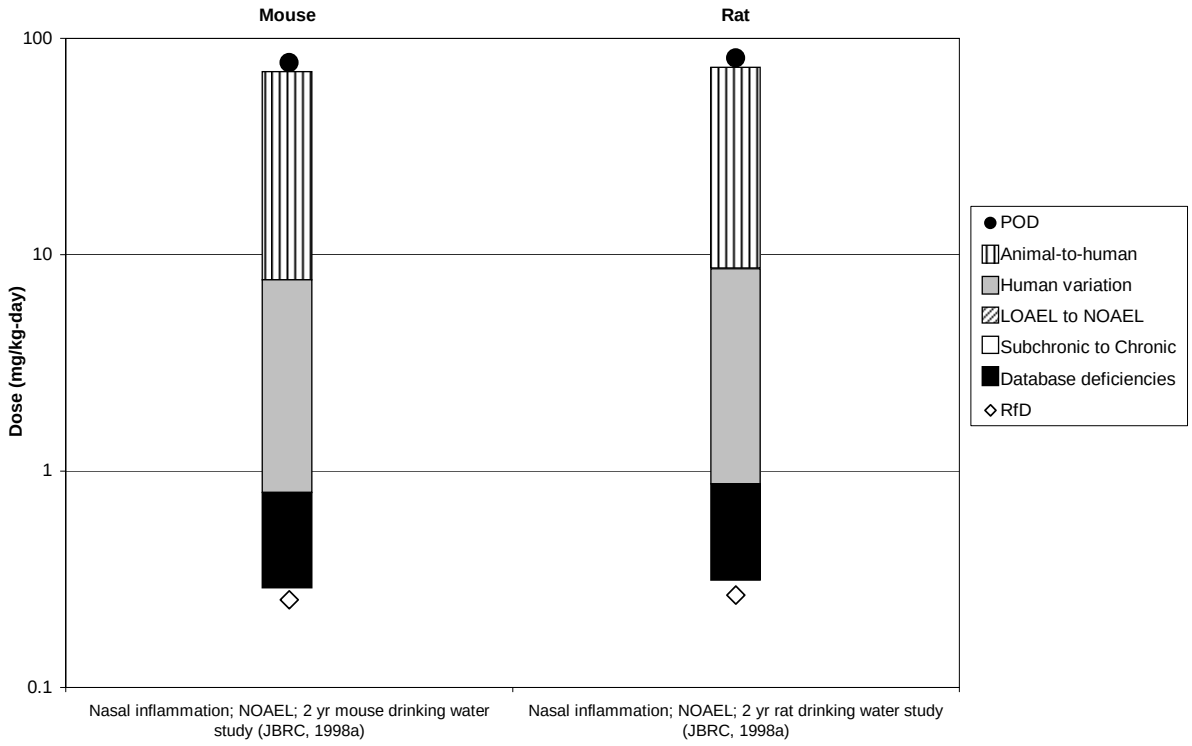

Figure 5-3. Points of departure (POD) for nasal inflammation with corresponding applied uncertainty factors and derived RfDs following oral expsorue to 1,4-dioxane.

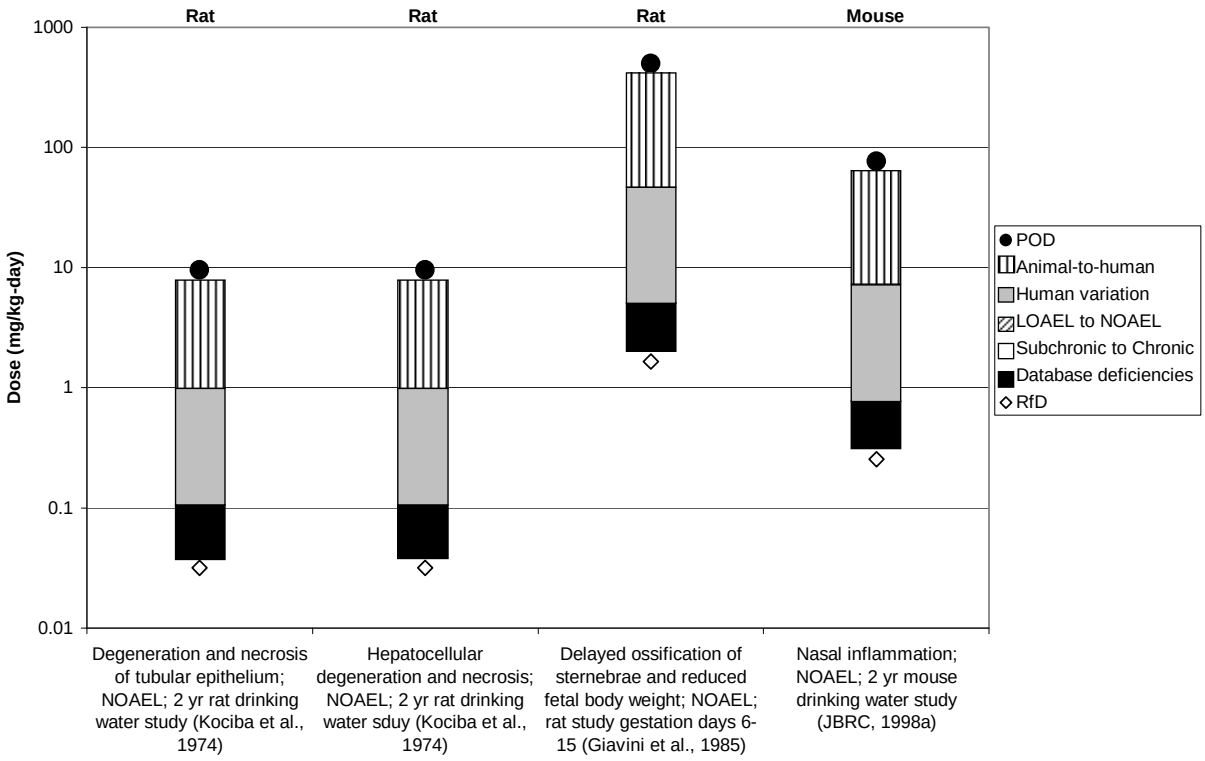

Figure 5-4. Points of departure (POD) for organ specific toxicity endpoints with corresponding applied uncertainty factors and derived RfDs following oral exposure to 1,4-dioxane.

5.1.5. Previous RfD Assessment

An assessment for 1,4-dioxane was previously posted on the IRIS database in 1988. An oral RfD was not developed as part of the 1988 assessment.

5.2. INHALATION REFERENCE CONCENTRATION (RFC)

Inhalation studies for 1,4-dioxane evaluated in this assessment were not adequate for the determination of an RfC value. Only one subchronic study (Fairley et al., 1934) and one chronic inhalation study (Torkelson et al., 1974) were identified. In the subchronic study, rabbits, guinea pigs, rats, and mice (3–6/species/group) were exposed to 1,000, 2,000, 5,000, or 10,000 ppm of 1,4-dioxane vapor for 16.5 hours/week. Animals were exposed until death occurred or were sacrificed at varying time periods (up to 12 weeks). Severe liver and kidney damage and acute vascular congestion of the lungs were observed at concentrations ≥ 1,000 ppm. Kidney damage was described as patchy degeneration of cortical tubules with vascular congestion and hemorrhage. Liver lesions varied from cloudy hepatocyte swelling to large areas of necrosis.

Torkelson et al. (1974) performed a chronic inhalation study in which male and female Wistar rats (288/sex) were exposed to 111 ppm 1,4-dioxane vapor for 7 hours/day, 5 days/week for 2 years. Control rats (192/sex) were exposed to filtered air. No significant effects were

observed on BWs, survival, organ weights, hematology, clinical chemistry, or histopathology. Because Fairley et al. (1934) identified a free-standing LOAEL only, and Torkelson et al. (1974) identified a free-standing NOAEL only, neither study was sufficient to characterize the inhalation risks of 1,4-dioxane. A route extrapolation from oral toxicity data was not performed because 1,4-dioxane inhalation causes direct effects on the respiratory tract (i.e., respiratory irritation in humans, pulmonary congestion in animals) (Wirth and Klimmer, 1936; Fairley et al., 1934; Yant et al., 1930), which would not be accounted for in a cross-route extrapolation. In addition, available kinetic models are not suitable for this purpose (see Appendix B).

An assessment for 1,4-dioxane was previously posted on the IRIS database in 1988. An inhalation RfC was not developed as part of the 1988 assessment.

During the review of this assessment, new data regarding the toxicity of 1,4-dioxane through the inhalation route of exposure have become available. The Agency will evaluate the recently published 1,4-dioxane inhalation data for the potential to derive an RfC in a separate document to follow this assessment.

5.3. UNCERTAINTIES IN THE ORAL REFERENCE DOSE (RfD)

Risk assessments need to portray associated uncertainty. The following discussion identifies uncertainties associated with the RfD for 1,4-dioxane. As presented earlier in this section (5.1.2 and 5.1.3), the uncertainty factor approach (U.S. EPA, 2002a, 1994b), was applied to a POD. Factors accounting for uncertainties associated with a number of steps in the analyses were adopted to account for extrapolating from an animal bioassay to human exposure, a diverse population of varying susceptibilities, and to account for database deficiencies. These extrapolations are carried out with current approaches given the paucity of experimental 1,4-dioxane data to inform individual steps.

An adequate range of animal toxicology data are available for the hazard assessment of 1,4-dioxane, as described throughout the previous section (Chapter 4). The database of oral toxicity studies includes chronic drinking water studies in rats and mice, multiple subchronic drinking water studies conducted in rats and mice, and a developmental study in rats. Toxicity associated with oral exposure to 1,4-dioxane is observed predominately in the liver and kidney. The database of inhalation toxicity studies in animals includes one subchronic bioassay in rabbits, guinea pigs, and rats, and a chronic inhalation bioassay in rats. Although the subchronic bioassay observed degenerative effects in the liver, kidney, and lungs of all species tested, the information reported from the study was insufficient to determine an exposure level below which these effects did not occur. The only available chronic inhalation bioassay did not indicate any treatment related effects due to exposure to 1,4-dioxane. Thus, the inhalation database lacked sufficient information to derive toxicity values relevant to this route of exposure for 1,4-dioxane. In addition to oral and inhalation data, there are PBPK models and genotoxicity studies of

1,4-dioxane. Critical data gaps have been identified and uncertainties associated with data deficiencies of 1,4-dioxane are more fully discussed below.

Consideration of the available dose-response data led to the selection of the two-year drinking water bioassay in Sherman rats (Kociba et al., 1974) as the principal study and increased liver and kidney degeneration as the critical effects for deriving the RfD for 1,4-dioxane. The dose-response relationship for oral exposure to 1,4-dioxane and cortical tubule degeneration in Osborne-Mendel rats (NCI, 1978) was also suitable for deriving a RfD, but it is associated with higher a POD and sample RfD compared to Kociba et al. (1974).

The RfD was derived by applying UFs to a NOAEL for degenerative liver and kidney effects. The incidence data for the observed effects were not reported in the principal study (Kociba et al., 1974), precluding modeling of the dose-response. However confidence in the LOAEL can be derived from additional studies (JBRC, 1998a; NCI, 1978; Argus et al., 1973; 1965) that observed effects on the same organs at comparable dose levels and by the BMDL generated by modeling of the kidney dose-response data from the chronic NCI (1978) study.

Extrapolating from animals to humans embodies further issues and uncertainties. The effect and the magnitude associated with the dose at the POD in rodents are extrapolated to human response. Pharmacokinetic models are useful to examine species differences in pharmacokinetic processing; however, it was determined that dosimetric adjustment using pharmacokinetic modeling was to reduce uncertainty following oral exposure to 1,4-dioxane was not supported. Insufficient information was available to quantitatively assess toxicokinetic or toxicodynamic differences between animals and humans, so a 10-fold UF was used to account for uncertainty in extrapolating from laboratory animals to humans in the derivation of the RfD.

Heterogeneity among humans is another uncertainty associated with extrapolating doses from animals to humans. Uncertainty related to human variation needs consideration. In the absence of 1,4-dioxane-specific data on human variation, a factor of 10 was used to account for uncertainty associated with human variation in the derivation of the RfD. Human variation may be larger or smaller; however, 1,4-dioxane-specific data to examine the potential magnitude of over- or under-estimation is unavailable.

Uncertainties in the assessment of the health hazards of ingested 1,4-dioxane are associated with deficiencies in reproductive toxicity information. The oral database lacks a multigeneration reproductive toxicity study. A single oral prenatal developmental toxicity study in rats was available for 1,4-dioxane (Giavini et al., 1985). This developmental study indicates that the developing fetus may be a target of toxicity. The database of inhalation studies is of particular concern due to the lack of a basic toxicological studies, a multigenerational reproductive study, and developmental toxicity studies.

5.4. CANCER ASSESSMENT

5.4.1. Choice of Study/Data - with Rationale and Justification

Three chronic drinking water bioassays provided incidence data for liver tumors in rats and mice, and nasal cavity, peritoneal, and mammary gland tumors in rats only (JBRC, 1998a; NCI, 1978; Kociba et al., 1974). The dose-response data from each of these studies are summarized in Table 5-5. With the exception of the NCI (1978) study, the incidence of nasal cavity tumors was generally lower than the incidence of liver tumors in exposed rats. The JBRC (1998a) drinking water study was chosen as the principal study for derivation of an oral cancer slope factor (CSF) for 1,4-dioxane. This study used three dose groups in addition to controls and characterized the dose-response relationship at lower exposure levels, as compared to the high doses employed in the NCI (1978) bioassay. The Kociba et al. (1974) study also used three dose groups and low exposures; however, the study authors only reported the incidence of hepatocellular carcinoma, which may underestimate the combined incidence of rats with adenoma or carcinoma. In addition to increased incidence of liver tumors, chosen as the most sensitive target organ for tumor formation, the JBRC (1998a) study also noted increased incidence of peritoneal and mammary gland tumors. Nasal cavity tumors were also seen in high-dose male and female rats; however, the incidence of nasal tumors was much lower than the incidence of liver tumors in both rats and mice.

Table 5-5. Incidence of liver, nasal cavity, peritoneal, and mammary gland tumors in rats and mice exposed to 1,4-dioxane in drinking water for 2 years (based on survival to 12 months)

Study	Species/strain/gender	Animal dose (mg/kg-day)	Tumor Incidence			
			Liver	Nasal cavity	Peritoneal	Mammary gland
Kociba et al., 1974	Sherman rats, male and female combined[a,b]	0	1/106[h]	0/106[h]	NA	NA
		14	0/110	0/110	NA	NA
		121	1/106	0/106	NA	NA
		1,307	10/66[i]	3/66	NA	NA
NCI, 1978	Male Osborne-Mendel rats[b]	0	NA	0/33[h]	NA	NA
		240	NA	12/26	NA	NA
		530	NA	16/33[i]	NA	NA
	Female Osborne-Mendel rats[b,c]	0	0/31[h]	0/34[h]	NA	NA
		350	10/30[i]	10/30[i]	NA	NA
		640	11/29[i]	8/29[i]	NA	NA
	Male B6C3F$_1$ mice[d]	0	8/49[h]	NA	NA	NA
		720	19/50[i]	NA	NA	NA
		830	28/47[i]	NA	NA	NA
	Female B6C3F$_1$ mice[d]	0	0/50[h]	NA	NA	NA
		380	21/48[i]	NA	NA	NA

Study	Species/strain/gender	Animal dose (mg/kg-day)	Tumor Incidence			
			Liver	Nasal cavity	Peritoneal	Mammary gland
		860	35/37[i]	NA	NA	NA
JBRC, 1998a; email from Dr. Kazunori Yamazaki, JBRC, to Dr. Julie Stickney, SRC, dated 12/18/06.	Male F344/DuCrj rats[d,e,f,g]	0	0/50[h]	0/50[h]	2/50	1/50
		16	2/50	0/50	2/50	1/50
		81	4/49	0/50	5/50	0/50
		398	33/50[i]	7/50[i]	28/50[i]	4/50
	Female F344/DuCrj rats[d,e,f,g]	0	1/50[h]	0/50[h]	1/50	9/50
		21	0/50	0/50	0/50	9/50
		103	5/50	0/50	0/50	11/50
		514	40/50[i]	8/50[i]	0/50	19/50
	Male Crj:BDF_1 mice[d]	0	21/50	NA	NA	NA
		66	31/48	NA	NA	NA
		251	37/50	NA	NA	NA
		768	39/48[i]	NA	NA	NA
	Female Crj:BDF_1 mice[d]	0	4/50[h]	NA	NA	NA
		77	34/50[i]	NA	NA	NA
		323	41/48[i]	NA	NA	NA
		1,066	46/48[i]	NA	NA	NA

[a]Incidence of hepatocellular carcinoma.
[b]Incidence of nasal squamous cell carcinoma.
[c]Incidence of hepatocellular adenoma.
[d]Incidence of hepatocellular adenoma or carcinoma.
[e]Incidence of all nasal tumors including squamous cell carcinoma, sarcoma, rhabdomyosarcoma, and esthesioneuro-epithelioma.
[f]Incidence of peritoneal tumors (mesothelioma).
[g]Incidence of mammary gland tumors (fibroadenoma and adenoma combined)
[h]$p < 0.05$; positive dose-related trend (Cochran-Armitage or Peto test).
[i]$p < 0.05$; Fisher's Exact test.
NA = data were not available for modeling (no significant change from controls)

5.4.2. Dose-Response Data

Table 5-6 summarizes the incidence of hepatocellular adenoma or carcinoma in rats and mice from the JBRC (1998a) 2-year drinking water study. There were statistically significant increasing trends in tumorigenic response for males and females of both species. The dose-response curve for female mice is steep, with 68% incidence of liver tumors occurring in the low-dose group (77 mg/kg-day). Exposure to 1,4-dioxane increased the incidence of these tumors in a dose-related manner.

A significant increase in the incidence of peritoneal mesothelioma was observed in high-dose male rats only (28/50 rats, see Table 5-5). The incidence of peritoneal mesothelioma was lower than the observed incidence of hepatocellular adenoma or carcinoma in male rats (see Table 5-6); therefore, hepatocellular adenoma or carcinoma data were used to derive an oral CSF for 1,4-dioxane.

Table 5-6. Incidence of hepatocellular adenoma or carcinoma in rats and mice exposed to 1,4-dioxane in drinking water for 2 years

Species/strain/gender	Animal dose (mg/kg-day)	Incidence of liver tumors[a]
Male F344/DuCrj rats	0	0/50[b]
	16	2/50
	81	4/49
	398	33/50[c]
Female F344/DuCrj rats	0	1/50[b]
	21	0/50
	103	5/50
	514	40/50[c]
Male Crj:BDF_1 mice	0	21/50
	66	31/48
	251	37/50
	768	39/48[c]
Female Crj:BDF_1 mice	0	4/50[b]
	77	34/50[c]
	323	41/48[c]
	1066	46/48[c]

[a]Incidence of hepatocellular adenoma or carcinoma.
[b]$p < 0.05$; positive dose-related trend (Cochran-Armitage or Peto test).
[c]$p < 0.05$; Fisher's Exact test.

Source: JBRC (1998a).

5.4.3. Dose Adjustments and Extrapolation Method(s)

5.4.3.1. *Dose Adjustments*

Human equivalent doses (HEDs) were calculated from the administered animal doses using a BW scaling factor ($BW^{0.75}$). This was accomplished using the following equation:

$$\text{HED} = \text{animal dose (mg/kg)} \times \left[\frac{\text{animal BW (kg)}}{\text{human BW (kg)}}\right]^{0.25}$$

HEDs for the principal study (JBRC, 1998a) are given in Table 5-7. HEDs were also calculated for supporting studies (NCI, 1978; Kociba et al., 1974) and are also shown in Table 5-7.

Table 5-7. Calculated HEDs for the tumor incidence data used for dose-response modeling

Study	Species/strain/gender	Animal BW (g) TWA	Animal dose (mg/kg-day)	HED (mg/kg-day)[d]
JBRC, 1998a	Male F344/DuCrj rats	380[a]	16	4.3
		380[a]	81	22
		380[a]	398	108
	Female F344/DuCrj rats	229[a]	21	5.0
		229[a]	103	25
		229[a]	514	123
	Male Crj:BDF_1 mice	37.3[a]	66	10
		37.3[a]	251	38
		37.3[a]	768	117
	Female Crj:BDF_1 mice	35.3[a]	77	12
		35.3[a]	323	48
		35.3[a]	1066	160
Kociba et al., 1974	Male and female (combined) Sherman rats	325[b]	14	3.7
		325[b]	121	32
		285[c]	1307	330
NCI, 1978	Male Osborne-Mendel rats	470[b]	240	69
		470[b]	530	152
	Female Osborne-Mendel rats	310[b]	350	90
		310[b]	640	165
	Male $B6C3F_1$ mice	32[b]	720	105
		32[b]	830	121
	Female $B6C3F_1$ mice	30[b]	380	55
		30[b]	860	124

[a]JBRC (1998a) reported only terminal BWs. Default TWA BWs for F344 rats and $B6C3F_1$ mice in a chronic study were obtained from U.S. EPA (1988).
[b]TWA BWs were determined from BW curve provided for control animals.
[c]BWs of high dose male and female rats were significantly lower than controls throughout the study. TWA represents the mean of TWA for male and females (calculated separately from growth curves).
[d]HEDs are calculated as HED = (animal dose) × (animal BW / human BW)$^{0.25}$.

Sources: JBRC (1998a); Kociba et al. (1974); and NCI (1978).

5.4.3.2. *Extrapolation Method(s)*

The weight of evidence is inadequate to establish a MOA(s) by which 1,4-dioxane induces peritoneal, mammary, or nasal tumors in rats and liver tumors in rats and mice (see Section 4.7.3 for a more detailed discussion of 1,4-dioxane's hypothesized MOAs). Therefore, based on the U.S. EPA Guidelines for Carcinogen Risk Assessment (U.S. EPA, 2005a), a linear low dose extrapolation was used as a default option. Accordingly, the CSF for 1,4-dioxane was derived via a linear extrapolation from the POD calculated by curve fitting the experimental dose-response data. The POD is the 95% lower confidence limit on the dose associated with a benchmark response (BMR) near the lower end of the observed data. The BMD modeling analysis used to estimate the POD is described in detail in Appendix D and is summarized below in Section 5.4.4.

Model estimates were derived for all available bioassays and tumor endpoints (see Appendix D); however, the POD used to derive the CSF is based on the most sensitive species and target organ in the principal study (female mice; liver tumors; JBRC, 1998a).

The oral CSF was calculated using the following equation:

$$\text{CSF} = \frac{0.1}{\text{BMDL}_{10}}$$

5.4.4. Oral Slope Factor and Inhalation Unit Risk

The multistage model in the Benchmark Dose Software (BMDS, version 1.3.2) was fit to the incidence data for hepatocellular carcinoma and/or adenoma in rats and mice and mammary and peritoneal tumors in rats exposed to 1,4-dioxane in the drinking water (JBRC, 1998a) (Table 5-5). HEDs were used for BMD modeling (Table 5-7). Doses associated with a BMR of 10% extra risk were calculated with the polynomial degree initially set at (n–1) and lower. BMDs and BMDLs from the lowest degree polynomial models with an adequate fit (χ^2 $p \geq 0.1$) were reported (see Appendix D). A summary of the BMDS model predictions for the JBRC (1998a), NCI (1978), and Kociba et al. (1974) studies is shown in Table 5-8.

The multistage model did not provide an adequate fit (as determined by χ^2 $p > 0.1$) to the data for the incidence of hepatocellular adenoma or carcinoma in female mice (see Appendix D). The high dose was dropped for the female mouse liver tumor dataset in an attempt to achieve an adequate fit; however, an adequate fit was still not achieved. Because the female mice were clearly the most sensitive group tested, other BMD models were applied to the female mouse liver tumor dataset to achieve an adequate fit. The log-logistic model was the only model that provided adequate fit for this data set due to the steep rise in the dose-response curve (68% incidence at the low dose) followed by a plateau at near maximal tumor incidence in the mid- and high-dose regions (85 and 96% incidence, respectively). The predicted BMD_{10} and BMDL_{10} for the female mouse data are presented in Table 5-8. Similarly, the multistage model did not

provide an adequate fit of mammary tumor incidence data for the female rat. The log logistic model provided an adequate fit of this dataset. The predicted BMD_{10} and $BMDL_{10}$ for female rat mammary tumors and male peritoneal tumors are presented in Table 5-8.

A comparison of the model estimates derived for rats and mice from the JBRC (1998a), NCI (1978), and Kociba et al. (1974) studies (Table 5-8) indicates that female mice are more sensitive to liver carcinogenicity induced by 1,4-dioxane compared to other species or tumor types. Additionally, the combined risk of multiple tumor sites in the rat model was considered (See Appendix D, Tables D-16 through D-21) which also supports that liver carcinogenicity in female mice is the most sensitive response. The $BMDL_{10\,HED}$ for the female mouse data was chosen as the POD and the CSF of 0.19 $(mg/kg\text{-}day)^{-1}$ was calculated as follows:

$$CSF = \frac{0.1}{0.52\ mg/kg\text{-}day\ (BMDL_{10\,HED}\ for\ female\ mice)} = 0.19\ (mg/kg\text{-}day)^{-1}$$

Calculation of a CSF for 1,4-dioxane based on dose-response data for the most sensitive species and gender represents a health-protective approach; however, no data currently exist to determine which animal model (i.e., mouse or rat) is more representative of the potential cancer risk in humans.

Table 5-8. $BMD_{10\,HED}$ and $BMDL_{10\,HED}$ values from models fit to tumor incidence data for rats and mice exposed to 1,4-dioxane in drinking water for 2 years and corresponding oral CSFs

Study	Species/strain/gender	Tumor type	$BMD_{10\,HED}$ (mg/kg-day)	$BMDL_{10\,HED}$ (mg/kg-day)	Oral CSF $(mg/kg\text{-}day)^{-1}$
JBRC, 1998a	Male F344/DuCrj rats[a]	Hepatocellular adenoma or carcinoma	21.9	11.9	8.4×10^{-3}
	Female F344/DuCrj rats[b]		31.1	27.3	3.7×10^{-3}
	Male Crj:BDF_1 mice[c]		4.74	2.41	4.1×10^{-2}
	Female Crj:BDF_1 mice[c]		0.79	0.52	0.19
	Male F344/DuCrj rats[b]	Peritoneal tumors	39.3	33.6	3.0×10^{-3}
	Female F344/DuCrj rats[c]	Mammary tumors	40.9	20.9	4.8×10^{-3}
Kociba et al., 1974	Male and female (combined) Sherman rats[a]	Nasal squamous cell carcinomas	880.8	387.8	2.6×10^{-4}
NCI, 1978	Male Osborne Mendel rats[a]		18.8	13.9	7.2×10^{-3}
	Female Osborne Mendel rats[a]		36.9	25.6	3.9×10^{-3}

[a]Multistage model, degree of polynomial = 1.
[b]Multistage model, degree of polynomial = 2.
[c]Log logistic model, high dose dropped, degree of polynomial = 1.

Inhalation studies for 1,4-dioxane evaluated in this assessment were not adequate for the determination of an inhalation unit risk value. No treatment-related tumors were noted in a chronic inhalation study in rats; however, only a single exposure concentration was used (111 ppm 1,4-dioxane vapor for 7 hours/day, 5 days/week for 2 years) (Torkelson et al., 1974).

A route extrapolation from oral bioassay data was not performed (see Section 5.2). In addition, available kinetic models are not suitable for this purpose (see Appendix B).

During the review of this assessment, new data regarding the toxicity of 1,4-dioxane through the inhalation route of exposure have become available. The Agency will evaluate the recently published 1,4-dioxane inhalation data for the potential to derive an IUR in a separate document to follow this assessment.

5.4.5. Previous Cancer Assessment

A previous cancer assessment was posted for 1,4-dioxane on IRIS in 1988. 1,4-Dioxane was classified as a Group B2 Carcinogen (probable human carcinogen; sufficient evidence from animal studies and inadequate eveident or no data from human epidemiology studies [U.S. EPA, 1986c]) based on the induction of nasal cavity and liver carcinomas in multiple strains of rats, liver carcinomas in mice, and gall bladder carcinomas in guinea pigs. An oral CSF of 0.011 $(mg/kg\text{-}day)^{-1}$ was derived from the tumor incidence data for nasal squamous cell carcinoma in male rats exposed to 1,4-dioxane in drinking water for 2 years (NCI, 1978). The linearized multistage extra risk procedure was used for linear low dose extrapolation.

5.5. UNCERTAINTIES IN CANCER RISK VALUES

As in most risk assessments, extrapolation of study data to estimate potential risks to human populations from exposure to 1,4-dioxane has engendered some uncertainty in the results. Several types of uncertainty may be considered quantitatively, but other important uncertainties cannot be considered quantitatively. Thus an overall integrated quantitative uncertainty analysis is not presented. Principal uncertainties are summarized below and in Table 5-9.

5.5.1. Sources of Uncertainty

5.5.1.1. *Choice of Low-Dose Extrapolation Approach*

The range of possibilities for the low-dose extrapolation of tumor risk for exposure to 1,4-dioxane, or any chemical, ranges from linear to nonlinear, but is dependent upon a plausible MOA(s) for the observed tumors. The MOA is a key consideration in clarifying how risks should be estimated for low-dose exposure. Exposure to 1,4-dioxane has been observed in animal models to induce multiple tumor types, including liver adenomas and carcinomas, nasal carcinomas, mammary adenomas and fibroadenomas, and mesothiolomas of the peritoneal cavity (JBRC, 1998a). MOA information that is available for the carcinogenicity of 1,4-dioxane has largely focused on liver adenomas and carcinomas, with little or no MOA information available for the remaining tumor types. In Section 4.7.3, hypothesized MOAs, other than a mutagenic MOA, were explored due to the lack of mutagenicity observed in genetic toxicology tests performed for 1,4-dioxane. Information that would provide sufficient support for any MOA is

not available. In the absence of a MOA(s) for the observed tumor types, a linear low-dose extrapolation approach was used to estimate human carcinogenic risk associated with 1,4-dioxane exposure.

It is not possible to predict how additional MOA information would impact the dose-response assessment for 1,4-dioxane because of the variety of tumors observed and the lack of data on how 1,4-dioxane or a metabolite thereof, interacts with cells starting the progression to the observed tumors.

In general, the Agency has preferred to use the multistage model for analyses of tumor incidence and related endpoints because they have a generic biological motivation based on long-established mathematical models such as the Moolgavkar-Venzon-Knudsen (MVK) model.

The MVK model does not necessarily characterize all modes of tumor formation, but it is a starting point for most investigations and, much more often than not, has provided at least an adequate description of tumor incidence data.

In the studies evaluated (JBRC 1998a; NCI, 1978; Kociba et al., 1974), the multistage model provided good descriptions of the incidence of many tumor types in male and female rats and in male mice exposed to 1,4-dioxane (JBRC, 1998a). However, the multistage model did not provide an adequate fit for the female mouse liver tumor dataset based upon the following (U.S. EPA, 2000b):

Goodness-of-fit χ^2 p-value > 0.10.

Akaike's Information Criterion (AIC) less than any other competing models, even if the alternative models did not have a biological motivation.

No data greatly deviating from the fitted model, as measured by their χ^2 residuals.

BMDS software typically implements the guidance in the BMD technical guidance document (U.S.EPA, 2000b) by imposing constraints on the values of certain parameters of the models. When these constraints were imposed, the multistage model and most other models did not fit the incidence data for female mouse liver adenomas or carcinomas.

The log-logistic model provided an adequate fit for the female mouse data (JBRC, 1998a). Additionally, a log-logistic model with a slope of 1, as is the case for the female mouse data (JBRC, 1998a), represents a low-dose linear extrapolation that is consistent with Agency guidance (U.S. EPA, 2005a). Therefore, the log-logistic model was selected, with the $BMDL_{10\,HED}$ derived by applying the constraints, as consistent with recommended use of BMDS in the BMD technical guidance document (U.S. EPA, 2000b).

The human equivalent oral CSFs estimated from tumor datasets with statistically significant increases ranged from 2.6×10^{-4} to 0.19 per mg/kg-day (Table 5-8), a range of about three orders of magnitude, with the extremes coming from the combined male and female rat data for nasal carcinomas (Kociba et al., 1974) and the female mouse liver adenoma and carcinoma dataset (JBRC, 1998a).

5.5.1.2. *Dose Metric*

1,4-Dioxane is known to be metabolized in vivo. However, it is unknown whether a metabolite or the parent compound, or some combination of parent compound and metabolites, is responsible for the observed toxicity. If the actual carcinogenic moiety is proportional to administered exposure, then use of administered exposure as the dose metric is the least biased choice. On the other hand, if this is not the correct dose metric, then the impact on the CSF is unknown.

5.5.1.3. *Cross-Species Scaling*

An adjustment for cross-species scaling ($BW^{0.75}$) was applied to address toxicological equivalence of internal doses between each rodent species and humans, consistent with the 2005 Guidelines for Carcinogen Risk Assessment (US EPA, 2005a). It is assumed that equal risks result from equivalent constant lifetime exposures.

5.5.1.4. *Statistical Uncertainty at the POD*

Parameter uncertainty can be assessed through confidence intervals. Each description of parameter uncertainty assumes that the underlying model and associated assumptions are valid. For the log-logistic model applied to the female mouse data, there is a reasonably small degree of uncertainty at the 10% excess incidence level (the POD for linear low-dose extrapolation).

5.5.1.5. *Bioassay Selection*

The study by JBRC (1998a) was used for development of an oral CSF. This was a well-designed study, conducted in both sexes in two species with a sufficient number of animals per dose group. The number of test animals allocated among three dose levels and an untreated control group was adequate, with examination of appropriate toxicological endpoints in both sexes of rats and mice. Alternative bioassays (NCI, 1978; Kociba et al., 1974) are available and were fully considered for the derivation of the oral CSF.

5.5.1.6. *Choice of Species/Gender*

The oral CSF for 1,4-dioxane was quantified using the tumor incidence data for the female mouse, which was thought to be more sensitive than male mice or either sex of rats to the carcinogenicity of 1,4-dioxane. While all data, both species and sexes reported from the JBRC (1998a) study, were suitable for deriving an oral CSF, the female mouse data represented the most sensitive indicator of carcinogenicity in the rodent model. The lowest exposure level (77 mg/kg-day or 12 mg/kg-day [HED]) observed a considerable and significant increase in combined liver adenomas and carcinomas. Additional testing of doses within the range of control and the lowest dose (77 mg/kg-day or 12 mg/kg-day [HED]) could refine and reduce uncertainty for the oral CSF.

5.5.1.7. *Relevance to Humans*

The derivation of the oral CSF is derived using the tumor incidence in the liver of female mice. A thorough review of the available toxicological data available for 1,4-dioxane provides no scientific justification to propose that the liver adenomas and carcinomas observed in animal models due to exposure to 1,4-dioxane are not relevant to humans. As such, liver adenomas and carcinomas were considered relevant to humans due to exposure to 1,4-dioxane.

5.5.1.8. *Human Population Variability*

The extent of inter-individual variability in 1,4-dioxane metabolism has not been characterized. A separate issue is that the human variability in response to 1,4-dioxane is also unknown. Although a mutagenic MOA would indicate increased early-life susceptibility, the data exploring whether there is differential sensitivity to 1,4-dioxane carcinogenicity across life stages is unavailable. This lack of understanding about potential differences in metabolism and susceptibility across exposed human populations thus represents a source of uncertainty. Also, the lack of information linking a MOA for 1,4-dioxane to the observed carcinogenicity is a source of uncertainty.

Table 5-9. Summary of uncertainty in the 1,4-dioxane cancer risk assessment

Consideration/ approach	Impact on oral slope factor	Decision	Justification
Low-dose extrapolation procedure	Departure from EPA's *Guidelines for Carcinogen Risk Assessment* POD paradigm, if justified, could ↓ or ↑ unit risk an unknown extent	Log-logistic model to determine POD, linear low-dose extrapolation from POD	A linear low-dose extrapolation approach was used to estimate human carcinogenic risk associated with 1,4-dioxane exposure. Where data are insufficient to ascertain the MOA, EPA's 2005 Guidelines for Carcinogen Risk Assessment recommend application of a linear low-dose extrapolation approach.
Dose metric	Alternatives could ↑ or ↓ CSF by an unknown extent	Used administered exposure	Experimental evidence supports a role for metabolism in toxicity, but it is unclear if the parent compound, metabolite or both contribute to 1,4-dioxane toxicity.
Cross-species scaling	Alternatives could ↓ or ↑ CSF [e.g., 3.5-fold ↓ (scaling by BW) or ↑ twofold (scaling by $BW^{0.67}$)]	$BW^{0.75}$ (default approach)	There are no data to support alternatives. $BW^{0.75}$ scaling was used to calculate equivalent cumulative exposures for estimating equivalent human risks. PBPK modeling was conducted but not deemed suitable for interspecies extrapolation.
Bioassay	Alternatives could ↑ or ↓ CSF by an unknown extent	JBRC 1998a	Alternative bioassays were available and considered for derivation of oral CSF.

Consideration/ approach	Impact on oral slope factor	Decision	Justification
Species /gender combination	Human risk could ↓ or ↑, depending on relative sensitivity	Female mouse	There are no MOA data to guide extrapolation approach for any choice. It was assumed that humans are as sensitive as the most sensitive rodent gender/species tested; true correspondence is unknown. Calculation of the CSF for 1,4-dioxane was based on dose-response data from the most sensitive species and gender. The carcinogenic response occurs across species.
Human relevance of mouse tumor data	If rodent tumors proved not to be relevant to humans, unit risk would not apply i.e., could ↓ CSF	Liver adenomas and carcinomas are relevant to humans	1,4-dioxane is a multi-site carcinogen in rodents and the MOA(s) is unknown; carcinogenicity observed in the rodent studies is considered relevant to human exposure.
Human population variability in metabolism and response/ sensitive subpopulations	Low-dose risk ↑ or ↓ to an unknown extent	Considered qualitatively	No data to support range of human variability/sensitivity, including whether children are more sensitive.

6. MAJOR CONCLUSIONS IN THE CHARACTERIZATION OF HAZARD AND DOSE RESPONSE

6.1. HUMAN HAZARD POTENTIAL

1,4-Dioxane is absorbed rapidly following oral and inhalation exposure, with much less absorption occurring from the dermal route. 1,4-Dioxane is primarily metabolized to HEAA, which is excreted in the urine. Liver and kidney toxicity are the primary noncancer health effects associated with exposure to 1,4-dioxane in humans and laboratory animals. Several fatal cases of hemorrhagic nephritis and centrilobular necrosis of the liver were related to occupational exposure (i.e., inhalation and dermal contact) to 1,4-dioxane (Johnstone, 1959; Barber, 1934). Neurological changes were also reported in one case, including headache, elevation in blood pressure, agitation and restlessness, and coma (Johnstone, 1959). Perivascular widening was observed in the brain of this worker, with small foci of demyelination in several regions (e.g., cortex, basal nuclei). Severe liver and kidney degeneration and necrosis were observed frequently in acute oral and inhalation studies (≥ 1,000 mg/kg-day oral, ≥ 1,000 ppm inhalation) (JBRC, 1998b; Drew et al., 1978; David, 1964; Kesten et al., 1939; Laug et al., 1939; Schrenk and Yant, 1936; de Navasquez, 1935; Fairley et al., 1934).

Liver and kidney toxicity were the primary noncancer health effects of subchronic and chronic oral exposure to 1,4-dioxane in animals. Hepatocellular degeneration and necrosis were observed (Kociba et al., 1974) and preneoplastic changes were noted in the liver following chronic administration of 1,4-dioxane in drinking water (JBRC, 1998a, Argus et al., 1973). Liver and kidney toxicity appear to be related to saturation of clearance pathways and an increase in the 1,4-dioxane concentration in the blood (Kociba et al., 1975). Kidney damage was characterized by degeneration of the cortical tubule cells, necrosis with hemorrhage, and glomerulonephritis (NCI, 1978; Kociba et al., 1974; Argus et al., 1973, 1965; Fairley et al., 1934).

Several carcinogenicity bioassays have been conducted for 1,4-dioxane in mice, rats, and guinea pigs (JBRC, 1998a; NCI, 1978; Kociba et al., 1974; Torkelson et al., 1974; Argus et al., 1973; Hoch-Ligeti and Argus, 1970; Hoch-Ligeti et al., 1970; Argus et al., 1965). Liver tumors (hepatocellular adenomas and carcinomas) have been observed following drinking water exposure in several species and strains of rats, mice, and guinea pigs. Nasal (squamous cell carcinomas), peritoneal, and mammary tumors were also observed in rats, but were not seen in mice. With the exception of the NCI (1978) study, the incidence of nasal cavity tumors was generally lower than that of liver tumors in the same study population.

Under the Guidelines for Carcinogen Risk Assessment (U.S. EPA, 2005a), 1,4-dioxane can be classified as likely to be carcinogenic to humans, based on adequate evidence of liver

carcinogenicity in several 2-year bioassays conducted in three strains of rats, two strains of mice, and in guinea pigs (JBRC, 1998a; NCI, 1978; Kociba et al., 1974; Argus et al., 1973; Hoch-Ligeti and Argus, 1970; Hoch-Ligeti et al., 1970; Argus et al., 1965). Studies in humans found no conclusive evidence for a causal link between occupational exposure to 1,4-dioxane and increased risk for cancer; however, only two studies were available and these were limited by small cohort size and a small number of reported cancer cases (Buffler et al., 1978; Thiess et al., 1976).

The available evidence is inadequate to establish a MOA by which 1,4-dioxane induces liver tumors in rats and mice. The genotoxicity data for 1,4-dioxane is generally characterized as negative, although several studies may suggest the possibility of genotoxic effects (Roy et al., 2005; Morita and Hayashi, 1998; Mirkova, 1994; Kitchin and Brown, 1990; Galloway et al., 1987). A MOA hypothesis involving sustained proliferation of spontaneously transformed liver cells has some support by evidence that suggests 1,4-dioxane is a tumor promoter in mouse skin and rat liver bioassays (Lundberg et al., 1987; King et al., 1973). Dose-response and temporal evidence support the occurrence of cell proliferation and hyperplasia prior to the development of liver tumors (JBRC, 1998a; Kociba et al., 1974). However, the dose-response relationship for the induction of hepatic cell proliferation has not been characterized, and it is unknown if it would reflect the dose-response relationship for liver tumors in the 2-year rat and mouse studies. Conflicting data from rat and mouse bioassays (JBRC, 1998a; Kociba et al., 1974) suggest that cytotoxicity is not a required precursor event for 1,4-dioxane-induced cell proliferation. Data regarding a plausible dose response and temporal progression from cytotoxicity to cell proliferation and eventual liver tumor formation are not available.

6.2. DOSE RESPONSE

6.2.1. Noncancer/Oral

The RfD of 3×10^{-2} mg/kg-day was derived based on liver and kidney toxicity in rats exposed to 1,4-dioxane in the drinking water for 2 years (Kociba et al., 1974). This study was chosen as the critical study because it provides the most sensitive measure of adverse effects by 1,4-dioxane. The incidence of liver and kidney lesions was not reported for each dose group. Therefore, BMD modeling could not be used to derive a POD. Instead, the RfD is derived by dividing the NOAEL of 9.6 mg/kg-day by a composite UF of 300 (factors of 10 for animal-to-human extrapolation and interindividual variability, and a partial UF of 3 for database deficiencies). Information was unavailable to quantitatively assess toxicokinetic or toxicodynamic differences between animals and humans and the potential variability in human susceptibility; thus, the interspecies and intraspecies uncertainty factors of 10 were applied. In addition, a threefold database uncertainty factor was applied due to the lack of information addressing the potential reproductive toxicity associated with 1,4-dioxane.

The overall confidence in this RfD assessment is medium. Confidence in the principal study (Kociba et al., 1974) is medium. Confidence in the database is medium due to the lack of a multigeneration reproductive toxicity study. Reflecting medium confidence in the principal study and medium confidence in the database, confidence in the RfD is medium.

6.2.2. Noncancer/Inhalation

No inhalation RfC was derived for 1,4-dioxane. Inhalation data were inadequate and a route extrapolation from oral toxicity data was not performed, due to direct effects of 1,4-dioxane on the respiratory tract (i.e., respiratory irritation in humans, pulmonary congestion in animals) (Wirth and Klimmer, 1936; Fairley et al., 1934; Yant et al., 1930) and lack of a suitable kinetic model (see Appendix B).

6.2.3. Cancer/Oral

An oral CSF for 1,4-dioxane of 0.19 $(mg/kg\text{-}day)^{-1}$ was based on liver tumors in female mice from a chronic study (JBRC, 1998a). Because the MOA for liver carcinogenicity of 1,4-dioxane is not known, the CSF was derived by linear low-dose extrapolation. The POD was calculated by curve fitting the experimental dose-response data from the POD, the range of observation ($BMDL_{10\ HED}$ of 0.52 mg/kg-day).

The uncertainties associated with the quantitation of the oral CSF are discussed below.

6.2.3.1. *Choice of Low-Dose Extrapolation Approach*

The range of possibilities for the low-dose extrapolation of tumor risk for exposure to 1,4-dioxane, or any chemical, ranges from linear to nonlinear, but is dependent upon a plausible MOA(s) for the observed tumors. The MOA is a key consideration in clarifying how risks should be estimated for low-dose exposure. Exposure to 1,4-dioxane has been observed in animal models to induce multiple tumor types, including liver adenomas and carcinomas, nasal carcinomas, mammary adenomas and fibroadenomas, and mesothiolomas of the peritoneal cavity (JBRC, 1998a). MOA information that is available for the carcinogenicity of 1,4-dioxane has largely focused on liver adenomas and carcinomas, with little or no MOA information available for the remaining tumor types. In Section 4.7.3, hypothesized MOAs, other than a mutagenic MOA, were explored due to the lack of mutagenicity observed in genetic toxicology tests performed for 1,4-dioxane. Data are not available to support a carcinogenic MOA for 1,4-dioxane. In the absence of a MOA(s) for the observed tumor types due to exposure to 1,4-dioxane, a linear low-dose extrapolation approach was used to estimate human carcinogenic risk associated with 1,4-dioxane exposure.

The extent to which the overall uncertainty in low-dose risk estimation could be reduced if the MOA for 1,4-dioxane were known is of interest, but additional supporting data on the MOA(s) of 1,4-dioxane is not available. Even if it were available, incorporation of MOA into

dose-response modeling might not be straightforward and might not significantly reduce the uncertainty about low-dose extrapolation.

In general, the Agency has preferred to use the multistage model for analyses of tumor incidence and related endpoints because they have a generic biological motivation based on long-established mathematical models such as the MVK model. The MVK model does not necessarily characterize all modes of tumor formation, but it is a starting point for most investigations and, much more often than not, has provided at least an adequate description of tumor incidence data.

In the studies evaluated (JBRC 1998a; NCI, 1978; Kociba et al., 1974) the multistage model provided good descriptions of the incidence of many tumor types in male and female rats and in male mice exposed to 1,4-dioxane (JBRC, 1998a). However, the multistage model did not provide an adequate fit for female mouse liver tumor dataset based upon the following (U.S. EPA, 2000b):

Goodness-of-fit χ^2 p-value > 0.10;

AIC less than any other competing models, even if the alternative models did not have a biological motivation;

No data greatly deviating from the fitted model, as measured by their χ^2 residuals.

BMDS software typically implements the guidance in the BMD technical guidance document (U.S.EPA, 2000b) by imposing constraints on the values of certain parameters of the models. When these constraints were imposed, the multistage model and most other models did not fit the incidence data for female mouse liver adenomas or carcinomas.

The log-logistic model provided an adequate fit for the female mouse data (JBRC, 1998a). Additionally, a log-logistic model with a slope of 1, as is the case for the female mouse data (JBRC, 1998a), represents a low-dose linear extrapolation that is consistent with Agency guidance (U.S. EPA, 2005a). Therefore, the log-logistic model was selected, with the $BMDL_{10}$ derived by applying the constraints, as consistent with recommended use of BMDS in the BMD technical guidance document (U.S. EPA, 2000b).

The human equivalent oral CSF estimated from liver tumor datasets with statistically significant increases ranged from 2.58×10^{-4} to 0.19 per mg/kg-day, a range of about three orders of magnitude, with the extremes coming from the combined male and female data for nasal carcinomas (Kociba et al., 1974) and the female mouse liver adenoma and carcinoma dataset (JBRC, 1998a).

6.2.3.2. *Dose Metric*

1,4-Dioxane is known to be metabolized in vivo. However, it is unknown whether a metabolite or the parent compound, or some combination of parent compound and metabolites, is responsible for the observed toxicity. If the actual carcinogenic moiety is proportional to

administered exposure, then use of administered exposure as the dose metric is the least biased choice. On the other hand, if this is not the correct dose metric, then the impact on the CSF is unknown.

6.2.3.3. *Cross-Species Scaling*

An adjustment for cross-species scaling ($BW^{0.75}$) was applied to address toxicological equivalence of internal doses between each rodent species and humans, consistent with the 2005 Guidelines for Carcinogen Risk Assessment (US EPA, 2005a). It is assumed that equal risks result from equivalent constant lifetime exposures.

6.2.3.4. *Statistical Uncertainty at the POD*

Parameter uncertainty can be assessed through confidence intervals. Each description of parameter uncertainty assumes that the underlying model and associated assumptions are valid. For the log-logistic model applied to the female mouse data, there is a reasonably small degree of uncertainty at the 10% excess incidence level (the POD for linear low-dose extrapolation).

6.2.3.5. *Bioassay Selection*

The study by JBRC (1998a) was used for development of an oral CSF. This was a well-designed study, conducted in both sexes in two species with a sufficient number of animals per dose group. The number of test animals allocated among three dose levels and an untreated control group was adequate, with examination of appropriate toxicological endpoints in both sexes of rats and mice. Alternative bioassays (NCI, 1978; Kociba et al., 1974) are available and were fully considered for the derivation of the oral CSF.

6.2.3.6. *Choice of Species/Gender*

The oral CSF for 1,4-dioxane was quantified using the tumor incidence data for the female mouse, which was thought to be more sensitive than male mice or either sex of rats to the carcinogenicity of 1,4-dioxane. While all data, both species and sexes reported from the JBRC (1998a) study, were suitable for deriving an oral CSF, the female mouse data represented the most sensitive indicator of carcinogenicity in the rodent model. The lowest exposure level (77 mg/kg-day or 12 mg/kg-day [HED]) observed a considerable and significant increase in combined liver adenomas and carcinomas. Additional testing of doses within the range of control and the lowest dose (77 mg/kg-day or 12 mg/kg-day [HED]) could refine and reduce uncertainty for the oral CSF.

6.2.3.7. *Relevance to Humans*

The derivation of the oral CSF is derived using the tumor incidence in the liver of female mice. A thorough review of the available toxicological data available for 1,4-dioxane provides no scientific justification to propose the liver adenomas and carcinomas observed in animal models due to exposure to 1,4-dioxane are not plausible in humans. Liver adenomas and carcinomas were considered as a plausible outcome in humans due to exposure to 1,4-dioxane.

6.2.3.8. *Human Population Variability*

The extent of inter-individual variability in 1,4-dioxane metabolism has not been characterized. A separate issue is that the human variability in response to 1,4-dioxane is also unknown. Although a mutagenic MOA would indicate increased early-life susceptibility, the data exploring whether there is differential sensitivity to 1,4-dioxane carcinogenicity across life stages is unavailable. This lack of understanding about potential differences in metabolism and susceptibility across exposed human populations thus represents a source of uncertainty. Also, the lack of information linking a MOA for 1,4-dioxane to the observed carcinogenicity is a source of uncertainty.

6.2.4. Cancer/Inhalation

Inhalation studies for 1,4-dioxane were not adequate for the determination of an inhalation unit risk value. No treatment-related tumors were noted in a chronic inhalation study in rats; however only a single exposure concentration was used (111 ppm 1,4-dioxane vapor for 7 hours/day, 5 days/week for 2 years) (Torkelson et al., 1974). Route extrapolation from oral bioassay data was not performed because available kinetic models were not considered suitable for this purpose.

7. REFERENCES

ATSDR (Agency for Toxic Substances and Disease Registry). (2007) Toxicological profile for 1,4-dioxane. Draft for public comment. Atlanta, GA: U.S. Department of Health and Human Services, Public Health Service. Available online at http://www.atsdr.cdc.gov/toxpro2.html.

ATSDR. (2006) Toxicological profile for 1,1,1-trichloroethane. Atlanta, GA: U.S. Department of Health and Human Services, Public Health Service. Available online at http://www.atsdr.cdc.gov/toxpro2.html.

Agrawal, AK; Shapiro, BH. (2000) Differential expression of gender-dependent hepatic isoforms of cytochrome P-450 by pulse signals in the circulating masculine episodic growth hormone profile of the rat. J Pharmacol Exp Therap 292:228–237.

Andersen, ME; Clewell, HJ,III; Gargas, ML; et al. (1987) Physiologically-based pharmacokinetics and the risk assessment process for methylene chloride. Toxicol Appl Pharmacol 87:185-205.

Argus, MF; Arcos, JC; Hochligeti, C. (1965) Studies on the carcinogenic activity of protein-denaturing agents: hepatocarcinogenicity of dioxane. J Natl Cancer Inst 35:949–958.

Argus, MF; Sohal, RS; Bryant, GM; et al. (1973) Dose-response and ultrastructural alterations in dioxane carcinogenesis: Influence of methylcholanthrene on acute toxicity. Eur J Cancer 9:237–243.

Ashby, J. (1994) Series: current issues in mutagenesis and carcinogenesis, No. 45—The genotoxicity of 1,4-dioxane. Mutat Res 322(2):141–150.

Atkinson, R. (1989) Kinetics and mechanisms of the gas-phase reactions of the hydroxyl radical with organic compounds. J Phys Chem Ref Data. Monograph No. 1 p. 143.

Bannasch P. (2003) Comments on R. Karbe and R.L. Kerlin (2002) Cystic degeneration/spongiosis hepatic (Toxicol Pathol 30 (2), 216-227). Toxicol Pathol 31:566-570.

Barber, H. (1934) Haemorrhagic nephritis and necrosis of the liver from dioxane poisoning. Guys Hosp Rep 84:267–280.

Braun, WH; Young, JD. (1977) Identification of B-hydroxyethoxyacetic acid as the major urinary metabolite of 1,4-dioxane in the rat. Toxicol Appl Pharmacol 39:33–38.

Bronaugh, RL. (1982) Percutaneous absorption of cosmetic ingredients. In: Frost, P; Horwitz, SN, eds. Principles of cosmetics for the dermatologist. Minneapolis, MN: University of Minnesota Press, 277-284.

Brown, RP; Delp, MD; Lindstedt, SL; et al. (1997) Physiological parameter values for physiologically based pharmacokinetic models. Toxicol Ind Health 13(4):407–484.

Buffler, PA; Wood, SM; Suarez, L; et al. (1978) Mortality follow-up of workers exposed to 1,4-dioxane. J Occup Med 20(4):255–259.

Bull, RJ; Robinson, M; Laurie, RD. (1986) Association of carcinoma yield with early papilloma development in SENCAR mice. Environ Health Perspect 68:11–17.

Burmistrov, SO; Arutyunyan, AV; Stepanov, MG; et al. (2001) Effect of chronic inhalation of toluene and dioxane on activity of free radical processes in rat ovaries and brain. Bull Exp Biol Med 132(3):832–836.

Carpenter, SP; Lasker, JM; Raucy, JL. (1996) Expression, induction, and catalytic activity of the ethanol-inducible cytochrome P450 (CYP2E1) in human fetal liver and hepatocytes. Mol Pharmacol 49:260–268.

Clark, B; Furlong, JW; Ladner, A; et al. (1984) Dermal toxicity of dimethyl acetylene dicarboxylate, n-methyl pyrrolidone, triethylene glycol dimethyl ether, dioxane and tetraline in the rat. IRCS J Med Sci 12:296–297.

David, H. (1964) [Electron-microscopic findings in dioxane-dependent nephrosis in rat kidneys] Beitr Pathol Anat 130:187–212.

de Navasquez, S. (1935) Experimental tubular necrosis of the kidneys accompanied by liver changes due to dioxane poisoning. J Hyg 35:540–548.

Derosa, CT; Wilbur, S; Holler, J; et al. (1996) Health evaluation of 1,4-dioxane. Toxicol Ind Health 12(1):1-43.

Drew, RT; Patel, JM; Lin, F. (1978) Changes in serum enzymes in rats after inhalation of organic solvents singly and in combination. Toxicol Appl Pharmacol 45:809–819.

Ernstård, L; Iregren, A; Sjögren, B; et al. (2006) Acute effects of exposure to vapours of dioxane in humans. Human Experimental Toxicol 25:723-729.

Fairley, A; Linton, EC; Ford-Moore, AH. (1934) The toxicity to animals of 1,4-dioxane. J Hyg 34:486–501.

Fisher, J; Mahle, D; Bankston, L; et al. (1997) Lactational transfer of volatile chemicals in breast milk. Am Ind Hyg Assoc J 58(6):425–431.

Franke, C; Studinger, G; Berger, G; et al. (1994) The assessment of bioaccumulation. Chemosphere 29:1501–1514.

Frantik, R; Hornychova, M; Horvath, M. (1994) Relative acute neurotoxicity of solvents: isoeffective air concentrations of 48 compounds evaluated in rats and mice. Environ Res 66:173–185.

Galloway, SM; Armstrong, MJ; Reuben, C; et al. (1987) Chromosome aberrations and sister chromatid exchanges in Chinese hamster ovary cells: evaluations of 108 chemicals. Environ Mol Mutagen 10(supp 10):1-175.

Giavini, E; Vismara, C; Broccia, ML. (1985) Teratogenesis study of dioxane in rats. Toxicol Lett 26:85–88.

Goldberg, ME; Johnson, HE; Pozzani, UC; et al. (1964) Effect of repeated inhalation of vapors of industrial solvents on animal behavior. I. Evaluation of nine solvent vapors on pole-climb performance in rats. Am Ind Hyg Assoc J 25:369–375.

Goldsworthy, TL; Monticello, TM; Morgan, KT; et al. (1991) Examination of potential mechanisms of carcinogenicity of 1,4-dioxane in rat nasal epithelial cells and hepatocytes. Arch Toxicol 65:1–9.

Green, T., Lee, R., Moore, R., et al. (2000) Acetochlor-induced rat nasal tumors: Further studies on the mode of action and relevance to humans.

Grosjean, D. (1990) Atmospheric chemistry of toxic contaminants. 2. Saturated aliphatics:Acetaldehyde, dioxane, ethylene glycol ethers, propylene oxide. J Air Waste Mgmt Assoc 40:1522-1531.

Hansch, C; Leo, A; Hoekman, D. (1995) Exploring QSAR. Hydrophobic, electronic, and steric constants. ACS Professional Reference Book. Washington, DC: American Chemical Society., p. 9.

Haseman, JK; Hailey, JR, (1997) An update of the National Toxicology Program database on nasal carcinogens. Mutat Res 380:3–11.

Haworth, S; Lawlor, T; Mortelmans, K; et al. (1983) Salmonella mutagenicity test results for 250 chemicals. Environ Mutagen supp. 1:1, 10.

Hayashi, S; Watanabe, J; Kawajiri, K. (1991) Genetic polymorphisms in the 5'-flanking region change transcriptional regulation of the human cytochrome P450IIE1 gene. J Biochem 110:559–565.

Hellmer, L; Bolcsfoldi, G. (1992) An evaluation of the E coli K-12 uvrB/recA DNA repair host- mediated assay I In vitro sensitivity of the bacteria to 61 compounds. Mutat Res 272:145–160.

Hoch-Ligeti, C; Argus, MF. (1970) Effect of carcinogens on the lung of guinea pigs. In: Nettesheim, P; Hanna, MG; Deatherage, JW, eds. Morphology of experimental respiratory carcinogenesis. AEC Symp Ser 21National Cancer Institute and U.S. Atomic Energy Commission, pp. 267–279. CONF700501.

Hoch-Ligeti, C; Argus. MF; Arcos, JC. (1970) Induction of carcinomas in the nasal cavity of rats by dioxane. Br J Cancer 24(1):164–167.

HSDB (Hazardous Substances Data Bank) (2007) 1,4-dioxane. Last update dated 4/14/2006. National Library of Medicine, National Toxicology Program, Bethesda, Maryland.

Huang, CY; Huang, KL; Chong, TI; et al. (1997) The GSTT1 and CYP2E1 genotypes are possible factors causing vinyl chloride induced abnormal liver function. Arch Toxicol 71:482–488.

IARC (International Agency for Research on Cancer). (1999) Some chemicals that cause tumours of the kidney or urinary bladder in rodents and some other substances- 1,4-dioxane (group 2B). IARC Monogr Eval Carcinog Risks Hum 71 Lyon, France: World Health Organization, p. 589. Available online at http://www-cie.iarc.fr/htdocs/monographs/vol71/019-dioxane.html.

ICRP (International Commission of Radiological Protection). (1975) No. 23: Report of the Task Group on Reference Man. Pergamon Press, New York, NY.

JBRC. (1998a) Two-year studies of 1,4-dioxane in F344 rats and BDF_1 mice (drinking water). Kanagawa, Japan: Japan Bioassay Research Center.

JBRC. (1998b) Two-week studies of 1,4-dioxane in F344 rats and BDF_1 mice (drinking water studies). Kanagawa, Japan: Japan Bioassay Research Center.

Johnstone, RT. (1959) Death due to dioxane? AMA Arch Ind Health 20:445–447.

Kanada, M; Miyagawa, M; Sato, M; et al. (1994) Neurochemical profile of effects of 28 neurotoxic chemicals on the central nervous system in rats (1). Effects of oral administration on brain contents of biogenic amines and metabolites. Ind Health 32:145–164.

Kano, J; Umeda, Y; Saito, M; et al. (2008) Thirteen-week oral toxicity of 1,4-dioxane in rats and mice. J Toxicol Sci 33(2):141-153.

Karbe, E; Kerlin, RL. (2002) Cystic degeneration/spongiosis hepatic in rats. Toxicol Pathol 30(2):216–227.

Kasper, P., Uno, Y., Mauthe, R. et al. (2007) Follow-up testing of rodent carcinogens not positive in the standard genotoxicity testing battery: IWGT workgroup report. Mut Res 627:106-116.

Kesten, HD; Mulinos, MG; Pomerantz L. (1939) Pathologic effects of certain glycols and related compounds. Arch Pathol 27:447–465.

Khudoley, VV; Mizgireuv, I; Pliss, GB. (1987) The study of mutagenic activity of carcinogens and other chemical agents with *Salmonella typhimurium* assays: testing of 126 compounds. Arch Geschwulstforsch 57:453–462.

King, ME; Shefner, AM; Bates, RR. (1973) Carcinogenesis bioassay of chlorinated dibenzodioxins and related chemicals. Environ Health Perspect 5:163–170.

Kitchin, KT; Brown, JL. (1990) Is 1,4-dioxane a genotoxic carcinogen? Cancer Lett 53(1):67–71.

Knoefel, PK. (1935) Narcotic potency of some cyclic acetals. J Pharmacol Exp Ther 53:440–444.

Kociba, RJ; McCollister, SB; Park, C; et al. (1974) 1,4-dioxane. I. Results of a 2-year ingestion study in rats. Toxicol Appl Pharmacol 30:275–286.

Kociba, RJ; Torkelson, TR; Young, JD; et al. (1975) 1,4-dioxane: correlation of the results of chronic ingestion and inhalation studies with its dose-dependent fate in rat. In: Proceedings of the 6th Annual Conference on Environmental Toxicology. October 21–23, Aerospace Medical Research Laboratory, Wright-Patterson Air Force Base, Ohio, pp. 345–354.

Kurl, RN; Poellinger, L; Lund, J; et al. (1981) Effects of dioxane on RNA synthesis in the rat liver. Arch Toxicol 49(1):29–33.

Kwan, KK; Dutka, BJ; Rao, SS; et al. (1990) Mutatox test: a new test for monitoring environmental genotoxic agents. Environ Pollut 65:323–332.

Laug, EP; Calvery, HO; Morris, HJ; et al. (1939) The toxicity of some glycols and derivatives. J Ind Hyg Toxicol 21:173–201.

Lesage S; Jackson RE; Priddle MW; et al. (1990) Occurrence and fate of organic solvent residues in anoxic groundwater at the Gloucester Landfill, Canada. Environ Sci Technol 24:559-565.

Lewis, RJ, ed. (2000) Sax's dangerous properties of industrial materials. 10th edition. New York, NY: John Wiley & Sons, Inc., p.1509.

Lewis, RJ, ed. (2001) Hawley's condensed chemical dictionary. 14th edition. New York, NY: John Wiley & Sons, Inc., p. 406.

Lide, DR, ed. (2000) CRC handbook of chemistry and physics. 81st edition. Boca Raton, FL: CRC Press LLC, pp. 3-144.

Leung, H-W; Paustenbach, DJ. (1990) Cancer risk assessment for dioxane based upon a physiologically-based pharmacokinetic approach. Toxicol Lett 51:147–162.

Lundberg, I; Ekdahl, M; Kronevi, T; et al. (1986) Relative hepatotoxicity of some industrial solvents after intraperitoneal injection or inhalation exposure in rats. Environ Res 40:411–420.

Lundberg, I; Hogberg, J; Kronevi, T; et al. (1987) Three industrial solvents investigated for tumor promoting activity in the rat liver. Cancer Lett 36:29–33.

Lyman, WJ; Reehl, WF; Rosenblatt; et al. (1990) Handbook of chemical property estimation methods. Washington, DC: American Chemical Society, pp. 4–9.

Marzulli, F; Anjo, DM; Maibach, HI. (1981) In vivo skin penetration studies of 2,4-toluenediamine, 2,4-diaminoanisole, 2-nitro-p-phenylenediamine, p-dioxane and N-nitrosodiethanolamine in cosmetics. Food Cosmet Toxicol 19:743–747.

McFee, AF; Abbott, MG; Gulati, DK; et al. (1994) Results of mouse bone marrow micronucleus studies on 1,4-dioxane. Mutat Res 322:141–150.

McGregor, DB; Brown, AG; Howgate, S; et al. (1991) Responses of the L5178Y mouse lymphoma cell forward mutation assay. V. 27 coded chemicals. Environ Mol Mutagen 17(3):196–219.

Meylan, WM; Howard, PH; Boethling, RS; et al. (1999) Improved method for estimating bioconcentration/ bioaccumulation factor from octanol/water partition coefficient. Environ Toxicol Chem 18:664–672.

Mikheev, MI; Gorlinskaya, YE P; Solovyova, TV. (1990) The body distribution and biological action of xenobiotics. J Hyg Epidemiol Microbiol Immunol 34:329–336.

Mirkova, ET. (1994) Activity of the rodent carcinogen 1,4-dioxane in the mouse bone marrow micronucleus assay. Mutat Res 322:142–144.

Miyagawa, M; Shirotori, T; Tsuchitani, M; et al. (1999) Repeat-assessment of 1,4-dioxane in a rat-hepatocyte replicative DNA synthesis (RDS) test: evidence for stimulus of hepatocyte proliferation. Exp Toxicol Pathol 51:555–558.

Morita, T. (1994) No clastogenicity of 1,4-dioxane as examined in the mouse peripheral blood micronucleus test. MMS Commun 2:7–8.

Morita, T; Hayashi, M. (1998) 1,4-dioxane is not mutagenic in five in vitro assays and mouse peripheral blood micronucleus assay, but is in mouse liver micronucleus assay. Environ Mol Mutagen 32:269–280.

Mungikar, AM; Pawar, SS. (1978) Induction of the hepatic microsomal mixed function oxidase system in mice by p-dioxane. Bull Environ Contam Toxicol 20:797–804.

Munoz, ER; Barnett, BM. (2002) The rodent carcinogens 1,4-dioxane and thiourea induce meiotic non-disjunction in *Drosophila melanogaster* females. Mutat Res 517(1–2):231–238.

Nannelli, A; De Rubertis, A; Longo, V; et al. (2005) Effects of dioxane on cytochrome P450 enzymes in liver, kidney, lung and nasal mucosa of rat. Arch Toxicol 79(2):74–82.

NCI (National Cancer Institute). (1978) Bioassay of 1,4-dioxane for possible carcinogenicity. Bethesda, MD: National Cancer Institute. NIH Pub. No. 78-1330 NCICGTR-80.

Nelson, N. (1951) Solvent toxicity with particular reference to certain octyl alcohols and dioxanes. Med Bull 11:226–238.

Nestmann, ER; Otson, R; Kowbel, DJ; et al. (1984) Mutagenicity in a modified Salmonella assay of fabric-protecting products containing 1,1,1-trichloroethane. Environ Mutagen 6:71–80.

NRC (National Research Council). (1983) Risk assessment in the Federal government: managing the process. Committee on the Institutional Means for Assessment of Risks to Public Health, Commission on Life Sciences, NRC. Washington, DC; National Academy Press.

O'Neil, MJ, ed. (2001) The Merck index - An encyclopedia of chemicals, drugs, and biologicals. 13th edition. Whitehouse Station, NJ: Merck and Co., Inc., p. 581.

Park, JH; Hussam, A; Couasnon, P; et al. (1987) Experimental reexamination of selected partition coefficients from Rohrschneider's data set. Anal Chem 59:1970–1976.

Platz, J., Megelberg, T., Nielson, O., et al. (1997) Atmospheric chemistry of 1,4-dioxane. J Chem Soc Faraday Trans 93:2855-2863.

Pozzani, UC; Weil, CS; Carpenter, CP. (1959) The toxicological basis of threshold limit values: 5: The experimental inhalation of vapor mixtures by rats, with notes upon the relationship between single dose inhalation and single dose oral data. J Ind Hyg 20:364–369.

Ramsey, JC; Andersen, ME. (1984) A physiologically based description of the inhalation pharmacokinetics of styrene in rats and humans. Toxicol Appl Pharmacol 73:159-175.

Reitz, RH; McCroskey, PS; Park, CN; et al. (1990) Development of a physiologically based pharmacokinetic model for risk assessment with 1,4-dioxane. Toxicol Appl Pharmacol 105:37–54.

Rosenkranz, HS; Klopman, G. (1992) 1,4-dioxane: prediction of in vivo clastogenicity. Mutat Res 280:245–251.

Roy, SK; Thilagar, AK; Eastmond, DA. (2005) Chromosome breakage is primarily responsible for the micronuclei induced by 1,4-dioxane in the bone marrow and liver of young CD1 mice. Mutation Research 586:28–37.

Schrenk, HH; Yant, WP. (1936) Toxicity of dioxane. J Ind Hyg Toxicol 18:448–460.

Sheu, CW; Moreland, FM; Lee, JK; et al. (1988) In vitro BALB/3T3 cell transformation assay of nonoxynol-9 and 1,4-dioxane. Environ Mol Mutagen 11:41–48.

Silverman, L; Schulte, HF; First, MW. (1946) Further studies of sensory response to certain industrial solvent vapors. J Ind Hyg Toxicol 28:262–266.

Sina, JF; Bean, CL; Dysart, GR; et al. (1983) Evaluation of the alkaline elution/rat hepatocyte assay as a predictor of carcinogenic/mutagenic potential. Mutat Res 113:357–391.

Smyth, HFJ; Seaton, J; Fischer, L. (1941) The single dose toxicity of some glycols and derivatives. J Ind Hyg Toxicol 23(6):259–268.

Stoner, GD, Conran, PB; Greisiger, EA; et al. (1986) Comparison of two routes of chemical administration on the lung adenoma response in strain A/J mice. Toxicol Appl Pharmacol 82:19–31.

Stott, WT; Quast, JF; Watanabe, PG. (1981) Differentiation of the mechanisms of oncogenicity of 1,4-dioxane and 1,3-hexachlorobutadiene in the rat. Toxicol Appl Pharmacol 60:287–300.

Stroebel, P; Mayer, F; Zerban, H; et al. (1995) Spongiotic pericytoma: a benign neoplasm deriving from the perisinusoidal (Ito) cells in rat liver. Am J Pathol 146(4):903–913.

Suprenant, KS. (2002) Dioxane. In: Ullmann's encyclopedia of industrial chemistry. Article Online Posting Date June 15, 2000. Available from subscription to Wiley Interscience: Wiley-VCH Verlag GmbH and Co. KGaA, and online at http://www.mrw.interscience.wiley.com/ueic/ueic_search_fs.html.

Sweeney, L., Thrall, K., Poet, T., et al. (2008) Physiologically based pharmacokinetic modeling of 1,4-dioxane in rats, mice, and humans. Toxicol Sci 101(1):32-50.

Thiess, AM; Tress, E; Fleig, I. (1976) [Industrial-medical investigation results in the case of workers exposed to dioxane.] Arbeitsmed Sozialmed Pravent 11:35–46.

Thurman, GB; Simms, BG; Goldstein, AL; et al. (1978) The effects of organic compounds used in the manufacture of plastics on the responsivity of murine and human lymphocytes. Toxicol Appl Pharmacol 44(3):617–641.

Tinwell, H; Ashby, J. (1994) Activity of 1,4-dioxane in mouse bone marrow micronucleus assays. Mutat Res 322:148–150.

Torkelson, R; Leong, BKJ; Kociba, RJ; et al. (1974) 1,4-dioxane. II. Results of a 2-year inhalation study in rats. Toxicol Appl Pharmacol 30:287–298.

UNEP (United Nations Environment Programme). (2000) The Montreal Protocol on substances that deplete the ozone layer. United Nations Office at Nairobi (UNON), Nairobi, Kenya. Available online at http://www.unep.org/ozone/Treaties_and_Ratification/2B_montreal_protocol.asp.

Uno, Y; Takaswas, H; Miyagawa, M; et al. (1994) An in vivo-in vitro replications DNA synthesis (RDS) test using rat hepatocytes as an early prediction assay for nongenotoxic hepatocarcinogens: Screening of 22 known positives and 25 noncarcinogens. Mutat Res 320(3):189–205.

U.S. EPA (U.S. Environmental Protection Agency). (1986a) Guidelines for the health risk assessment of chemical mixtures. Federal Register 51(185):34014–34025.

U.S. EPA. (1986b) Guidelines for mutagenicity risk assessment. Federal Register 51(185):34006–34012.

U.S. EPA (1986c). Guidelines for Carcinogen Risk Assessment. Report #EPA/630/R-00/004. http://cfpub.epa.gov/ncea/cfm/recordisplay.cfm?deid=54933 Federal Register 51(185):33992–34003

U.S. EPA. (1988) Recommendations for and documentation of biological values for use in risk assessment. EPA 600/6-87/008. Available from National Technical Information Service, Springfield, VA; PB88-179874/AS.

U.S. EPA. (1990) Amendments to the Clean Air Act. Sec. 604. Phase-out of Production and Consumption of Class I Substances. Available online at http://www.epa.gov/oar/caa/caa604.txt.

U.S. EPA. (1991) Guidelines for developmental toxicity risk assessment. Federal Register 56(234):63798–63826.

U.S. EPA. (1994a) Interim policy for particle size and limit concentration issues in inhalation toxicity studies. Federal Register 59(206):53799.

U.S. EPA. (1994b) Methods for derivation of inhalation reference concentrations and application of inhalation dosimetry. EPA/600/8-90/066F. Available from: National Technical Information Service, Springfield, VA; PB2000-500023, and online at http://www.epa.gov/iris/backgr-d.htm.

U.S. EPA. (1995) Use of the benchmark dose approach in health risk assessment. U.S. Environmental Protection Agency. EPA/630/R-94/007. Available from: National Technical Information Service (NTIS), Springfield, VA; PB95-213765, and online at http://www.epa.gov/iris/backgr-d.htm.

U.S. EPA. (1996) Guidelines for reproductive toxicity risk assessment. Federal Register 61(212):56274–56322.

U.S. EPA. (1998) Guidelines for neurotoxicity risk assessment. Federal Register 63(93):26926–26954.

U.S. EPA. (2000a) Science policy council handbook: risk characterization. Prepared by the Office of Science Policy, Office of Research and Development, Washington, DC. EPA 100-B-00-002. Available online at http://www.epa.gov/iris/backgr-d.htm.

U.S. EPA. (2000b) Benchmark dose technical guidance document [external review draft]. EPA/630/R-00/001. Available online at http://www.epa.gov/iris/backgr-d.htm.

U.S. EPA. (2000c) Supplemental guidance for conducting for health risk assessment of chemical mixtures. EPA/630/R-00/002. Available online at http://www.epa.gov/iris/backgr-d.htm.

U.S. EPA. (2002a) A review of the reference dose and reference concentration processes. Risk Assessment Forum, Washington, DC; EPA/630/P-02/0002F. Available online at http://www.epa.gov/iris/backgr-d.htm.

U.S. EPA. (2002b) Toxic Substances Control Act (TSCA) Inventory Update Database. Available online at http://www.epa.gov/oppt/iur/iur02/index.htm.

U.S. EPA. (2005a) Guidelines for carcinogen risk assessment. Risk Assessment Forum, Washington, DC; EPA/630/P-03/001B. Available online at http://www.epa.gov/iris/backgr-d.htm.

U.S. EPA. (2005b) Supplemental guidance for assessing susceptibility from early-life exposure to carcinogens. Risk Assessment Forum, Washington, DC; EPA/630/R-03/003F. Available online at http://www.epa.gov/iris/backgr-d.htm.

U.S. EPA. (2006a) Peer review handbook. 3rd edition. Science Policy Council, Washington, DC. Available online at http://www.epa.gov/peerreview/pdfs/Peer%20Review%20HandbookMay06.pdf.

U.S. EPA. (2006b) A Framework for Assessing Health Risk of Environmental Exposures to Children. National Center for Environmental Assessment, Washington, DC, EPA/600/R-05/093F. Available from: <http://cfpub.epa.gov/ncea/cfm/recordisplay.cfm?deid=158363>.

van Delft, JHM; Van Agen, E; van Breda, SGJ; et al. (2004) Discrimination of genotoxic from non-genotoxic carcinogens by gene expression profiling. Carcinogenesis 25(7):1265–1276.

Vieira, I; Sonnier, M; Cresteil, T. (1996) Developmental expression of CYP2E1 in the human liver. Hypermethylation control of gene expression during the neonatal period. Eur J Biochem 238:476–483.

Watanabe, J; Hayashi, S; Kawajiri, K. (1994) Different regulation and expression of the human CYP2E1 gene due to the Rsa1 polymorphism in the 5'-flanking region. J Biochem 116:321–326.

Waxman, DJ; Pampori, NA; Prabha, AR. (1991) Interpulse interval in circulating growth hormone patterns regulates sexually dimorphic expression of hepatic cytochrome P450. Proc Natl Acad Sci 88:6868–6872.

Wirth, W; Klimmer, O. (1936) [On the toxicology of organic solvents. 1,4-dioxane (diethylene dioxide).] Arch Gewerbepathol Gewerbehyg 17:192–206.

Wolfe, NL; Jeffers PM. (2000) Hydrolysis. In: Boethling RS, Mackay D, eds. Handbook of property estimation methods for chemicals: Environmental and health sciences. Boca Raton, FL: Lewis Publishers.

Wolford, ST; Schroer, RA; Gohs, FX; et al. (1986) Reference range data base for serum chemistry and hematology values in laboratory animals. J Toxicol Environ Health 18:161–188.

Woo, Y-T; Argus, MF; Arcos, JC. (1977a) Tissue and subcellular distribution of 3H-dioxane in the rat and apparent lack of microsome-catalyzed covalent binding in the target tissue. Life Sci 21(10):1447–1456.

Woo, Y; Arcos, JC; Argus, MF; et al. (1977b) Structural identification of p-dioxane-2-one as the major urinary metabolite of p-dioxane. Naunyn-Schmiedebergs Arch Pharmacol 299:283–287.

Woo, Y; Argus, MF; Arcos, JC. (1977c) Metabolism in vivo of dioxane: effect of inducers and inhibitors of hepatic mixed-function oxidases. Biochem Pharmacol 25:1539–1542.

Woo, YT; Argus, MF; Arcos, JC. (1978) Effect of mixed-function oxidase modifiers on metabolism and toxicity of the oncogen dioxane. Cancer Res 38:1621–1625.

Woo, Y-T; Neuburger, BJ; Arcos, JC; et al. (1980) Enhancement of toxicity and enzyme-repressing activity of p-dioxane by chlorination: stereoselective effects. Toxicol Lett 5(1):69–75.

Yamamoto, S; Urano, K; Nomura, T. (1998a) Validation of transgenic mice harboring the human prototype c-Ha-ras gene as a bioassay model for rapid carcinogenicity testing. Toxicol Lett 102–103:473–478.

Yamamoto, S; Urano, K; Koizumi, H; et al. (1998b) Validation of transgenic mice carrying the human prototype c-Ha-ras gene as a bioassay model for rapid carcinogenicity testing. Environ Health Perspect 106:57–69.

Yamazaki, K; Ohno, H; Asakura, M; et al. (1994) Two-year toxicological and carcingenesis studies of 1,4-dioxane in F344 rats and BDF_1 mice. In: Sumino K, Sato S, eds. Second Asia-Pacific Symposium on Environmental and Occupational Health, 22-24 July, 1993, Kobe: proceedings. Kobe: International Center for Medical Research Kobe, University School of Medicine, 193-198.

Yant, WP; Schrenk, HH; Waite, CP; et al. (1930) Acute response of guinea pigs to vapors of some new commercial organic compounds --VI Dioxane. Public Health Rep 45:2023–2032.

Yasuhara A; Shiraishi H; Nishikawa M; et al. (1997) Determination of organic components in leachates from hazardous waste disposal sites in Japan by gas chromatography-mass spectrometry. J Chromatogr A 774:321-332.

Yasuhara A; Tanaka Y; Tanabe A; et al. (2003) Elution of 1,4-dioxane from waste landfill sites. Bull Environ Contam Toxicol 71:641-647.

Yoon, JS; Mason, JM; Nalencia, R; et al. (1985) Chemical mutagenesis testing in drosophila. IV. Results of 45 coded compounds tested for the national toxicology program. Environ Mutagen 7:349–367.

Young, JD; Braun, WH; Gehring, PJ; et al. (1976) Short communication. 1,4-dioxane and beta-hydroxyethoxyacetic acid excretion in urine of humans exposed to dioxane vapors. Toxicol Appl Pharmacol 38:643–646.

Young, JD; Braun, WH; Rampy, LW. (1977) Pharmacokinetics of 1,4-dioxane in humans. J Toxicol Environ Health 3:507–520.

Young, JD; Braun, WH; Gehring, PJ. (1978a) The dose-dependent fate of 1,4-dioxane in rats. J Environ Pathol Toxicol 2:263–282.

Young, JD; Braun, WH; Gehring, PJ. (1978b) Dose-dependent fate of 1,4-dioxane in rats. J Toxicol Environ Health 4(5–6):709–726.

Zimmermann, FK; Mayer, VW; Scheel, I; et al. (1985) Acetone, methyl ethyl ketone, ethyl acetate, acetonitrile and other polar aprotic solvents are strong inducers of aneuploidy in *Saccharomyces cerevisiae*. Mutat Res 149:339–351.

APPENDIX A. EXTERNAL REVIEW COMMENTS AND DISPOSITION

APPENDIX B. EVALUATION OF EXISTING PBPK MODELS FOR 1,4-dioxane

B.1. BACKGROUND

Several pharmacokinetic models have been developed to predict the absorption, distribution, metabolism, and elimination of 1,4-dioxane in rats and humans. Single compartment, empirical models for rats (Young et al., 1978a, b) and humans (Young et al., 1977) were developed that predict blood levels of 1,4-dioxane and urine levels of the primary metabolite, β-hydroxyethoxy acetic acid (HEAA). Physiologically based pharmacokinetic (PBPK) models, which describe the kinetics of 1,4-dioxane using biologically realistic flow rates, tissue volumes and affinities, metabolic processes, and elimination behaviors, were also developed (Fisher et al., 1997; Leung and Paustenbach, 1990; Reitz et al., 1990).

In developing updated toxicity values for 1,4-dioxane, the available PBPK models were evaluated for their ability to predict observations made in experimental studies of rat and human exposures to 1,4-dioxane. The model of Reitz et al. (1990) was identified for further consideration to assist in the derivation of toxicity values. Issues related to the biological plausibility of parameter values in the human model were identified. Specifically, the model's ability to predict the only available human inhalation data set (50 ppm 1,4-dioxane for 6 hours; Young et al., 1977) relies on increasing (i.e., doubling) of parameter values for human alveolar ventilation, cardiac output, and the blood:air partition coefficient above the measured values. Furthermore, the measured value for the slowly perfused tissue:air partition coefficient (i.e., muscle) was replaced with the measured liver value to improve the fit. Analysis of the Young et al. (1977) human data suggested that the apparent volume of distribution (V_d) for 1,4-dioxane was approximately 10-fold higher in rats than humans, presumably due to species differences in tissue partitioning or other process not represented in the model. Subsequent exercising of the model demonstrated that selecting a human slowly perfused tissue:air partition coefficient much lower than the measured rat value resulted in better agreement between model predictions of 1,4-dioxane in blood and experimental observations. Based upon these observations, the model (e.g., metabolism/elimination parameters) was re-calibrated using biologically plausible values for flow rates and tissue:air partition coefficients.

This appendix describes activities conducted in the evaluation of the empirical models (Young et al. 1978a, b, 1977) and re-calibration and exercising of the Reitz et al. (1990) PBPK model to determine the potential utility of the PBPK models for 1,4-dioxane for interspecies and route to route extrapolation.

B.2. SCOPE

The scope of this effort consisted of implementation of the Young et al. (1978a, b, 1977) empirical rat and human models using the acslXtreme simulation software and re-calibration of the Reitz et al. (1990) human PBPK model. Using the model descriptions and equations given in Young et al. (1978a, b, 1977), model code was developed for the empirical models and executed, simulating the reported experimental conditions. The model output was then compared with the model output reported in Young et al. (1978a, b, 1977).

The PBPK model of Reitz et al. (1990) was re-calibrated using measured values for cardiac and alveolar flow rates and tissue:air partition coefficients. The predictions of blood and urine levels of 1,4-dioxane and HEAA, respectively, from the re-calibrated model were compared with the empirical model predictions of the same dosimeters to determine whether the re-calibrated PBPK model could perform similarly to the empirical model. As part of the PBPK model evaluation, a sensitivity analysis was performed to identify the model parameters having the greatest influence on the primary dosimeter of interest, the blood level of 1,4-dioxane. Variability data for the experimental measurements of the tissue:air partition coefficients were incorporated to determine a range of model outputs bounded by biologically plausible values for these parameters.

B.3. IMPLEMENTATION OF THE EMPIRICAL MODELS IN ACSLXTREME

The empirical models of Young et al. (1978a, b, 1977) for 1,4-dioxane in rats and humans were reproduced using acslXtreme, version 2.3 (Aegis Technologies, Huntsville, AL). Model code files were developed using the equations described in the published papers. Additional files containing experiment-specific information (i.e., BWs, exposure levels, and duration) were also generated.

B.3.1. Model Descriptions

The empirical model of Young et al. (1978a, b) for 1,4-dioxane in rats is shown in Figure B-1. This is a single-compartment model that describes the absorption and metabolism kinetics of 1,4-dioxane in blood and urine. No information is reported describing pulmonary absorption or intravenous (i.v.) injection/infusion of 1,4-dioxane. The metabolism of 1,4-dioxane and subsequent appearance of HEAA is described by Michaelis-Menten kinetics governed by a maximum rate (V_{max}, μg/mL-hour) and affinity constant (K_m, μg/mL) . Both 1,4-dioxane and HEAA are eliminated via the first-order elimination rate constants, k_e and k_{me}, respectively ($hour^{-1}$) by which 35% of 1,4-dioxane and 100% of HEAA appear in the urine, while 65% of 1,4-dioxane is exhaled. Blood concentration of 1,4-dioxane is determined by dividing the instantaneous amount of 1,4-dioxane in blood by a V_d of 301 mL/kg BW.

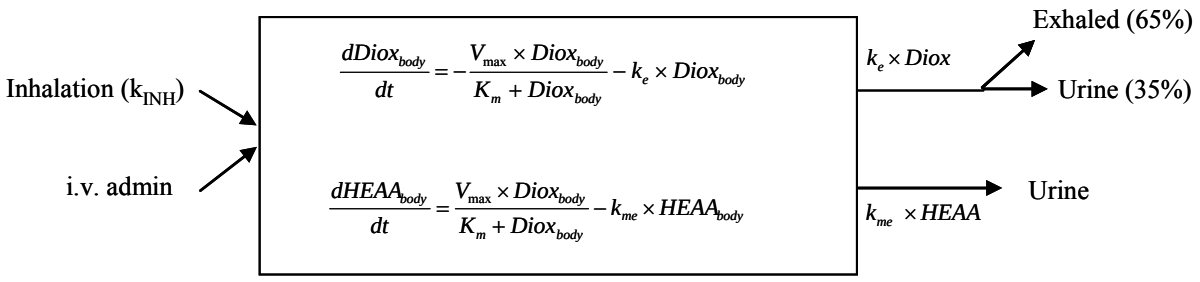

Source: Young et al. (1978a, b).

Figure B-1. Schematic representation of empirical model for 1,4-dioxane in rats.

Figure B-2 illustrates the empirical model for 1,4-dioxane in humans as described in Young et al. (1977). Like the rat model, the human model predicts blood 1,4-dioxane and urinary 1,4-dioxane and HEAA levels using a single-compartment structure. However, the metabolism of 1,4-dioxane to HEAA in humans is modeled as a first-order process governed by a rate constant, K_M (hour^{-1}). Urinary deposition of 1,4-dioxane and HEAA is described using the first order rate constants, $k_{e(diox)}$ and $k_{me(HEAA)}$, respectively. Pulmonary absorption is described by a fixed rate of 76.1 mg/hour (k_{INH}). Blood concentrations of 1,4-dioxane and HEAA are calculated as instantaneous amount (mg) divided by $V_{d(diox)}$ or $V_{d(HEAA)}$, respectively (104 and 480 mL/kg BW, respectively).

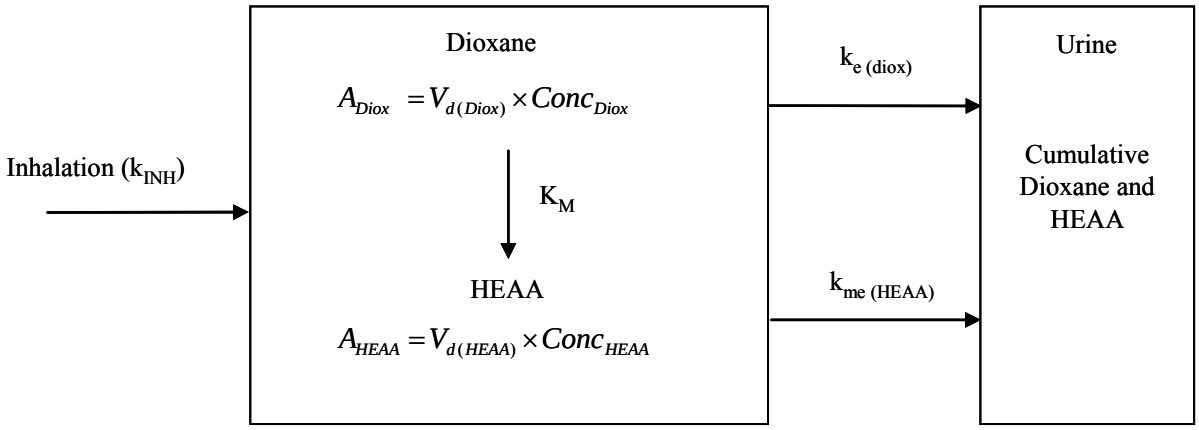

Source: Young et al. (1977).

Figure B-2. Schematic representation of empirical model for 1,4-dioxane in humans.

B.3.2. Modifications to the Empirical Models

Several modifications were made to the empirical models. The need for the modifications arose in some cases from incomplete reporting of the Young et al. (1978a, b, 1977)

studies and in other cases from the desire to add capabilities to the models to assist in the derivation of toxicity values.

For the rat model, no information was given by Young et al. (1978a, b) regarding the parameterization of pulmonary absorption (or exhalation) or i.v. administration of 1,4-dioxane. Therefore, additional parameters were added to simulate these processes in the simplest form. To replicate 1,4-dioxane inhalation, a first-order rate constant, k_{INH} ($hour^{-1}$), was introduced. k_{INH} was multiplied by the inhalation concentration and the respiratory minute volume of 0.238 L/minute (Young et al., 1978a, b). The value for k_{INH} was estimated by optimization against the blood time course data of Young et al. (1978a, b). Intravenous (i.v.) administration was modeled as instantaneous appearance of the full dose at the start of the simulation. Rat urinary HEAA data were reported by Young et al. (1978a, b) in units of concentration. To simulate urinary HEAA concentration, an estimate of urine volume was required. Since observed urinary volumes were not reported by Young et al. (1978a, b), a standard rat urine production rate of 0.00145 L/hour was used.

For humans, Young et al. (1977) used a fixed 1,4-dioxane inhalation uptake rate of 76.1 mg/hour, which corresponded to observations during a 50 ppm exposure. In order to facilitate user-specified inhalation concentrations, pulmonary absorption was modeled. The modeling was performed identically to the rat model, but using a human minute volume of 7 L/minute. Urinary HEAA data were reported by Young et al. (1977) as a cumulative amount (mg) of HEAA. Cumulative amount of HEAA in the urine is readily calculated from the rate of transfer of HEAA from plasma to urine, so no modification was necessary to simulate this dose metric for humans.

Neither empirical model of Young et al. (1978a, b;1977) described oral uptake of 1,4-dioxane. Adequate data to estimate oral absorption parameters are not available for either rats or humans; therefore, neither empirical model was modified to include oral uptake.

B.3.3. Results

The acslXtreme implementation of the Young et al. (1978a, b) rat empirical model simulates the 1,4-dioxane blood levels from the i.v. experiments identically to the model output reported in the published paper (Figure B-3). However, the acslXtreme version predicts urinary HEAA concentrations in rats that are approximately threefold lower and reach a maximum sooner than the predicted levels reported in the paper (Figure B-4). These discrepancies may be due, at least in part, to the reliance in the acslXtreme implementation on a constant, standard, urine volume rather than experimental measurements, which may have been different from the assumed value and may have varied over time. Unreported model parameters (e.g., lag times for appearance of excreted HEAA in bladder urine) may also contribute to the discrepancy.

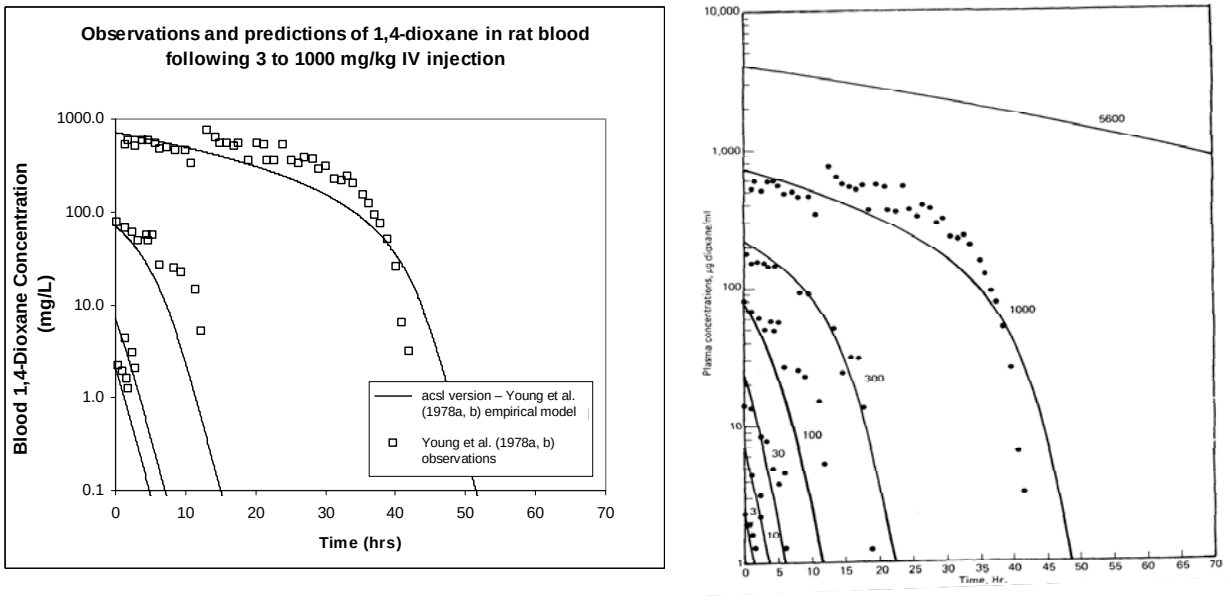

Source: Young et al. (1978a, b).

Figure B-3. Output of 1,4-dioxane blood level data from the acslXtreme implementation (left) and published (right) empirical rat model simulations of i.v. administration experiments.

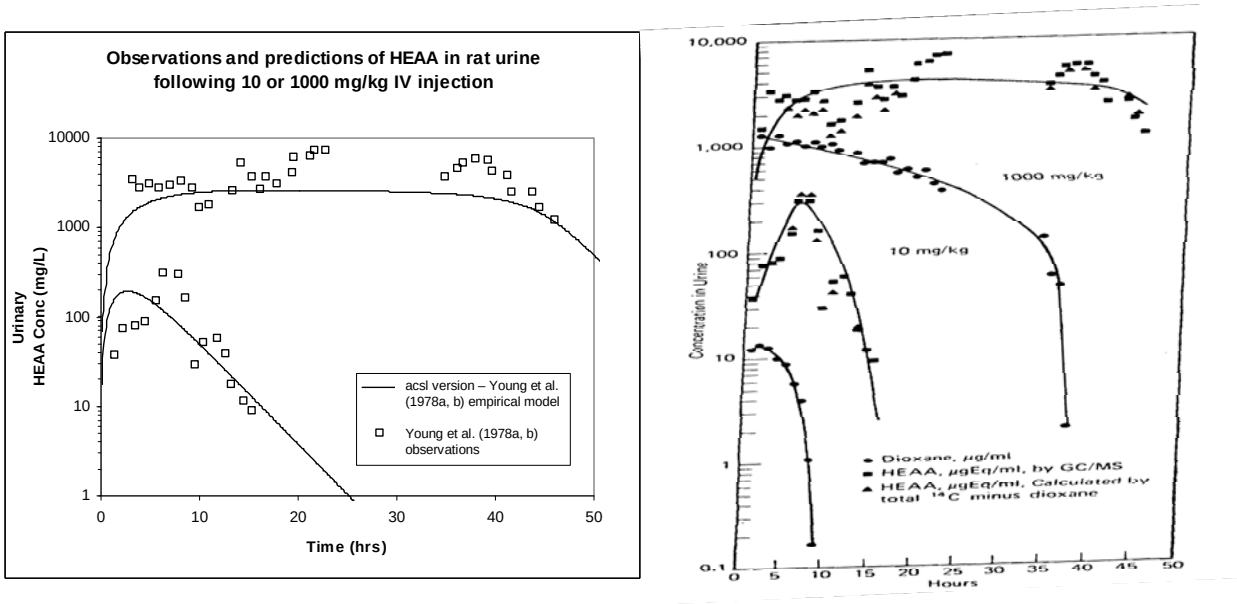

Source: Young et al. (1978a, b).

Figure B-4. Output of HEAA urine level data from acslXtreme implementation (left) and published (right) empirical rat model simulations of i.v. administration experiments.

The Young et al. (1978a, b) report did not provide model predictions for the 50-ppm inhalation experiment. However, the acslXtreme implementation produces blood 1,4-dioxane predictions that are quite similar to the reported observations (Figure B-5). As with the urine data from the i.v. experiment, the acslXtreme-predicted urinary HEAA concentrations are approximately threefold lower than the observations, presumably for the same reasons discussed above for the i.v. predictions.

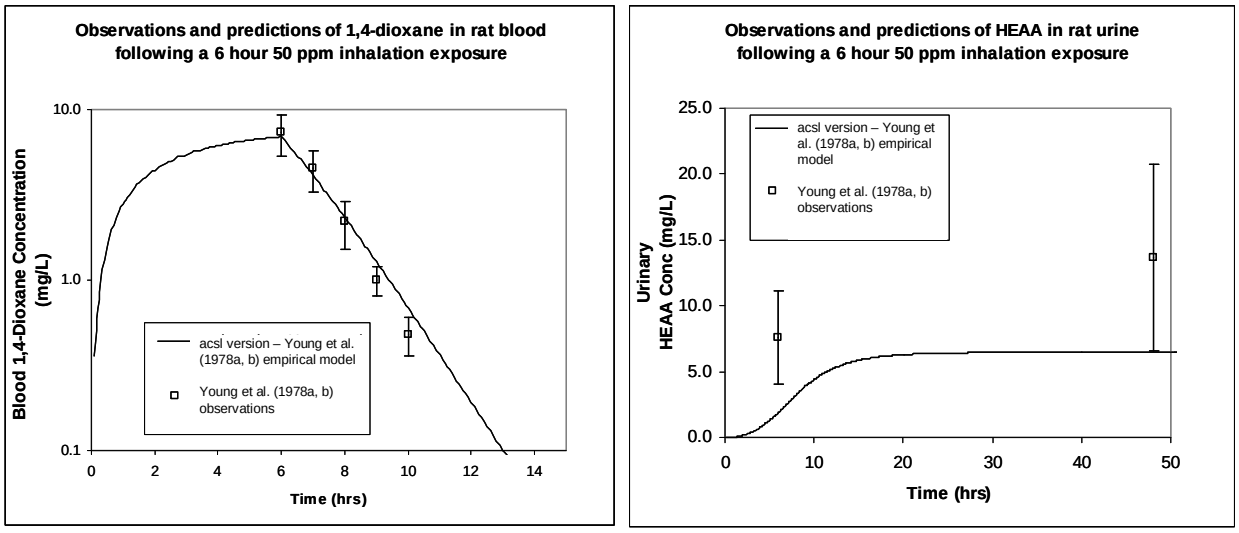

Source: Young et al. (1978a, b).

Figure B-5. acslXtreme predictions of blood 1,4-dioxane and urine HEAA levels from the empirical rat model simulations of a 6-hour, 50-ppm inhalation exposure.

Inhalation data for a single exposure level (50 ppm) are available for humans. The acslXtreme predictions of the blood 1,4-dioxane observations are identical to the predictions reported in Young et al. (1977) (Figure B-6). Limited blood HEAA data were reported, and the specimen analysis was highly problematic (e.g., an analytical interference was sometimes present from which HEAA could not be separated). For this reason, Young et al. (1977) did not compare predictions of the blood HEAA data to observations in their manuscript.

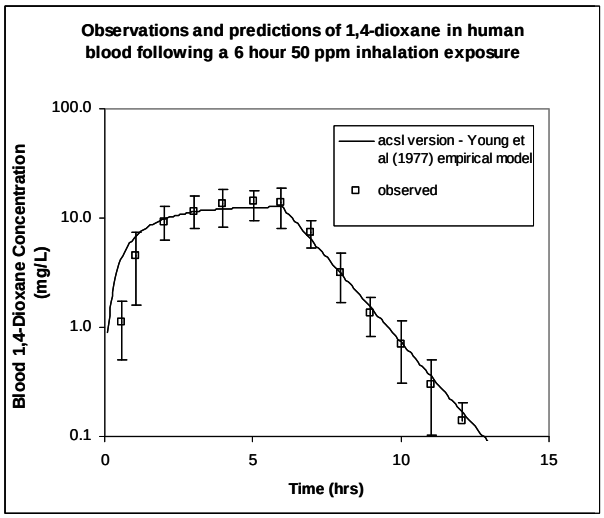

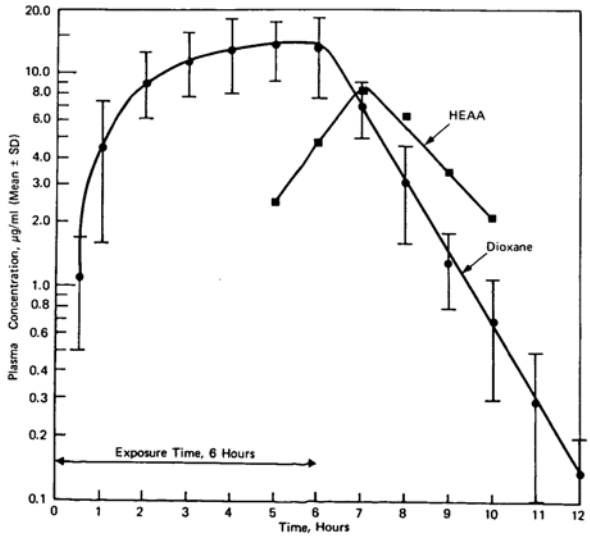

Source: Young et al. (1978a, b).

Figure B-6. Output of 1,4-dioxane blood level data from the acslXtreme implementation (left) and published (right) empirical human model simulations of a 6-hour, 50-ppm inhalation exposure.

Data for cumulative urinary HEAA amounts are provided in Young et al. (1977), and no analytical problems for these data were reported. Nevertheless, model predictions for urinary HEAA were not presented in the manuscript. The acslXtreme prediction of the HEAA kinetics profile is similar to the observations, although predicted values are approximately 1.5- to 2-fold lower than the observed values (Figure B-7). Unlike urinary HEAA observations in the rat, human observations were reported as cumulative amount produced, negating the need for urine volume data. Therefore, discrepancies between model predictions and experimental observations for humans cannot be attributed to uncertainties in urine volumes in the subjects.

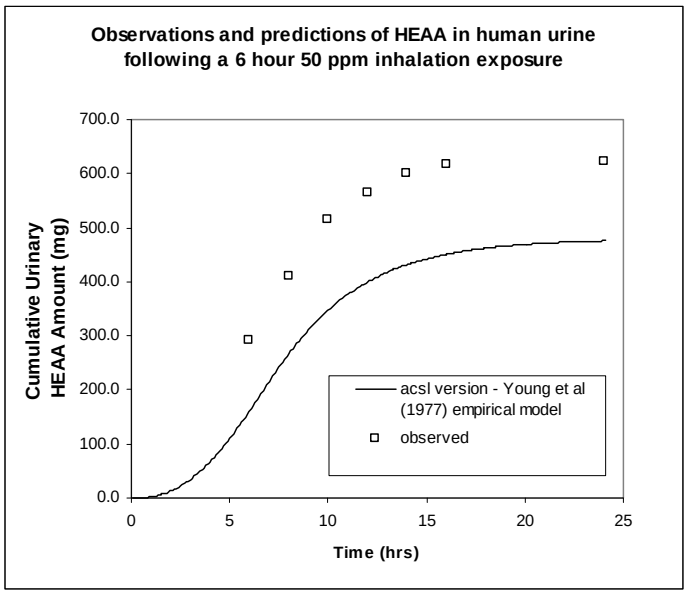

Source: Young et al. (1977).

Figure B-7. Observations and acslXtreme predictions of cumulative HEAA in human urine following a 6-hour, 50-ppm inhalation exposure.

B.3.4. Conclusions for Empirical Model Implementation

The empirical models described by Young et al. (1978a, b, 1977) for rats and humans were implemented using acslXtreme. The models were modified to allow for user-defined inhalation levels by addition of a first-order rate constant for pulmonary uptake of 1,4-dioxane, fitted to the inhalation data. No modifications were made for oral absorption as adequate data are not available for parameter estimation. The acslXtreme predictions of 1,4-dioxane in the blood are identical to the published predictions for simulations of 6-hour, 50-ppm inhalation exposures in rats and humans and 3 to 1,000 mg/kg i.v. doses in rats (Figures B-3, B-5, and B-6). However, the acslXtreme version predicts lower urinary HEAA concentrations in rats appearing earlier than either the Young et al. (1978a, b) model predictions or the experimental observations. The lower predicted urinary HEAA levels in the acslXtreme implementation for rats is likely due to use of default values for urine volume in the absence of measured volumes. The reason for differences in time-to-peak levels is unknown, but may be the result of an unreported adjustment by Young et al. (1978a, b) in model parameter values. For humans, Young et al. (1977) did not report model predictions of urinary HEAA levels. The urinary HEAA levels predicted by acslXtreme were low relative to the observations. However, unlike the situation in rats, these data are not dependent on unreported urine volumes (observations were reported as cumulative HEAA amount rather than HEAA concentration), but reflect the model parameter values reported by Young et al. (1977). Presently, there is no explanation for the lack of fit of the reported urinary HEAA elimination rate constant to the observations.

B.4. INITIAL RE-CALIBRATION OF THE PBPK MODEL

Concern regarding adjustments made to some of the parameter values in Reitz et al. (1990) prompted a re-calibration of the human PBPK model using more biologically plausible values for all measured parameter values. Reitz et al. (1990) doubled the measured physiological flows and blood:air partition coefficient and substituted the slowly-perfused tissue:air partition coefficient with the liver:air value in order to attain an adequate fit to the observations. This approach increases uncertainty in these parameter values, and in the utilization of the model for cross-species dose extrapolation. Therefore, the model was re-calibrated using parameter values that are more biologically plausible to determine whether an adequate fit of the model to the available data can be attained.

B.4.1. Sources of Values for Flow Rates

The cardiac output of 30 L/hour/kg$^{0.74}$ (Table B-1) reported by Reitz et al. (1990) is approximately double the mean resting value of 14 L/hour/kg$^{0.74}$ reported in the widely accepted compendium of Brown et al. (1997). Brown et al. (1997) cite the work of Astrand (1983) in which resting cardiac output was measured to be 5.2 L/minute (or 14 L/hour/kg$^{0.74}$), while strenuous exercise resulted in a flow of 9.9 L/minute (or 26 L/hour/kg$^{0.74}$). Brown et al. (1997) also cite the ICRP (1975) as having a mean respiratory minute volume of 7.5 L/minute, which results in an alveolar ventilation rate of 5 L/minute (assuming 33% lung dead space), or 13 L/minute/kg$^{0.74}$. Again, this is roughly half the value of 30 L/hour/kg$^{0.74}$ employed for this parameter by Reitz et al. (1990). Young et al. (1977) reported that the human subjects exposed to 50 ppm for 6 hours were resting inside a walk-in exposure chamber. Thus, use of cardiac output and alveolar ventilation rates of 30 L/hour/kg$^{0.74}$ is not consistent with the experimental conditions being simulated.

Table B-1. Human PBPK model parameter values for 1,4-dioxane

Parameter	Reitz et al. (1990)	Leung and Paustenbach (1990)	Sweeney et al. (2008)	EPA[c]
Physiological Flows				
Cardiac output (QCC)[a]	30	--	--	17.0
Alveolar ventilation (QPC)[a]	30	--	--	17.7
Partition Coefficients (PCs)				
Blood:air (PB)	3,650	1,825 ± 94	1,666 ± 287	1,850
Fat:air (PFA)	851	851 ± 118	--	851
Liver:air (PLA)	1,557	1,557 ± 114	1,862 ± 739[b]	1,557
Rapidly perfused tissue:air (PRA)	1,557	--	--	1,557
Slowly perfused tissue:air (PSA)	1,557	997 ± 254	1,348 ± 290[b]	166
Metabolic Constants				
Maximum rate for 1,4-dioxane metabolism (V_{maxC})[d]	6.35	--	--	5.49

Parameter	Reitz et al. (1990)	Leung and Paustenbach (1990)	Sweeney et al. (2008)	EPA[c]
Metabolic dissociation constant (K_m)[e]	3.00	--	--	9.8
HEAA urinary elimination rate constant (k_{me})[f]	0.56	--	--	0.44

[a]L/hour/kg $BW^{0.74}$
[b]Measurement for rat tissue
[c]Biologically plausible values utilized by EPA in this assessment
[d]mg/hour/kg $BW^{0.75}$
[e]mg/L
[f]$hour^{-1}$

Examination of the experimental data of Young et al. (1977) yields an estimated alveolar ventilation to be 7 L/minute (or 16 L/hour/$kg^{0.74}$) for volunteers having a mean BW of 84 kg. This rate is based on the Young et al. (1977) estimate of 76.1 mg/hour for 1,4-dioxane uptake. Based on these findings, the cardiac output and alveolar ventilation rates of 17.0 and 17.7 L/hour/$kg^{0.74}$ were biologically plausible for the experimental subjects. These rate estimates are based on calculations made using empirical data and are consistent with standard human values and the experimental conditions (i.e., subject exertion level) reported by Young et al. (1977). Therefore, these flow values were chosen for the model re-calibration.

B.4.2. Sources of Values for Partition Coefficients

Two data sources are available for the tissue:air equilibrium partition coefficients for 1,4-dioxane: Leung and Paustenbach (1990) and Sweeney et al. (2008). Both investigators report mean values and standard deviations for human blood:air, rat liver:air, and rat muscle:air (e.g., slowly perfused tissue:air), while Leung and Paustenbach et al. (1990) also reported values for rat fat:air (Table B-1).

B.4.3. Calibration Method

The PBPK model was twice re-calibrated using the physiological flow values suggested values (current EPA assessment, see Table B-1) and the partition coefficients of Leung and Paustenbach (1990) and Sweeney et al. (2008) separately. For each calibration, the metabolic parameters V_{maxC} and K_m, were simultaneously fit (using the parameter estimation tool provided in the acslXtreme software) to the output of 1,4-dioxane blood concentrations generated by the acslXtreme implementation of the Young et al. (1977) empirical human model for a 6 hour, 50 ppm inhalation exposure. Subsequently, the HEAA urinary elimination rate constant, k_{me}, was fitted to the urine HEAA predictions from the empirical model. The empirical model predictions, rather than experimental observations, were used to provide a more robust data set for model fitting, as the empirical model simulation provided 240 data points (one prediction

every 0.1 hour) compared with hourly experimental observations, and to avoid introducing error by calibrating the model to data digitally captured from Young et al. (1977).

B.4.4. Results

Results of the model re-calibration are provided in Table B-2. The re-calibrated values for V_{maxC} and k_{me} associated with the Leung and Paustenbach (1990) or Sweeney et al. (2008) tissue:air partition coefficients are very similar. However, the fitted value for K_m using the Sweeney et al. (2008) partition coefficients is far lower (0.0001 mg/L) than that resulting from use of the Leung and Paustenbach (1990) partition coefficients (2.5 mg/L). This appears to be due to the higher slowly perfused tissue:air partition coefficient determined by Sweeney et al. (2008) (1,348 vs. 997), resulting in a higher apparent V_d than if the Leung and Paustenbach (1990) value is used. Thus, the optimization algorithm selects a low K_m, artificially saturating metabolism in an effort to drive predicted blood 1,4-dioxane levels closer to the empirical model output. Saturation of metabolism during a 50 ppm inhalation exposure is inconsistent with the observed kinetics.

Table B-2. PBPK metabolic and elimination parameter values resulting from re-calibration of the human model using alternative values for physiological flow rates[a] and tissue:air partition coefficients

Source of Partition Coefficients	Leung and Paustenbach (1990)	Sweeney et al. (2008)
Maximum rate for 1,4-dioxane metabolism (V_{maxC})[b]	16.9	20.36
Metabolic dissociation constant (K_m)[c]	2.5	0.0001
HEAA urinary elimination rate constant (k_{me})[d]	0.18	0.17

[a]Cardiac output = 17.0 L/hour/kg $BW^{0.74}$, alveolar ventilation = 17.7 L/hour/kg $BW^{0.74}$
[b]mg/hour/kg $BW^{0.75}$
[c]mg/L
[d]$hour^{-1}$

Plots of predicted and experimentally observed blood 1,4-dioxane and urinary HEAA levels are shown in Figures 4-1 and 4-2. Neither re-calibration resulted in an adequate fit to the blood 1,4-dioxane data from the empirical model output or the experimental observations. Re-calibration using either the Leung and Paustenbach (1990) or Sweeney et al. (2008) partition coefficients resulted in blood 1,4-dioxane predictions that were at least 10-fold lower than empirical model predictions or observations.

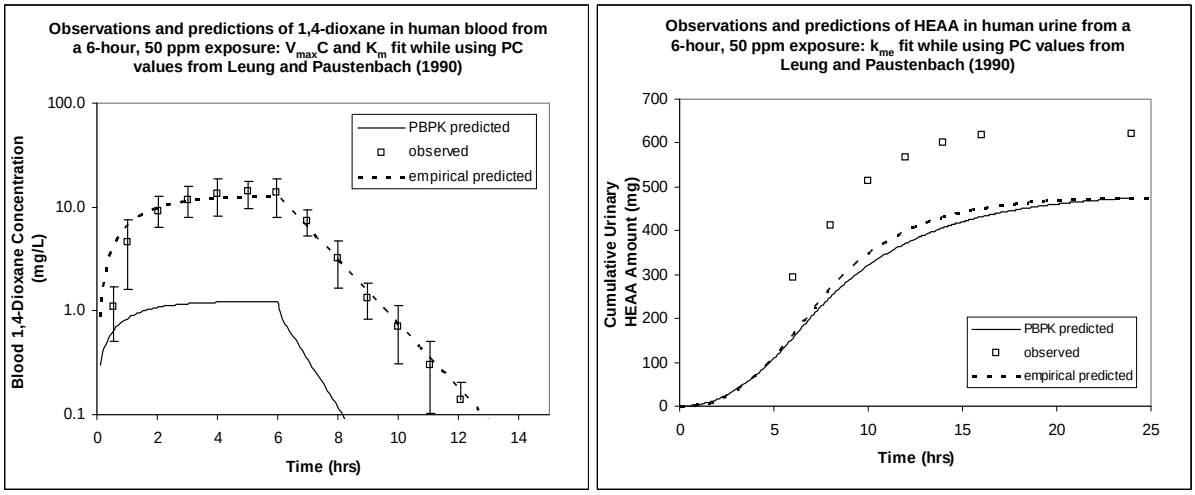

Source: Leung and Paustenbach (1990).

Figure B-8. Predicted and observed blood 1,4-dioxane concentrations (left) and urinary HEAA levels (right) following re-calibration of the human PBPK model with tissue:air partition coefficient values.

The refitted values for k_{me} resulted in HEAA levels in urine that were very similar to the empirical model output (compare Figures B-7, B-8, and B-9), which was not surprising, given the fitting of a single parameter to the data.

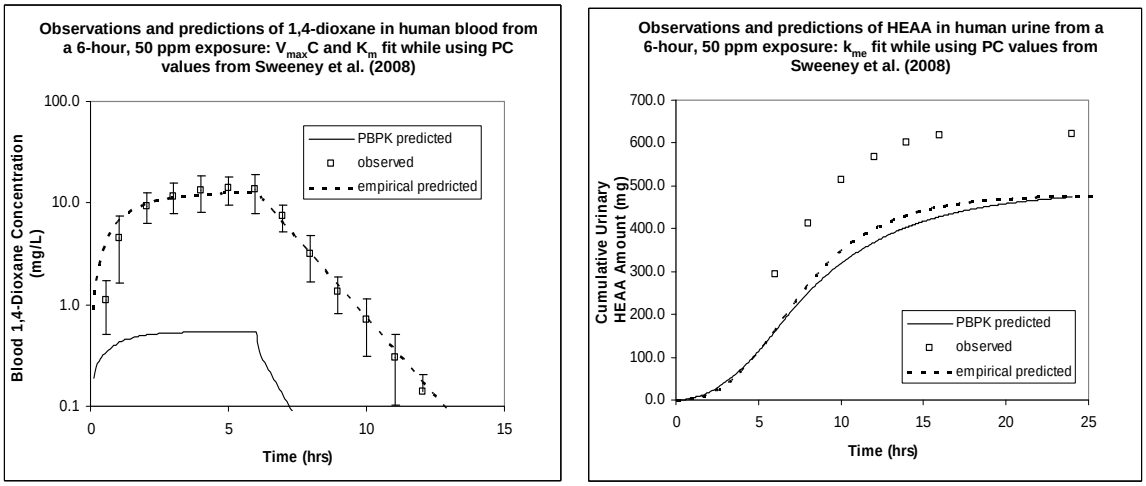

Source: Sweeney et al. (2008).

Figure B-9. Predicted and observed blood 1,4-dioxane concentrations (left) and urinary HEAA levels (right) following re-calibration of the human PBPK model with tissue:air partition coefficient values.

Outputs of the blood 1,4-dioxane and urinary HEAA levels using the suggested (see Table B-1) parameters are shown in Figure B-10. These outputs rely on a very low value for the slowly perfused tissue:air partition coefficient (166) that is six- to eightfold lower than the

measured values reported in Leung and Paustenbach (1990) and Sweeney et al. (2008), and 10-fold lower than the value used by Reitz et al. (1990). While the predicted maximum blood 1,4-dioxane levels are much closer to the observations, the elimination kinetics are markedly different, producing higher predicted elimination rates compared to observations during the post-exposure phase of the experiment.

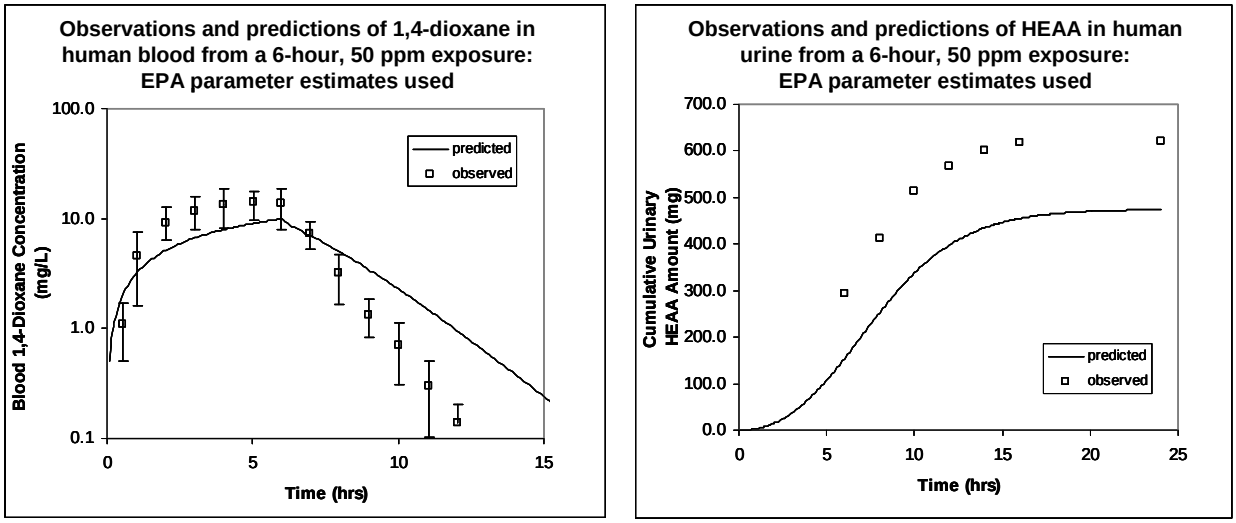

Figure B-10. Predicted and observed blood 1,4-dioxane concentrations (left) and urinary HEAA levels (right) using EPA estimated biologically plausible parameters (see Table B-1).

B.4.5. Conclusions for Empirical Model Implementation

Re-calibration of the human PBPK model was performed using experiment-specific values for cardiac output and alveolar ventilation (values derived from Young et al., 1977) and measured mean tissue:air 1,4-dioxane partition coefficients reported by Leung and Paustenbach (1990) or Sweeney et al. (2008). The resulting predictions of 1,4-dioxane in blood following a 6-hour, 50-ppm inhalation exposure were 10-fold (or more) lower than either the observations or the empirical model predictions, while the predictions of urinary HEAA by the PBPK and empirical models were similar to each other, but lower than observed values (Figures B-8 and B-9). Output from the model using biologically plausible parameter values (see Table B-1), Figure B-10 shows that application of a value for the slowly perfused tissue:air partition coefficient, which is 10-fold lower than the measured value reported by Leung and Paustenbach (1990), results in closer agreement of the predictions to observations during the exposure phase, but not during the elimination phase. Thus, model re-calibration using experiment-specific flow rates and mean measured partition coefficients does not result in an adequate fit of the PBPK model to the available data.

B.4.6. SENSITIVITY ANALYSIS

A sensitivity analysis of the Reitz et al. (1990) model was performed to determine which PBPK model parameters exert the greatest influence on the outcome of dosimeters of interest—in this case, the concentration of 1,4-dioxane in blood. Knowledge of model sensitivity is useful for guiding the choice of parameter values to minimize model uncertainty.

B.4.7. Method

A univariate sensitivity analysis was performed on all of the model parameters for two endpoints: blood 1,4-dioxane concentrations after 1 and 4 hours of exposure. These time points were chosen to assess sensitivity during periods of rapid uptake (1 hour) and as the model approached steady state (4 hours) for blood 1,4-dioxane. Model parameters were perturbated 1% above and below nominal values and sensitivity coefficients were calculated as follows:

$$f'(x) \approx \frac{f(x+\Delta x) - f(x)}{\Delta x} \cdot \frac{x}{f(x)}$$

where x is the model parameter, f(x) is the output variable, Δx is the perturbation of the parameter from the nominal value, and f'(x) is the sensitivity coefficient. The sensitivity coefficients were scaled to the nominal value of x and f(x) to eliminate the potential effect of units of expression. As a result, the sensitivity coefficient is a measure of the proportional change in the blood 1,4-dioxane concentration produced by a proportional change in the parameter value, with a maximum value of 1.

B.4.8. Results

The sensitivity coefficients for the seven most influential model parameters at 1 and 4 hours of exposure are shown in Figure B-11. The three parameters with the highest sensitivity coefficients in descending order are alveolar ventilation (QPC) (1.0), the blood:air partition coefficient (PB) (0.65), and the slowly perfused tissue:air partition coefficient (PSA) (0.51). Not surprisingly, these were the parameters that were doubled or given surrogate values in the Reitz et al. (1990) model in order to achieve an adequate fit to the data. Because of the large influence of these parameters on the model, it is important to assign values to these parameters in which high confidence is placed, in order to reduce model uncertainty.

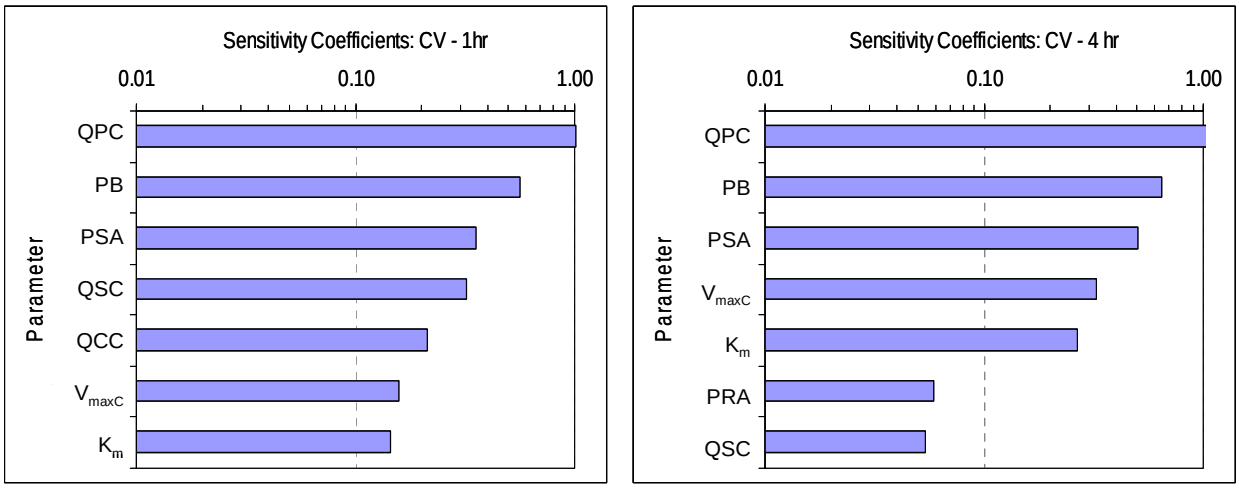

Figure B-11. The highest seven sensitivity coefficients (and associated parameters) for blood 1,4-dioxane concentrations (CV) at 1 (left) and 4 (right) hours of a 50-ppm inhalation exposure.

B.5. PBPK MODEL EXERCISES USING BIOLOGICALLY PLAUSIBLE PARAMETER BOUNDARIES

The PBPK model includes numerous physiological parameters whose values are typically taken from experimental observations. In particular, values for the flow rates (cardiac output and alveolar ventilation) and tissue:air partition coefficients (i.e., mean and standard deviations) are available from multiple sources as means and variances. The PBPK model was exercised by varying the partition coefficients over the range of biological plausibility (parameter mean ± 2 standard deviations), re-calibrating the metabolism and elimination parameters, and exploring the resulting range of blood 1,4-dioxane concentration time course predictions. Cardiac output and alveolar ventilation were not varied because the experiment-specific values used did not include any measure of inter-individual variation.

B.5.1. Observations Regarding the Volume of Distribution

Young et al. (1978a, b) used experimental observations to estimate a V_d for 1,4-dioxane in rats of 301 mL, or 1,204 mL/kg BW. For humans, the V_d was estimated to be 104 mL/kg BW (Young et al., 1977). It is possible that a very large volume of the slowly perfused tissues in the body of rats and humans may be a significant contributor to the estimated 10-fold difference in distribution volumes for the two species. This raises doubt regarding the appropriateness of using the measured rat slowly perfused tissue:air partition coefficient as a surrogate values for humans in the PBPK model.

B.5.2. Defining Boundaries for Parameter Values

Given the possible 10-fold species differences in the apparent V_d for 1,4-dioxane in rats and humans, boundary values for the partition coefficients were chosen to exercise the PBPK model across its performance range to either minimize or maximize the simulated V_d. This was accomplished by defining biologically plausible values for the partition coefficients as the mean ± 2 standard deviations of the measured values. Thus, to minimize the simulated V_d for 1,4-dioxane, the selected blood:air partition coefficient was chosen to be the mean + 2 standard deviations, while all of the other tissue:air partition coefficients were chosen to be the mean – 2 standard deviations. This created conditions that would sequester 1,4-dioxane in the blood, away from other tissues. To maximize the simulated 1,4-dioxane V_d, the opposite selections were made: blood and other tissue:air partition coefficients were chosen as the mean – 2 standard deviations and mean + 2 standard deviations, respectively. Subsequently, V_{maxC}, K_m, and k_{me} were optimized to the empirical model output data as described in Section B.4.3. This procedure was performed for both the Leung and Paustenbach (1990) and Sweeney et al. (2008) partition coefficients (Table B-1). The two predicted time courses resulting from the re-calibrated model with partition coefficients chosen to minimize or maximize the 1,4-dioxane V_d represent the range of model performance as bounded by biologically plausible parameter values.

B.5.3. Results

The predicted time courses for a 6-hour, 50-ppm inhalation exposure for the re-calibrated human PBPK model with mean (central tendency) and ± 2 standard deviations from the mean values for partition coefficients are shown in Figure B-12 for the Leung and Paustenbach (1990) values and Figure B-13 for the Sweeney et al. (2008) values. The resulting fitted values for V_{maxC}, K_m, and k_{me}, are given in Table B-3. By bounding the tissue:air partition coefficients with upper and lower limits on biologically plausible values from Leung and Paustenbach (1990) or Sweeney et al. (2008), the model predictions are still at least six- to sevenfold lower than either the empirical model output or the experimental observations. The range of possible urinary HEAA predictions brackets the prediction of the empirical model, but this agreement is not surprising, as the cumulative rate of excretion depends only on the rate of metabolism of 1,4-dioxane, and not on the apparent V_d for 1,4-dioxane. These data show that the PBPK model cannot adequately reproduce the predictions of blood 1,4-dioxane concentrations of the Young et al. (1977) human empirical model or the experimental observations when constrained by biologically plausible values for physiological flow rates and tissue:air partition coefficients.

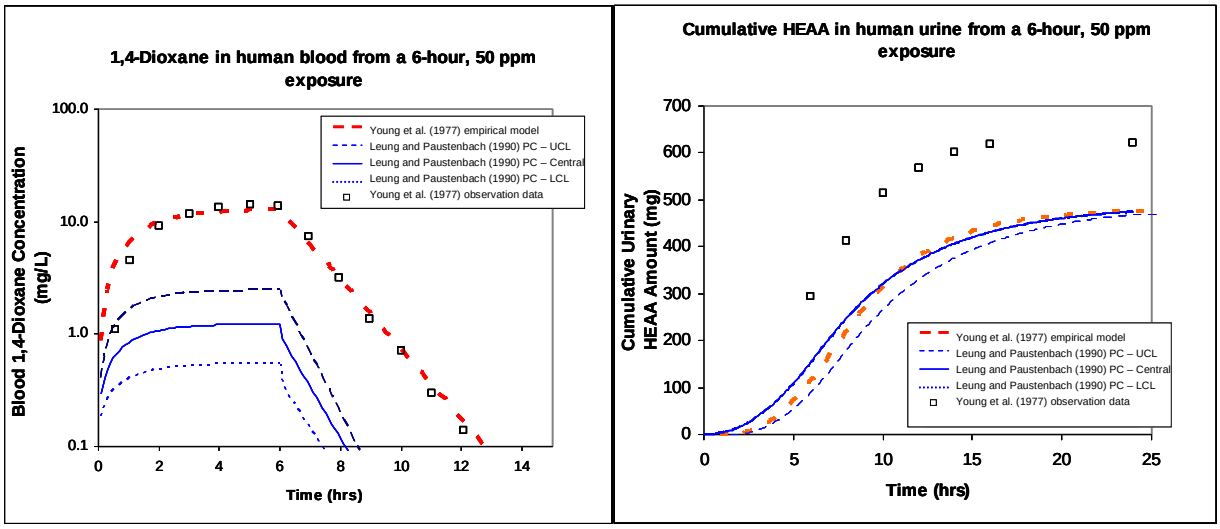

Source: Leung and Paustenbach (1990)

Figure B-12. Comparisons of the range of PBPK model predictions from upper and lower boundaries on partition coefficients with empirical model predictions and experimental observations for blood 1,4-dioxane concentrations (left) and urinary HEAA levels (right) from a 6-hour, 50-ppm inhalation exposure.

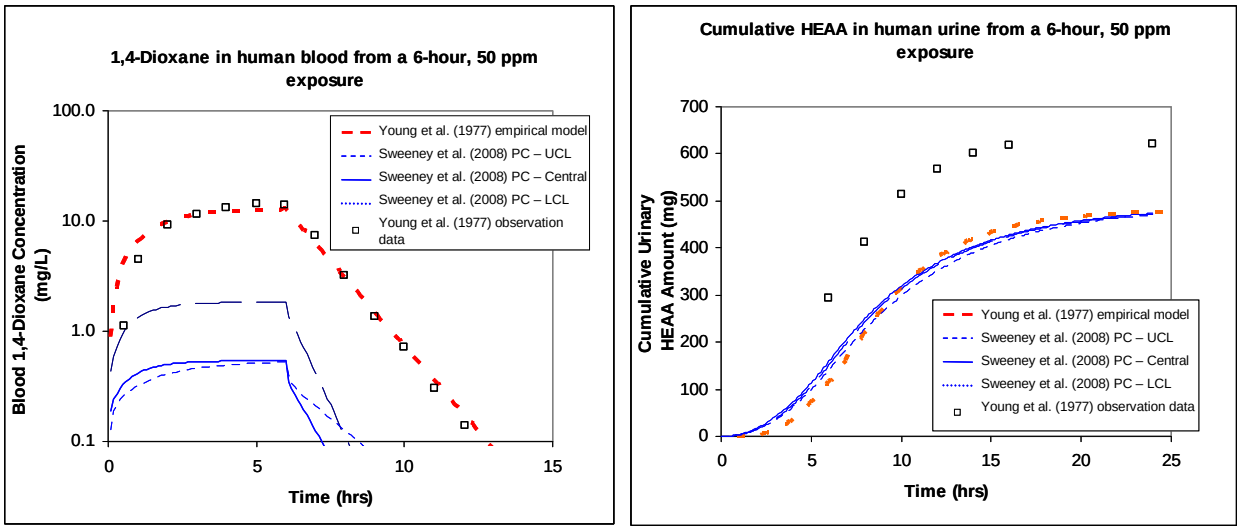

Source: Sweeney et al. (2008); Young et al. (1977).

Figure B-13. Comparisons of the range of PBPK model predictions from upper and lower boundaries on partition coefficients with empirical model predictions and experimental observations for blood 1,4-dioxane concentrations (left) and urinary HEAA levels (right) from a 6-hour, 50-ppm inhalation exposure.

Table B-3. PBPK metabolic and elimination parameter values resulting from recalibration of the human model using biologically plausible values for physiological flow rates[a] and selected upper and lower boundary values for tissue:air partition coefficients

Source of partition coefficients	Leung and Pausenbach (1990)		Sweeney et al. (2008)	
	For maximal V_d	For minimal V_d	For maximal V_d	For minimal V_d
Maximum rate for 1,4-dioxane metabolism (V_{maxC})[b]	14.95	18.24	17.37	21.75
Metabolic dissociation constant (K_m)[c]	5.97	0.0001	4.88	0.0001
HEAA urinary elimination rate constant (k_{me})[d]	0.18	0.17	0.26	0.19

[a]Cardiac output = 17.0 L/hour/kg $BW^{0.74,}$ alveolar ventilation = 17.7 L/hour/kg $BW^{0.74}$
[b]mg/hour/kg $BW^{0.75}$
[c]mg/L
[d]$hour^{-1}$

B.5.4. Alternative Model Parameterization

Since the PBPK model does not predict the experimental observations of Young et al. (1977) when parameterized by biologically plausible values, an exercise was performed to explore alternative parameters and values capable of producing an adequate fit of the data. Since the metabolism of 1,4-dioxane appears to be linear in humans for a 50-ppm exposure (Young et al., 1977), the parameters V_{maxC} and K_m were replaced by a first-order, non-saturable metabolism rate constant, k_{LC}. This rate constant was fitted to the experimental blood 1,4-dioxane data using partition coefficient values of Sweeney et al. (2008) to minimize the V_d (i.e., maximize the blood 1,4-dioxane levels). The resulting model predictions are shown in Figure B-14. As before, the maximum blood 1,4-dioxane levels were approximately sevenfold lower than the observed values.

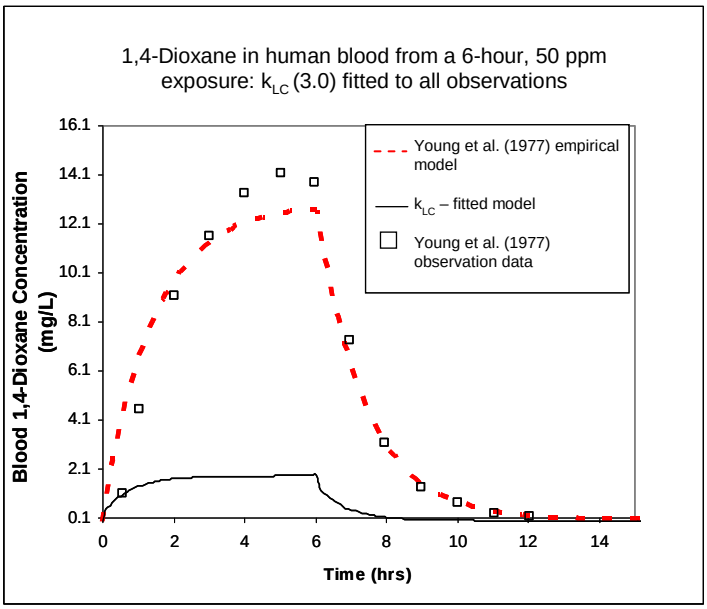

Figure B-14. Predictions of blood 1,4-dioxane concentration following calibration of a first-order metabolism rate constant, k_{LC}, to the experimental data.

A re-calibration was performed using only the data from the exposure phase of the experiment, such that the elimination data did not influence the initial metabolism and tissue distribution. The model predictions from this exercise are shown in Figure B-15. These predictions are more similar to the observations made during the exposure phase of the experiment; however, this is achieved at greatly reduced elimination rate (compare Figures B-10 and B-15).

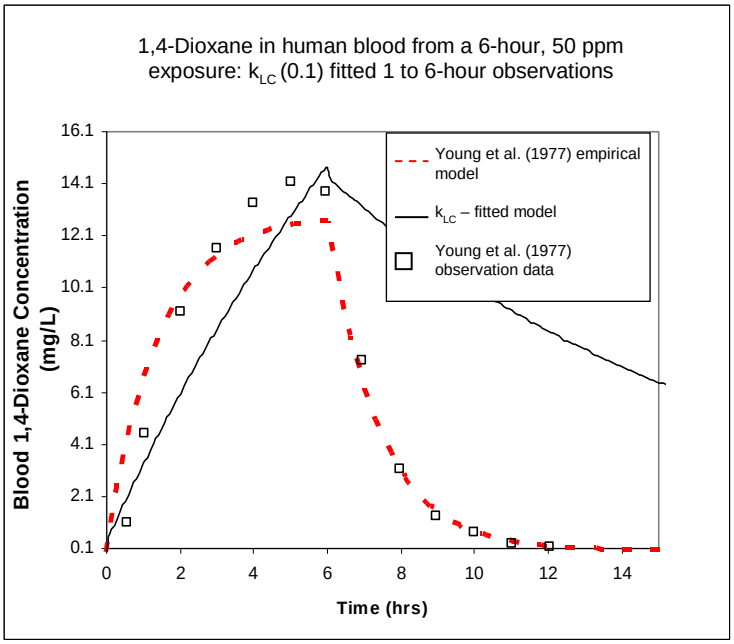

Figure B-15. Predictions of blood 1,4-dioxane concentration following calibration of a first-order metabolism rate constant, k_{LC}, to only the exposure phase of the experimental data.

Finally, the model was re-calibrated by simultaneously fitting k_{LC} and the slowly perfused tissue:air partition coefficient to the experimental data with no bounds on possible values (except that they be non-zero). The fitted slowly perfused tissue:air partition coefficient was an extremely low (and biologically unlikely) value of 0.0001. The resulting model predictions, however, were closer to the observations than even the empirical model predictions (Figure B-16). These exercises show that better fits to the observed blood 1,4-dioxane kinetics are achieved only when parameter values are adjusted in a way that corresponds to a substantial decrease in apparent V_d of 1,4-dioxane in the human, relative to the rat (e.g., decreasing the slowly perfused tissue:air partition coefficient to extremely low values, relative to observations). Downward adjustment of the elimination parameters (e.g., decreasing k_{LC}) increases the predicted blood concentrations of 1,4-dioxane, achieving better agreement with observations during the exposure phase of the experiment; however, it results in unacceptably slow elimination kinetics, relative to observations following cessation of exposure. These observations suggest that some other process not captured in the present PBPK model structure is responsible for the species differences in 1,4-dioxane V_d and the inability to reproduce the human experimental inhalation data with biologically plausible parameter values.

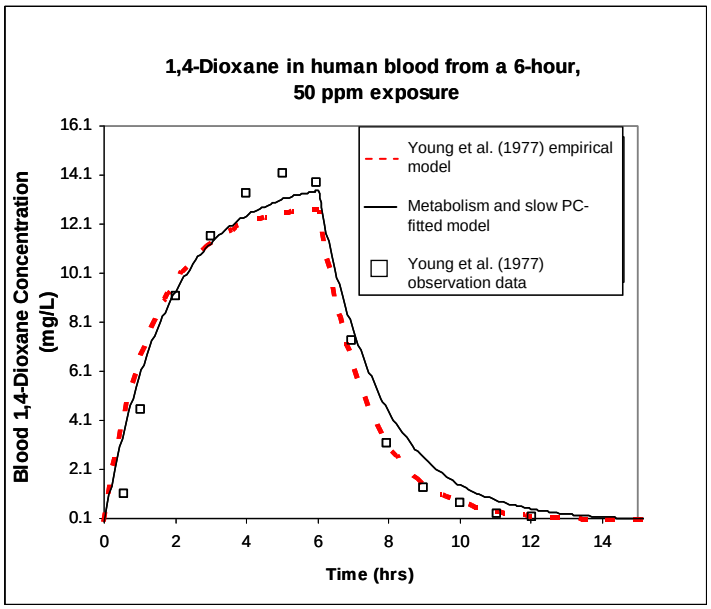

Figure B-16. Predictions of blood 1,4-dioxane concentration following simultaneous calibration of a first-order metabolism rate constant, k_{LC}, and slowly perfused tissue:air partition coefficient to the experimental data.

B.6. CONCLUSIONS

The rat and human empirical models of Young et al. (1978a, b, 1977) were successfully implemented in acslXtreme and perform identically to the models reported in the published papers (Figures 3-3 through 3-6), with the exception of the lower predicted HEAA concentrations and early appearance of the peak HEAA levels in rat urine. The early appearance of peak HEAA levels cannot presently be explained, but may result from manipulations of k_{me} or other parameters by Young et al. (1978a, b) that were not reported. The lower predictions of HEAA levels are likely due to reliance on a standard urine volume production rate in the absence of measured (but unreported) urine volumes. While the human urinary HEAA predictions were lower than observations, this is due to parameter fitting of Young et al. (1977). No model output was published in Young et al. (1977) for comparison. The empirical models were modified to allow for user-defined inhalation exposure levels. However, no modifications were made to model oral exposures because adequate data to parameterize such modifications do not exist for rats or humans.

Several procedures were applied to the human PBPK model to determine if an adequate fit of the model to the empirical model output or experimental observations could be attained using biologically plausible values for the model parameters. The re-calibrated model predictions for blood 1,4-dioxane levels do not come within 10-fold of the experimental values using measured tissue:air partition coefficients from Leung and Paustenbach (1990) or Sweeney et al. (2008) (Figures B-8 and B-9). Use of a slowly perfused tissue:air partition coefficient 10-

fold lower than measured values produces exposure-phase predictions that are much closer to observations, but does not replicate the elimination kinetics (Figure B-10). Re-calibration of the model with upper bounds on the tissue:air partition coefficients results in predictions that are still six- to sevenfold lower than empirical model prediction or observations (Figures B-12 and B-13). Exploration of the model space using an assumption of first-order metabolism (valid for the 50-ppm inhalation exposure) showed that an adequate fit to the exposure and elimination data can be achieved only when unrealistically low values are assumed for the slowly perfused tissue:air partition coefficient (Figure B-16). Artificially low values for the other tissue:air partition coefficients are not expected to improve the model fit, because the sensitivity analysis to exert less influence on blood 1,4-dioxane than V_{maxC} and K_m. This suggests that the model structure is insufficient to capture the apparent 10-fold species difference in the blood 1,4-dioxane V_d between rats and humans. In the absence of actual measurements for the human slowly perfused tissue:air partition coefficient, high uncertainty exists for this model parameter value. Differences in the ability of rat and human blood to bind 1,4-dioxane may contribute to the difference in V_d. However, this is expected to be evident in very different values for rat and human blood:air partition coefficients, which is not the case (Table B-1). Therefore, some other, as yet unknown, modification to model structure may be necessary.

B.7. RECOMMENDATIONS FOR UTILIZING EXISTING PBPK MODELS

The use of empirical or PBPK models to reduce uncertainty in extrapolation of dose-responses (in terms of internal dosimetry) requires accurate representation of exposure and biological reality. In the case of the empirical models of Young et al. (1978a, b, 1977), the acslXtreme implementations are adequate for predicting blood 1,4-dioxane levels for a variety of inhalation exposure levels in rats and up to 50 ppm in humans. However, the absence of data with which to evaluate simulated oral absorption in either species precludes the inclusion of this route of exposure in the models. Therefore, the empirical models may be useful for assessment of toxicity by inhalation exposure, but not by oral exposure, and not for route-to-route extrapolation. For the PBPK model, an apparent gap in the model structure exists such that experimental observations of blood 1,4-dioxane levels in humans during and following inhalation exposures to 1,4-dioxane cannot be reproduced under the constraints of biologically plausible parameter values for all parameters. Therefore, the use of the PBPK model (in its present form) is not recommended for application to the derivation of toxicity values for 1,4-dioxane.

B.8. ACSLXTREME CODE FOR THE YOUNG ET AL. (1978A, B) EMPIRCAL MODEL FOR 1,4-DIOXANE IN RATS

```
PROGRAM: Young 1978 rat.csl
!-------------------------------------------------------------
! Created by Michael Lumpkin, Syracuse Research Corporation, 08/06
! This program implements the 1-compartment empirical model for 1,4-dioxane
! in rats, developed by Young et al. 1978a, b. Program was modified to run
! in ACSL Xtreme and to include user-defined i.v. and inhalation concentrations
!(MLumpkin, 08/06)
!-------------------------------------------------------------

INITIAL

!*****Timing and Integration Commands*****
ALGORITHM IALG=2        !Gear integration algorithm for stiff systems
!MERROR %%%%=0.01       !Relative error for lead in plasma
NSTEPS NSTP=1000 !Number of integration steps per communication interval
CINTERVAL CINT=0.1      !Communication interval
CONSTANT TSTART=0.      !Start of simulation (hr)
CONSTANT TSTOP=70.      !End of simulation (hr)

!*****MODEL PARAMETERS*****
CONSTANT BW=0.215       !Body weight (kg)
CONSTANT MINVOL=0.238 !respiratory minute volume (L/min) estimated from Young et al.
(1978)
CONSTANT IVDOSE = 0.   !IV dose (mg/kg)!
CONSTANT CONC = 0.   !inhalation concentration (ppm)

CONSTANT MOLWT=88.105 !mol weight of 1,4-dioxane
CONSTANT TCHNG=6.0      !Exposure pulse 1 width (hr)
CONSTANT TDUR=24.0    !Exposure duration (hr)
CONSTANT TCHNG2=120.0 !Exposure pulse 2 width (hr)
CONSTANT TDUR2=168.0  !Exposure duration 2 (hr)

CONSTANT Vmax=4.008   !(mcg/mL/hr)
CONSTANT Km=6.308     !(mcg/mL)
CONSTANT Kinh=0.43          !pulmonary absorption constant (/hr)
CONSTANT Ke=0.0149    !(/hr)
CONSTANT Kme=0.2593   !(/hr)
CONSTANT Vd=0.3014     !(L)

IV = IVDOSE*BW
AmDIOXi=IV

END                     !Of Initial Section

DYNAMIC
```

```
DERIVATIVE

!*** Dioxane inhalation concentration ***
CIZONE=PULSE(0.0, TDUR, TCHNG) * PULSE(0.0, TDUR2, TCHNG2)
        !First pulse is hours/day, second pulse is hours/week
CI=CONC*CIZONE*MOLWT/24450.        !Convert to mg/L

!*** Dioxane metabolism/1st order elimination ***
dAmDIOX=(Kinh*CI*(MINVOL*60))-((Vmax*(AmDIOX))/(Km+(AmDIOX)))-
(Ke*(AmDIOX))
AmDIOX=INTEG(dAmDIOX,AmDIOXi)
ConcDIOX=AmDIOX/Vd     !plasma dioxane concentration (mcg/mL)
AUCDIOX=INTEG(ConcDIOX,0) !plasma dioxane AUC

!*** HEAA production and 1st order metabolism ***
dAmHEAA=((Vmax*(AmDIOX))/(Km+(AmDIOX)))-(Kme*(AmHEAA))
AmHEAA=INTEG(dAmHEAA,0.)
ConcHEAA=AmHEAA/Vd !plasma HEAA concentration

!*** 1st order dioxane elimination to urine ***
dAmDIOXu=(Ke*(AmDIOX))*0.35
AmDIOXu=INTEG(dAmDIOXu,0.)
ConcDIOXu=Ke*AmDIOX*0.35/1.45e-3 !urine production approx 1.45e-3 L/hr in SD rats

!*** 1st order dioxane exhaled ***
dAmDIOXex=(Ke*(AmDIOX))*0.65
AmDIOXex=INTEG(dAmDIOXex,0.)

!*** 1st order HEAA elimination to urine ***
dAmHEAAu=(Kme*(AmHEAA))
AmHEAAu=INTEG(dAmHEAAu,0.)
ConcHEAAu=Kme*AmHEAA/1.45e-3 !urine production approx 1.45e-3 L/hr in SD rats

END !of Derivative Section

DISCRETE

END    !of Discrete Section

TERMT (T .GT. TSTOP)

END !of Dynamic Section

TERMINAL

END    !of Terminal Section

END    !of Program
```

B.9. ACSLXTREME CODE FOR THE YOUNG ET AL. (1977) EMPIRICAL MODEL FOR 1,4-DIOXANE IN HUMANS

```
PROGRAM: Young 1977 human.csl
!-------------------------------------------------------------
! Created by Michael Lumpkin, Syracuse Research Corporation, 01/06
! This program implements the 1-compartment model for 1,4-dioxane in humans,
! developed by Young et al., 1977. Program was modified to run
! in acslXtreme (MLumpkin, 08/06)
!-------------------------------------------------------------

INITIAL

!*****Timing and Integration Commands*****
ALGORITHM IALG=2        !Gear integration algorithm for stiff systems
!MERROR %%%%=0.01       !Relative error for lead in plasma
NSTEPS NSTP=1000 !Number of integration steps per communication interval
CINTERVAL CINT=0.1      !Communication interval
CONSTANT TSTART=0.      !Start of simulation (hr)
CONSTANT TSTOP=120.     !End of simulation (hr)

!*****MODEL PARAMETERS*****
!CONSTANT DATA=1        !Optimization dataset
CONSTANT MOLWT=88.105 !mol weight for 1,4-dioxane
CONSTANT DOSE=0.        !Dose (mg/kg
CONSTANT CONC=0.        !Inhalation concentration (ppm)
CONSTANT BW=84.1        !Body weight (kg)
CONSTANT MINVOL=7.0  !pulmonary minute volume (L/min)
CONSTANT F=1.0          !Fraction of dose absorbed
CONSTANT kinh=1.06      !Rate constant for inhalation (mg/hr); optimized by MHL
CONSTANT ke=0.0033      !Rate constant for dioxane elim to urine (hr-1)
CONSTANT km=0.7096      !Rate constant for metab of dioxane to HEAA (hr-1)
CONSTANT kme=0.2593     !Rate constant for transfer from rapid to blood (hr-1)
CONSTANT VdDkg=0.104   !Volume of distribution for dioxane (L/kg BW)

CONSTANT VdMkg=0.480  !Volume of distribution for HEAA (L/kg BW)
CONSTANT OStart=0.      !Time of first oral dose (hr)
CONSTANT OPeriod=120.   !Oral Dose pulse period (hr)
CONSTANT OWidth=1.      !Width (gavage/drink time) of oral dose (hr)

CONSTANT IStart=0.      !Time of inhalation onset (hr)
CONSTANT IPeriod=120.   !Inhalation pulse period (hr)
CONSTANT IWidth=6.      !Width (duration) of inhalation exposure (hr)

END                     !Of Initial Section

DYNAMIC

DERIVATIVE
```

```
!****VARIABLES and DEFINED VALUES*****
VdD=BW*VdDkg     !Volume of distribution for dioxane
VdM=BW*VdMkg     !Volume of distribution for HEAA

InhalePulse=PULSE(IStart,IPeriod,IWidth)
Inhale=CONC*InhalePulse*MOLWT/24450.          !Convert to mg/L

!*****DIFFERENTIAL EQUATIONS FOR COMPARTMENTS****

!*** Dioxane in the body (plasma) ***
dAMTbD=(Kinh*Inhale*(MINVOL*60))-(AMTbD*km)-(AMTbD*ke)
AMTbD=INTEG(dAMTbD,0.)
CbD=AMTbD/VdD
AUCbD=INTEG(CbD,0)

!*** HEAA in the body  (plasma)***
dAMTbM=AMTbD*km-AMTbM*kme
AMTbM=INTEG(dAMTbM,0.)
CbM=AMTbM/VdM

!*** Cumulative Dioxane in the urine ***
dAMTuD=(AMTbD*ke)
AMTuD=INTEG(dAMTuD,0.)

!*** Cumulative HEAA in the urine ***
dAMTuM=(AMTbM*kme)
AMTuM=INTEG(dAMTuM,0.)

END                    !Of Derivative Section

DISCRETE

END                    !of Discrete Section

TERMT (T .GT. TSTOP)

END                    !Of Dynamic Section

TERMINAL

END                    !of Terminal Section

END                    !of Program
```

B.10. ACSLXTEME CODE FOR THE REITZ ET AL. (1990) PBPK MODEL FOR 1,4-DIOXANE

```
PROGRAM: DIOXANE.CSL (Used in Risk Estimation Procedures)
  !Added a venous blood compartment and 1st order elim of metab.'
  !Mass Balance Checked OK for Inhal, IV, Oral, and Water RHR'
  !Defined Dose Surrogates for Risk Assessment 01/04/89'
  !Modified the Inhal Route to use PULSE for exposure conditions'
  !Modifications by GLDiamond, Aug2004, marked as !**
  !
  !Metabolism of dioxane modified by MLumpkin, Oct2006, to include 1st order
  !or saturable kinetics. For 1st order, set VmaxC=0; for M-Menten, set KlC=0.
  !
INITIAL

  INTEGER I
   I=1
!  ARRAY TDATA(20)  !  CONSTANT TDATA=999, 19*1.0E-6 !**
  CONSTANT    BW = 0.40   !'Body weight (kg)'
  CONSTANT   QPC = 15.    !'Alveolar ventilation rate (l/hr)'
  CONSTANT   QCC = 15.    !'Cardiac output (l/hr)'

!Flows to Tissue Compartments'
  CONSTANT   QLC = 0.25   !'Fractional blood flow to liver'
  CONSTANT   QFC = 0.05   !'Fractional blood flow to fat'
  CONSTANT   QSC = 0.18   !'Fractional blood flow to slow'
         QRC = 1.0 - (QFC + QSC + QLC)
  CONSTANT   SPDC = 1.0  ! diffusion constant for slowly perfused tissues

!Volumes of Tissue/Blood Compartments'
  CONSTANT   VLC = 0.04   !'Fraction liver tissue'
  CONSTANT   VFC = 0.07   !'Fraction fat tissue'
  CONSTANT   VRC = 0.05   !'Fraction Rapidly Perf tissue'
  CONSTANT   VBC = 0.05   !'Fraction as Blood'
         VSC = 0.91 - (VLC + VFC + VRC + VBC)

!Partition Coefficients'
  CONSTANT   PLA = 1557.  !'Liver/air partition coefficient'
  CONSTANT   PFA =  851.  !'Fat/air partition coefficient'
  CONSTANT   PSA = 2065.  !'Muscle/air (Slow Perf) partition'
  CONSTANT   PRA = 1557.  !'Richly perfused tissue/air partition'
  CONSTANT    PB = 1850.  !'Blood/air partition coefficient'

!Other Compound Specific Parameters'
  CONSTANT    MW = 88.1   !'Molecular weight (g/mol)'
  CONSTANT   KLC = 12.0   ! temp 1st order metab constant
  CONSTANT VMAXC = 13.8   !'Maximum Velocity of Metabol.'
  CONSTANT    KM = 29.4   !'Michaelis Menten Constant'
  CONSTANT  ORAL = 0.0    !'Oral Bolus Dose (mg/kg)'
```

```
  CONSTANT    KA = 5.0    !'Oral uptake rate (/hr)'
  CONSTANT WATER = 0.0    !'Conc in Water (mg/liter, ppm)'
  CONSTANT WDOSE=0.0    !Water dose (mg/kg/day) **
  CONSTANT    IV = 0.0    !'IV dose (mg/kg)'
  CONSTANT  CONC = 0.0    !'Inhaled concentration (ppm)'
  CONSTANT   KME = 0.276  !'Urinary Elim constant for met (hr-1)'

!Timing commands'
  CONSTANT   TSTOP = 50   !'Length of experiment (hrs)'
  CONSTANT   TCHNG =  6   !'Length of inhalation exposure (hrs)'
  CINTERVAL CINT=0.1
  CONSTANT WIDD=24.    !**
  CONSTANT PERD=24.    !**
  CONSTANT PERW=168.  !**
  CONSTANT WIDW=168.  !**
  CONSTANT DAT=0.017   !**

!Scaled parameters calculated in this section of Program'
  QC=QCC*BW**0.74
      QP=QPC*BW**0.74
  QL=QLC*QC
      QF=QFC*QC
      QS=QSC*QC
      QR=QRC*QC
  VL=VLC*BW
      VF=VFC*BW
      VS=VSC*BW
      VR=VRC*BW
      VB=VBC*BW
  PL=PLA/PB
      PR=PRA/PB
      PS=PSA/PB
      PF=PFA/PB
      KL = KLC*bw**0.7 ! 1st order metab constant
      VMAX = VMAXC*BW**0.7
  DOSE = ORAL*BW              !'Initial Amount in Stomach'
  AB0 = IV*BW                 !'Initial Amount in Blood'
  !DRINK = 0.102*BW**0.7*WATER/24 !'Input from water (mg/hr)' !**
  !DRINKA = 0.102*BW**0.7*WATER/DAT !'Input from water (mg/hr)'  !**
      DRINKA=WDOSE*BW/DAT
  CV = AB0/VB             !'Initialize CV'

END    !'End of INITIAL'

DYNAMIC

      ALGORITHM IALG = 2       !'Gear method for stiff systems'
      TERMT( T .GE. TSTOP )
      CR = AR/VR
```

```
            CS = AS/VS
            CF = AF/VF
            BODY = AL + AR + AS + AF + AB + TUMMY
            BURDEN = AM + BODY
            TMASS = BURDEN + AX + AMEX

!Calculate the Interval Excretion Data here:'
 !          DAX = AMEX-AMEX2
 !          IF( DOSE .LE. 0.0 .AND. IV .LE. 0.0 ) GO TO SKIP1
 !          PCTAX = 100*(AX - AX2)/(DOSE + IV*BW)
 !          PCTMX = 100*(AMEX - AMEX2)/(DOSE + IV*BW)
!           SKIP1.. CONTINUE
 !          IF( T .LT. TDATA(I) .OR. I .GE. 20 ) GO TO SKIP
  !         AX2=AX
!           AMEX2=AMEX
!           I=I+1
!           SKIP.. CONTINUE

!DISCRETE EXPOSE
!   CIZONE = 1.0  ! CALL LOGD(.TRUE.) Turns on inhalation exposure?
!END
!DISCRETE CLEAR
!   CIZONE = 0.0  ! CALL LOGD(.TRUE.)
!END

DERIVATIVE

!Use Zero-Crossing Form of DISCRETE Function Here'
!  SCHEDULE command must be in DERIVATIVE section'
 !  DAILY = PULSE ( 0.0, PER1, TCHNG )
 !  WEEKLY = PULSE ( 0.0, PER2, LEN2  )
  ! SWITCHY = DAILY * WEEKLY
!SCHEDULE EXPOSE .XP. SWITCHY - 0.995
!SCHEDULE CLEAR  .XN. SWITCHY - 0.005

DAILY=PULSE(0.0,PERD,WIDD)
WEEKLY=PULSE(0.0,PERW,WIDW)
SWITCHY = DAILY * WEEKLY

!**********************Modified Here for Wong*****************'
            CI = CONC * MW / 24451.0 * SWITCHY!**

        !CA = Concentration in arterial blood (mg/l)'
         CA = (QC*CV+QP*CI)/(QC+(QP/PB))
         CX = CA/PB

            DRINK=DRINKA*SWITCHY        !**

    !TUMMY = Amount in stomach'
```

```
1       RTUMMY = -KA*TUMMY
2        TUMMY = INTEG(RTUMMY,DOSE)
3         !RAX = Rate of Elimination in Exhaled air'
4         RAX = QP*CX
5          AX = INTEG(RAX, 0.0)
6
7         !AS = Amount in slowly perfused tissues (mg)'
8         RAS = SPDC*(CA-CVS) !now governed by diffusion-limited constant, SPDC, instead of QS
9          AS = INTEG(RAS,0.)
10        CVS = AS/(VS*PS)
11
12        !AR = Amount in rapidly perfused tissues (mg)'
13        RAR = QR*(CA-CVR)
14         AR = INTEG(RAR,0.)
15        CVR = AR/(VR*PR)
16
17        !AF = Amount in fat tissue (mg)'
18        RAF = QF*(CA-CVF)
19         AF = INTEG(RAF,0.)
20        CVF = AF/(VF*PF)
21
22        !AL = Amount in liver tissue (mg)'
23        RAL = QL*(CA-CVL) - KL*CVL - VMAX*CVL/(KM+CVL) + KA*TUMMY + DRINK
24                AL = INTEG(RAL,0.)
25        CVL = AL/(VL*PL)
26
27        !AM = Amount metabolized (mg)'
28       RMEX = (KL*CVL)+(VMAX*CVL/(KM+CVL))
29        RAM = (KL*CVL)+(VMAX*CVL)/(KM+CVL) - KME*AM
30
31                  AM = INTEG(RAM, 0.0)              !'Amt Metabol'
32        CAM = AM/BW                         !'Conc Metabol in body'
33       AMEX = INTEG(KME*AM, 0.0)            !'Amt Met Excret'
34
35        !AB = Amount in Venous Blood'
36        RAB = QF*CVF + QL*CVL + QS*CVS + QR*CVR  - QC*CV
37         AB = INTEG(RAB, AB0)
38         CV = AB/VB
39        AUCV = INTEG(CV, 0.0)
40
41    !Possible Dose Surrogates for Risk Assessment Defined Here'
42
43        CEX = 0.667*CX + 0.333*CI         !'Conc in Exhal Air'
44      AVECON = PLA * (CEX+CI)/2            !'Ave Conc in Nose Tissue'
45      AUCCON = INTEG(AVECON, 0.0)          !'Area under Curve (Nose)'
46
47      AUCMET = INTEG(CAM, 0.0)             !'Area under Curve (Metab)'
48
49        CL = AL/VL                    !'Conc Liver Tissue'
```

```
      AUCL = INTEG(CL, 0.0)            !'Area under Curve (Liver)'
           AAUCL=AUCL/TIME

!  Dose Surrogates are Average Area under Time/Conc Curve per 24 hrs'
IF (T .GT. 0) TIME=T
     DAYS = TIME/24.0
     NOSE = AUCCON/DAYS              !'Nasal Turbinates'
    LIVER = AUCL/DAYS               !'Liver Tissues'
    METAB = AUCMET/DAYS              !'Stable Metabolite'

END      !'End of dynamic'

END  ! End of TERMINAL

END      !'End of PROGRAM
```

APPENDIX C. DETAILS OF BMD ANALYSIS FOR ORAL RfD FOR 1,4-dioxane

C.1. CORTICAL TUBULE DEGENERATION.

All available dichotomous models in the Benchmark Dose Software (version 1.3.2) were fit to the incidence data shown in Table C-1, for cortical tubule degeneration in male and female Osborne-Mendel rats exposed to 1,4-dioxane in the drinking water (NCI, 1978). Doses associated with a BMR of a 10% extra risk was calculated.

Table C-1. Incidence of cortical tubule degeneration in Osborne-Mendel rats exposed to 1,4-dioxane in drinking water for 2 years

Males (mg/kg-day)			Females (mg/kg-day)		
0	**240**	**530**	**0**	**350**	**640**
0/31[a]	20/31[b] (65%)	27/33[b] (82%)	0/31[a]	0/34	10/32[b] (31%)

[a]Statistically significant trend for increased incidence by Cochran-Armitage test ($p < 0.05$) performed for this review.
[b]Incidence significantly elevated compared to control by Fisher's exact test ($p < 0.05$) performed for this review.

Source: NCI (1978).

As assessed by the χ^2 goodness-of-fit test, several models in the software provided adequate fits to the data for the incidence of cortical tubule degeneration in male and female rats (χ^2 $p \geq$ 0.1) (Table C-2). Comparing across models, a better fit is indicated by a lower AIC value (U.S. EPA, 2000b). As assessed by Akaike's Information Criterion (AIC), the log-probit model provided the best fit to the cortical tubule degeneration incidence data for male rats (Table C-2, Figure C-1) and the log-logistic and Weibull models provided the best fit to the data for female rats (Table C-2, Figures C-2 and C-3). For those models that exhibit adequate fit, models with the lower AIC values are preferred. Differences in AIC values of less than 1 are generally not considered important. Benchmark doses (BMDs) and benchmark dose lower confidence limits (BMDLs) associated with an extra risk of 10% were calculated for all models. These values are also shown in Table C-2.

Table C-2. Goodness-of-fit statistics and BMD_{10} and $BMDL_{10}$ values from models fit to incidence data for cortical tubule degeneration in male and female Osborne-Mendel rats exposed to 1,4-dioxane in drinking water

Model	χ^2 Goodness-of-Fit Test *p*-Value[a]	AIC	BMD_{10} (mg/kg-day)	$BMDL_{10}$ (mg/kg-day)
Male				
Gamma[b]	0.65	74.46	28.80	22.27
Logistic	0.001	89.01	88.48	65.84
Log-logistic[c]	1.00	75.62	20.85	8.59
MS[e]	0.65	74.46	28.80	22.27
Probit	0.001	88.78	87.10	66.32
Log-probit[c,d]	0.75	74.17	51.41	38.53
Weibull[b]	0.65	74.46	28.80	22.27
Female				
Gamma[b]	0.95	41.97	524.73	437.08
Logistic	0.9996	43.75	617.44	471.92
Log-logistic[c,d]	0.9999	41.75	591.82	447.21
MS[e]	0.03	52.30	306.21	189.49
Probit	0.9997	43.75	596.02	456.42
Log-probit[c]	0.9997	43.75	584.22	436.19
Quantal quadratic	0.14	48.20	399.29	314.00
Weibull[b]	0.9999	41.75	596.44	452.36

[a] *p*-Value from the χ^2 goodness-of-fit test for the selected model. Values < 0.1 indicate that the model exhibited a statistically significant lack of fit, and thus a different model should be chosen.
[b]Power restricted to ≥1.
[c]Slope restricted to >1.
[d]Best-fitting model.
[e]Betas restricted to ≥0.

Source: NCI (1978).

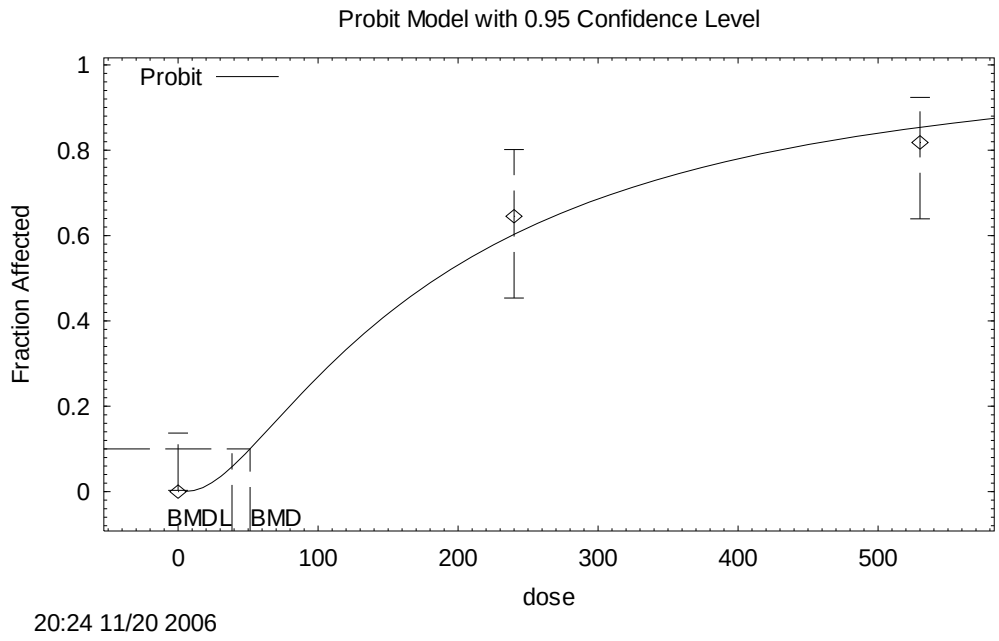

Source: NCI (1978).

Figure C-1. BMD log probit model of cortical tubule degeneration incidence data for male rats exposed to 1,4-dioxane in drinking water for 2 years to support the results in Table C-2.

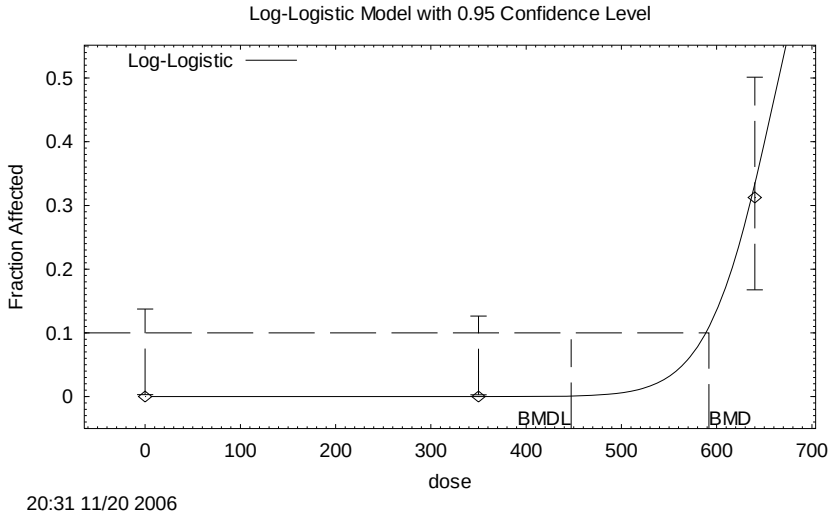

Source: NCI (1978).

Figure C-2. BMD log-logistic model of cortical tubule degeneration incidence data for female rats exposed to 1,4-dioxane in drinking water for 2 years to support results Table C-2.

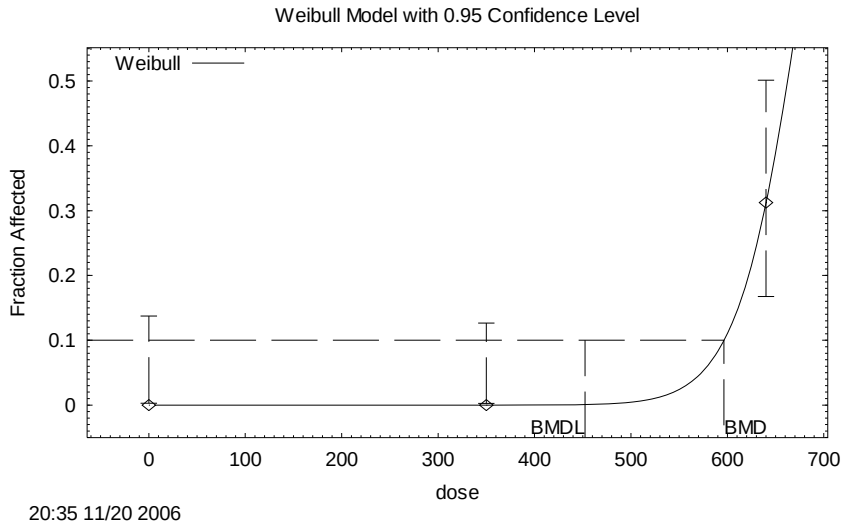

Source: NCI (1978).

Figure C-3. BMD Weibull model of cortical tubule degeneration incidence data for female rats exposed to 1,4-dioxane in drinking water for 2 years to support the results in Table C-2.

An alternative BMR of 20% was calculated from the best fitting model for each data set. The doses associated with the 20% extra risk (BMD_{20}) and the 95% lower confidence limits ($BMDL_{20}$) for the incidence of cortical tubule degeneration in male rats are 79.81 and 59.82 mg/kg-day, respectively. The doses associated with the BMD_{20} and the $BMDL_{20}$ for female rats are 619.09 and 533.88 mg/kg-day for the log-logistic model, and 621.84 and 541.58 mg/kg-day for the Weibull model.

C.2. LIVER HYPERPLASIA.

All available dichotomous models in the Benchmark Dose Software (version 1.3.2) were fit to the incidence data shown in Table C-1, for cortical tubule degeneration in male and female Osborne-Mendel rats exposed to 1,4-dioxane in the drinking water (NCI, 1978). Doses associated with a BMR of a 10% extra risk was calculated.

Table C-3. Incidence of liver hyperplasia in F344/DuCrj rats exposed to 1,4-dioxane in drinking water

Males (mg/kg-day)				Females (mg/kg-day)			
0	16	81	398	0	21	103	514
3/40	2/45	9/35[a]	12/22[b]	0/38[a]	0/37	1/38	14/24[b]

[a]Statistically significant compared to controls by the Dunnett's test ($p < 0.05$).
[b]Incidence significantly elevated compared to control by χ^2 test ($p < 0.01$).

Source: JBRC (1998a).

For incidence of liver hyperplasia, the logistic and probit models both exhibited a statistically significant lack of fit (i.e., χ^2 p-value < 0.1; see Table C-4), and thus should not be considered further for identification of a POD. All of the remaining models exhibited adequate fit, but the AIC values for the gamma, multistage, quantal-linear, and Weibull models were significantly lower than the AIC values for the log-logistic and log-probit models. Thus, the log-logistic and log-probit models should also be eliminated from further consideration for POD determination. Finally, the AIC values for gamma, multistage, quantal-linear, and Weibull models in Table C-4 are equivalent and, in this case, essentially represent the same model. Therefore, consistent with the "Benchmark Dose Technical Guidance" (EPA, 2000b), any of the highlighted models could be used to identify a POD for this endpoint of 34.7 mg/kg-day.

Table C-4. Benchmark dose modeling results based on the incidence of liver hyperplasias in F344 male rats exposed to 1,4-dioxane in drinking water for 2 years

Fitted Dichotomous Model[a]	χ^2 Goodness-of-Fit Test p-Value[a]	AIC	BMD_{10} (mg/kg-day)	$BMDL_{10}$ (mg/kg-day)
Gamma	0.35	114.13	52.3	34.7
Logistic	0.07	116.99	121.4	92.0
Log-Logistic	0.19	115.73	49.0	24.8
MS (1-degree)	0.35	114.13	52.3	34.7
Probit	0.09	116.61	111.4	85.2
Log-Probit	0.15	115.47	79.9	54.1
Quantal-Linear	0.35	114.13	52.3	34.7
Weibull	0.35	114.13	52.3	34.7

[a]p-Value from the χ^2 goodness-of-fit test for the selected model. Values < 0.1 indicate that the model exhibited a statistically significant lack of fit, and thus a different model should be chosen.

Source: JBRC (1998a).

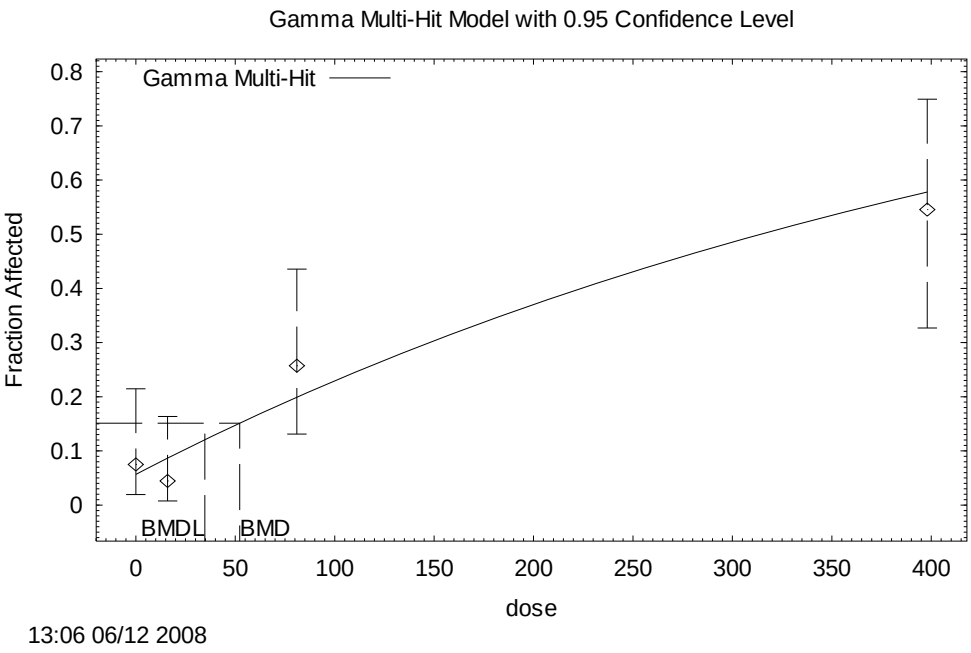

Figure C-4. BMD gamma model of liver hyperplasia incidence data for F344 male rats exposed to 1,4-dioxane in drinking water for 2 years to support results Table C-4.

```
1   ================================================================
2            Gamma Model. (Version: 2.8;  Date: 02/20/2007)
3            Input Data File: M:\DIOXANE DOSE-RESPONSE
4   MODELING\MALE_RATS_LIVER_HYPERPLASIA_JBRC_1998.(d)
5            Gnuplot Plotting File:  M:\DIOXANE DOSE-RESPONSE
6   MODELING\MALE_RATS_LIVER_HYPERPLASIA_JBRC_1998.plt
7                                                 Thu Jun 12 13:06:46 2008
8   ================================================================
9   BMDS MODEL RUN
10  ~~~~~~~~~~~~~~~~~~~~~~~~~~~~~~~~~~~~~~~~~~~~~~~~~~~~~~~~~~~~~~~~~~~~
11     The form of the probability function is:
12     P[response]= background+(1-background)*CumGamma[slope*dose,power],
13     where CumGamma(.) is the cummulative Gamma distribution function
14     Dependent variable = Response
15     Independent variable = Dose
16     Power parameter is restricted as power >=1
17     Total number of observations = 4
18     Total number of records with missing values = 0
19     Maximum number of iterations = 250
20     Relative Function Convergence has been set to: 1e-008
21     Parameter Convergence has been set to: 1e-008
22                     Default Initial (and Specified) Parameter Values
23                        Background =    0.0853659
24                             Slope =   0.00334063
25                             Power =          1.3
26
27              Asymptotic Correlation Matrix of Parameter Estimates
28  ( *** The model parameter(s)  -Power, have been estimated at a boundary point, or have
29  been specified by the user, and do not appear in the correlation matrix )
30
31                Background        Slope
32  Background             1        -0.36
33       Slope        -0.36            1
```

Parameter Estimates

Variable	Estimate	Std. Err.	95.0% Wald Confidence Interval Lower Conf. Limit	Upper Conf. Limit
Background	0.0567425	0.0277768	0.00230091	0.111184
Slope	0.00201574	0.000558241	0.000921605	0.00310987
Power	1	NA		

NA - Indicates that this parameter has hit a bound implied by some inequality constraint and thus has no standard error.

Analysis of Deviance Table

Model	Log(likelihood)	# Param's	Deviance	Test d.f.	P-value
Full model	-53.9471	4			
Fitted model	-55.0634	2	2.23256	2	0.3275
Reduced model	-67.6005	1	27.3066	3	<.0001

AIC: 114.127

Goodness of Fit

Dose	Est._Prob.	Expected	Observed	Size	Scaled Residual
0.0000	0.0567	2.270	3	40	0.499
16.0000	0.0867	3.901	2	45	-1.007
81.0000	0.1988	6.959	9	35	0.864
398.0000	0.5771	12.697	12	22	-0.301

Chi^2 = 2.10 d.f. = 2 P-value = 0.3499

Benchmark Dose Computation

Specified effect = 0.1
Risk Type = Extra risk
Confidence level = 0.95
BMD = 52.269
BMDL = 34.6825

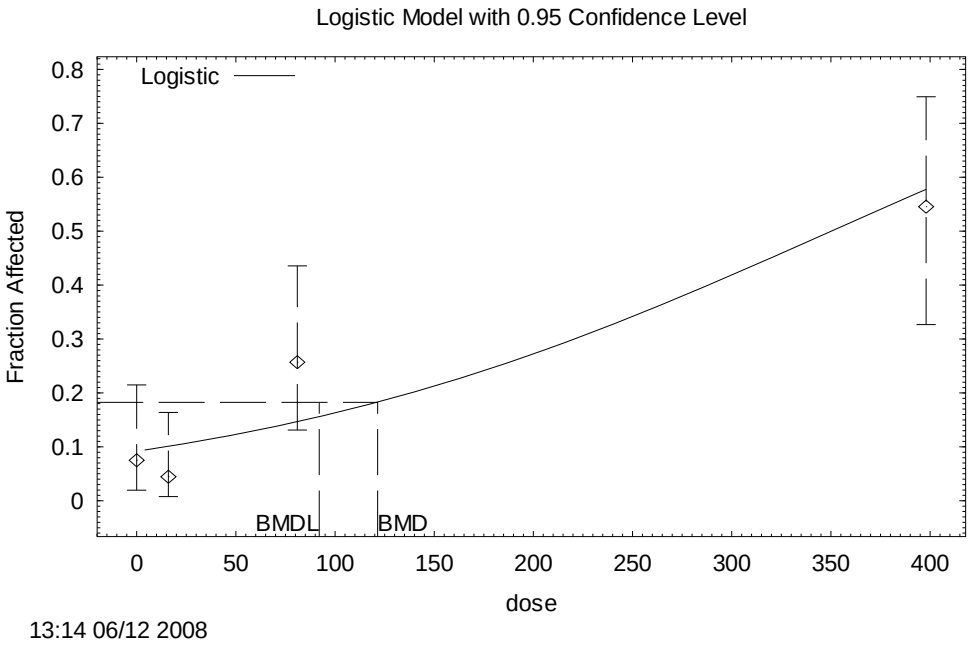

Figure C-5. BMD logistic model of liver hyperplasia incidence data for F344 male rats exposed to 1,4-dioxane in drinking water for 2 years to support results Table C-4.

```
1   ================================================================
2           Logistic Model. (Version: 2.9; Date: 02/20/2007)
3           Input Data File: M:\DIOXANE DOSE-RESPONSE
4   MODELING\MALE_RATS_LIVER_HYPERPLASIA_JBRC_1998.(d)
5           Gnuplot Plotting File:  M:\DIOXANE DOSE-RESPONSE
6   MODELING\MALE_RATS_LIVER_HYPERPLASIA_JBRC_1998.plt
7                                                 Thu Jun 12 13:14:11 2008
8   ================================================================
9    BMDS MODEL RUN
10  ~~~~~~~~~~~~~~~~~~~~~~~~~~~~~~~~~~~~~~~~~~~~~~~~~~~~~~~~~~~~~~~~~~~~
11     The form of the probability function is:
12
13     P[response] = 1/[1+EXP(-intercept-slope*dose)]
14
15     Dependent variable = Response
16     Independent variable = Dose
17     Slope parameter is not restricted
18
19     Total number of observations = 4
20     Total number of records with missing values = 0
21     Maximum number of iterations = 250
22     Relative Function Convergence has been set to: 1e-008
23     Parameter Convergence has been set to: 1e-008
24
25                     Default Initial Parameter Values
26                        background =            0   Specified
27                         intercept =      -2.3447
28                             slope =   0.00666513
29
30              Asymptotic Correlation Matrix of Parameter Estimates
31  ( *** The model parameter(s)  -background,have been estimated at a boundary point, or
32  have been specified by the user, and do not appear in the correlation matrix )
33
34                  intercept        slope
35   intercept              1        -0.66
36       slope          -0.66            1
```

Parameter Estimates

Variable	Estimate	Std. Err.	95.0% Wald Confidence Interval Lower Conf. Limit	Upper Conf. Limit
intercept	-2.29444	0.320777	-2.92315	-1.66572
slope	0.00654235	0.00141544	0.00376813	0.00931657

Analysis of Deviance Table

Model	Log(likelihood)	# Param's	Deviance	Test d.f.	P-value
Full model	-53.9471	4			
Fitted model	-56.4957	2	5.09704	2	0.0782
Reduced model	-67.6005	1	27.3066	3	<.0001

AIC: 116.991

Goodness of Fit

Dose	Est._Prob.	Expected	Observed	Size	Scaled Residual
0.0000	0.0916	3.663	3	40	-0.364
16.0000	0.1007	4.530	2	45	-1.254
81.0000	0.1462	5.118	9	35	1.857
398.0000	0.5767	12.688	12	22	-0.297

Chi^2 = 5.24 d.f. = 2 P-value = 0.0728

Benchmark Dose Computation

Specified effect = 0.1
Risk Type = Extra risk
Confidence level = 0.95
BMD = 121.431
BMDL = 92.0138

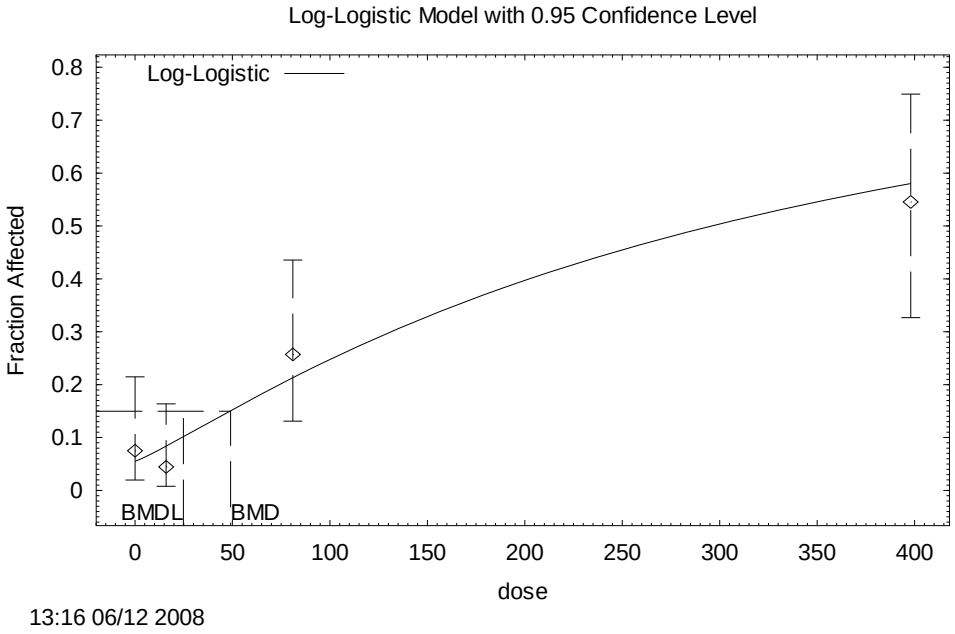

Figure C-6. BMD log-logistic model of liver hyperplasia incidence data for F344 male rats exposed to 1,4-dioxane in drinking water for 2 years to support the results in Table C-4.

```
================================================================
        Logistic Model. (Version: 2.9; Date: 02/20/2007)
        Input Data File: M:\DIOXANE DOSE-RESPONSE
MODELING\MALE_RATS_LIVER_HYPERPLASIA_JBRC_1998.(d)
        Gnuplot Plotting File:  M:\DIOXANE DOSE-RESPONSE
MODELING\MALE_RATS_LIVER_HYPERPLASIA_JBRC_1998.plt
                                          Thu Jun 12 13:16:30 2008
================================================================
 BMDS MODEL RUN
~~~~~~~~~~~~~~~~~~~~~~~~~~~~~~~~~~~~~~~~~~~~~~~~~~~~~~~~~~~~~~~~
   The form of the probability function is:

   P[response] = background+(1-background)/[1+EXP(-intercept-slope*Log(dose))]

   Dependent variable = Response
   Independent variable = Dose
   Slope parameter is restricted as slope >= 1

   Total number of observations = 4
   Total number of records with missing values = 0
   Maximum number of iterations = 250
   Relative Function Convergence has been set to: 1e-008
   Parameter Convergence has been set to: 1e-008

   User has chosen the log transformed model

                Default Initial Parameter Values
                   background =       0.075
                    intercept =    -8.16843
                        slope =     1.41583
```

Asymptotic Correlation Matrix of Parameter Estimates

	background	intercept	slope
background	1	-0.34	0.28
intercept	-0.34	1	-0.98
slope	0.28	-0.98	1

Parameter Estimates

Variable	Estimate	Std. Err.	95.0% Wald Confidence Interval Lower Conf. Limit	Upper Conf. Limit
background	0.0550676	*	*	*
intercept	-6.66232	*	*	*
slope	1.1471	*	*	*

* - Indicates that this value is not calculated.

Analysis of Deviance Table

Model	Log(likelihood)	# Param's	Deviance	Test d.f.	P-value
Full model	-53.9471	4			
Fitted model	-54.8671	3	1.83982	1	0.175
Reduced model	-67.6005	1	27.3066	3	<.0001

AIC: 115.734

Goodness of Fit

Dose	Est._Prob.	Expected	Observed	Size	Scaled Residual
0.0000	0.0551	2.203	3	40	0.553
16.0000	0.0833	3.747	2	45	-0.942
81.0000	0.2110	7.385	9	35	0.669
398.0000	0.5757	12.666	12	22	-0.287

Chi^2 = 1.72 d.f. = 1 P-value = 0.1892

Benchmark Dose Computation

Specified effect = 0.1
Risk Type = Extra risk
Confidence level = 0.95
BMD = 49.0334
BMDL = 24.8079

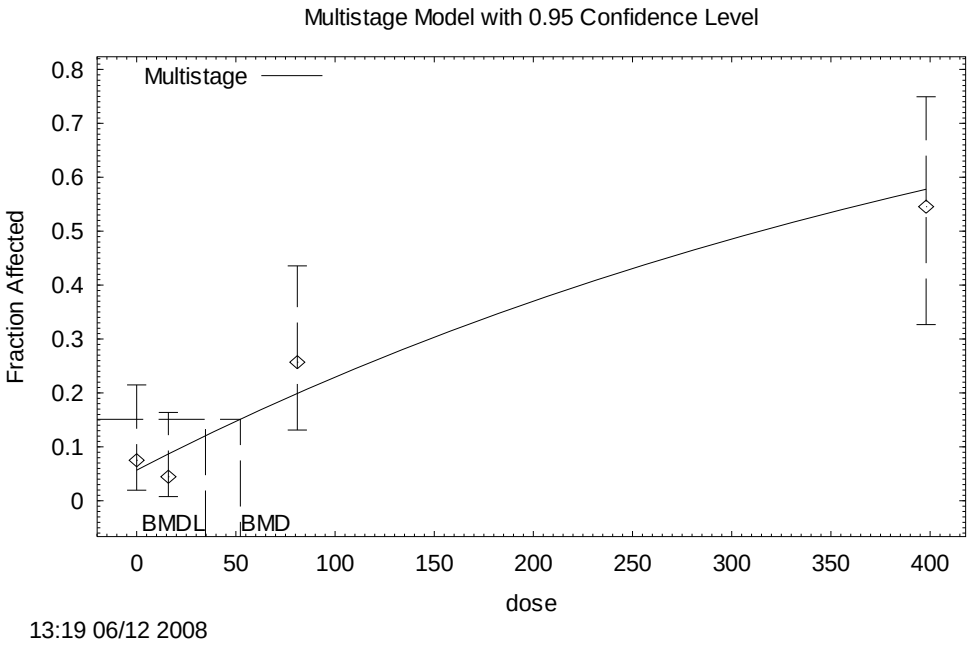

Figure C-7. BMD multistage model of liver hyperplasia incidence data for F344 male rats exposed to 1,4-dioxane in drinking water for 2 years to support the results in Table C-4.

```
1  ========================================================================
2           Multistage Model. (Version: 2.8;  Date: 02/20/2007)
3           Input Data File: M:\DIOXANE DOSE-RESPONSE
4  MODELING\MALE_RATS_LIVER_HYPERPLASIA_JBRC_1998.(d)
5           Gnuplot Plotting File:  M:\DIOXANE DOSE-RESPONSE
6  MODELING\MALE_RATS_LIVER_HYPERPLASIA_JBRC_1998.plt
7                                                 Thu Jun 12 13:19:53 2008
8  ========================================================================
9   BMDS MODEL RUN
10 ~~~~~~~~~~~~~~~~~~~~~~~~~~~~~~~~~~~~~~~~~~~~~~~~~~~~~~~~~~~~~~~~~~~~~~~~
11    The form of the probability function is:
12
13    P[response] = background + (1-background)*[1-EXP(-beta1*dose^1)]
14
15    The parameter betas are restricted to be positive
16
17    Dependent variable = Response
18    Independent variable = Dose
19
20   Total number of observations = 4
21   Total number of records with missing values = 0
22   Total number of parameters in model = 2
23   Total number of specified parameters = 0
24   Degree of polynomial = 1
25   Maximum number of iterations = 250
26   Relative Function Convergence has been set to: 1e-008
27   Parameter Convergence has been set to: 1e-008
28
29                    Default Initial Parameter Values
30                       Background =    0.0744232
31                           Beta(1) =   0.00181774
```

Asymptotic Correlation Matrix of Parameter Estimates

	Background	Beta(1)
Background	1	-0.49
Beta(1)	-0.49	1

Parameter Estimates

Variable	Estimate	Std. Err.	95.0% Wald Confidence Interval Lower Conf. Limit	Upper Conf. Limit
Background	0.0567425	*	*	*
Beta(1)	0.00201574	*	*	*

* - Indicates that this value is not calculated.

Analysis of Deviance Table

Model	Log(likelihood)	# Param's	Deviance	Test d.f.	P-value
Full model	-53.9471	4			
Fitted model	-55.0634	2	2.23256	2	0.3275
Reduced model	-67.6005	1	27.3066	3	<.0001

AIC: 114.127

Goodness of Fit

Dose	Est._Prob.	Expected	Observed	Size	Scaled Residual
0.0000	0.0567	2.270	3	40	0.499
16.0000	0.0867	3.901	2	45	-1.007
81.0000	0.1988	6.959	9	35	0.864
398.0000	0.5771	12.697	12	22	-0.301

Chi^2 = 2.10 d.f. = 2 P-value = 0.3499

Benchmark Dose Computation

Specified effect = 0.1

Risk Type = Extra risk
Confidence level = 0.95
BMD = 52.269
BMDL = 34.6825
BMDU = 88.4683

Taken together, (34.6825, 88.4683) is a 90% two-sided confidence interval for the BMD

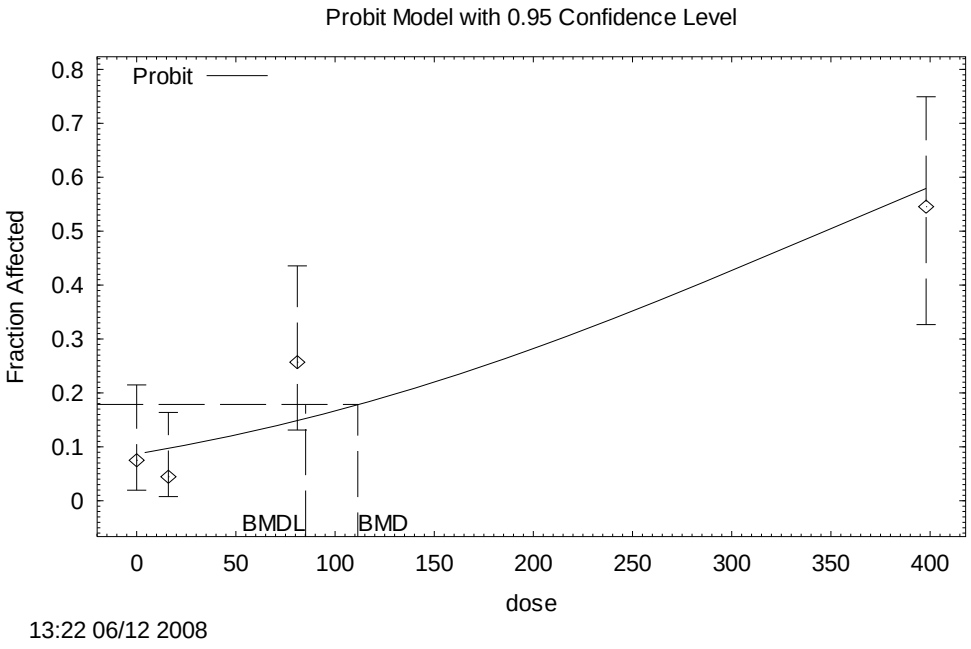

Figure C-8. BMD probit model of liver hyperplasia incidence data for F344 male rats exposed to 1,4-dioxane in drinking water for 2 years to support results Table C-4.

```
1  ================================================================
2           Probit Model. (Version: 2.8;  Date: 02/20/2007)
3           Input Data File: M:\DIOXANE DOSE-RESPONSE
4  MODELING\MALE_RATS_LIVER_HYPERPLASIA_JBRC_1998.(d)
5           Gnuplot Plotting File:  M:\DIOXANE DOSE-RESPONSE
6  MODELING\MALE_RATS_LIVER_HYPERPLASIA_JBRC_1998.plt
7                                                 Thu Jun 12 13:21:59 2008
8  ================================================================
9   BMDS MODEL RUN
10 ~~~~~~~~~~~~~~~~~~~~~~~~~~~~~~~~~~~~~~~~~~~~~~~~~~~~~~~~~~~~~~~~~~~~
11    The form of the probability function is:
12
13    P[response] = CumNorm(Intercept+Slope*Dose),
14
15    where CumNorm(.) is the cumulative normal distribution function
16
17    Dependent variable = Response
18    Independent variable = Dose
19    Slope parameter is not restricted
20    Total number of observations = 4
21    Total number of records with missing values = 0
22    Maximum number of iterations = 250
23    Relative Function Convergence has been set to: 1e-008
24    Parameter Convergence has been set to: 1e-008
25                    Default Initial (and Specified) Parameter Values
26                       background =            0   Specified
27                        intercept =     -1.43942
28                            slope =   0.00420358
```

Asymptotic Correlation Matrix of Parameter Estimates

(*** The model parameter(s) -background, have been estimated at a boundary point, or have been specified by the user, and do not appear in the correlation matrix)

	intercept	slope
intercept	1	-0.62
slope	-0.62	1

Parameter Estimates

Variable	Estimate	Std. Err.	95.0% Wald Confidence Interval Lower Conf. Limit	Upper Conf. Limit
intercept	-1.35669	0.169086	-1.68809	-1.02528
slope	0.00391559	0.000838003	0.00227313	0.00555805

Analysis of Deviance Table

Model	Log(likelihood)	# Param's	Deviance	Test d.f.	P-value
Full model	-53.9471	4			
Fitted model	-56.3042	2	4.71415	2	0.0947
Reduced model	-67.6005	1	27.3066	3	<.0001

AIC: 116.608

Goodness of Fit

Dose	Est._Prob.	Expected	Observed	Size	Scaled Residual
0.0000	0.0874	3.498	3	40	-0.279
16.0000	0.0978	4.402	2	45	-1.205
81.0000	0.1493	5.225	9	35	1.791
398.0000	0.5799	12.758	12	22	-0.328

Chi^2 = 4.84 d.f. = 2 P-value = 0.0887

Benchmark Dose Computation

Specified effect = 0.1
Risk Type = Extra risk
Confidence level = 0.95
BMD = 111.437
BMDL = 85.1525

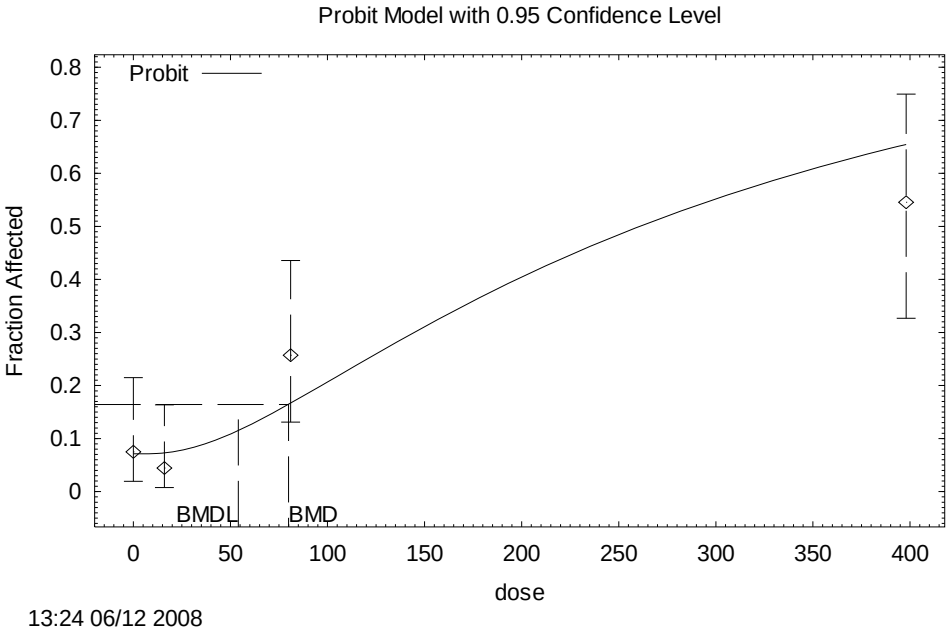

Figure C-9. BMD probit model of liver hyperplasia incidence data for F344 male rats exposed to 1,4-dioxane in drinking water for 2 years, accounting for background incidence.

```
1   ================================================================
2            Probit Model. (Version: 2.8;  Date: 02/20/2007)
3            Input Data File: M:\DIOXANE DOSE-RESPONSE
4   MODELING\MALE_RATS_LIVER_HYPERPLASIA_JBRC_1998.(d)
5            Gnuplot Plotting File:  M:\DIOXANE DOSE-RESPONSE
6   MODELING\MALE_RATS_LIVER_HYPERPLASIA_JBRC_1998.plt
7                                                 Thu Jun 12 13:24:01 2008
8   ================================================================
9    BMDS MODEL RUN
10  ~~~~~~~~~~~~~~~~~~~~~~~~~~~~~~~~~~~~~~~~~~~~~~~~~~~~~~~~~~~~~~~~~~~~
11     The form of the probability function is:
12
13     P[response] = Background + (1-Background) * CumNorm(Intercept+Slope*Log(Dose)),
14
15     where CumNorm(.) is the cumulative normal distribution function
16
17     Dependent variable = Response
18     Independent variable = Dose
19     Slope parameter is restricted as slope >= 1
20     Total number of observations = 4
21     Total number of records with missing values = 0
22     Maximum number of iterations = 250
23     Relative Function Convergence has been set to: 1e-008
24     Parameter Convergence has been set to: 1e-008
25     User has chosen the log transformed model
26                   Default Initial (and Specified) Parameter Values
27                      background =       0.075
28                       intercept =    -5.64933
29                           slope =           1
```

Asymptotic Correlation Matrix of Parameter Estimates

(*** The model parameter(s) -slope, have been estimated at a boundary point, or have been specified by the user, and do not appear in the correlation matrix)

	background	intercept
background	1	-0.45
intercept	-0.45	1

Parameter Estimates

Variable	Estimate	Std. Err.	95.0% Wald Confidence Interval Lower Conf. Limit	Upper Conf. Limit
background	0.0712134	0.0303379	0.0117523	0.130675
intercept	-5.66248	0.263846	-6.17961	-5.14535
slope	1	NA		

NA - Indicates that this parameter has hit a bound implied by some inequality constraint and thus has no standard error.

Analysis of Deviance Table

Model	Log(likelihood)	# Param's	Deviance	Test d.f.	P-value
Full model	-53.9471	4			
Fitted model	-55.7325	2	3.57078	2	0.1677
Reduced model	-67.6005	1	27.3066	3	<.0001

AIC: 115.465

Goodness of Fit

Dose	Est._Prob.	Expected	Observed	Size	Scaled Residual
0.0000	0.0712	2.849	3	40	0.093
16.0000	0.0730	3.285	2	45	-0.736
81.0000	0.1663	5.821	9	35	1.443
398.0000	0.6536	14.379	12	22	-1.066

Chi^2 = 3.77 d.f. = 2 P-value = 0.1519

Benchmark Dose Computation

Specified effect = 0.1
Risk Type = Extra risk
Confidence level = 0.95
BMD = 79.9119
BMDL = 54.0772

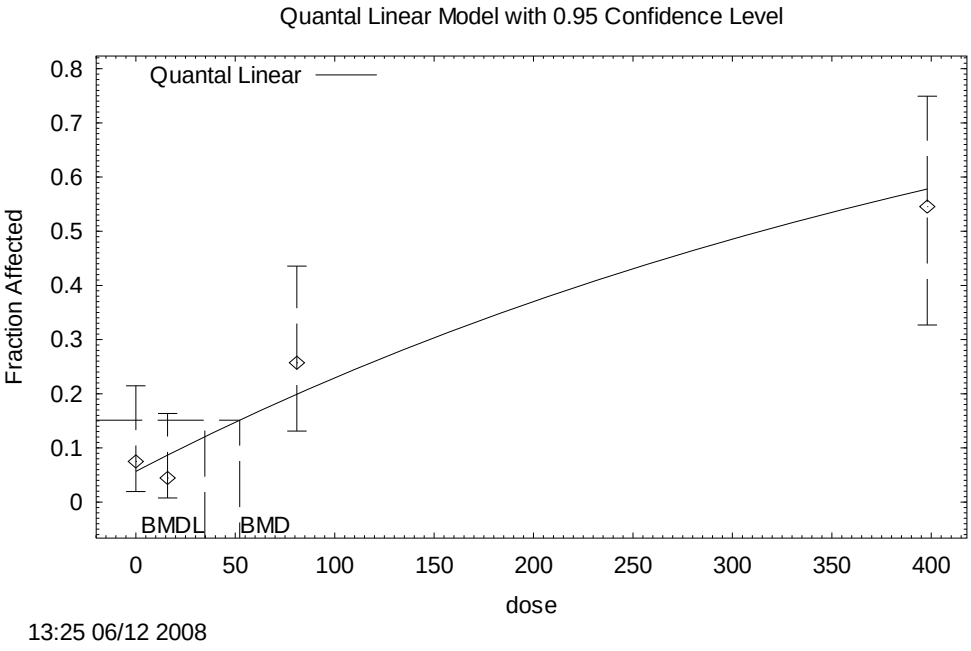

Figure C-10. BMD quantal linear model of liver hyperplasia incidence data for F344 male rats exposed to 1,4-dioxane in drinking water for 2 years to support the results in Table C-4.

```
1   ================================================================
2            Quantal Linear Model using Weibull Model (Version: 2.7;  Date: 2/20/2007)
3            Input Data File: M:\DIOXANE DOSE-RESPONSE
4   MODELING\MALE_RATS_LIVER_HYPERPLASIA_JBRC_1998.(d)
5            Gnuplot Plotting File:  M:\DIOXANE DOSE-RESPONSE
6   MODELING\MALE_RATS_LIVER_HYPERPLASIA_JBRC_1998.plt
7                                                 Thu Jun 12 13:25:58 2008
8   ================================================================
9    BMDS MODEL RUN
10  ~~~~~~~~~~~~~~~~~~~~~~~~~~~~~~~~~~~~~~~~~~~~~~~~~~~~~~~~~~~~~~~~~~~~
11      The form of the probability function is:
12
13     P[response] = background + (1-background)*[1-EXP(-slope*dose)]
14
15     Dependent variable = Response
16     Independent variable = Dose
17
18     Total number of observations = 4
19     Total number of records with missing values = 0
20     Maximum number of iterations = 250
21     Relative Function Convergence has been set to: 1e-008
22     Parameter Convergence has been set to: 1e-008
23
24                     Default Initial (and Specified) Parameter Values
25                        Background =    0.0853659
26                             Slope =   0.00174595
27                             Power =            1   Specified
28
29
30              Asymptotic Correlation Matrix of Parameter Estimates
31  ( *** The model parameter(s)  -Power, have been estimated at a boundary point, or have
32  been specified by the user, and do not appear in the correlation matrix )
33
34                Background        Slope
35  Background             1        -0.36
36       Slope         -0.36            1
```

Parameter Estimates

Variable	Estimate	Std. Err.	95.0% Wald Confidence Interval Lower Conf. Limit	Upper Conf. Limit
Background	0.0567426	0.0277774	0.00229997	0.111185
Slope	0.00201574	0.000558246	0.000921598	0.00310988

Analysis of Deviance Table

Model	Log(likelihood)	# Param's	Deviance	Test d.f.	P-value
Full model	-53.9471	4			
Fitted model	-55.0634	2	2.23256	2	0.3275
Reduced model	-67.6005	1	27.3066	3	<.0001

AIC: 114.127

Goodness of Fit

Dose	Est._Prob.	Expected	Observed	Size	Scaled Residual
0.0000	0.0567	2.270	3	40	0.499
16.0000	0.0867	3.901	2	45	-1.007
81.0000	0.1988	6.959	9	35	0.864
398.0000	0.5771	12.697	12	22	-0.301

Chi^2 = 2.10 d.f. = 2 P-value = 0.3499

Benchmark Dose Computation

Specified effect = 0.1
Risk Type = Extra risk
Confidence level = 0.95
BMD = 52.2689
BMDL = 34.6825

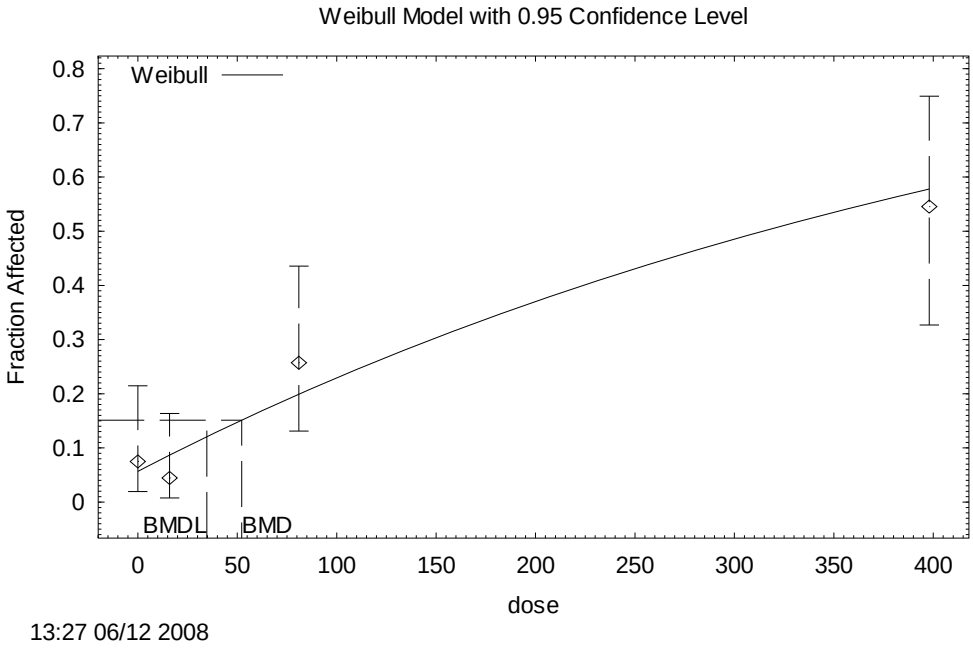

Figure C-11. BMD Weibull model of liver hyperplasia incidence data for F344 male rats exposed to 1,4-dioxane in drinking water for 2 years to support the results in Table C-4.

```
 ================================================================
        Weibull Model using Weibull Model (Version: 2.7;  Date: 2/20/2007)
        Input Data File: M:\DIOXANE DOSE-RESPONSE
MODELING\MALE_RATS_LIVER_HYPERPLASIA_JBRC_1998.(d)
        Gnuplot Plotting File:  M:\DIOXANE DOSE-RESPONSE
MODELING\MALE_RATS_LIVER_HYPERPLASIA_JBRC_1998.plt
                                          Thu Jun 12 13:27:47 2008
 ================================================================
 BMDS MODEL RUN
~~~~~~~~~~~~~~~~~~~~~~~~~~~~~~~~~~~~~~~~~~~~~~~~~~~~~~~~~~~~~~~~~~~~
   The form of the probability function is:

   P[response] = background + (1-background)*[1-EXP(-slope*dose^power)]

   Dependent variable = Response
   Independent variable = Dose
   Power parameter is restricted as power >=1

   Total number of observations = 4
   Total number of records with missing values = 0
   Maximum number of iterations = 250
   Relative Function Convergence has been set to: 1e-008
   Parameter Convergence has been set to: 1e-008

                  Default Initial (and Specified) Parameter Values
                     Background =    0.0853659
                          Slope =   0.00174595
                          Power =            1
```

```
          Asymptotic Correlation Matrix of Parameter Estimates
( *** The model parameter(s)  -Power, have been estimated at a boundary point, or have
been specified by the user, and do not appear in the correlation matrix )

             Background        Slope
Background            1        -0.36
     Slope        -0.36            1
                              Parameter Estimates

                                                      95.0% Wald Confidence Interval
       Variable     Estimate      Std. Err.     Lower Conf. Limit   Upper Conf. Limit
     Background     0.0567426     0.0277773      0.00229996           0.111185
          Slope     0.00201574    0.000558245    0.000921596          0.00310988
          Power                1               NA

NA - Indicates that this parameter has hit a bound implied by some inequality
constraint and thus has no standard error.

                        Analysis of Deviance Table

       Model      Log(likelihood)  # Param's  Deviance  Test d.f.   P-value
     Full model        -53.9471         4
   Fitted model        -55.0634         2       2.23256      2          0.3275
  Reduced model        -67.6005         1       27.3066      3         <.0001

           AIC:         114.127

                                  Goodness  of  Fit
                                                                      Scaled
     Dose     Est._Prob.    Expected    Observed     Size       Residual
  ---------------------------------------------------------------------------
    0.0000     0.0567         2.270         3          40        0.499
   16.0000     0.0867         3.901         2          45       -1.007
   81.0000     0.1988         6.959         9          35        0.864
  398.0000     0.5771        12.697        12          22       -0.301

 Chi^2 = 2.10      d.f. = 2        P-value = 0.3499


   Benchmark Dose Computation

Specified effect =            0.1
Risk Type        =      Extra risk
Confidence level =           0.95
             BMD =         52.269
            BMDL =        34.6825
```

For liver hyperplasias in F344 female rats exosed to 1,4-dioxane, the quantal-linear model exhibited a statistically significant lack of fit (i.e., χ^2 *p*-value < 0.1; See Table C-5), and thus should not be considered further for identification of a POD. All of the remaining models exhibited adequate fit, but the AIC values for the logistic, multistage, and probit models were significantly lower than the AIC values for the gamma, log-logistic, log-probit, and Weibull models. Thus, the gamma, log-logistic, log-probit, and Weibull models should also be eliminated from further consideration for POD determination. Finally, the AIC values for the three highlighted models in Table C-5 were essentially equivalent. Therefore, consistent with the "Benchmark Dose Technical Guidance" (EPA, 2000b), the BMDLs from these three highlighted models were averaged to yield a POD for this endpoint of 45.7 mg/kg-day.

Table C-5. Benchmark dose modeling results based on the incidence of liver hyperplasias in F344 female rats exposed to 1,4-dioxane in drinking water for 2 years

Fitted Dichotomous Model	χ^2 Goodness-of-Fit Test *p*-Value[a]	AIC	BMD_{10} (mg/kg-day)	$BMDL_{10}$ (mg/kg-day)
Gamma	0.98	78.84	88.7	51.2
Logistic	0.92	77.03	67.6	50.8
Log-Logistic	0.98	78.84	96.7	64.2
MS (2-degree)	0.95	77.01	69.0	38.7
Probit	0.92	77.02	64.8	47.5
Log-Probit	0.98	78.84	92.8	64.0
Quantal-Linear	0.02	87.66	26.2	19.0
Weibull	1.0	78.83	81.7	45.3

[a]*p*-Value from the χ^2 goodness-of-fit test for the selected model. Values < 0.1 indicate that the model exhibits a statistically significant lack of fit, and thus a different model should be chosen.

Source: JBRC (1998a).

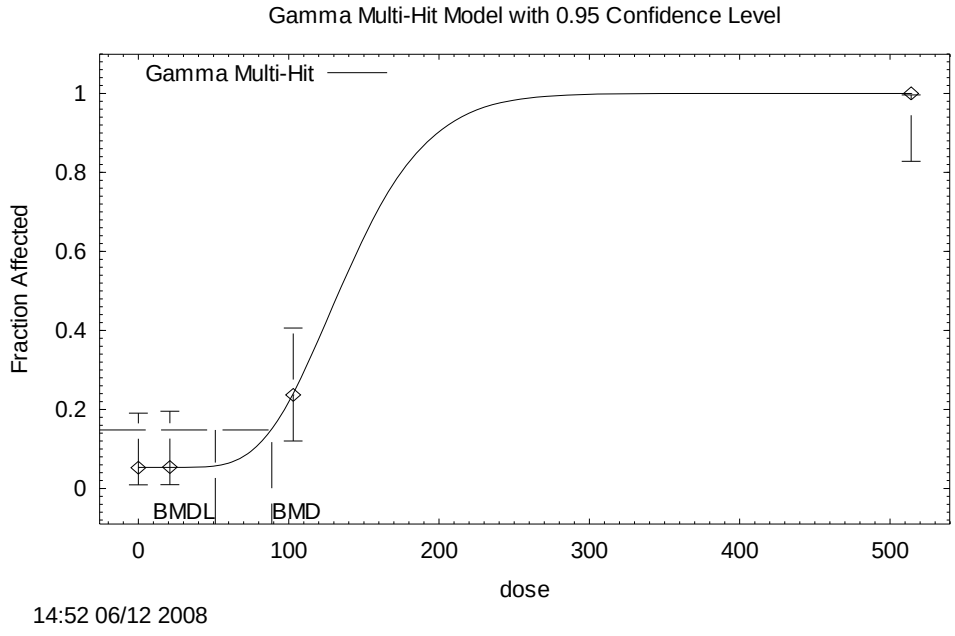

Source: JBRC (1998a).

Figure C-12. BMD gamma model of liver hyperplasia incidence data for F344 female rats exposed to 1,4-dioxane in drinking water for 2 years to support the results in Table C-5.

```
================================================================
        Gamma Model. (Version: 2.8;  Date: 02/20/2007)
        Input Data File: M:\DIOXANE DOSE-RESPONSE
MODELING\FEMALE_RATS_LIVER_HYPERPLASIA_JBRC_1998.(d)
        Gnuplot Plotting File:  M:\DIOXANE DOSE-RESPONSE
MODELING\FEMALE_RATS_LIVER_HYPERPLASIA_JBRC_1998.plt
                                              Thu Jun 12 14:52:14 2008
================================================================
 BMDS MODEL RUN
~~~~~~~~~~~~~~~~~~~~~~~~~~~~~~~~~~~~~~~~~~~~~~~~~~~~~~~~~~~~~~~~~~~~
   The form of the probability function is:

   P[response]= background+(1-background)*CumGamma[slope*dose,power],

   where CumGamma(.) is the cummulative Gamma distribution function
   Dependent variable = Response
   Independent variable = Dose
   Power parameter is restricted as power >=1
   Total number of observations = 4
   Total number of records with missing values = 0
   Maximum number of iterations = 250
   Relative Function Convergence has been set to: 1e-008
   Parameter Convergence has been set to: 1e-008
                  Default Initial (and Specified) Parameter Values
                     Background =    0.0641026
                          Slope =   0.00375157
                          Power =          1.3
           Asymptotic Correlation Matrix of Parameter Estimates
             Background        Slope        Power
Background            1        0.021        0.021
     Slope        0.021            1            1
     Power        0.021            1            1
                               Parameter Estimates

                                                    95.0% Wald Confidence Interval
       Variable      Estimate      Std. Err.     Lower Conf. Limit   Upper Conf. Limit
     Background      0.0533319     0.0259525          0.00246604            0.104198
          Slope      0.0713984     3.22468            -6.24886             6.39166
          Power        10.1413     385.373            -745.176             765.459


                         Analysis of Deviance Table

        Model      Log(likelihood)  # Param's  Deviance  Test d.f.   P-value
      Full model        -36.4175         4
    Fitted model        -36.4178         3   0.000751059      1          0.9781
  Reduced model         -79.9164         1       86.9979      3         <.0001

           AIC:         78.8357


                                  Goodness  of  Fit
                                                                    Scaled
     Dose     Est._Prob.    Expected    Observed     Size       Residual
   ---------------------------------------------------------------------
    0.0000     0.0533         2.027         2          38       -0.019
   21.0000     0.0533         1.973         2          37        0.019
  103.0000     0.2368         8.999         9          38        0.000
  514.0000     1.0000        24.000        24          24        0.001

 Chi^2 = 0.00      d.f. = 1        P-value = 0.9782
   Benchmark Dose Computation
Specified effect =            0.1
Risk Type        =      Extra risk
Confidence level =           0.95
             BMD =        88.7086
            BMDL =       51.1769
```

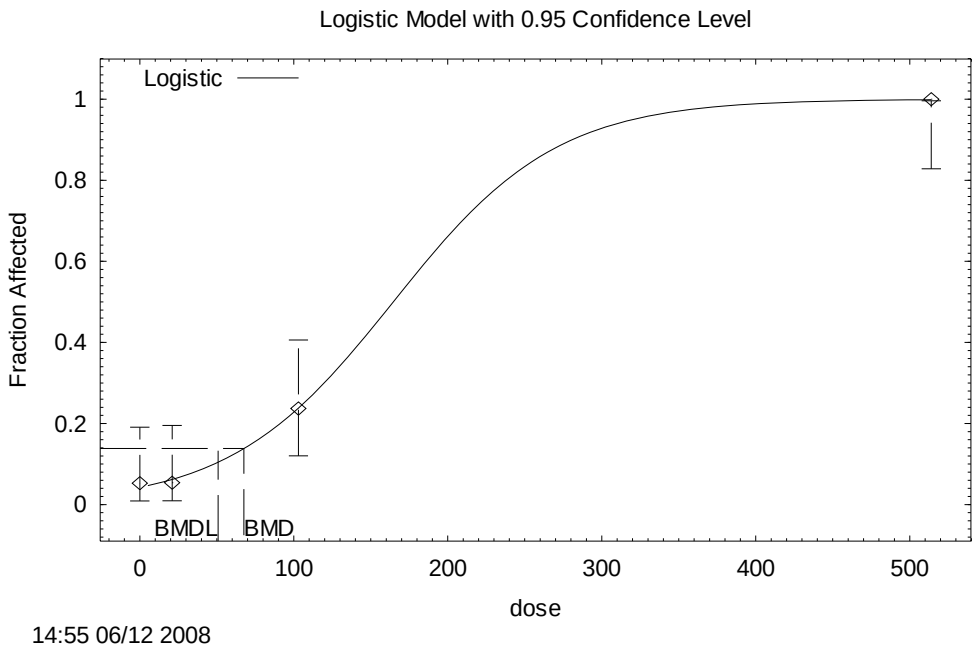

Source: JBRC (1998a).

Figure C-13. BMD logistic model of liver hyperplasia incidence data for F344 female rats exposed to 1,4-dioxane in drinking water for 2 years to support the results in Table C-5.

```
1   ================================================================
2            Logistic Model. (Version: 2.9; Date: 02/20/2007)
3            Input Data File: M:\DIOXANE DOSE-RESPONSE
4   MODELING\FEMALE_RATS_LIVER_HYPERPLASIA_JBRC_1998.(d)
5            Gnuplot Plotting File:  M:\DIOXANE DOSE-RESPONSE
6   MODELING\FEMALE_RATS_LIVER_HYPERPLASIA_JBRC_1998.plt
7                                                 Thu Jun 12 14:55:04 2008
8    ================================================================
9    BMDS MODEL RUN
10  ~~~~~~~~~~~~~~~~~~~~~~~~~~~~~~~~~~~~~~~~~~~~~~~~~~~~~~~~~~~~~~~~~~~~
11      The form of the probability function is:
12
13     P[response] = 1/[1+EXP(-intercept-slope*dose)]
14
15     Dependent variable = Response
16     Independent variable = Dose
17     Slope parameter is not restricted
18     Total number of observations = 4
19     Total number of records with missing values = 0
20     Maximum number of iterations = 250
21     Relative Function Convergence has been set to: 1e-008
22     Parameter Convergence has been set to: 1e-008
23                     Default Initial Parameter Values
24                        background =            0   Specified
25                         intercept =     -2.70218
26                             slope =    0.0129047
```

Asymptotic Correlation Matrix of Parameter Estimates

(*** The model parameter(s) -background, have been estimated at a boundary point, or have been specified by the user, and do not appear in the correlation matrix)

	intercept	slope
intercept	1	-0.82
slope	-0.82	1

Parameter Estimates

Variable	Estimate	Std. Err.	95.0% Wald Confidence Interval Lower Conf. Limit	Upper Conf. Limit
intercept	-3.1071	0.540423	-4.16631	-2.04789
slope	0.01894	0.00613873	0.00690836	0.0309717

Analysis of Deviance Table

Model	Log(likelihood)	# Param's	Deviance	Test d.f.	P-value
Full model	-36.4175	4			
Fitted model	-36.5147	2	0.194506	2	0.9073
Reduced model	-79.9164	1	86.9979	3	<.0001

AIC: 77.0294

Goodness of Fit

Dose	Est._Prob.	Expected	Observed	Size	Scaled Residual
0.0000	0.0428	1.627	2	38	0.299
21.0000	0.0624	2.310	2	37	-0.210
103.0000	0.2393	9.095	9	38	-0.036
514.0000	0.9987	23.968	24	24	0.178

Chi^2 = 0.17 d.f. = 2 P-value = 0.9200

Benchmark Dose Computation

Specified effect = 0.1
Risk Type = Extra risk
Confidence level = 0.95
BMD = 67.5596
BMDL = 50.8415

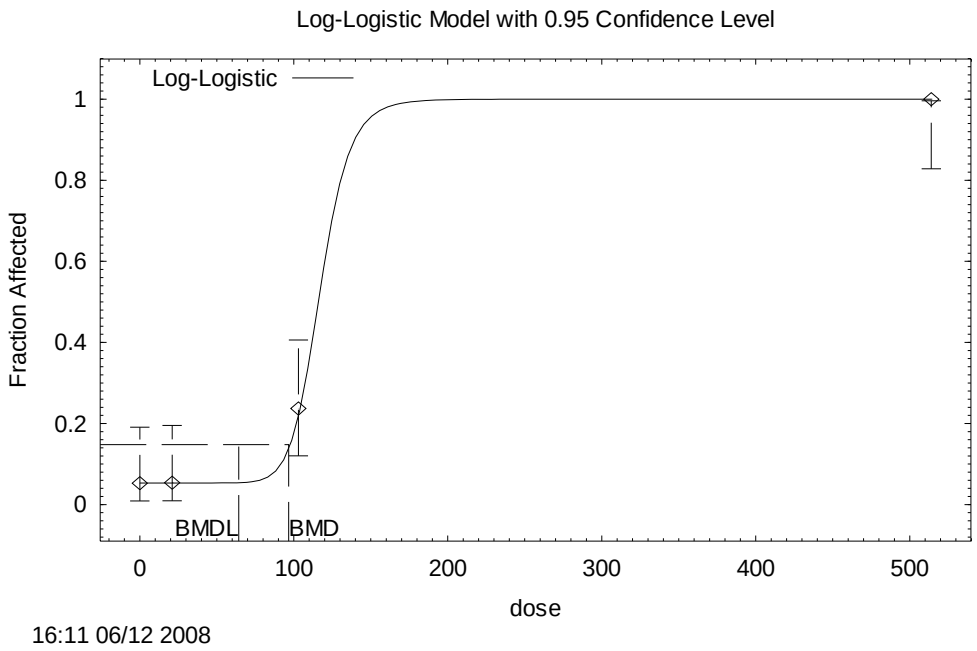

Source: JBRC (1998a).

Figure C-14. BMD log-logistic model of liver hyperplasia incidence data for F344 female rats exposed to 1,4-dioxane in drinking water for 2 years to support the results in Table C-5.

```
1   ================================================================
2            Logistic Model. (Version: 2.9; Date: 02/20/2007)
3            Input Data File: M:\DIOXANE DOSE-RESPONSE
4   MODELING\FEMALE_RATS_LIVER_HYPERPLASIA_JBRC_1998.(d)
5            Gnuplot Plotting File:  M:\DIOXANE DOSE-RESPONSE
6   MODELING\FEMALE_RATS_LIVER_HYPERPLASIA_JBRC_1998.plt
7                                                 Thu Jun 12 16:11:17 2008
8   ================================================================
9    BMDS MODEL RUN
10  ~~~~~~~~~~~~~~~~~~~~~~~~~~~~~~~~~~~~~~~~~~~~~~~~~~~~~~~~~~~~~~~~~~~~
11     The form of the probability function is:
12
13     P[response] = background+(1-background)/[1+EXP(-intercept-slope*Log(dose))]
14
15     Dependent variable = Response
16     Independent variable = Dose
17     Slope parameter is restricted as slope >= 1
18     Total number of observations = 4
19     Total number of records with missing values = 0
20     Maximum number of iterations = 250
21     Relative Function Convergence has been set to: 1e-008
22     Parameter Convergence has been set to: 1e-008
23     User has chosen the log transformed model
24
25                    Default Initial Parameter Values
26                       background =    0.0526316
27                        intercept =     -16.4238
28                            slope =      3.24981
```

Asymptotic Correlation Matrix of Parameter Estimates

	background	intercept	slope
background	1	0.018	-0.018
intercept	0.018	1	-1
slope	-0.018	-1	1

Parameter Estimates

Variable	Estimate	Std. Err.	95.0% Wald Confidence Interval Lower Conf. Limit	Upper Conf. Limit
background	0.0533333	*	*	*
intercept	-58.0881	*	*	*
slope	12.2257	*	*	*

* - Indicates that this value is not calculated.

Analysis of Deviance Table

Model	Log(likelihood)	# Param's	Deviance	Test d.f.	P-value
Full model	-36.4175	4			
Fitted model	-36.4178	3	0.000751795	1	0.9781
Reduced model	-79.9164	1	86.9979	3	<.0001

AIC: 78.8357

Goodness of Fit

Dose	Est._Prob.	Expected	Observed	Size	Scaled Residual
0.0000	0.0533	2.027	2	38	-0.019
21.0000	0.0533	1.973	2	37	0.020
103.0000	0.2368	9.000	9	38	0.000
514.0000	1.0000	24.000	24	24	0.001

Chi^2 = 0.00 d.f. = 1 P-value = 0.9781

Benchmark Dose Computation

Specified effect = 0.1
Risk Type = Extra risk
Confidence level = 0.95
BMD = 96.6969
BMDL = 64.2472

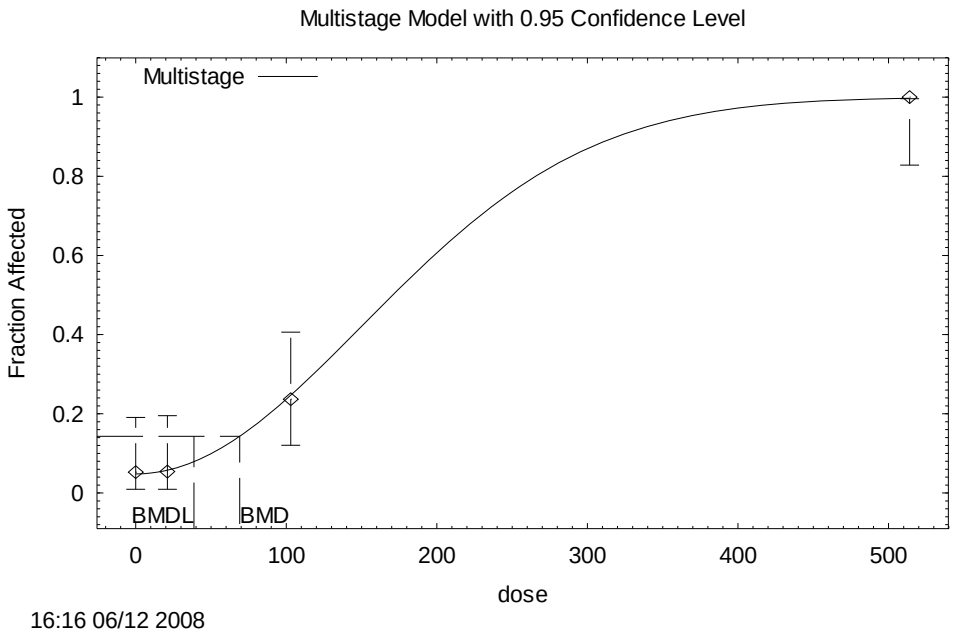

Source: JBRC (1998a).

Figure C-15. BMD multistage model of liver hyperplasia incidence data for F344 female rats exposed to 1,4-dioxane in drinking water for 2 years to support the results in Table C-5.

```
1   ================================================================
2            Multistage Model. (Version: 2.8;  Date: 02/20/2007)
3            Input Data File: M:\DIOXANE DOSE-RESPONSE
4   MODELING\FEMALE_RATS_LIVER_HYPERPLASIA_JBRC_1998.(d)
5            Gnuplot Plotting File:  M:\DIOXANE DOSE-RESPONSE
6   MODELING\FEMALE_RATS_LIVER_HYPERPLASIA_JBRC_1998.plt
7                                                 Thu Jun 12 16:16:25 2008
8   ================================================================
9    BMDS MODEL RUN
10  ~~~~~~~~~~~~~~~~~~~~~~~~~~~~~~~~~~~~~~~~~~~~~~~~~~~~~~~~~~~~~~~~~~~~
11   The form of the probability function is:
12
13     P[response] = background + (1-background)*[1-EXP(-beta1*dose^1-beta2*dose^2)]
14
15   The parameter betas are restricted to be positive
16
17   Dependent variable = Response
18   Independent variable = Dose
19   Total number of observations = 4
20   Total number of records with missing values = 0
21   Total number of parameters in model = 3
22   Total number of specified parameters = 0
23   Degree of polynomial = 2
24   Maximum number of iterations = 250
25   Relative Function Convergence has been set to: 1e-008
26   Parameter Convergence has been set to: 1e-008
27
28                     Default Initial Parameter Values
29                        Background =           0
30                           Beta(1) =           0
31                           Beta(2) = 3.83316e+014
```

Asymptotic Correlation Matrix of Parameter Estimates

(*** The model parameter(s) -Beta(1), have been estimated at a boundary point, or have been specified by the user, and do not appear in the correlation matrix)

	Background	Beta(2)
Background	1	-0.37
Beta(2)	-0.37	1

Parameter Estimates

Variable	Estimate	Std. Err.	95.0% Wald Confidence Interval Lower Conf. Limit	Upper Conf. Limit
Background	0.0480711	*	*	*
Beta(1)	0	*	*	*
Beta(2)	2.21049e-005	*	*	*

* - Indicates that this value is not calculated.

Analysis of Deviance Table

Model	Log(likelihood)	# Param's	Deviance	Test d.f.	P-value
Full model	-36.4175	4			
Fitted model	-36.5069	2	0.178792	2	0.9145
Reduced model	-79.9164	1	86.9979	3	<.0001

AIC: 77.0137

Goodness of Fit

Dose	Est._Prob.	Expected	Observed	Size	Scaled Residual
0.0000	0.0481	1.827	2	38	0.131
21.0000	0.0573	2.120	2	37	-0.085
103.0000	0.2471	9.388	9	38	-0.146
514.0000	0.9972	23.934	24	24	0.258

Chi^2 = 0.11 d.f. = 2 P-value = 0.9453

Benchmark Dose Computation

Specified effect = 0.1
Risk Type = Extra risk
Confidence level = 0.95
BMD = 69.0391
BMDL = 38.6809
BMDU = 92.891

Taken together, (38.6809, 92.891) is a 90% two-sided confidence interval for the BMD

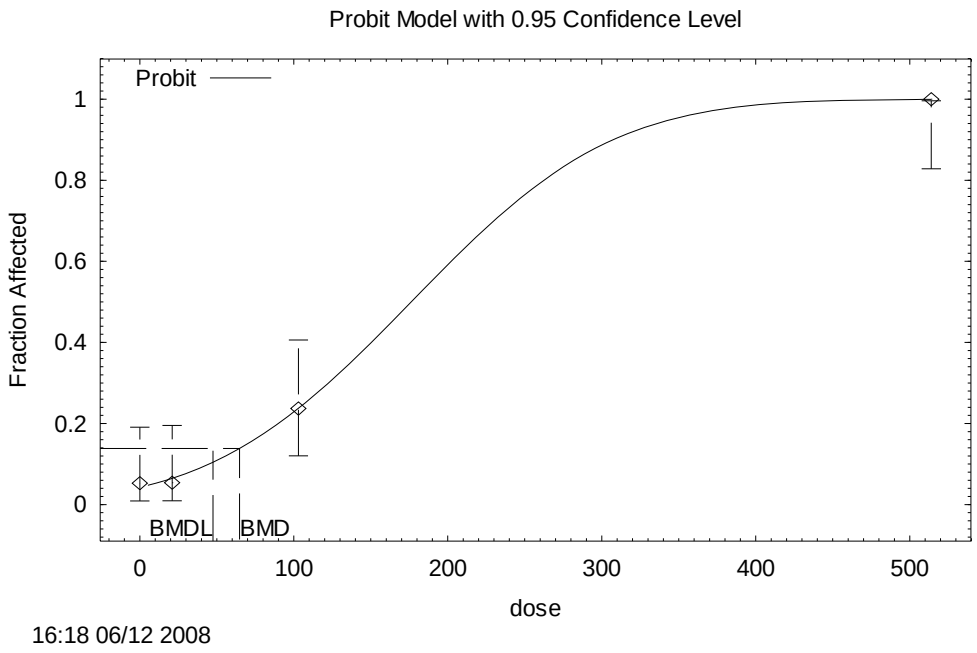

Source: JBRC (1998a).

Figure C-16. BMD probit model of liver hyperplasia incidence data for F344 female rats exposed to 1,4-dioxane in drinking water for 2 years to support the results in Table C-5.

```
=============================================================================
         Probit Model. (Version: 2.8;  Date: 02/20/2007)
         Input Data File: M:\DIOXANE DOSE-RESPONSE
MODELING\FEMALE_RATS_LIVER_HYPERPLASIA_JBRC_1998.(d)
         Gnuplot Plotting File:  M:\DIOXANE DOSE-RESPONSE
MODELING\FEMALE_RATS_LIVER_HYPERPLASIA_JBRC_1998.plt
                                                Thu Jun 12 16:17:59 2008
=============================================================================
 BMDS MODEL RUN
~~~~~~~~~~~~~~~~~~~~~~~~~~~~~~~~~~~~~~~~~~~~~~~~~~~~~~~~~~~~~~~~~~~~~~~~~~~~~
   The form of the probability function is:

   P[response] = CumNorm(Intercept+Slope*Dose),

   where CumNorm(.) is the cumulative normal distribution function

   Dependent variable = Response
   Independent variable = Dose
   Slope parameter is not restricted
   Total number of observations = 4
   Total number of records with missing values = 0
   Maximum number of iterations = 250
   Relative Function Convergence has been set to: 1e-008
   Parameter Convergence has been set to: 1e-008

                  Default Initial (and Specified) Parameter Values
                     background =            0   Specified
                      intercept =     -1.61994
                          slope =   0.00769493
```

Asymptotic Correlation Matrix of Parameter Estimates

(*** The model parameter(s) -background have been estimated at a boundary point, or have been specified by the user, and do not appear in the correlation matrix)

	intercept	slope
intercept	1	-0.76
slope	-0.76	1

Parameter Estimates

Variable	Estimate	Std. Err.	95.0% Wald Confidence Interval Lower Conf. Limit	Upper Conf. Limit
intercept	-1.71967	0.249073	-2.20785	-1.2315
slope	0.00975802	0.00303637	0.00380686	0.0157092

Analysis of Deviance Table

Model	Log(likelihood)	# Param's	Deviance	Test d.f.	P-value
Full model	-36.4175	4			
Fitted model	-36.5097	2	0.184385	2	0.9119
Reduced model	-79.9164	1	86.9979	3	<.0001

AIC: 77.0193

Goodness of Fit

Dose	Est._Prob.	Expected	Observed	Size	Scaled Residual
0.0000	0.0427	1.624	2	38	0.301
21.0000	0.0649	2.402	2	37	-0.268
103.0000	0.2374	9.022	9	38	-0.009
514.0000	0.9995	23.988	24	24	0.109

Chi^2 = 0.17 d.f. = 2 P-value = 0.9164

Benchmark Dose Computation

Specified effect = 0.1
Risk Type = Extra risk
Confidence level = 0.95
BMD = 64.8143
BMDL = 47.5376

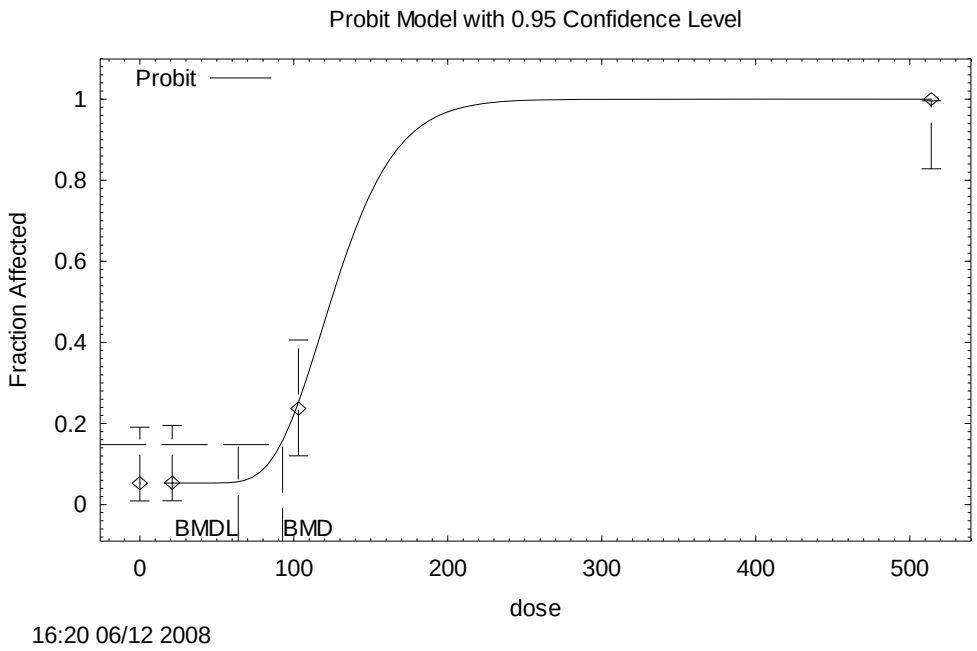

Source: JBRC (1998a).

Figure C-17. BMD log-probit model of liver hyperplasia incidence data for F344 female rats exposed to 1,4-dioxane in drinking water for 2 years to support the results in Table C-5.

```
1   ================================================================
2            Probit Model. (Version: 2.8;  Date: 02/20/2007)
3            Input Data File: M:\DIOXANE DOSE-RESPONSE
4   MODELING\FEMALE_RATS_LIVER_HYPERPLASIA_JBRC_1998.(d)
5            Gnuplot Plotting File:  M:\DIOXANE DOSE-RESPONSE
6   MODELING\FEMALE_RATS_LIVER_HYPERPLASIA_JBRC_1998.plt
7                                                 Thu Jun 12 16:20:01 2008
8   ================================================================
9    BMDS MODEL RUN
10  ~~~~~~~~~~~~~~~~~~~~~~~~~~~~~~~~~~~~~~~~~~~~~~~~~~~~~~~~~~~~~~~~~~~~
11
12     The form of the probability function is:
13
14     P[response] = Background + (1-Background) * CumNorm(Intercept+Slope*Log(Dose)),
15
16     where CumNorm(.) is the cumulative normal distribution function
17
18     Dependent variable = Response
19     Independent variable = Dose
20     Slope parameter is restricted as slope >= 1
21
22     Total number of observations = 4
23     Total number of records with missing values = 0
24     Maximum number of iterations = 250
25     Relative Function Convergence has been set to: 1e-008
26     Parameter Convergence has been set to: 1e-008
27
28     User has chosen the log transformed model
```

Default Initial (and Specified) Parameter Values
background = 0.0526316
intercept = -7.80926
slope = 1.55016

Asymptotic Correlation Matrix of Parameter Estimates

	background	intercept	slope
background	1	-0.0044	0.0043
intercept	-0.0044	1	-1
slope	0.0043	-1	1

Parameter Estimates

Variable	Estimate	Std. Err.	95.0% Wald Confidence Interval Lower Conf. Limit	Upper Conf. Limit
background	0.0533333	0.0259454	0.0024812	0.104185
intercept	-19.3386	742.282	-1474.19	1435.51
slope	3.98616	160.156	-309.915	317.887

Analysis of Deviance Table

Model	Log(likelihood)	# Param's	Deviance	Test d.f.	P-value
Full model	-36.4175	4			
Fitted model	-36.4178	3	0.000751916	1	0.9781
Reduced model	-79.9164	1	86.9979	3	<.0001

AIC: 78.8357

Goodness of Fit

Dose	Est._Prob.	Expected	Observed	Size	Scaled Residual
0.0000	0.0533	2.027	2	38	-0.019
21.0000	0.0533	1.973	2	37	0.020
103.0000	0.2368	9.000	9	38	0.000
514.0000	1.0000	24.000	24	24	0.001

Chi^2 = 0.00 d.f. = 1 P-value = 0.9781

Benchmark Dose Computation

Specified effect = 0.1
Risk Type = Extra risk
Confidence level = 0.95
BMD = 92.7521
BMDL = 63.951

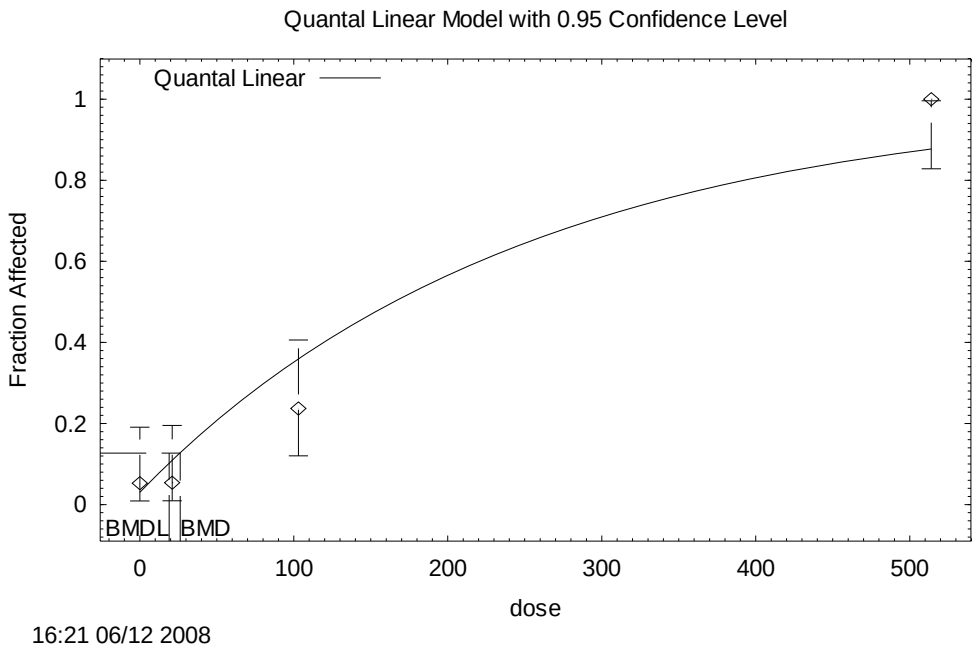

Source: JBRC (1998a).

Figure C-18. BMD quantal linear model of liver hyperplasia incidence data for F344 female rats exposed to 1,4-dioxane in drinking water for 2 years to support the results in Table C-5.

```
1   ================================================================
2            Quantal Linear Model using Weibull Model (Version: 2.7;  Date: 2/20/2007)
3            Input Data File: M:\DIOXANE DOSE-RESPONSE
4   MODELING\FEMALE_RATS_LIVER_HYPERPLASIA_JBRC_1998.(d)
5            Gnuplot Plotting File:  M:\DIOXANE DOSE-RESPONSE
6   MODELING\FEMALE_RATS_LIVER_HYPERPLASIA_JBRC_1998.plt
7                                                 Thu Jun 12 16:21:35 2008
8   ================================================================
9    BMDS MODEL RUN
10  ~~~~~~~~~~~~~~~~~~~~~~~~~~~~~~~~~~~~~~~~~~~~~~~~~~~~~~~~~~~~~~~~~~~~
11     The form of the probability function is:
12
13     P[response] = background + (1-background)*[1-EXP(-slope*dose)]
14
15     Dependent variable = Response
16     Independent variable = Dose
17     Total number of observations = 4
18     Total number of records with missing values = 0
19     Maximum number of iterations = 250
20     Relative Function Convergence has been set to: 1e-008
21     Parameter Convergence has been set to: 1e-008
22
23                    Default Initial (and Specified) Parameter Values
24                       Background =    0.0641026
25                            Slope =   0.00748205
26                            Power =            1   Specified
```

Asymptotic Correlation Matrix of Parameter Estimates

(*** The model parameter(s) -Power, have been estimated at a boundary point, or have been specified by the user, and do not appear in the correlation matrix)

	Background	Slope
Background	1	-0.16
Slope	-0.16	1

Parameter Estimates

Variable	Estimate	Std. Err.	95.0% Wald Confidence Interval Lower Conf. Limit	Upper Conf. Limit
Background	0.0302097	0.0203846	-0.00974332	0.0701627
Slope	0.00402312	0.000813792	0.00242812	0.00561813

Analysis of Deviance Table

Model	Log(likelihood)	# Param's	Deviance	Test d.f.	P-value
Full model	-36.4175	4			
Fitted model	-41.8322	2	10.8294	2	0.004451
Reduced model	-79.9164	1	86.9979	3	<.0001

AIC: 87.6644

Goodness of Fit

Dose	Est._Prob.	Expected	Observed	Size	Scaled Residual
0.0000	0.0302	1.148	2	38	0.808
21.0000	0.1088	4.025	2	37	-1.069
103.0000	0.3592	13.650	9	38	-1.572
514.0000	0.8774	21.057	24	24	1.832

Chi^2 = 7.62 d.f. = 2 P-value = 0.0221

Benchmark Dose Computation

Specified effect = 0.1
Risk Type = Extra risk
Confidence level = 0.95
BMD = 26.1887
BMDL = 19.0079

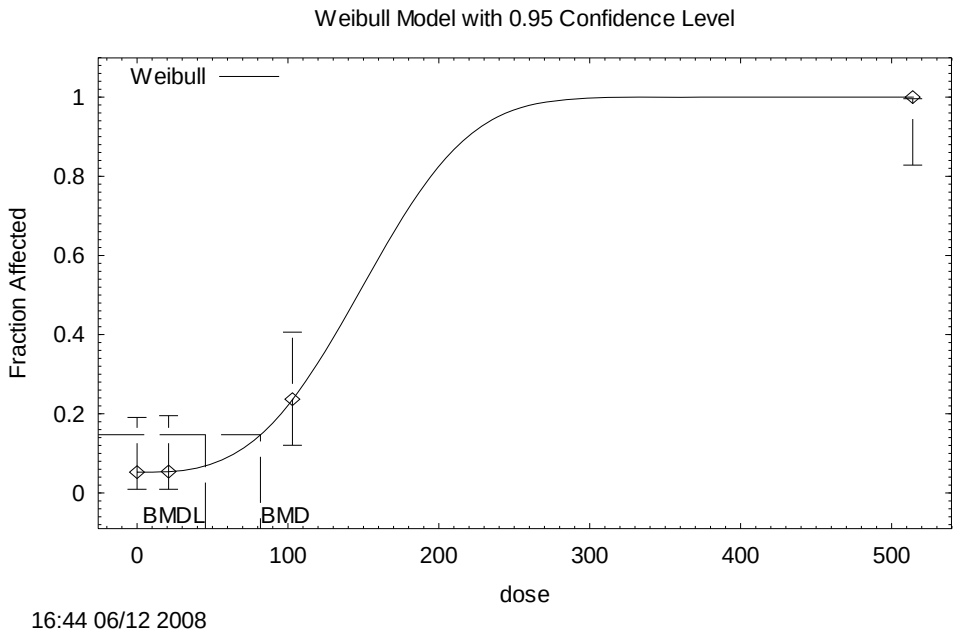

Source: JBRC (1998a).

Figure C-19. BMD Weibull model of liver hyperplasia incidence data for F344 female rats exposed to 1,4-dioxane in drinking water for 2 years to support the results in Table C-5.

```
1   ================================================================
2           Weibull Model using Weibull Model (Version: 2.7;  Date: 2/20/2007)
3           Input Data File: M:\DIOXANE DOSE-RESPONSE
4   MODELING\FEMALE_RATS_LIVER_HYPERPLASIA_JBRC_1998.(d)
5           Gnuplot Plotting File:  M:\DIOXANE DOSE-RESPONSE
6   MODELING\FEMALE_RATS_LIVER_HYPERPLASIA_JBRC_1998.plt
7                                                 Thu Jun 12 16:44:49 2008
8   ================================================================
9    BMDS MODEL RUN
10  ~~~~~~~~~~~~~~~~~~~~~~~~~~~~~~~~~~~~~~~~~~~~~~~~~~~~~~~~~~~~~~~~~~~~
11     The form of the probability function is:
12
13     P[response] = background + (1-background)*[1-EXP(-slope*dose^power)]
14
15     Dependent variable = Response
16     Independent variable = Dose
17     Power parameter is restricted as power >=1
18     Total number of observations = 4
19     Total number of records with missing values = 0
20     Maximum number of iterations = 250
21     Relative Function Convergence has been set to: 1e-008
22     Parameter Convergence has been set to: 1e-008
23
24                     Default Initial (and Specified) Parameter Values
25                        Background =    0.0641026
26                             Slope = 5.51356e-007
27                             Power =       2.5244
```

Asymptotic Correlation Matrix of Parameter Estimates

	Background	Slope	Power
Background	1	-0.42	0.42
Slope	-0.42	1	-1
Power	0.42	-1	1

Parameter Estimates

Variable	Estimate	Std. Err.	95.0% Wald Confidence Interval Lower Conf. Limit	Upper Conf. Limit
Background	0.052616	0.0286871	-0.00360976	0.108842
Slope	1.18324e-007	5.88858e-006	-1.14231e-005	1.16597e-005
Power	3.11095	10.7258	-17.9112	24.1331

Analysis of Deviance Table

Model	Log(likelihood)	# Param's	Deviance	Test d.f.	P-value
Full model	-36.4175	4			
Fitted model	-36.4175	3	3.92191e-007	1	0.9995
Reduced model	-79.9164	1	86.9979	3	<.0001

AIC: 78.8349

Goodness of Fit

Dose	Est._Prob.	Expected	Observed	Size	Scaled Residual
0.0000	0.0526	1.999	2	38	0.000
21.0000	0.0541	2.001	2	37	-0.000
103.0000	0.2368	9.000	9	38	0.000
514.0000	1.0000	24.000	24	24	0.000

Chi^2 = 0.00 d.f. = 1 P-value = 0.9995

Benchmark Dose Computation

Specified effect = 0.1
Risk Type = Extra risk
Confidence level = 0.95
BMD = 81.747
BMDL = 45.2828

APPENDIX D. DETAILS OF BMD ANALYSIS FOR ORAL CSF FOR 1,4-dioxane

The multistage (MS) model in the Benchmark Dose Software (BMDS) (version 1.3.2) was fit to the incidence data for hepatocellular carcinoma and/or adenoma for mice and rats, nasal cavity tumors, peritoneal mesothelioma, and mammary gland adenomas in rats and mice exposed to 1,4-dioxane in the drinking water. Doses associated with a benchmark response (BMR) of a 10% extra risk were calculated with the polynomial degree initially set at n–1 and lower. BMD_{10} and $BMDL_{10}$ values from the lowest degree polynomial models with an adequate fit (χ^2 $p \geq$ 0.1) were reported (U.S. EPA, 2000b). A summary of the model predictions for the JBRC (1998a) study are shown in Table D-1. The data and BMD modeling results are presented separately for each dataset as follows:

- Hepatic adenomas and carcinomas in female F344 rats (Tables D-2 and D-3; Figures D-1, D-2, and D-3)
- Hepatic adenomas and carcinomas in male F344 rats (Tables D-4 and D-5; Figures D-4 and D-5)
- Significant tumor incidence data at sites other than the liver (i.e., nasal cavity, mammary gland adenoma, and peritoneal mesothelioma) in male and female F344 rats (Table D-6)
  - Nasal cavity tumors in female F344 rats (Table D-7; Figures D-6 and D-7)
  - Nasal cavity tumors in male F344 rats (Table D-8)
  - Mammary gland adenomas in female F344 rats (Table D-9; Figures D-8 and D-9)
  - Peritoneal mesotheliomas in male F344 rats (Table D-10; Figures D-10)
- Hepatic adenomas and carcinomas in female BDF_1 mice (Tables D-11 and D-12; Figure D-11)
- Hepatic adenomas and carcinomas in male BDF_1 mice (Tables D-13 and D-14; Figure D-12)
- MS models for male and female F344 rats (Table D-15)
  - MS-Combo analysis for F344 rats (Tables D-16 and D-17)

Data and BMD modeling results from the additional chronic bioassays (NCI, 1978; Kociba et al., 1974) were evaluated in comparison to the JBRC (1998a) study. These results are presented as follows:

- Calculation of HEDs for additional studies reporting the incidence of liver and nasal cavity tumors in rats and mice exposed to 1,4-dioxane in the drinking water for 2 years (Table D-18)
- Summary of BMD modeling estimates and CSF values associated with liver and nasal tumor incidence data from chronic oral exposure to 1,4-dioxane in rats and mice (Table D-19)

- Incidence of hepatocellular carcinoma and nasal squamous cell carcinoma in male and female Sherman rats (combined) treated with 1,4-dioxane in the drinking water for 2 years (Table D-20)
  - Goodness-of-fit statistics, $BMD_{10\ HED}$ and $BMDL_{10\ HED}$ values from MS models fit to incidence data for hepatocellular carcinoma and nasal tumors in male and female Sherman rats (combined) exposed to 1,4-dioxane in drinking water for 2 years (Table D-21; Figures D-13 and D-14)
- Incidence of nasal cavity squamous cell carcinoma and hepatocellular adenoma in Osborne-Mendel rats exposed to 1,4-dioxane in the drinking water (Table D-22)
  - Goodness-of-fit statistics and $BMD_{10\ HED}$ and $BMDL_{10\ HED}$ values from MS models fit to incidence data for hepatocellular adenoma and nasal tumors in male and female Osborne-Mendel rats exposed to 1,4-dioxane in the drinking water for 2 years (Table D-23; Figures D-15, D-16, and D-17)
- Incidence of hepatocellular adenoma or carcinoma in $B6C3F_1$ mice exposed to 1,4-dioxane in drinking water (Table D-24)
  - Goodness-of-fit statistics and $BMD_{10\ HED}$ and $BMDL_{10\ HED}$ values from MS models fit to incidence data for hepatocellular adenoma or carcinoma in male and female $B6C3F_1$ mice exposed to 1,4-dioxane in the drinking water for 2 years (Table D-25)

D.1. GENERAL ISSUES AND APPROACHES TO BMDS MODELING

D.1.1. Combining Data on Adenomas and Carcinomas

The incidence of adenomas and the incidence of carcinomas within a dose group at a site or tissue in rodents are sometimes combined. This practice is based upon the hypothesis that adenomas are a severe endpoint by themselves and most would have developed into carcinomas if exposure at the same dose was continued (U.S. EPA, 2005a). The incidence at high doses of both tumors in rat and mouse liver is high in the key study (JBRC, 1998a). Consequently it is necessary to add the incidence of hepatic adenomas and carcinomas without double-counting them so as to calculate the combined incidence of either a hepatic carcinoma or a hepatic adenoma or both in rodents.

The variable N is used to denote the total number of animals tested in the dose group. The variable Y is used here to denote the number of rodents within a dose group that have characteristic X, and the notation Y(X) is used to identify the number with a specific characteristic X. Modeling was performed on the adenomas and carcinomas separately and the following combinations of tumor types:

- Y(adenomas) = number of animals with adenomas, whether or not carcinomas are present;
- Y(carcinomas) = number of animals with carcinomas, whether or not adenomas are also present;
- Y(adenomas and carcinomas) = number of animals with both adenomas and carcinomas present in the same animal;
- Y(either adenomas or carcinomas) = number of animals with adenomas, or carcinomas, or both = Y(adenomas) + Y(carcinomas) – Y(both adenomas and carcinomas);
- Y(neither adenomas nor carcinomas) = number of animals with no adenomas and no carcinomas = N - Y(either adenomas or carcinomas;
- Y(only carcinomas and not adenomas) = Y(carcinomas) - Y(adenomas and carcinomas);
- Y(only adenomas and not carcinomas) = Y(adenomas) - Y(adenomas and carcinomas).

D.1.2. Model Development Strategy

If the incidence data shown graphically appeared to have a monotone non-decreasing dose-response function for adenomas, carcinomas, or both, the following sequence of models were fit to the data: (1) A Weibull model was fit to evaluate the single power or exponent for which the MS models might best fit. The MS models with a single polynomial term might be considered as Weibull models whose exponents are integers (whole numbers); (2) MS models might be considered a simplified special case of the clonal expansion model or MVK model of carcinogenesis. Because of the limited number of dose groups (4 in the JBRC 1998a study, only 3 if the highest dose is dropped) and if a background parameter is included in the MS model, then in order to have enough degrees of freedom to calculate a goodness-of-fit *p*-value at most two polynomial terms can be included within the exponential part of the MS model. This can be done using the "Advanced" option in BMDS and specifying all but one or two polynomial coefficients to be equal to 0. Additional considerations occur when there is no response at any dose except for the highest dose, in which case BMDS will try to fit the highest-order polynomial possible. This occurs in a number of models for carcinomas only shown in the output. An additional ad hoc criterion was imposed to deal with this case: fit the lowest-order polynomial whose AIC and *p*-value are not measurably worse than those of the highest-order polynomial that can be fit, with the assumption that it seems more plausible that the formation of carcinomas does not require an extremely large number of distinct stages. In any case, by way of sensitivity analyses, results of fitting both acceptable models with a small number of stages and a

model with the current maximum number of stages (8) are reported. Higher-order MS monomial models with up to eighteen stages can be fit using the Weibull model with a user-specified power or exponent, which is the reason that analysis started with the Weibull model.

Other BMDS quantal models were fit in the following sequence: gamma, (log)-logistic, (log)-probit. In some cases where the power (slope in the log-transformed-dose models) is estimated as less than one in the unconstrained case, it may be worthwhile to also fit a model with the power or slope constrained to be greater than or equal to one, or more easily by setting the exponent or power equal to one.

Section D.2 reports results for fitting hepatic adenomas and carcinomas in female F344 rats, Section D.3 reports results for fitting hepatic adenomas and carcinomas in male F344 rats, Section D.4 reports results for fitting certain adenomas and carcinomas at other sites in female or male F344 rats, and Section D.5 reports results for fitting the combined incidence of hepatic adenomas or carcinomas and tumors at other sites in female and male rats using the best-fitting models for hepatic and other tumors shown in Sections D.2 through D.4.

The mouse data had a profoundly non-monotonic dose-response function and thus the combined incidence of hepatic adenomas and carcinomas retained some of this character due to the much larger incidence of adenomas at the lower doses. This is discussed in Sections D.6 and D.7.

Software for fitting combined tumor incidence in the liver or at one other site is currently available in a program ("MS-combo") whose structure and output are virtually identical to that of BMDS, but currently is limited to MS models at only two distinct sites. Results are presented in Section D.7 so as to evaluate the sensitivity of the BMDL estimates to using as an adverse effect the occurrence of tumors at one site, the other site, or tumors at both sites. In those cases where there were strong dose-response relationships for tumors at other sites with other models, analyses were restricted to the best-fitting MS models.

D.1.3. Model Selection Criteria

Multiple models were fit to each data set. The model selection criteria used in the BMDS Benchmark Dose Technical Guidance Document (U.S. EPA, 2000b) were applied as follows:

- p-value for goodness-of-fit > 0.10
- AIC smaller than other acceptable models
- χ^2 residuals as small as possible
- No systematic patterns of deviation of model from data

Additional criteria were applied to eliminate implausible dose-response functions:

- Monotonic dose-response functions, e.g. no negative coefficients of polynomials in MS models
- No infinitely steep dose-response functions near 0 (control dose), achieved by requiring the estimated parameters "power" in the Weibull and Gamma models and "slope" in the log-logistic and log-probit models to have values ≥1.
- When combining risk estimates for different sites using the MS-Combo program, the program automatically includes a linear term in the polynomial part of the MS model so there is currently no ideal way to fit an optimal MS model in MS-Combo consistent with the same model taken by itself if the optimal does not have a linear term.

Because no single set of criteria covers all contingencies, an extended list of preferred models are presented below.

D.1.4. Summary

The BMDS models recommended to calculate rodent BMD_{10} and $BMDL_{10}$ values and corresponding human $BMD_{10\ HED}$ and $BMDL_{10\ HED}$ values are summarized in Table D-1.

Table D-1. Recommended models for rodents exposed to 1,4-dioxane in drinking water (JBRC, 1998a)

Sex/ strain/ species	Endpoint	Model selection criterion	Model type	Model parameters	AIC	*p*-value	BMD_{10}	$BMDL_{10}$	$BMD_{10\ HED}$	$BMDL_{10\ HED}$
Female F344 Rat	Hepatic Tumors	Lowest AIC	MS	2	98.49	0.473	130	114	31.11	27.30
		Lowest AIC with linear term	MS in MS-Combo	1, 2	100.5	0.449	73.8	42.6	17.66	10.19
	Mammary Gland Tumors	Lowest AIC	MS	1	193.8	0.845	163	91.8	39.00	21.97
	Nasal Cavity Tumors	Lowest AIC	MS	8	45.97	1.000	483	452	115.6	108.2
		Low AIC lowest order non-linear	MS	2	46.68	0.947	409	413	97.87	98.83
Male F344 Rat	Hepatic Tumors	Lowest AIC	MS	1,8	113.5	0.574	88.0	37.6	23.88	10.20
		Low AIC, lowest order non-linear	MS in MS-Combo	1,2	114.0	0.368	73.8	42.6	20.03	11.56
	Peritoneal Mesothelioma	Lowest AIC	MS	2	139.0	0.760	145	124	39.35	33.65
		Low AIC	MS in MS-Combo	1, 2	140.5	0.809	112	51.0	30.39	13.84
	Nasal Cavity Tumors	Lowest AIC	MS	8	44.50	1.000	371	235	100.7	63.77
		Low AIC, lowest order that fits well	MS	2	43.12	0.956	340	257	92.27	69.74
Female BDF_1 Mouse	Hepatic Tumors	AIC-estim.	Log-logistic	0.854	153.3	0.635	2.94	0.0864	0.4413	0.01297
		Power =1		1	151.6	0.749	5.28	3.47	0.7926	0.5209
Male BDF_1 Mouse	Hepatic Tumors	AIC-estim.	Log-logistic	0.484	240.1	0.984	1.77	0+	0.2697	0
		Power =1		1	240.5	0.284	31.1	15.8	4.738	2.4071

D.2. FEMALE F344 RATS: HEPATIC CARCINOMAS AND ADENOMAS

The data for hepatic carcinomas and adenomas in female F344 rats (JBRC, 1998a) are shown in Table D-2.

Table D-2. Data for hepatic adenomas and carcinomas in female F344 rats (JBRC, 1998a)

Tumor type	Dose (mg/kg-day)			
	0	**21**	**103**	**514**
Adenomas	1	0	5	38
Carcinomas	1	0	0	10
Either adenomas or carcinomas	1	0	5	40
Neither adenomas nor carcinomas	49	50	45	10
Both adenomas and carcinomas	1	0	0	8
Total number per group	50	50	50	50

Source: JBRC (1998a).

Note that the incidence of rats with adenomas, with carcinomas, and with either adenomas or carcinomas or both (combined incidence) are monotone non-decreasing functions of dose except for 1 female rat in the control group. These data therefore appear to be appropriate for dose-response modeling using BMDS.

The results of the BMDS modeling for the entire suite of models are presented in Table D-3 in the order described in Section D.1.

Table D-3. Summary of BMDS dose-response modeling results for the combined incidence of hepatic adenomas and carcinomas in female F344 rats

Model	Power	Estim.	Std. Err.	AIC	*p*-value	BMD_{10} mg/kg-day	$BMDL_{10}$ mg/kg-day	Max χ^{2a}	Dose max[b] mg/kg-day	BMD_{10} HED	$BMDL_{10}$ HED
Weibull	Est.	1.837	0.320	100.262	0.2638	116	75.2	0.873	21	27.8	18.0
MS	1			110.201	0.0057	45.8	35.6	2.016	103	11.0	8.52
	2[c]			98.492	0.4734	130	114	0.861	21	31.1	27.3
	3			102.598	0.0555	207	186	2.007	103	49.5	44.5
	4			104.046	0.0302	261	243	2.141	103	62.5	58.2
	1&2[d]			100.463	0.2357	126	77.2	0.892	21	30.2	18.5
	2&3			100.157	0.2736	112	76.4	0.847	21	26.8	18.3
	2&4			100.196	0.2700	111	77.0	0.857	21	26.6	18.4
	2&5			100.136	0.2753	111	75.6	0.841	21	26.6	18.1
	2&6			100.135	0.2754	111	77.6	0.841	21	26.6	18.6
Gamma	Est.	2.484	0.648	100.020	0.2883	113	75.8	0.803	21	27.0	18.1
Log-Logistic	Est.	2.337	0.382	99.993	0.2905	111	76.6	0.796	21	26.6	18.3
Log-Probit	Est.	1.355	0.204	99.773	0.3130	108	76.4	0.721	21	25.8	18.3

[a]Maximum absolute χ^2 residual deviation between observed and predicted count. Values much larger than 1 are undesirable.
[b]Dose at which the maximum χ^2 residual deviation occurred.
[c]Best-fitting model.
[d]Utilized in combined analyses with tumors at other sites for consistency with male F344 rat model and because MS-Combo software requires a linear term at this time; differs from optimal by < 2 AIC units.

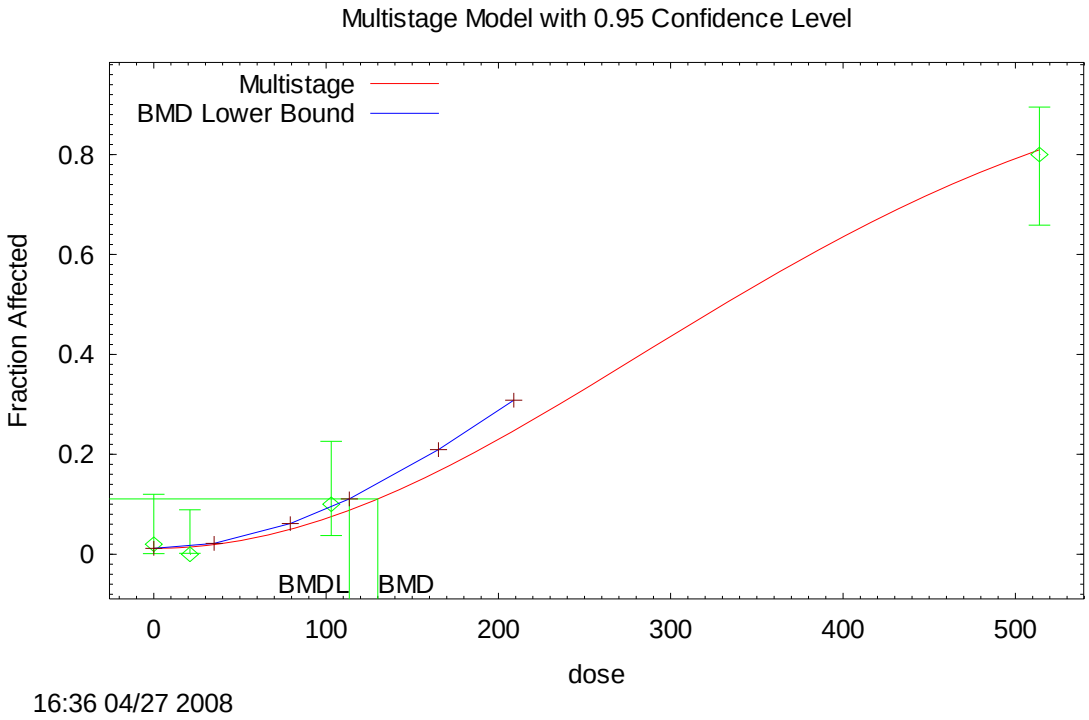

Source: JBRC (1998a).

Figure D-1. Multistage BMD model (2 degree) for the combined incidence of hepatic adenomas and carcinomas in female F344 rats.

```
1   ================================================================
2            Multistage Model. (Version: 2.5;  Date: 10/17/2005)
3            Input Data File: U:\DIOXANE\JBRCLIVER.(d)
4            Gnuplot Plotting File:  U:\DIOXANE\JBRCLIVER.plt
5                                                  Sun Apr 27 16:36:47 2008
6   ================================================================
7    JBRC FEMALE carcino+adenomas multi deg 2 Table D-3
8   ~~~~~~~~~~~~~~~~~~~~~~~~~~~~~~~~~~~~~~~~~~~~~~~~~~~~~~~~~~~~~~~~~~~~
9   Observation # < parameter # for Multistage model.
10     The form of the probability function is:
11
12     P[response] = background + (1-background)*[1-EXP(-beta1*dose^1-beta2*dose^2-
13         beta3*dose^3-beta4*dose^4-beta5*dose^5-beta6*dose^6-beta7*dose^7-beta8*dose^8)]
14
15     The parameter betas are not restricted
16
17     Dependent variable = EITHERRATF
18     Independent variable = DOSERATF
19
20     User specifies the following parameters:
21           Beta(1) =          0
22           Beta(3) =          0
23           Beta(4) =          0
24           Beta(5) =          0
25           Beta(6) =          0
26           Beta(7) =          0
27           Beta(8) =          0
28
29    Total number of observations = 4
30    Total number of records with missing values = 0
31    Total number of parameters in model = 9
32    Total number of specified parameters = 7
```

```
 Degree of polynomial = 8
 Maximum number of iterations = 250
 Relative Function Convergence has been set to: 1e-008
 Parameter Convergence has been set to: 1e-008

                 User Inputs Initial Parameter Values
                     Background =         0.08
                        Beta(1) =            1   Specified
                        Beta(2) =            0
                        Beta(3) =            1   Specified
                        Beta(4) =            1   Specified
                        Beta(5) =            1   Specified
                        Beta(6) =            1   Specified
                        Beta(7) =            1   Specified
                        Beta(8) =            1   Specified

           Asymptotic Correlation Matrix of Parameter Estimates

(*** The model parameter(s) -Beta(1), -Beta(3), -Beta(4), -Beta(5), -Beta(6),
-Beta(7), -Beta(8) have been estimated at a boundary point, or have been specified by
the user, and do not appear in the correlation matrix)

             Background      Beta(2)
Background            1        -0.31
   Beta(2)        -0.31            1

                                Parameter Estimates

                                                        95.0% Wald Confidence Interval
       Variable      Estimate      Std. Err.     Lower Conf. Limit   Upper Conf. Limit
     Background      0.0119049     0.0839009       -0.152538         0.176348
        Beta(2)      6.2293e-006   1.29099e-006    3.699e-006        8.75959e-006

                           Analysis of Deviance Table

        Model      Log(likelihood)  # Param's Deviance  Test d.f.   P-value
     Full model        -46.1762         4
    Fitted model       -47.2461         2       2.13973      2          0.3431
   Reduced model       -107.855         1       123.358      3         <.0001

           AIC:         98.4922

                                  Goodness  of  Fit
                                                                      Scaled
     Dose     Est._Prob.    Expected    Observed     Size       Residual
   ---------------------------------------------------------------------
    0.0000     0.0119         0.595         1          50         0.528
   21.0000     0.0146         0.731         0          50        -0.861
  103.0000     0.0751         3.755         5          50         0.668
  514.0000     0.8094        40.471        40          50        -0.170

 Chi^2 = 1.50      d.f. = 2        P-value = 0.4734


   Benchmark Dose Computation

Specified effect =           0.1
Risk Type        =      Extra risk
Confidence level =          0.95
             BMD =       130.053
            BMDL =       113.537
```

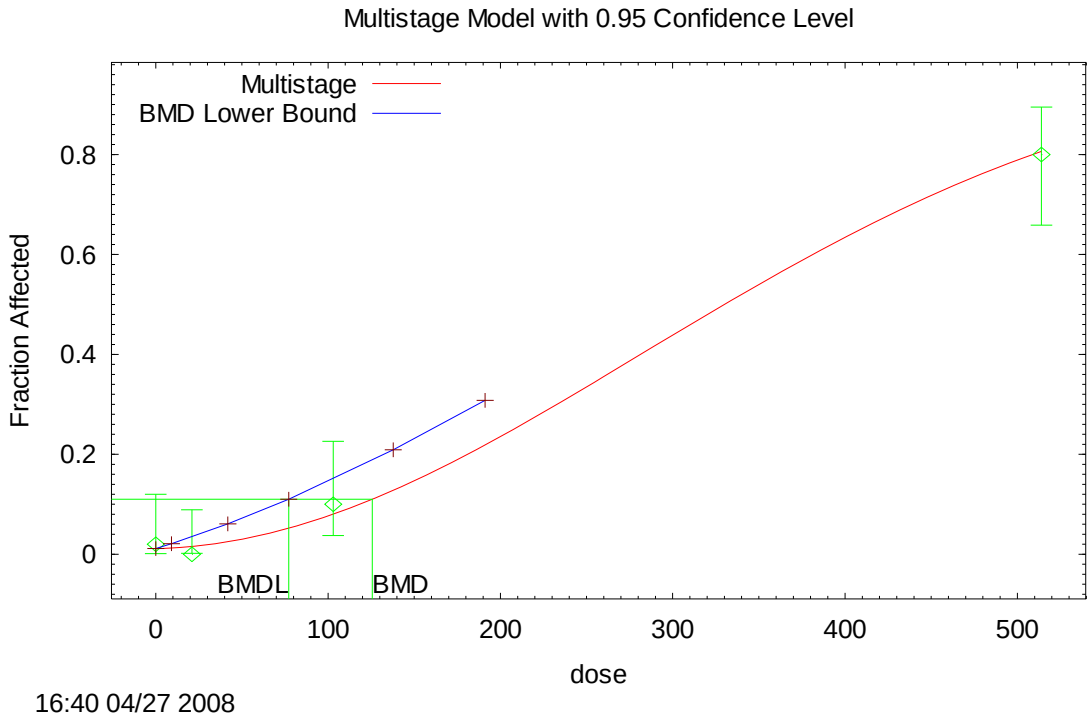

Source: JBRC (1998a).

Figure D-2. Multistage BMD model (1 & 2 degree) for the combined incidence of hepatic adenomas and carcinomas in female F344 rats.

```
1   ========================================================================
2            Multistage Model. (Version: 2.5;  Date: 10/17/2005)
3            Input Data File: U:\DIOXANE\JBRCLIVER.(d)
4            Gnuplot Plotting File:  U:\DIOXANE\JBRCLIVER.plt
5                                                  Sun Apr 27 16:40:47 2008
6   ========================================================================
7    JBRC FEMALE carcino+adenomas multi deg 1&2 Table D-3
8   ~~~~~~~~~~~~~~~~~~~~~~~~~~~~~~~~~~~~~~~~~~~~~~~~~~~~~~~~~~~~~~~~~~~~~~~~
9
10  Observation # < parameter # for Multistage model.
11     The form of the probability function is:
12
13     P[response] = background + (1-background)*[1-EXP(
14                  -beta1*dose^1-beta2*dose^2-beta3*dose^3-beta4*dose^4-beta5*dose^5-
15                  beta6*dose^6-beta7*dose^7-beta8*dose^8)]
16
17     The parameter betas are not restricted
18
19     Dependent variable = EITHERRATF
20     Independent variable = DOSERATF
21
22     User specifies the following parameters:
23           Beta(3) =          0
24           Beta(4) =          0
25           Beta(5) =          0
26           Beta(6) =          0
27           Beta(7) =          0
28           Beta(8) =          0
29
30    Total number of observations = 4
31    Total number of records with missing values = 0
32    Total number of parameters in model = 9
```

```
 Total number of specified parameters = 6
 Degree of polynomial = 8

 Maximum number of iterations = 250
 Relative Function Convergence has been set to: 1e-008
 Parameter Convergence has been set to: 1e-008

                 User Inputs Initial Parameter Values
                     Background =         0.08
                        Beta(1) =            0
                        Beta(2) =            0
                        Beta(3) =            1   Specified
                        Beta(4) =            1   Specified
                        Beta(5) =            1   Specified
                        Beta(6) =            1   Specified
                        Beta(7) =            1   Specified
                        Beta(8) =            1   Specified

           Asymptotic Correlation Matrix of Parameter Estimates

(*** The model parameter(s)  -Beta(3), -Beta(4), -Beta(5), -Beta(6), -Beta(7),
-Beta(8) have been estimated at a boundary point, or have been specified by the user,
and do not appear in the correlation matrix)

             Background      Beta(1)      Beta(2)
Background            1        -0.61          0.5
   Beta(1)        -0.61            1        -0.95
   Beta(2)          0.5        -0.95            1

                                Parameter Estimates
                                                        95.0% Wald Confidence Interval
        Variable     Estimate       Std. Err.     Lower Conf. Limit   Upper Conf. Limit
      Background     0.0113405      0.106071        -0.196554           0.219235
         Beta(1)     8.31025e-005   0.00204065      -0.0039165          0.00408271
         Beta(2)      6.0135e-006   4.0241e-006     -1.87358e-006       1.39006e-005

                           Analysis of Deviance Table

        Model      Log(likelihood)  # Param's Deviance  Test d.f.   P-value
      Full model        -46.1762         4
     Fitted model       -47.2315         3       2.11046      1          0.1463
   Reduced model        -107.855         1       123.358      3         <.0001

           AIC:         100.463

                                  Goodness  of  Fit
                                                                    Scaled
      Dose     Est._Prob.    Expected    Observed     Size        Residual
   ---------------------------------------------------------------------
     0.0000     0.0113         0.567         1          50         0.578
    21.0000     0.0157         0.784         0          50        -0.892
   103.0000     0.0803         4.017         5          50         0.511
   514.0000     0.8066        40.329        40          50        -0.118

 Chi^2 = 1.41      d.f. = 1        P-value = 0.2357


   Benchmark Dose Computation
Specified effect =           0.1
Risk Type        =      Extra risk
Confidence level =          0.95
             BMD =       125.636
            BMDL =       77.1768
```

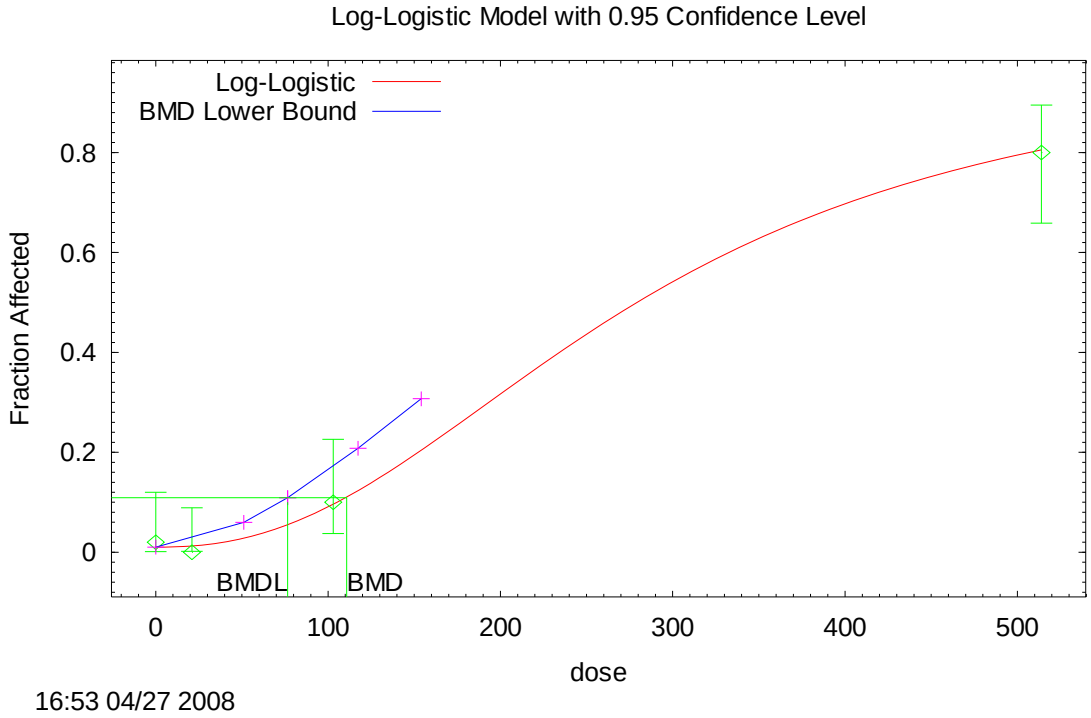

Source: JBRC (1998a).

Figure D-3. Log-logistic BMD model for the combined incidence of hepatic adenomas and carcinomas in female F344 rats.

```
==========================================================================
         Logistic Model. (Version: 2.5; Date: 09/24/2005)
         Input Data File: U:\DIOXANE\JBRCLIVER.(d)
         Gnuplot Plotting File:  U:\DIOXANE\JBRCLIVER.plt
                                                Sun Apr 27 16:53:34 2008
==========================================================================
 JBRC FEMALE carcino+adenomas log-logistic Table D-3
~~~~~~~~~~~~~~~~~~~~~~~~~~~~~~~~~~~~~~~~~~~~~~~~~~~~~~~~~~~~~~~~~~~~~~~~~~
   The form of the probability function is:

   P[response] = background+(1-background)/[1+EXP(-intercept-slope*Log(dose))]

   Dependent variable = EITHERRATF
   Independent variable = DOSERATF
   Slope parameter is not restricted

   Total number of observations = 4
   Total number of records with missing values = 0
   Maximum number of iterations = 250
   Relative Function Convergence has been set to: 1e-008
   Parameter Convergence has been set to: 1e-008
   User has chosen the log transformed model

                  Default Initial Parameter Values
                     background =         0.02
                      intercept =     -10.5681
                          slope =      1.86975



            Asymptotic Correlation Matrix of Parameter Estimates
```

	background	intercept	slope
background	1	-0.18	0.16
intercept	-0.18	1	-0.99
slope	0.16	-0.99	1

Parameter Estimates

Variable	Estimate	Std. Err.	95.0% Wald Confidence Interval Lower Conf. Limit	Upper Conf. Limit
background	0.0102565	0.01019	-0.00971556	0.0302286
intercept	-13.1982	2.21197	-17.5335	-8.86278
slope	2.33662	0.381529	1.58884	3.08441

Analysis of Deviance Table

Model	Log(likelihood)	# Param's	Deviance	Test d.f.	P-value
Full model	-46.1762	4			
Fitted model	-46.9966	3	1.64065	1	0.2002
Reduced model	-107.855	1	123.358	3	<.0001

AIC: 99.9931

Goodness of Fit

Dose	Est._Prob.	Expected	Observed	Size	Scaled Residual
0.0000	0.0103	0.513	1	50	0.684
21.0000	0.0125	0.625	0	50	-0.796
103.0000	0.0950	4.749	5	50	0.121
514.0000	0.8023	40.113	40	50	-0.040

Chi^2 = 1.12 d.f. = 1 P-value = 0.2905

Benchmark Dose Computation

Specified effect = 0.1
Risk Type = Extra risk
Confidence level = 0.95
BMD = 110.835
BMDL = 76.5788

D.3. MALE F344 RATS: HEPATIC CARCINOMAS AND ADENOMAS

The data for hepatic adenomas and carcinomas in male F344 rats (JBRC, 1998a) are shown in Table D-4.

Table D-4. Data for hepatic adenomas and carcinomas in male F344 rats (JBRC, 1998a)

Tumor type	Dose (mg/kg-day)			
	0	16	81	398
Adenomas	0	2	4	24
Carcinomas	0	0	0	14
Either adenomas or carcinomas	0	2	4	33
Neither adenomas nor carcinomas	50	48	45	17
Both adenomas and carcinomas	0	0	0	5
Total number per group	50	50	49	50

Note that the incidence of rats with hepatic adenomas, carcinomas, and with either adenomas or carcinomas or both (combined incidence) are monotone non-decreasing functions of dose. These data therefore appear to be appropriate for dose-response modeling using BMDS.

The results of the BMDS modeling for the entire suite of models tested using the data for hepatic adenomas and carcinomas for male F344 rats are presented in Table D-5 in the order described in Section D.1.

Table D-5. Summary of BMDS dose-response modeling results for the combined incidence of adenomas and carcinomas in livers of male F344 rats

Model	Power	Estim.	Std. Err.	AIC	*p*-value	BMD_{10} mg/kg-day	$BMDL_{10}$ mg/kg-day	Max χ^{2a}	Dose max[b] mg/kg-day	BMD_{10} HED	$BMDL_{10}$ HED
Weibull	Est.	1.427	0.746	116.801	0.1424	79.6	39.0	1.178	16	21.60	10.58
MS	1			114.636	0.3223	45.7	35.2	1.650	81	12.40	9.55
	2			115.532	0.3678	124	108			33.65	29.31
	1&2 [d]			113.973	0.4485	73.8	42.6	1.079	16	20.03	11.56
	1&3			113.623	0.5448	79.0	43.8	0.990	16	21.44	11.89
	1&4			113.553	0.5678	80.2	44.0	0.965	16	21.76	11.94
	1&8 [c]			113.535	0.5738	80.6	44.0	0.958	16	21.87	11.94
Gamma	Est.	1.831	1.200	117.075	0.1447	88.0	37.6	1.132	16	23.88	10.20
Log-Logistic	Est.	1.956	0.552	117.134	0.1555	94.2	42.6	1.079	16	25.56	11.56
Log-Probit	Est.	1.200	0.251	117.394	0.1530	98.6	51.8	1.021	16	26.76	14.06

[a]Maximum absolute χ^2 residual deviation between observed and predicted count. Values much larger than 1 are undesirable.
[b]Dose at which the maximum χ^2 residual deviation occurred.
[c]Best-fitting model.
[d]This model fits the data nearly as well as the optimal model. It is simpler and is at least as plausible, thus will be carried forward into combined analyses with tumors at another site as a sensitivity analysis.

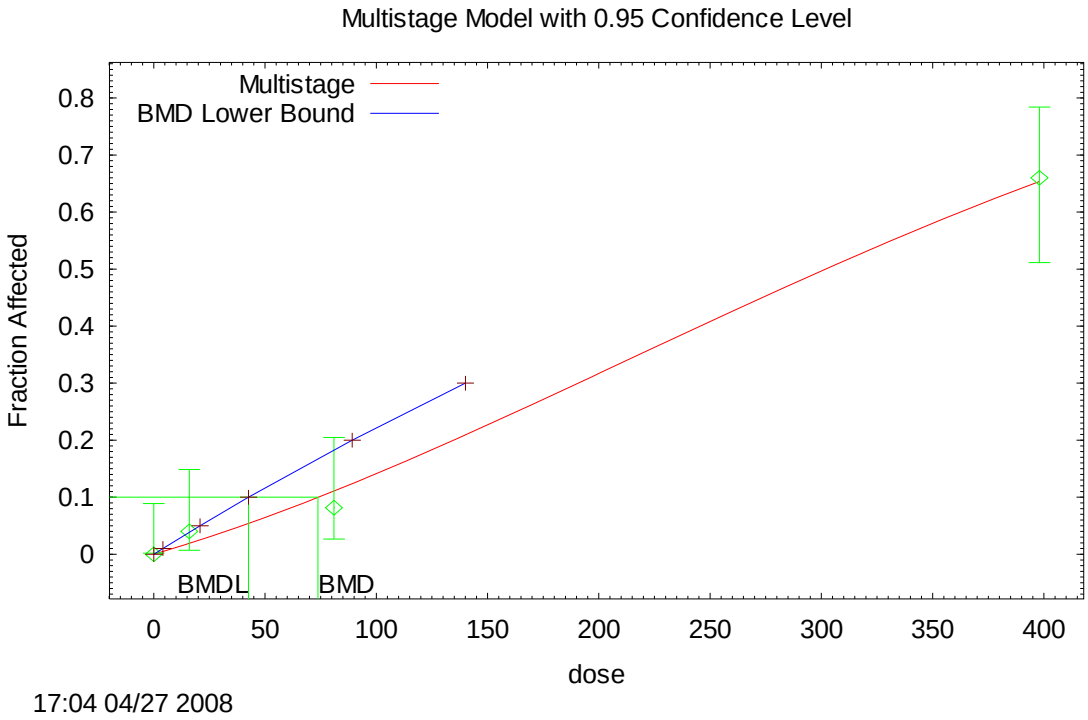

Source: JBRC (1998a).

Figure D-4. Multistage BMD model (1 & 2 degree) for the combined incidence of hepatic adenomas and carcinomas in male F344 rats.

```
=================================================================
         Multistage Model. (Version: 2.5;  Date: 10/17/2005)
         Input Data File: U:\DIOXANE\JBRCLIVER.(d)
         Gnuplot Plotting File:  U:\DIOXANE\JBRCLIVER.plt
                                              Sun Apr 27 17:04:35 2008
=================================================================
 JBRC MALE carcino+adenomas multi deg 1&2 Table D-5
~~~~~~~~~~~~~~~~~~~~~~~~~~~~~~~~~~~~~~~~~~~~~~~~~~~~~~~~~~~~~~~~~~~
Observation # < parameter # for Multistage model.
   The form of the probability function is:

   P[response] = background + (1-background)*[1-EXP(-beta1*dose^1-beta2*dose^2-
       beta3*dose^3-beta4*dose^4-beta5*dose^5-beta6*dose^6-beta7*dose^7-beta8*dose^8)]

   The parameter betas are not restricted

   Dependent variable = EITHERRATM
   Independent variable = DOSERATM

   User specifies the following parameters:
         Beta(3) =          0
         Beta(4) =          0
         Beta(5) =          0
         Beta(6) =          0
         Beta(7) =          0
         Beta(8) =          0

 Total number of observations = 4
 Total number of records with missing values = 0
 Total number of parameters in model = 9
 Total number of specified parameters = 6
 Degree of polynomial = 8
```

```
 Maximum number of iterations = 250
 Relative Function Convergence has been set to: 1e-008
 Parameter Convergence has been set to: 1e-008

                 User Inputs Initial Parameter Values
                     Background =         0.08
                        Beta(1) =            0
                        Beta(2) =            0
                        Beta(3) =            1   Specified
                        Beta(4) =            1   Specified
                        Beta(5) =            1   Specified
                        Beta(6) =            1   Specified
                        Beta(7) =            1   Specified
                        Beta(8) =            1   Specified

           Asymptotic Correlation Matrix of Parameter Estimates

(*** The model parameter(s) -Background, -Beta(3), -Beta(4), -Beta(5), -Beta(6),
-Beta(7), -Beta(8) have been estimated at a boundary point, or have been specified by
the user, and do not appear in the correlation matrix)

                Beta(1)      Beta(2)
   Beta(1)            1        -0.97
   Beta(2)        -0.97            1

                                Parameter Estimates

                                                        95.0% Wald Confidence Interval
       Variable     Estimate      Std. Err.     Lower Conf. Limit   Upper Conf. Limit
     Background            0             NA
        Beta(1)    0.00114469    0.00252448     -0.0038032          0.00609257
        Beta(2)    3.82589e-006  6.59789e-006   -9.10573e-006       1.67575e-005

NA - Indicates that this parameter has hit a bound implied by some inequality
constraint and thus has no standard error.

                        Analysis of Deviance Table

        Model      Log(likelihood)  # Param's Deviance  Test d.f.   P-value
     Full model        -54.3032         4
   Fitted model        -54.9865         2       1.36669      2          0.5049
  Reduced model        -98.4609         1       88.3155      3         <.0001

           AIC:         113.973

                                Goodness  of  Fit
                                                                    Scaled
     Dose     Est._Prob.    Expected    Observed     Size       Residual
  ---------------------------------------------------------------------
     0.0000     0.0000         0.000         0          50        0.000
    16.0000     0.0191         0.955         2          50        1.079
    81.0000     0.1111         5.446         4          49       -0.657
   398.0000     0.6541        32.705        33          50        0.088

 Chi^2 = 1.60      d.f. = 2        P-value = 0.4485

   Benchmark Dose Computation
Specified effect =           0.1
Risk Type        =      Extra risk
Confidence level =          0.95
             BMD =       73.8264
            BMDL =       42.6043
```

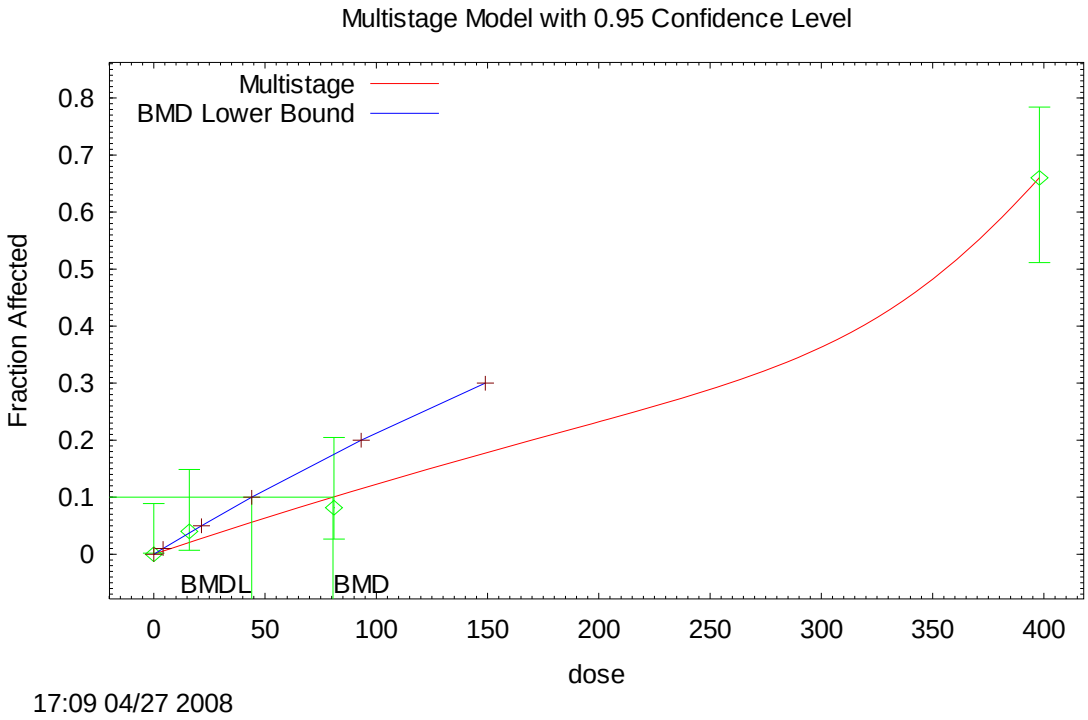

Source: JBRC (1998a).

Figure D-5. Multistage BMD model (1 & 8 degree) for the combined incidence of hepatic adenomas and carcinomas in male F344 rats.

```
=================================================================
         Multistage Model. (Version: 2.5;  Date: 10/17/2005)
         Input Data File: U:\DIOXANE\JBRCLIVER.(d)
         Gnuplot Plotting File:  U:\DIOXANE\JBRCLIVER.plt
                                              Sun Apr 27 17:09:20 2008
=================================================================
 JBRC MALE carcino+adenomas multi deg 1&8 Table D-5
~~~~~~~~~~~~~~~~~~~~~~~~~~~~~~~~~~~~~~~~~~~~~~~~~~~~~~~~~~~~~~~~~~~
Observation # < parameter # for Multistage model.
   The form of the probability function is:

   P[response] = background + (1-background)*[1-EXP(-beta1*dose^1-beta2*dose^2-
       beta3*dose^3-beta4*dose^4-beta5*dose^5-beta6*dose^6-beta7*dose^7-beta8*dose^8)]

   The parameter betas are not restricted

   Dependent variable = EITHERRATM
   Independent variable = DOSERATM

   User specifies the following parameters:
         Beta(2) =          0
         Beta(3) =          0
         Beta(4) =          0
         Beta(5) =          0
         Beta(6) =          0
         Beta(7) =          0

 Total number of observations = 4
 Total number of records with missing values = 0
 Total number of parameters in model = 9
 Total number of specified parameters = 6
 Degree of polynomial = 8
```

```
 Maximum number of iterations = 250
 Relative Function Convergence has been set to: 1e-008
 Parameter Convergence has been set to: 1e-008

                 User Inputs Initial Parameter Values
                     Background =         0.08
                        Beta(1) =            0
                        Beta(2) =            1   Specified
                        Beta(3) =            1   Specified
                        Beta(4) =            1   Specified
                        Beta(5) =            1   Specified
                        Beta(6) =            1   Specified
                        Beta(7) =            1   Specified
                        Beta(8) =            0

           Asymptotic Correlation Matrix of Parameter Estimates

(*** The model parameter(s) -Background, -Beta(2), -Beta(3), -Beta(4), -Beta(5),
-Beta(6), -Beta(7) have been estimated at a boundary point, or have been specified by
the user, and do not appear in the correlation matrix )

                Beta(1)      Beta(8)
   Beta(1)            1        -0.96
   Beta(8)        -0.96            1

                                Parameter Estimates

                                                        95.0% Wald Confidence Interval
       Variable     Estimate      Std. Err.     Lower Conf. Limit   Upper Conf. Limit
     Background            0           NA
        Beta(1)     0.00130773    0.00196467         -0.00254296       0.00515841
        Beta(8)     8.86808e-022  1.30033e-021       -1.6618e-021      3.43541e-021

NA - Indicates that this parameter has hit a bound implied by some inequality
constraint and thus has no standard error.

                        Analysis of Deviance Table

        Model      Log(likelihood)  # Param's Deviance  Test d.f.   P-value
     Full model        -54.3032         4
   Fitted model        -54.7675         2      0.928571      2          0.6286
  Reduced model        -98.4609         1       88.3155      3         <.0001

           AIC:         113.535

                                Goodness  of  Fit
                                                                    Scaled
     Dose     Est._Prob.    Expected    Observed     Size       Residual
  ---------------------------------------------------------------------
    0.0000     0.0000         0.000         0          50        0.000
   16.0000     0.0207         1.035         2          50        0.958
   81.0000     0.1005         4.925         4          49       -0.439
  398.0000     0.6600        33.000        33          50        0.000

 Chi^2 = 1.11      d.f. = 2        P-value = 0.5738

   Benchmark Dose Computation
Specified effect =           0.1
Risk Type        =      Extra risk
Confidence level =          0.95
             BMD =       80.5665
            BMDL =       44.0259
```

D.4. F344 RATS: TUMORS AT OTHER SITES

The data for tumors at sites other than the liver in male and female F344 rats (JBRC, 1998a) are shown in Table D-6. Note that the incidence of rats with these endpoints are monotone non-decreasing functions of dose whose estimated incidence at the highest dose is greater than the BMR of 10% so that the BMD and BMDL are expected to be well within the range of the observed data. These data therefore appear to be appropriate for dose-response modeling using BMDS.

Table D-6. Data for significant tumors at other sites in male and female F344 rats

Tumor site and type	Dose (mg/kg-day)							
	Female				Male			
	0	21	103	514	0	16	81	398
Nasal cavity carcinomas	0	0	0	8	0	0	0	7
Peritoneal mesothelioma	Not available				2	2	5	28
Mammary gland adenoma	6	7	10	16	No relation for BMR 0.10			
Total Number per Group	50	50	50	50	50	50	49	50

Source: JBRC (1998a).

The results of the BMDS modeling for the entire suite of models are presented in Tables D-7 through Table D-10 for tumors in the nasal cavity, mammary gland, and peritoneal cavity in the order described in Section D.1.

Table D-7. Summary of BMDS dose-response modeling results for the incidence of nasal cavity tumors in female F344 rats [e]

Model	Power	Estim	Std Err	AIC	*p*-value	BMD_{10} mg/kg-day	$BMDL_{10}$ mg/kg-day	Max χ^2 [a]	Dose max [b] mg/kg-day	BMD_{10} HED	$BMDL_{10}$ HED
Weibull	Est.	10.98	NE	47.967	1.0000	491	312	0.000	NA	117.5	74.66
MS	1			49.700	0.5488	392	231	1.184	103	93.80	55.28
	2[d]			46.680	0.9472	409	313	0.580	103	97.87	74.90
	3			46.108	0.9951	436	365	0.264	103	104.3	87.34
	4			45.995	0.9996	453	397	0.118	103	108.4	95.00
	8[c]			45.967	1.0000	483	452	0.005	103	115.6	108.2
Gamma	Est.	14.74	NE	47.967	1.0000	473	306	0.001	103	113.2	73.22
Log-Logistic	Est.	10.92	NE	47.967	1.0000	489	305	0.000	NA	117.0	72.98
Log-Probit	Est.	2.942	154	47.967	1.0000	466	283	0.001	103	111.5	67.72

[a]Maximum absolute χ^2 residual deviation between observed and predicted count. Values much larger than 1 are undesirable.
[b]Dose at which the maximum χ^2 residual deviation occurred.
[c]Best-fitting model.
[d]This model fits the data nearly as well as the optimal model. It is simpler and is at least as plausible, thus will be carried forward into combined analyses with liver tumors as a sensitivity analysis.
[e]Nasal cavity tumors in female F344 rats include squamous cell carcinoma and esthesioneuro-epithelioma.

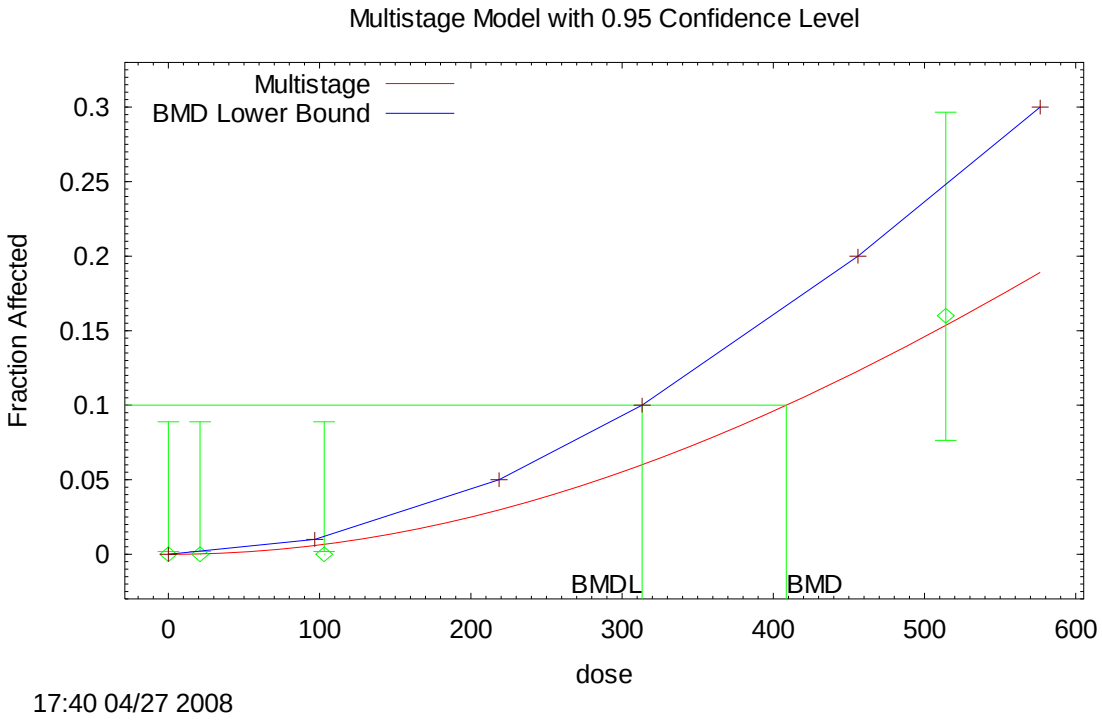

Source: JBRC (1998a).

Figure D-6. Multistage BMD model (2 degree) for the nasal cavity tumors in female F344 rats.

```
=============================================================================
         Multistage Model. (Version: 2.5;  Date: 10/17/2005)
         Input Data File: U:\DIOXANE\JBRCLIVER.(d)
         Gnuplot Plotting File:  U:\DIOXANE\JBRCLIVER.plt
                                                Sun Apr 27 17:40:07 2008
=============================================================================
 JBRC FEMALE RAT Nasal Cavity Tumors multistage deg 2 Table D-7
~~~~~~~~~~~~~~~~~~~~~~~~~~~~~~~~~~~~~~~~~~~~~~~~~~~~~~~~~~~~~~~~~~~~~~~~~~~~
Observation # < parameter # for Multistage model.
   The form of the probability function is:

   P[response] = background + (1-background)*[1-EXP(-beta1*dose^1-beta2*dose^2-
       beta3*dose^3-beta4*dose^4-beta5*dose^5-beta6*dose^6-beta7*dose^7-beta8*dose^8)]

   The parameter betas are restricted to be positive

   Dependent variable = NASALCAVITYF
   Independent variable = DOSERATF

   User specifies the following parameters:
         Beta(1) =          0
         Beta(3) =          0
         Beta(4) =          0
         Beta(5) =          0
         Beta(6) =          0
         Beta(7) =          0
         Beta(8) =          0

 Total number of observations = 4
 Total number of records with missing values = 0
 Total number of parameters in model = 9
 Total number of specified parameters = 7
```

```
 Degree of polynomial = 8
 Maximum number of iterations = 250
 Relative Function Convergence has been set to: 1e-008
 Parameter Convergence has been set to: 1e-008

                  Default Initial Parameter Values
                     Background =            0
                        Beta(1) =            0   Specified
                        Beta(2) =            0
                        Beta(3) =            0   Specified
                        Beta(4) =            0   Specified
                        Beta(5) =            0   Specified
                        Beta(6) = 9.47989e-018   Specified
                        Beta(7) =            0   Specified
                        Beta(8) =            0   Specified

           Asymptotic Correlation Matrix of Parameter Estimates

(*** The model parameter(s) -Background, -Beta(1), -Beta(3), -Beta(4), -Beta(5),
-Beta(6), -Beta(7), -Beta(8) have been estimated at a boundary point, or have been
specified by the user, and do not appear in the correlation matrix)

               Beta(2)
   Beta(2)           1

                                Parameter Estimates

                                                        95.0% Wald Confidence Interval
       Variable     Estimate       Std. Err.     Lower Conf. Limit   Upper Conf. Limit
     Background       0             NA
        Beta(2)     6.31106e-007    5.7003e-007  -4.86132e-007        1.74834e-006

NA - Indicates that this parameter has hit a bound implied by some inequality
constraint and thus has no standard error.


                        Analysis of Deviance Table

        Model      Log(likelihood)  # Param's Deviance  Test d.f.   P-value
     Full model        -21.9835         4
   Fitted model          -22.34         1      0.713065      3          0.8701
  Reduced model        -33.5888         1       23.2107      3         <.0001

           AIC:         46.6801

                                 Goodness  of  Fit
                                                                      Scaled
     Dose     Est._Prob.    Expected    Observed     Size       Residual
  ---------------------------------------------------------------------------
    0.0000     0.0000         0.000         0          50        0.000
   21.0000     0.0003         0.014         0          50       -0.118
  103.0000     0.0067         0.334         0          50       -0.580
  514.0000     0.1536         7.679         8          50        0.126

 Chi^2 = 0.37      d.f. = 3        P-value = 0.9472

   Benchmark Dose Computation
Specified effect =           0.1
Risk Type        =      Extra risk
Confidence level =          0.95
             BMD =        408.59
            BMDL =       313.309
```

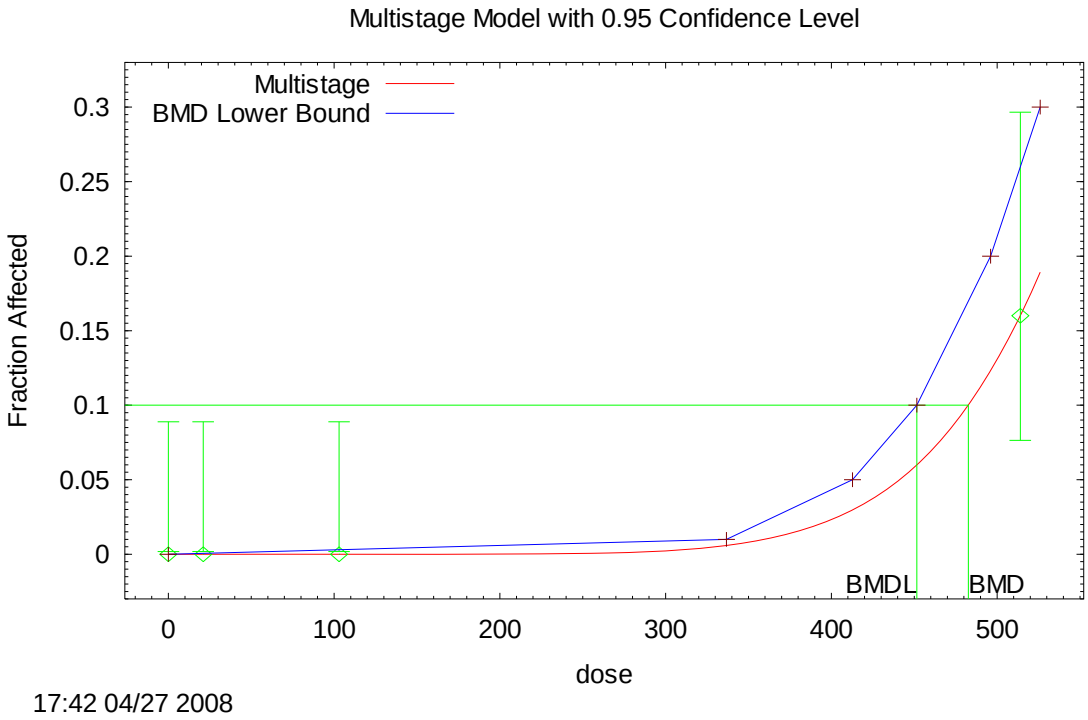

Source: JBRC (1998a).

Figure D-7. Multistage BMD model (8 degree) for the nasal cavity tumors in female F344 rats.

```
1   ================================================================
2            Multistage Model. (Version: 2.5;  Date: 10/17/2005)
3            Input Data File: U:\DIOXANE\JBRCLIVER.(d)
4            Gnuplot Plotting File:  U:\DIOXANE\JBRCLIVER.plt
5                                                  Sun Apr 27 17:42:03 2008
6   ================================================================
7    JBRC FEMALE RAT Nasal Cavity Tumors multistage deg 8 Table D-7
8   ~~~~~~~~~~~~~~~~~~~~~~~~~~~~~~~~~~~~~~~~~~~~~~~~~~~~~~~~~~~~~~~~
9   Observation # < parameter # for Multistage model.
10     The form of the probability function is:
11
12     P[response] = background + (1-background)*[1-EXP(-beta1*dose^1-beta2*dose^2-
13         beta3*dose^3-beta4*dose^4-beta5*dose^5-beta6*dose^6-beta7*dose^7-beta8*dose^8)]
14
15     The parameter betas are restricted to be positive
16
17     Dependent variable = NASALCAVITYF
18     Independent variable = DOSERATF
19
20     User specifies the following parameters:
21           Beta(1) =          0
22           Beta(2) =          0
23           Beta(3) =          0
24           Beta(4) =          0
25           Beta(5) =          0
26           Beta(6) =          0
27           Beta(7) =          0
28
29    Total number of observations = 4
30    Total number of records with missing values = 0
31    Total number of parameters in model = 9
32    Total number of specified parameters = 7
```

```
 Degree of polynomial = 8
 Maximum number of iterations = 250
 Relative Function Convergence has been set to: 1e-008
 Parameter Convergence has been set to: 1e-008

                  Default Initial Parameter Values
                     Background =            0
                        Beta(1) =            0   Specified
                        Beta(2) =            0   Specified
                        Beta(3) =            0   Specified
                        Beta(4) =            0   Specified
                        Beta(5) =            0   Specified
                        Beta(6) = 9.47989e-018   Specified
                        Beta(7) =            0   Specified
                        Beta(8) =            0

           Asymptotic Correlation Matrix of Parameter Estimates

(*** The model parameter(s) -Background, -Beta(1), -Beta(2), -Beta(3), -Beta(4),
-Beta(5), -Beta(6), -Beta(7) have been estimated at a boundary point, or have been
specified by the user, and do not appear in the correlation matrix)

               Beta(8)
  Beta(8)            1

                                Parameter Estimates

                                                      95.0% Wald Confidence Interval
       Variable     Estimate     Std. Err.     Lower Conf. Limit   Upper Conf. Limit
     Background           0              NA
        Beta(8)    3.57866e-023  3.16715e-023  -2.62883e-023       9.78616e-023

NA - Indicates that this parameter has hit a bound implied by some inequality
constraint and thus has no standard error.

                         Analysis of Deviance Table

        Model      Log(likelihood)  # Param's Deviance  Test d.f.   P-value
     Full model        -21.9835         4
   Fitted model        -21.9835         1  4.53344e-005      3              1
  Reduced model        -33.5888         1       23.2107      3         <.0001

           AIC:          45.967

                                 Goodness  of  Fit
                                                                    Scaled
     Dose     Est._Prob.    Expected    Observed     Size       Residual
  ---------------------------------------------------------------------
    0.0000     0.0000         0.000         0          50        0.000
   21.0000     0.0000         0.000         0          50       -0.000
  103.0000     0.0000         0.000         0          50       -0.005
  514.0000     0.1600         8.000         8          50        0.000

 Chi^2 = 0.00      d.f. = 3        P-value = 1.0000

   Benchmark Dose Computation
Specified effect =           0.1
Risk Type        =      Extra risk
Confidence level =          0.95
             BMD =       482.636
            BMDL =       451.634
```

Table D-8. Summary of BMDS dose-response modeling results for the incidence of nasal cavity tumors in male F344 rats

Model	Power	Estim	Std. Err	AIC	*p*-value	BMD_{10} mg/kg-day	$BMDL_{10}$ mg/kg-day	Max χ^2 [a]	Dose max [b] mg/kg-day	BMD_{10} HED	$BMDL_{10}$ HED
Weibull	Est.	10.74	NE	44.496	1.0000	385	256	0.001	81	104.48	69.47
MS	1			45.711	0.6113	350	199	1.100	81	94.98	54.00
	2 [d]			43.119	0.9564	340	257	0.542	81	92.27	69.74
	3			43.571	0.9101	379	328	0.666	81	102.85	89.01
	4			42.522	0.9996	364	316	0.113	81	98.78	85.75
	8 [c]			42.496	1.0000	378	349	0.010	81	102.58	94.71
Gamma	Est.	14.65	NE	44.496	1.0000	375	252	0.001	81	101.76	68.39
Log-Logistic	Est.	11.09	NE	44.496	1.0000	489	305	0.000	NA	132.70	82.77
Log-Probit	Est.	2.919	174	44.496	1.0000	371	235	0.000	NA	100.67	63.77

[a]Maximum absolute χ^2 residual deviation between observed and predicted count. Values much larger than 1 are undesirable.
[b]Dose at which the maximum χ^2 residual deviation occurred.
[c]Best-fitting model.
[d]This model fits the data nearly as well as the optimal model. It is simpler and is at least as plausible, thus will be carried forward into combined analyses with liver tumors as a sensitivity analysis.
[e]Nasal cavity tumors in male F344 rats include squamous cell carcinoma, Sarcoma: NOS, rhabdomyosarcoma, and esthesioneuro-epithelioma.

Table D-9. Summary of BMDS dose-response modeling results for the incidence of mammary gland adenomas in female F344 rats

Model	Power	Estim.	Std. Err.	AIC	*p*-value	BMD_{10} mg/kg-day	$BMDL_{10}$ mg/kg-day	Max χ^2 [a]	Dose max [b] mg/kg-day	BMD_{10} HED	$BMDL_{10}$ HED
Weibull	Est.	0.659	0.496	195.941	0.8757	129	4.90	0.115	21	30.87	1.17
MS	1[c]			194.197	0.8671	211	119	0.443	103	50.49	28.48
	2			194.964	0.5851	349	256	0.832	103	83.51	61.26
	1&2			194.945	0.8652	270	4.57	0.123	21	64.61	1.09
Gamma	Est.	0.611	0.492	195.505	0.8403	97.0	2.98	0.144	21	23.21	0.71
	Fixed	1		194.256	0.8388	201	118	0.544	103	48.10	28.24
Log-Logistic	Est.	0.707	0.518	195.934	0.8930	127	5.23	0.098	21	30.39	1.25
	Fixed	1		194.128	0.8982	193	98.4	0.382	103	46.18	23.55
Log-Probit	Est.	0.375	0.263	195.920	0.9502	122	5.90	0.044	21	29.19	1.41
	Fixed	1		195.008	0.5718	323	209	0.853	103	77.29	50.01

[a]Maximum absolute χ^2 residual deviation between observed and predicted count. Values much larger than 1 are undesirable.
[b]Dose at which the maximum χ^2 residual deviation occurred.
[c]Best-fitting model. It is simple and plausible, thus will be carried forward into combined analyses with liver tumors as a sensitivity analysis.

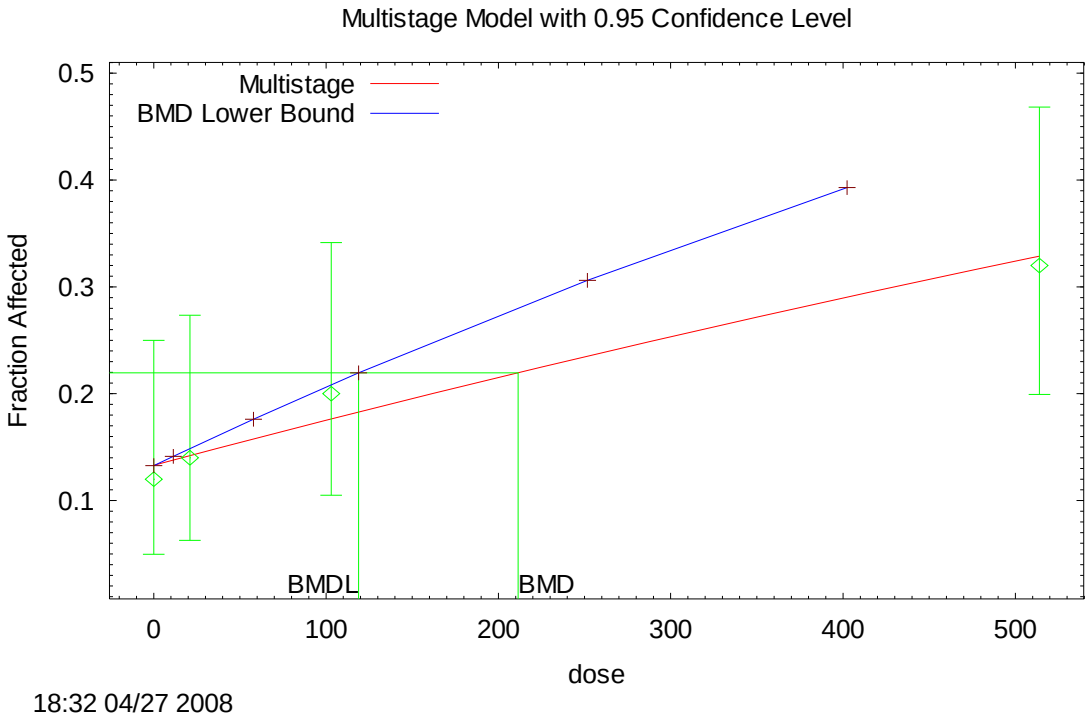

Source: JBRC (1998a).

Figure D-8. Multistage BMD model (1 degree) for mammary gland adenomas in female F344 rats.

```
1   ======================================================================
2            Multistage Model. (Version: 2.5;  Date: 10/17/2005)
3            Input Data File: U:\DIOXANE\JBRCLIVER.(d)
4            Gnuplot Plotting File:  U:\DIOXANE\JBRCLIVER.plt
5                                                  Sun Apr 27 18:32:45 2008
6   ======================================================================
7    JBRC FEMALE RAT Mammary Gland Adenoma multi deg 1 Table D-9
8   ~~~~~~~~~~~~~~~~~~~~~~~~~~~~~~~~~~~~~~~~~~~~~~~~~~~~~~~~~~~~~~~~~~~~~~~
9
10  Observation # < parameter # for Multistage model.
11     The form of the probability function is:
12
13     P[response] = background + (1-background)*[1-EXP(-beta1*dose^1-beta2*dose^2-
14             beta3*dose^3-beta4*dose^4-beta5*dose^5-beta6*dose^6-beta7*dose^7-
15             beta8*dose^8)]
16
17     The parameter betas are not restricted
18
19     Dependent variable = MAMMGLANDF
20     Independent variable = DOSERATF
21
22     User specifies the following parameters:
23           Beta(2) =          0
24           Beta(3) =          0
25           Beta(4) =          0
26           Beta(5) =          0
27           Beta(6) =          0
28           Beta(7) =          0
29           Beta(8) =          0
30
31    Total number of observations = 4
32    Total number of records with missing values = 0
```

```
 Total number of parameters in model = 9
 Total number of specified parameters = 7
 Degree of polynomial = 8

 Maximum number of iterations = 250
 Relative Function Convergence has been set to: 1e-008
 Parameter Convergence has been set to: 1e-008

                  Default Initial Parameter Values
                     Background =    0.0104878
                        Beta(1) =   0.00347368
                        Beta(2) = -4.98817e-006   Specified
                        Beta(3) = 5.12249e-009   Specified
                        Beta(4) = -8.5135e-012   Specified
                        Beta(5) =  4.0469e-014   Specified
                        Beta(6) = -7.50662e-017   Specified
                        Beta(7) = -1.84537e-019   Specified
                        Beta(8) = -3.25974e-023   Specified

           Asymptotic Correlation Matrix of Parameter Estimates

(*** The model parameter(s) -Beta(2), -Beta(3), -Beta(4), -Beta(5), -Beta(6), -
Beta(7), -Beta(8) have been estimated at a boundary point, or have been specified by
the user, and do not appear in the correlation matrix)

             Background      Beta(1)
Background            1        -0.59
   Beta(1)        -0.59            1

                                Parameter Estimates

                                                      95.0% Wald Confidence Interval
        Variable     Estimate       Std. Err.     Lower Conf. Limit   Upper Conf. Limit
      Background     0.132761        0.0843828     -0.0326261            0.298148
         Beta(1)     0.000498383     0.000408202   -0.000301679          0.00129844


                           Analysis of Deviance Table

         Model      Log(likelihood)  # Param's Deviance  Test d.f.   P-value
       Full model         -94.958         4
      Fitted model        -95.0985        2      0.280866      2           0.869
     Reduced model        -98.6785        1        7.4409      3          0.0591

           AIC:         194.197


                                  Goodness  of  Fit
                                                                      Scaled
      Dose     Est._Prob.    Expected    Observed     Size       Residual
    ---------------------------------------------------------------------
      0.0000     0.1328         6.638         6          50       -0.266
     21.0000     0.1418         7.090         7          50       -0.036
    103.0000     0.1762         8.808        10          50        0.443
    514.0000     0.3287        16.437        16          50       -0.132

 Chi^2 = 0.29      d.f. = 2        P-value = 0.8671

    Benchmark Dose Computation
Specified effect =            0.1
Risk Type        =      Extra risk
Confidence level =           0.95
             BMD =        211.405
            BMDL =        118.855
```

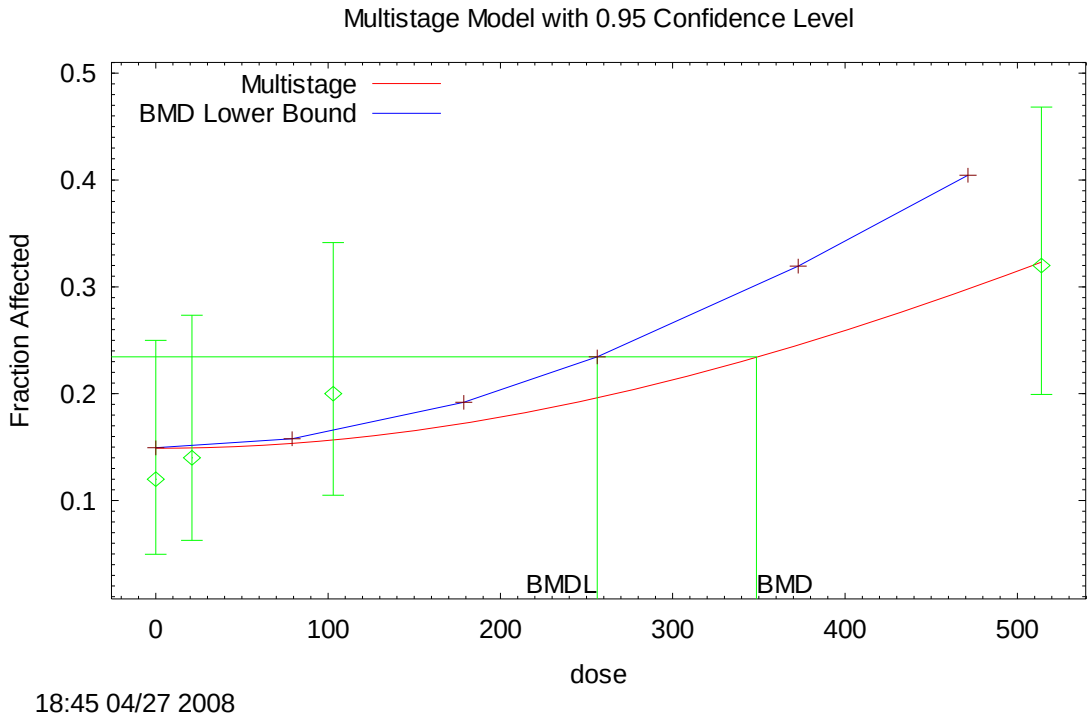

Source: JBRC (1998a).

Figure D-9. Multistage BMD model (2 degree) for mammary gland adenomas in female F344 rats.

```
1   ================================================================
2            Multistage Model. (Version: 2.5;  Date: 10/17/2005)
3            Input Data File: U:\DIOXANE\JBRCLIVER.(d)
4            Gnuplot Plotting File:  U:\DIOXANE\JBRCLIVER.plt
5                                                  Sun Apr 27 18:45:19 2008
6   ================================================================
7    JBRC FEMALE RAT Mammary Gland Adenoma multi deg 2 Table D-9
8   ~~~~~~~~~~~~~~~~~~~~~~~~~~~~~~~~~~~~~~~~~~~~~~~~~~~~~~~~~~~~~~~~
9   Observation # < parameter # for Multistage model.
10     The form of the probability function is:
11
12     P[response] = background + (1-background)*[1-EXP(-beta1*dose^1-beta2*dose^2-
13         beta3*dose^3-beta4*dose^4-beta5*dose^5-beta6*dose^6-beta7*dose^7-beta8*dose^8)]
14
15     The parameter betas are restricted to be positive
16
17     Dependent variable = MAMMGLANDF
18     Independent variable = DOSERATF
19
20     User specifies the following parameters:
21           Beta(1) =          0
22           Beta(3) =          0
23           Beta(4) =          0
24           Beta(5) =          0
25           Beta(6) =          0
26           Beta(7) =          0
27           Beta(8) =          0
28
29    Total number of observations = 4
30    Total number of records with missing values = 0
31    Total number of parameters in model = 9
32    Total number of specified parameters = 7
```

```
 Degree of polynomial = 8
 Maximum number of iterations = 250
 Relative Function Convergence has been set to: 1e-008
 Parameter Convergence has been set to: 1e-008

                  Default Initial Parameter Values
                     Background =     0.135593
                        Beta(1) =  0.000477455   Specified
                        Beta(2) =            0
                        Beta(3) =            0   Specified
                        Beta(4) =            0   Specified
                        Beta(5) =            0   Specified
                        Beta(6) =            0   Specified
                        Beta(7) =            0   Specified
                        Beta(8) =            0   Specified


           Asymptotic Correlation Matrix of Parameter Estimates

(*** The model parameter(s) -Beta(1), -Beta(3), -Beta(4), -Beta(5), -Beta(6), -
Beta(7), -Beta(8)  have been estimated at a boundary point, or have been specified by
the user, and do not appear in the correlation matrix)

             Background      Beta(2)
Background            1        -0.49
   Beta(2)        -0.49            1

                                Parameter Estimates

                                                      95.0% Wald Confidence Interval
        Variable    Estimate       Std. Err.     Lower Conf. Limit   Upper Conf. Limit
      Background    0.14939        0.0766837       -0.000907529         0.299687
         Beta(2)    8.66886e-007   7.47534e-007    -5.98253e-007        2.33203e-006


                         Analysis of Deviance Table

        Model      Log(likelihood)  # Param's Deviance  Test d.f.   P-value
      Full model         -94.958         4
     Fitted model       -95.4821         2       1.04822      2          0.5921
   Reduced model        -98.6785         1        7.4409      3          0.0591

           AIC:         194.964

                                Goodness  of  Fit
                                                                    Scaled
      Dose     Est._Prob.    Expected    Observed     Size        Residual
   ----------------------------------------------------------------------
     0.0000     0.1494         7.469         6          50       -0.583
    21.0000     0.1497         7.486         7          50       -0.193
   103.0000     0.1572         7.859        10          50        0.832
   514.0000     0.3235        16.175        16          50       -0.053

 Chi^2 = 1.07      d.f. = 2        P-value = 0.5851

   Benchmark Dose Computation
Specified effect =           0.1
Risk Type        =      Extra risk
Confidence level =          0.95
             BMD =       348.624
            BMDL =        256.18
```

Table D-10. Summary of BMDS dose-response modeling results for the incidence of peritoneal mesotheliomas in male F344 rats

Model	Power	Estim.	Std. Err.	AIC	*p*-value	BMD_{10} mg/kg-day	$BMDL_{10}$ mg/kg-day	Max χ^2 [a]	Dose max [b] mg/kg-day	BMD_{10} HED	$BMDL_{10}$ HED
Weibull	Est.	1.537	0.505	140.497	0.8885	107.9	50.9	0.108	16	29.31	13.81
MS	1			140.557	0.3711	59.5	44.2	1.049	81	16.15	11.99
	2 [c]			138.996	0.7602	145	124	0.651	81	39.35	33.65
	3			140.149	0.4073	205	184	1.119	81	55.63	49.93
	4			140.472	0.3432	243	224	1.049	81	65.94	60.79
	8			140.559	0.3279	311	298	1.223	81	84.40	80.87
	1&2			140.537	0.8808	112	50.8	0.191	16	30.39	13.79
	2&3			140.482	0.9426	103	61.6	0.053	16	27.95	16.72
Gamma	Est.	1.796	0.810	140.488	0.9164	106	50.9	0.080	16	28.77	13.81
Log-Logistic	Est.	1.776	0.537	140.487	0.8930	127	5.23	0.098	16	34.46	1.42
Log-Probit	Est.	1.017	0.267	140.477	0.9848	102	53.7	0.014	16	27.68	14.57

[a]Maximum absolute χ^2 residual deviation between observed and predicted count. Values much larger than 1 are undesirable.
[b]Dose at which the maximum χ^2 residual deviation occurred.
[c]Best-fitting model will be carried forward into combined analyses with liver tumors.

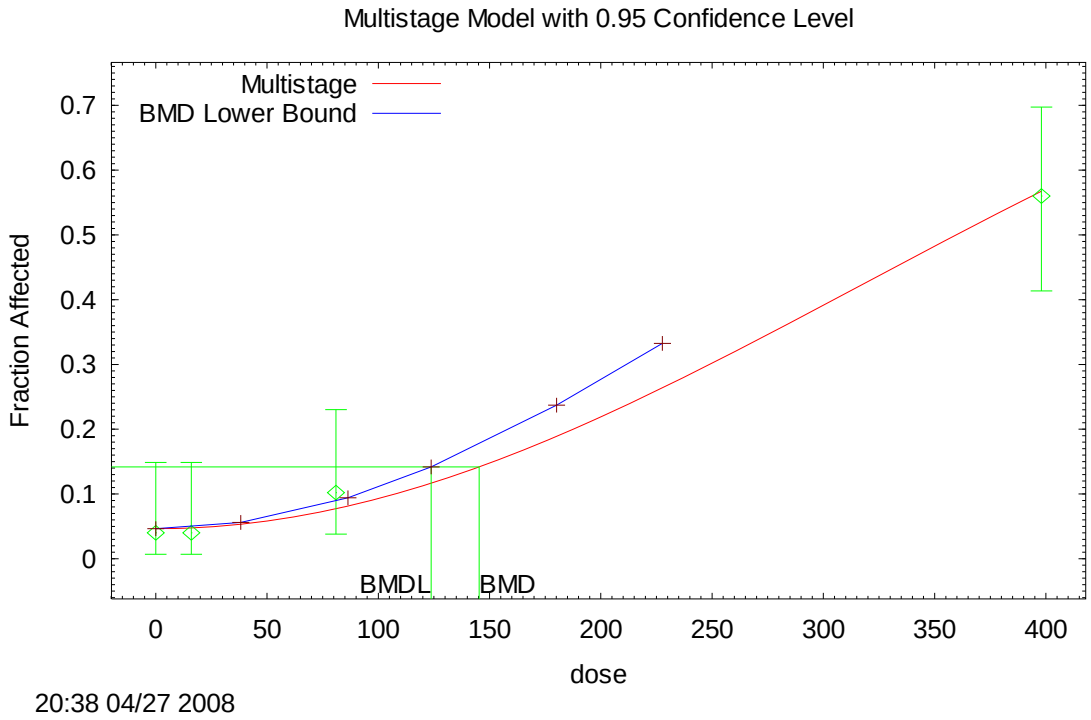

Source: JBRC (1998a).

Figure D-10. Multistage BMD model (2 degree) for peritoneal mesotheliomas in male F344 rats.

```
1   ================================================================
2            Multistage Model. (Version: 2.5;  Date: 10/17/2005)
3            Input Data File: U:\DIOXANE\JBRCLIVER.(d)
4            Gnuplot Plotting File:  U:\DIOXANE\JBRCLIVER.plt
5                                                  Sun Apr 27 20:38:46 2008
6   ================================================================
7    JBRC MALE RAT Peritoneal Mesotheliama multi deg 2 Table D-10
8   ~~~~~~~~~~~~~~~~~~~~~~~~~~~~~~~~~~~~~~~~~~~~~~~~~~~~~~~~~~~~~~~~
9   Observation # < parameter # for Multistage model.
10     The form of the probability function is:
11
12     P[response] = background + (1-background)*[1-EXP(-beta1*dose^1-beta2*dose^2-
13         beta3*dose^3-beta4*dose^4-beta5*dose^5-beta6*dose^6-beta7*dose^7-beta8*dose^8)]
14
15     The parameter betas are restricted to be positive
16
17     Dependent variable = PERITMESOTHELM
18     Independent variable = DOSERATM
19
20     User specifies the following parameters:
21           Beta(1) =          0
22           Beta(3) =          0
23           Beta(4) =          0
24           Beta(5) =          0
25           Beta(6) =          0
26           Beta(7) =          0
27           Beta(8) =          0
28
29    Total number of observations = 4
30    Total number of records with missing values = 0
31    Total number of parameters in model = 9
32    Total number of specified parameters = 7
```

```
 Degree of polynomial = 8
 Maximum number of iterations = 250
 Relative Function Convergence has been set to: 1e-008
 Parameter Convergence has been set to: 1e-008

                  Default Initial Parameter Values
                     Background =     0.035746
                        Beta(1) =                0   Specified
                        Beta(2) = 3.49814e-006
                        Beta(3) =            0   Specified
                        Beta(4) =            0   Specified
                        Beta(5) =            0   Specified
                        Beta(6) =            0   Specified
                        Beta(7) =            0   Specified
                        Beta(8) =            0   Specified

           Asymptotic Correlation Matrix of Parameter Estimates

(*** The model parameter(s) -Beta(1), -Beta(3), -Beta(4), -Beta(5), -Beta(6),
-Beta(7), -Beta(8) have been estimated at a boundary point, or have been specified by
the user, and do not appear in the correlation matrix)

             Background      Beta(2)
Background            1        -0.41
   Beta(2)        -0.41            1


                                Parameter Estimates

                                                    95.0% Wald Confidence Interval
        Variable    Estimate        Std. Err.     Lower Conf. Limit   Upper Conf. Limit
      Background    0.0465221       0.0819877       -0.114171            0.207215
         Beta(2)    4.98704e-006    1.49071e-006     2.06529e-006        7.90878e-006


                         Analysis of Deviance Table

         Model      Log(likelihood)  # Param's Deviance  Test d.f.   P-value
       Full model        -67.2386         4
      Fitted model       -67.4978         2      0.518389      2          0.7717
    Reduced model        -95.5731         1       56.6691      3         <.0001

           AIC:         138.996


                                Goodness  of  Fit
                                                                      Scaled
      Dose     Est._Prob.    Expected    Observed     Size       Residual
   ----------------------------------------------------------------------
     0.0000     0.0465         2.326         2          50       -0.219
    16.0000     0.0477         2.387         2          50       -0.257
    81.0000     0.0772         3.784         5          49        0.651
   398.0000     0.5673        28.363        28          50       -0.104

 Chi^2 = 0.55      d.f. = 2        P-value = 0.7602


   Benchmark Dose Computation
Specified effect =           0.1
Risk Type        =      Extra risk
Confidence level =          0.95
             BMD =       145.351
            BMDL =       123.748
```

D.5. FEMALE BDF_1 MICE: HEPATIC CARCINOMAS AND ADENOMAS

Data for female BDF_1 mouse hepatic carcinomas and adenomas are shown in Table D-11. Note that the incidence of carcinomas and the incidence of either adenomas or carcinomas or both (combined incidence) are monotone non-decreasing functions of dose. These data therefore appear to be appropriate for dose-response modeling using BMDS. However, the incidence of adenomas clearly reaches a peak value at 77 mg/kg-day and then decreases sharply with increasing dose. This cannot be modeled by a MS model using only non-negative coefficients. To some extent the incidence of "either adenomas or carcinomas or both" retains some of the inverted-U shaped dose-response of the adenomas, which dominate based on their high incidence at the lowest dose groups (77 and 323 mg/kg-day), thus is not well characterized by any MS model such as those that provided consistently good descriptions of the rat data.

Table D-11. Data for hepatic adenomas and carcinomas in female BDF_1 mice

Tumor type	Dose(mg/kg-day)			
	0	**77**	**323**	**1066**
Adenomas	4	30	20	2
Carcinomas	0	6	30	45
Either adenomas or carcinomas	4	34	41	46
Neither adenomas nor carcinomas	46	16	7	2
Both adenomas and carcinomas	0	2	9	1
Total number per group	50	50	48	48

Source: JBRC (1998a).

The results of the BMDS modeling for the entire suite of models for hepatic adenomas and carcinomas in female BDF_1 mice are presented in Table D-12 in the order described in Section D.1.

The graphical output from fitting these models suggested that a simpler model obtained by dropping the data point for the highest dose (1,066 mg/kg-day) might also be adequate.

Table D-12. Summary of BMDS dose-response modeling results for the combined incidence of hepatic adenomas and carcinomas in female BDF_1 mice

Model	Power	Estim	Std. Err.	AIC	*p*-value	BMD_{10} mg/kg-day	$BMDL_{10}$ mg/kg-day	Max χ^{2a}	Dose max[b] mg/kg-day	BMD_{10} HED	$BMDL_{10}$ HED
Weibull	Est.	0.407	0.112	153.087	0.9001	0.274	0.0011	0.046	77	0.04113	0.000165
MS	1			172.372	0.0000	19.3	14.8	3.335	77	2.897	2.222
Gamma	Est.	0.195	0.083	153.092	0.8846	0.0046	0.0004	0.116	323	0.00069	0.0006
Log-Logistic	Est.	0.854	0.248	153.298	0.6349	2.94	0.0864	0.355	323	0.4413	0.01297
	Fixed[c]	1.000		151.629	0.7494	5.28	3.47	0.604	323	0.7926	0.5209
Log-Probit	Est.	0.478	0.134	153.181	0.7403	2.43	0.062	0.256	323	0.3648	0.009307
	Fixed	1.000		164.002	0.0000	23.2	17.8	3.656	1,066	3.482	2.672

[a]Maximum absolute χ^2 residual deviation between observed and predicted count. Values much larger than1 are undesirable.
[b]Dose at which the maximum χ^2 residual deviation occurred.
[c]Best-fitting model not supra-linear will be carried forward into combined analyses with tumors at another site.

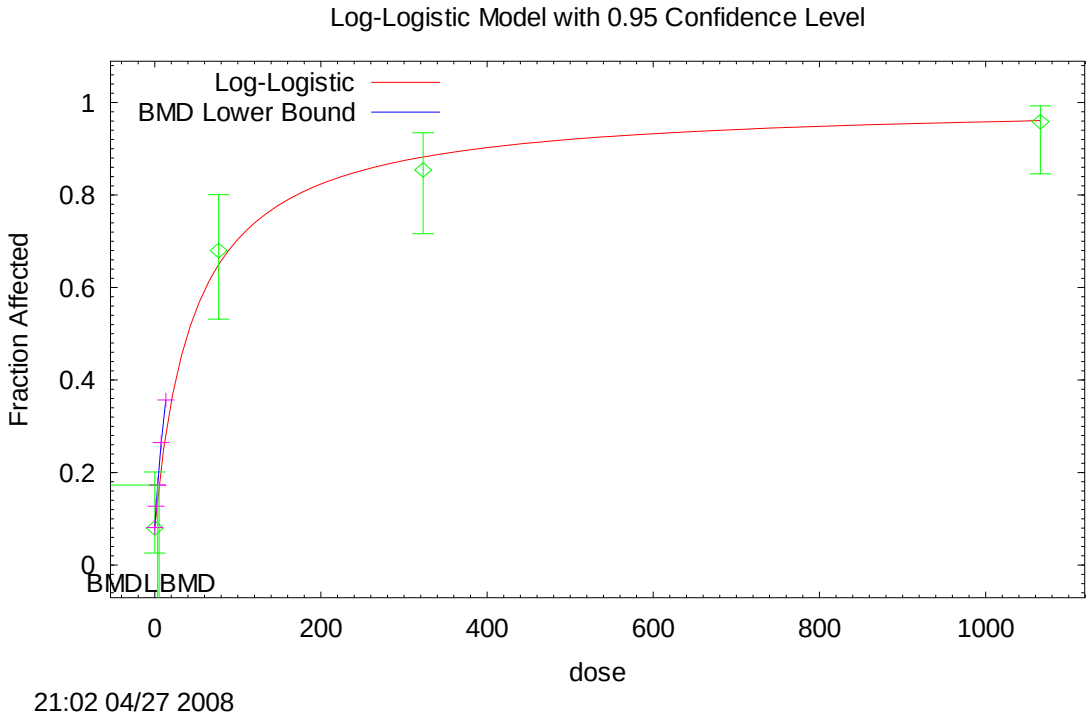

Source: JBRC (1998a).

Figure D-11. Log-logistic BMD model (Fixed power=1) for the combined incidence of hepatic adenomas and carcinomas in female BDF_1 mice.

```
==========================================================================
        Logistic Model. (Version: 2.5; Date: 09/24/2005)
        Input Data File: U:\DIOXANE\JBRCLIVER.(d)
        Gnuplot Plotting File:  U:\DIOXANE\JBRCLIVER.plt
                                              Sun Apr 27 21:02:47 2008
==========================================================================
 JBRC FEMALE MOUSEcarcino+adenoma slope = 1 loglogit Tbl D-12
~~~~~~~~~~~~~~~~~~~~~~~~~~~~~~~~~~~~~~~~~~~~~~~~~~~~~~~~~~~~~~~~~~~~~~~~~~

   The form of the probability function is:

   P[response] = background+(1-background)/[1+EXP(-intercept-slope*Log(dose))]

   Dependent variable = EITHERMUSF
   Independent variable = DOSEMUSF
   Slope parameter is restricted as slope >= 1

   Total number of observations = 4
   Total number of records with missing values = 0
   Maximum number of iterations = 250
   Relative Function Convergence has been set to: 1e-008
   Parameter Convergence has been set to: 1e-008

   User has chosen the log transformed model

                 Default Initial Parameter Values
                    background =         0.08
                     intercept =     -3.96538
                         slope =            1
             Asymptotic Correlation Matrix of Parameter Estimates
(*** The model parameter(s) -slope have been estimated at a boundary point, or have
been specified by the user, and do not appear in the correlation matrix)

             background    intercept
background            1        -0.25
 intercept        -0.25            1


                                Parameter Estimates

                                                    95.0% Wald Confidence Interval
       Variable     Estimate      Std. Err.     Lower Conf. Limit   Upper Conf. Limit
     background     0.0811252     0.0388749      0.00493183          0.157319
      intercept    -3.86024       0.250749      -4.3517            -3.36878
          slope               1              NA

NA - Indicates that this parameter has hit a bound
     implied by some inequality constraint and thus
     has no standard error.


                        Analysis of Deviance Table

       Model      Log(likelihood)  # Param's Deviance  Test d.f.   P-value
     Full model        -73.5356         4
   Fitted model        -73.8143         2      0.557285      2          0.7568
  Reduced model        -128.321         1       109.571      3         <.0001

           AIC:         151.629


```

```
                                Goodness  of  Fit

                                                                      Scaled
     Dose     Est._Prob.    Expected    Observed     Size       Residual
   ---------------------------------------------------------------------------
      0.0000     0.0811         4.056         4          50       -0.029
     77.0000     0.6495        32.477        34          50        0.452
    323.0000     0.8822        42.348        41          48       -0.604
   1066.0000     0.9608        46.119        46          48       -0.089

   Chi^2 = 0.58      d.f. = 2        P-value = 0.7494


     Benchmark Dose Computation
Specified effect =            0.1
Risk Type        =      Extra risk
Confidence level =           0.95
             BMD =         5.2752
            BMDL =        3.46551
```

D.6. MALE BDF_1 MICE: HEPATIC CARCINOMAS AND ADENOMAS

Data for hepatic carcinomas and adenomas in male BDF_1 mice (JBRC, 1998a) are shown in Table D-13. Note that the incidence of carcinomas and the incidence of either adenomas or carcinomas or both (combined incidence) are monotone non-decreasing functions of dose. These data therefore appear to be appropriate for dose-response modeling using BMDS. However, the incidence of adenomas clearly reaches a peak value at 251 mg/kg-day and then decreases sharply with increasing dose. This cannot be modeled by a MS model using only non-negative coefficients. To some extent the incidence of "either adenomas or carcinomas or both" retains some of the inverted-U shaped dose-response of the adenomas, which dominate based on their high incidence at the lowest dose groups (66 and 251 mg/kg-day), thus is not well characterized by any MS model such as those that provided consistently good descriptions of the rat data.

Table D-13. Data for hepatic adenomas and carcinomas in male BDF_1 mice

Tumor type	Dose (mg/kg-day)			
	0	**66**	**251**	**768**
Adenomas	7	18	22	8
Carcinomas	15	20	23	36
Either adenomas or carcinomas	21	31	37	39
Neither adenomas nor carcinomas	29	17	13	9
Both adenomas and carcinomas	1	7	8	5
Total number per group	50	48	50	48

Source: JBRC (1998a).

The results of the BMDS modeling for the entire suite of models for hepatic adenomas and carcinomas in male BDF_1 mice are presented in Table D-14 in the order described in Section D.1. Fit in these models was also evaluated using a simpler model obtained by dropping the data point for the highest dose (768 mg/kg-day). This did not appear to offer any great advantages over using all four dose groups.

Table D-14. Summary of BMDS dose-response modeling results for the combined incidence of hepatic adenomas and carcinomas in male BDF_1 mice

Model	Power	Estim	Std. Err	AIC	*p*-value	BMD_{10} mg/kg-day	$BMDL_{10}$ mg/kg-day	Max χ^{2a}	Dose max[b] mg/kg-day	$BMD_{10\ HED}$	$BMDL_{10\ HED}$
Weibull	Est	0.334	0.196	240.070	0.9248	0.616	0+	0.020	251	0.09385	0
MS	1			242.941	0.0885	68.8	44.4	1.120	66	10.48	6.764
	1&2			241.266	0.2740	24.3	14.6	0.879	66	3.702	2.224
	1&3			241.635	0.2119	29.4	18.0	1.014	66	4.479	2.742
	2&3			243.964	0.0496	87.0	64.6	1.494	66	13.25	9.842
Gamma	Est	0.228	0.157	240.088	0.8701	0.149	0+	0.130	66	0.0227	0
	Fixed	1		242.941	0.0885	68.8	44.4	1.120	66	10.48	6.764
Log-Logistic	Est.	0.484	0.277	240.062	0.9845	1.77	0+	0.015	251	0.2697	0
	Fixed[c]	1		240.543	0.2836	31.1	15.8	1.059	66	4.738	2.407
Log-Probit	Est.	0.301	0.171	240.062	0.9801	2.35	0+	0.020	251	0.3580	0
	Fixed	1		244.833	0.0339	128	77.6	1.701	0	19.50	11.82

[a]Maximum absolute χ^2 residual deviation between observed and predicted count. Values much larger than 1 are undesirable.
[b]Dose at which the maximum χ^2 residual deviation occurred.
[c]Best-fitting model not supra-linear.

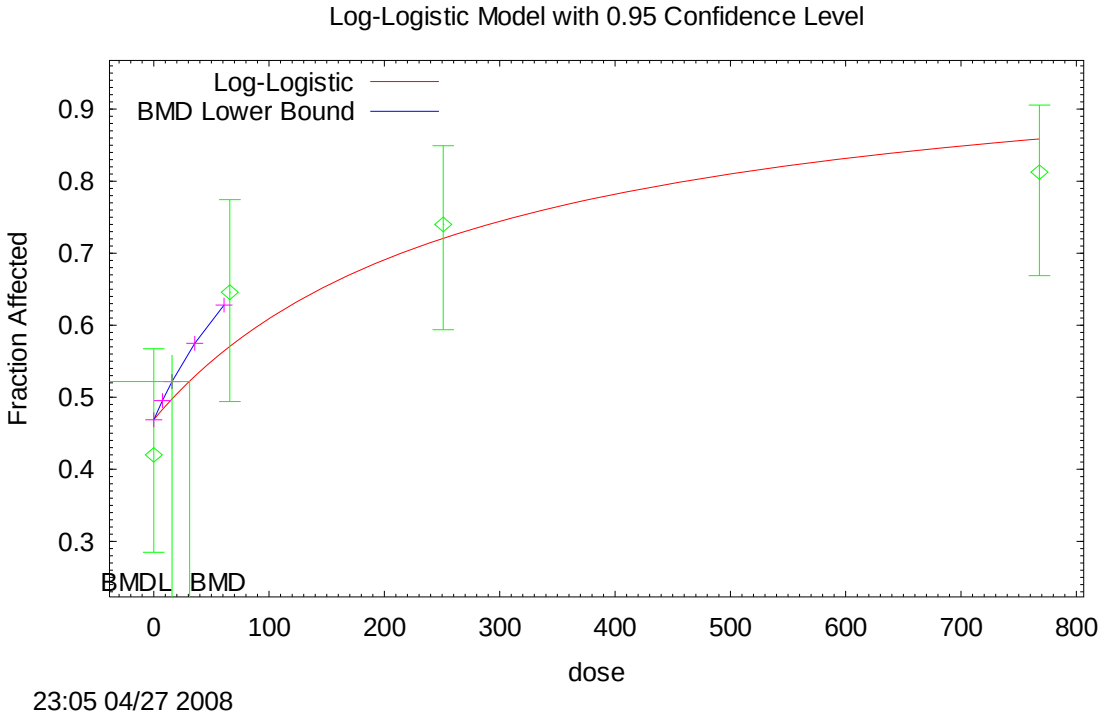

Source: JBRC (1998a).

Figure D-12. Log-logistic BMD model (Fixed power=1) for the combined incidence of hepatic adenomas and carcinomas in male BDF_1 mice.

```
1   ================================================================
2            Logistic Model. (Version: 2.5; Date: 09/24/2005)
3            Input Data File: U:\DIOXANE\JBRCLIVER.(d)
4            Gnuplot Plotting File:  U:\DIOXANE\JBRCLIVER.plt
5                                                  Sun Apr 27 23:05:00 2008
6   ================================================================
7    JBRC MALE MOUSE carcino+adenoma slope = 1 loglogit Tbl D-14
8   ~~~~~~~~~~~~~~~~~~~~~~~~~~~~~~~~~~~~~~~~~~~~~~~~~~~~~~~~~~~~~~~~
9
10     The form of the probability function is:
11
12     P[response] = background+(1-background)/[1+EXP(-intercept-slope*Log(dose))]
13
14     Dependent variable = EITHERMUSM
15     Independent variable = DOSEMUSM
16     Slope parameter is restricted as slope >= 1
17
18     Total number of observations = 4
19     Total number of records with missing values = 0
20     Maximum number of iterations = 250
21     Relative Function Convergence has been set to: 1e-008
22     Parameter Convergence has been set to: 1e-008
23
24     User has chosen the log transformed model
25
26                    Default Initial Parameter Values
27                       background =         0.42
28                        intercept =     -5.54398
29                            slope =            1
```

```
           Asymptotic Correlation Matrix of Parameter Estimates
( *** The model parameter(s) -slope have been estimated at a boundary point, or have
been specified by the user, and do not appear in the correlation matrix )

             background    intercept
background            1        -0.69
 intercept        -0.69            1


                                Parameter Estimates

                                                      95.0% Wald Confidence Interval
      Variable     Estimate      Std. Err.     Lower Conf. Limit   Upper Conf. Limit
    background     0.468776      0.0671164       0.33723            0.600322
     intercept    -5.63385       0.455627       -6.52686           -4.74084
         slope               1               NA

NA - Indicates that this parameter has hit a bound
     implied by some inequality constraint and thus
     has no standard error.


                        Analysis of Deviance Table

       Model      Log(likelihood)  # Param's Deviance  Test d.f.   P-value
     Full model        -117.031         4
   Fitted model        -118.272         2       2.48218      2          0.2891
  Reduced model        -126.524         1        18.987      3       0.0002751

           AIC:         240.543


                                Goodness  of  Fit
                                                                      Scaled
     Dose     Est._Prob.    Expected    Observed     Size       Residual
  ---------------------------------------------------------------------------
    0.0000     0.4688        23.439        21          50       -0.691
   66.0000     0.5702        27.369        31          48        1.059
  251.0000     0.7200        36.000        37          50        0.315
  768.0000     0.8582        41.192        39          48       -0.907

 Chi^2 = 2.52      d.f. = 2        P-value = 0.2836


   Benchmark Dose Computation
Specified effect =            0.1
Risk Type        =      Extra risk
Confidence level =           0.95
             BMD =        31.0819
            BMDL =        15.7951
```

D.7. COMBINING RISKS FOR DIFFERENT ENDPOINTS USING MULTISTAGE MODELS

Analyses were restricted to those endpoints for which there were statistically significant dose-response functions as determined by the criterion $p > 0.10$. Table D-15 lists these for F344 female and male rats separately because there were sex differences.

Table D-15. Statistically significant MS dose-response models for F344 rats

Endpoint	Female		Male	
	Coefficients used in model	*p*-value	Coefficients used in model	*p*-value
Liver adenomas and carcinomas	1, 2	0.2357	1,2	0.4485
Nasal cavity tumors	1,2	0.5488	1,2	0.9564
Peritoneal mesotheliomas	No significant dose-response		1,2	0.8088
Mammary gland adenomas	1	0.8671	No significant dose-response	

The risks for the tumor type with the highest response at the largest dose (liver adenomas and carcinomas, the key endpoint) were combined with the other statistically significant tumors at other sites whose response at the highest dose also exceeded the BMR of 10% excess risk. The MS-combo software was used. This software was recently developed by EPA to evaluate the sensitivity of the BMDL for liver tumors to the inclusion of additional tumor sites. The risks in the tables below were combined for liver tumors and an additional tumor type to better evaluate how much the BMD and BMDL could be decreased when the excess risk is the occurrence of a liver tumor or another significant tumor type, rather than just the occurrence of a liver tumor. The sensitivity analysis was not extended to multiple tumor types including other less significant or non-significant tumors occurring at other sites. The BMDLs in the following tables are thus to be taken as upper bounds on the BMDL for the tumor types evaluated, generally adenomas and carcinomas.

The effects can be examined on calculated human equivalent doses if several tumor types are considered with the following example for F344 rats. The liver tumors are the most significant tumor type for either sex. There are other sites for which a significant dose-response relationship can be detected below the highest dose in the study: in male rats, peritoneal mesotheliomas, and in female rats mammary gland mesotheliomas. A significant increase in nasal cavity tumors occurs in the highest dose group only. One might hypothesize that when risks are combined in the sense of finding a tumor either at one site or at the other, the greatest decrease in BMD or BMDL occurs when the strength of the dose-response relationship at the secondary site is nearly as large as at the primary site. The six pairwise combinations of tumors have been ranked in order of increasing BMDL, and this hypothesis is demonstrated by the data in the following tables.

Note that a very large reduction in $BMD_{10\ HED}$ and $BMDL_{10\ HED}$ occurs in Table D-17 relative to the separate $BMD_{10\ HED}$ and $BMDL_{10\ HED}$ for either the liver tumors or the peritoneal mesotheliomas. When nasal cavity tumors are the secondary type, the reduction in $BMD_{10\ HED}$ and $BMDL_{10\ HED}$ is relatively very small compared to the primary tumor type, either liver or peritoneal mesotheliomas (Table D-17). For the female rats, one obtains similar findings with a modest reduction in the $BMD_{10\ HED}$ and $BMDL_{10\ HED}$ when mammary gland adenomas are

considered in addition to liver tumors (Table D-16), and relatively minor reductions in $BMDL_{10\ HED}$ when nasal cavity tumors are combined with liver tumors or mammary gland tumors (Table D-16). It therefore seems highly likely that considerably increasing the number of rat tumor sites will yield substantial further reductions in $BMD_{10\ HED}$ and $BMDL_{10\ HED}$.

Note that the smallest rat $BMD_{10\ HED}$ and $BMDL_{10\ HED}$ for combined liver tumors and peritoneal mesotheliomas in male rats is 13.9 and 7.76 mg/kg-day respectively (Table D-17), about 15-fold larger than the female mouse $BMD_{10\ HED}$ and $BMDL_{10\ HED}$ of 0.792 and 0.521 mg/kg-day respectively, and five- to sixfold larger than the male mouse $BMD_{10\ HED}$ and $BMDL_{10\ HED}$ of 4.74 and 2.41 mg/kg-day respectively. If tumor data from other sites in the mouse were available then one would expect the mouse $BMD_{10\ HED}$ and $BMDL_{10\ HED}$ values combined over tumor sites would also be smaller. Therefore it is concluded that the mouse is the more sensitive species and provides an appropriate basis for extrapolation to humans in a health risk assessment.

Table D-16. MS-combo analysis of excess risks for liver adenomas/ carcinomas, mammary gland adenomas, or nasal cavity tumors in female F344 rats using MS models

Tumor site	Coefficients	AIC	*p*-value	BMD_{10}	$BMDL_{10}$	$BMD_{10\ HED}$	$BMDL_{10\ HED}$
				mg/kg-day		mg/kg-day	
Liver	1, 2	100.463	0.2357	126	77.2	30.2	18.5
Mammary	1	194.197	0.8671	211	119	50.5	28.5
Nasal cavity	1	49.701	0.5488	392	231	93.8	55.3
Either	Liver or mammary			92.6	57.1	22.2	13.7
	Liver or nasal cavity			106	65.8	25.4	15.7
	Mammary or nasal cavity			137	88.7	32.8	21.25

```
================================================================
        MS_COMBO. (Version: 1.0;  Date: 07/06/2007)
        Input Data File: FLV2MM1.(d)
        Gnuplot Plotting File:  FLV2MM1.plt
                                          Wed Apr 23 15:03:14 2008
================================================================
 Female Rat Liver Carcinomas or Adenomas AND Mammary Adenomas Degree 2, Tbl D-16
~~~~~~~~~~~~~~~~~~~~~~~~~~~~~~~~~~~~~~~~~~~~~~~~~~~~~~~~~~~~~~~~~~~~
   The form of the probability function is:

   P[response] = background + (1-background)*[1-EXP(-beta1*dose^1-beta2*dose^2)]

   The parameter betas are restricted to be positive

   Dependent variable = LIVCARAD
   Independent variable = DOSE

 Total number of observations = 4
 Total number of records with missing values = 0
 Total number of parameters in model = 3
 Total number of specified parameters = 0
 Degree of polynomial = 2
 Maximum number of iterations = 250
 Relative Function Convergence has been set to: 1e-008
```

```
 Parameter Convergence has been set to: 1e-008

                  Default Initial Parameter Values
                     Background =   0.00712897
                        Beta(1) =  0.000360374
                        Beta(2) = 5.36416e-006

            Asymptotic Correlation Matrix of Parameter Estimates

              Background      Beta(1)      Beta(2)
Background             1        -0.61          0.5
   Beta(1)         -0.61            1        -0.95
   Beta(2)           0.5        -0.95            1

                                Parameter Estimates
                                                        95.0% Wald Confidence Interval
       Variable     Estimate        Std. Err.     Lower Conf. Limit   Upper Conf.Limit
     Background     0.0113405           *               *                   *
        Beta(1)     8.30975e-005        *               *                   *
        Beta(2)     6.01351e-006        *               *                   *

* - Indicates that this value is not calculated.

                        Analysis of Deviance Table

       Model      Log(likelihood)  # Param's  Deviance  Test d.f.   P-value
     Full model        -46.1762         4
    Fitted model       -47.2315         3       2.11046      1          0.1463
   Reduced model       -107.855         1       123.358      3         <.0001

           AIC:         100.463

 Log-likelihood Constant             41.531079239232298
                                Goodness  of  Fit
                                                                    Scaled
     Dose     Est._Prob.    Expected    Observed     Size       Residual
  ---------------------------------------------------------------------------
    0.0000     0.0113         0.567         1          50        0.578
   21.0000     0.0157         0.784         0          50       -0.892
  103.0000     0.0803         4.017         5          50        0.511
  514.0000     0.8066        40.329        40          50       -0.118

 Chi^2 = 1.41      d.f. = 1        P-value = 0.2357

   Benchmark Dose Computation
Specified effect =            0.1
Risk Type        =      Extra risk
Confidence level =           0.95
             BMD =        125.636
            BMDL =        77.1768
            BMDU =         150.31

Taken together, (77.1768, 150.31 ) is a 90% two-sided confidence interval for the BMD

=====================================================================
         MS_COMBO. (Version: 1.0;  Date: 07/06/2007)
         Input Data File: FLV2MM1.(d)
         Gnuplot Plotting File:  FLV2MM1.plt
                                              Wed Apr 23 15:03:14 2008
=====================================================================
Female Rat Liver Carcinomas or Adenomas OR Mammary Adenomas Degree 2, Tbl D-16
~~~~~~~~~~~~~~~~~~~~~~~~~~~~~~~~~~~~~~~~~~~~~~~~~~~~~~~~~~~~~~~~~~~~~
    The form of the probability function is:

   P[response] = background + (1-background)*[1-EXP(-beta1*dose^1)]

   The parameter betas are restricted to be positive
```

```
  Dependent variable = MAMMADEN
  Independent variable = DOSE

 Total number of observations = 4
 Total number of records with missing values = 0
 Total number of parameters in model = 2
 Total number of specified parameters = 0
 Degree of polynomial = 1
 Maximum number of iterations = 250
 Relative Function Convergence has been set to: 1e-008
 Parameter Convergence has been set to: 1e-008

                 Default Initial Parameter Values
                    Background =     0.135593
                       Beta(1) =  0.000477455

           Asymptotic Correlation Matrix of Parameter Estimates

             Background      Beta(1)
Background            1        -0.59
   Beta(1)        -0.59            1
                                Parameter Estimates

                                                      95.0% Wald Confidence Interval
       Variable      Estimate      Std. Err.     Lower Conf. Limit   Upper Conf. Limit
     Background      0.132761          *                 *                   *
        Beta(1)      0.000498383       *                 *                   *

* - Indicates that this value is not calculated.
                        Analysis of Deviance Table

       Model      Log(likelihood)  # Param's  Deviance  Test d.f.   P-value
     Full model         -94.958         4
   Fitted model        -95.0985         2      0.280866      2           0.869
  Reduced model        -98.6785         1        7.4409      3          0.0591

           AIC:         194.197

 Log-likelihood Constant            87.278562633109985

                                 Goodness  of  Fit
                                                                      Scaled
    Dose     Est._Prob.    Expected    Observed     Size       Residual
  ----------------------------------------------------------------------
     0.0000     0.1328         6.638         6          50       -0.266
    21.0000     0.1418         7.090         7          50       -0.036
   103.0000     0.1762         8.808        10          50        0.443
   514.0000     0.3287        16.437        16          50       -0.132

 Chi^2 = 0.29      d.f. = 2        P-value = 0.8671

   Benchmark Dose Computation
Specified effect =           0.1
Risk Type        =      Extra risk
Confidence level =          0.95
             BMD =       211.405
            BMDL =       118.855
            BMDU =       597.799

Taken together, (118.855, 597.799) is a 90     % two-sided confidence
interval for the BMD
```

```
(Female Liver Carcinomas and Adenomas or Mammary Adenomas)
**** Start of combined BMD and BMDL Calculations.****

  Combined Log-Likelihood                    -142.32990579511375

  Combined Log-likelihood Constant             128.8096418723423


   Benchmark Dose Computation
Specified effect =            0.1
Risk Type        =      Extra risk
Confidence level =           0.95
             BMD =        92.5711
            BMDL =        57.0564
=====================================================================
         MS_COMBO. (Version: 1.0;  Date: 07/06/2007)
         Input Data File: FLIV2NC2.(d)
         Gnuplot Plotting File:  FLIV2NC2.plt
                                                 Wed Apr 23 15:03:53 2008
=====================================================================
Female Rat Liver Carcinomas or Adenomas And Nasal Cavity Tumors Degree 2, Tbl D-16
~~~~~~~~~~~~~~~~~~~~~~~~~~~~~~~~~~~~~~~~~~~~~~~~~~~~~~~~~~~~~~~~~~~~~~~~~
    The form of the probability function is:

   P[response] = background + (1-background)*[1-EXP(-beta1*dose^1)]

   The parameter betas are restricted to be positive

   Dependent variable = NASALCAV
   Independent variable = DOSE

 Total number of observations = 4
 Total number of records with missing values = 0
 Total number of parameters in model = 2
 Total number of specified parameters = 0
 Degree of polynomial = 1
 Maximum number of iterations = 250
 Relative Function Convergence has been set to: 1e-008
 Parameter Convergence has been set to: 1e-008

                  Default Initial Parameter Values
                     Background =            0
                        Beta(1) =  0.000356274

           Asymptotic Correlation Matrix of Parameter Estimates

(*** The model parameter(s) -Background, have been estimated at a boundary point, or
have been specified by the user, and do not appear in the correlation matrix)

                Beta(1)
   Beta(1)           1

                               Parameter Estimates

                                                    95.0% Wald Confidence Interval
       Variable      Estimate      Std. Err.     Lower Conf. Limit   Upper Conf. Limit
     Background             0          *                *                   *
        Beta(1)     0.000268486       *                *                   *

* - Indicates that this value is not calculated.

                          Analysis of Deviance Table

        Model      Log(likelihood)  # Param's  Deviance  Test d.f.   P-value
      Full model        -21.9835         4
    Fitted model        -23.8503         1       3.73353      3          0.2917
   Reduced model        -33.5888         1       23.2107      3         <.0001
```

```
            AIC:         49.7005

 Log-likelihood Constant             20.101282649283011
                                  Goodness  of  Fit
                                                                      Scaled
      Dose      Est._Prob.    Expected    Observed     Size        Residual
   ----------------------------------------------------------------------
     0.0000     0.0000         0.000         0          50         0.000
    21.0000     0.0056         0.281         0          50        -0.532
   103.0000     0.0273         1.364         0          50        -1.184
   514.0000     0.1289         6.445         8          50         0.656
  Chi^2 = 2.12      d.f. = 3        P-value = 0.5488
    Benchmark Dose Computation
Specified effect =            0.1
Risk Type        =      Extra risk
Confidence level =           0.95
              BMD =        392.425
             BMDL =        230.801
             BMDU =        747.347

Taken together, (230.801, 747.347) is a 90% two-sided confidence interval for the BMD

(Female Liver Carcinomas and Adenomas or Nasal Cavity Tumors)
**** Start of combined BMD and BMDL Calculations.****

  Combined Log-Likelihood                    -71.081712052481365

  Combined Log-likelihood Constant            61.632361888515305

    Benchmark Dose Computation
Specified effect =            0.1
Risk Type        =      Extra risk
Confidence level =           0.95
              BMD =        106.322
             BMDL =        65.8109

(Female Mammary Adenomas or Nasal Cavity Tumors)
**** Start of combined BMD and BMDL Calculations.****

  Combined Log-Likelihood                        -118.9487081361909

  Combined Log-likelihood Constant               107.37984528239299

    Benchmark Dose Computation
Specified effect =            0.1
Risk Type        =      Extra risk
Confidence level =           0.95
              BMD =        137.391
             BMDL =        88.7463
```

Table D-17. MS-combo analysis of excess risks for liver adenomas, liver carcinomas, nasal cavity tumors, or peritoneal mesotheliomas in male F344 rats using MS models

Tumor site	Coefficients	AIC	*p*-value	BMD_{10}	$BMDL_{10}$	$BMD_{10\ HED}$	$BMDL_{10\ HED}$
				mg/kg-day		mg/kg-day	
Liver	1, 2	113.973	0.4485	73.8	42.6	20.0	11.6
Peritoneal Mesothelioma	2	140.537	0.8088	112.0	51.0	30.4	13.8
Nasal cavity	2	43.119	0.9564	340	255	92.3	69.7
Either	Liver or peritoneal mesothelioma			51.1	28.6	13.9	7.76
	Liver or nasal cavity			71.1	42.0	19.3	11.4
	Peritoneal mesothelioma or nasal cavity			104	49.9	28.2	13.5

```
================================================================
         MS_COMBO. (Version: 1.0;  Date: 07/06/2007)
         Input Data File: MLV12NC2.(d)
         Gnuplot Plotting File:  MLV12NC2.plt
                                              Wed Apr 23 15:02:29 2008
 ================================================================
Male Rat Liver Carcinomas or Adenomas AND and Nasal Cavity Degree 1&2, Tbl D-17
~~~~~~~~~~~~~~~~~~~~~~~~~~~~~~~~~~~~~~~~~~~~~~~~~~~~~~~~~~~~~~~~~~~~
    The form of the probability function is:

   P[response] = background + (1-background)*[1-EXP(-beta1*dose^1-beta2*dose^2)]

   The parameter betas are restricted to be positive

   Dependent variable = LIVCARAD
   Independent variable = DOSE

 Total number of observations = 4
 Total number of records with missing values = 0
 Total number of parameters in model = 3
 Total number of specified parameters = 0
 Degree of polynomial = 2
 Maximum number of iterations = 250
 Relative Function Convergence has been set to: 1e-008
 Parameter Convergence has been set to: 1e-008

                  Default Initial Parameter Values
                     Background =    0.0136508
                        Beta(1) =  0.000489073
                        Beta(2) = 5.49397e-006


           Asymptotic Correlation Matrix of Parameter Estimates

           ( *** The model parameter(s)  -Background
                 have been estimated at a boundary point, or have been specified by
the user, and do not appear in the correlation matrix )

                Beta(1)      Beta(2)
   Beta(1)            1        -0.97
   Beta(2)        -0.97            1
```

```
                                Parameter Estimates

                                                        95.0% Wald Confidence Interval
        Variable      Estimate      Std. Err.     Lower Conf. Limit   Upper Conf. Limit
      Background             0              *                     *                   *
         Beta(1)     0.00114469              *                     *                   *
         Beta(2)     3.82589e-006            *                     *                   *

* - Indicates that this value is not calculated.


                         Analysis of Deviance Table

        Model      Log(likelihood)  # Param's  Deviance  Test d.f.   P-value
      Full model         -54.3032          4
     Fitted model        -54.9865          2       1.36669      2          0.5049
    Reduced model        -98.4609          1       88.3155      3         <.0001

            AIC:          113.973

 Log-likelihood Constant             49.292679083903337


                                  Goodness  of  Fit
                                                                          Scaled
      Dose     Est._Prob.    Expected    Observed     Size       Residual
   ----------------------------------------------------------------------------
     0.0000     0.0000         0.000         0          50        0.000
    16.0000     0.0191         0.955         2          50        1.079
    81.0000     0.1111         5.446         4          49       -0.657
   398.0000     0.6541        32.705        33          50        0.088

 Chi^2 = 1.60      d.f. = 2        P-value = 0.4485


    Benchmark Dose Computation

Specified effect =           0.1
Risk Type        =      Extra risk
Confidence level =          0.95
             BMD =       73.8264
            BMDL =       42.6043
            BMDU =       137.575

Taken together, (42.6043, 137.575) is a 90% two-sided confidence interval for the BMD

=====================================================================
         MS_COMBO. (Version: 1.0;  Date: 07/06/2007)
         Input Data File: MLV12NC2.(d)
         Gnuplot Plotting File:  MLV12NC2.plt
                                              Wed Apr 23 15:02:29 2008
=====================================================================
Male Rat Liver Carcinomas or Adenomas AND and Nasal Cavity Degree 1&2, Tbl D-17
~~~~~~~~~~~~~~~~~~~~~~~~~~~~~~~~~~~~~~~~~~~~~~~~~~~~~~~~~~~~~~~~~~~~~
    The form of the probability function is:

    P[response] = background + (1-background)*[1-EXP(-beta1*dose^1-beta2*dose^2)]

    The parameter betas are restricted to be positive

    Dependent variable = NASALCAV
    Independent variable = DOSE

 Total number of observations = 4
 Total number of records with missing values = 0
 Total number of parameters in model = 3
 Total number of specified parameters = 0
```

```
Degree of polynomial = 2
Maximum number of iterations = 250
Relative Function Convergence has been set to: 1e-008
Parameter Convergence has been set to: 1e-008

                 Default Initial Parameter Values
                    Background =           0
                       Beta(1) =           0
                       Beta(2) = 9.64541e-007

          Asymptotic Correlation Matrix of Parameter Estimates

          ( *** The model parameter(s)  -Background    -Beta(1)
                have been estimated at a boundary point, or have been specified by
               the user, and do not appear in the correlation matrix )

                Beta(2)
  Beta(2)            1

                                  Parameter Estimates
                                                      95.0% Wald Confidence Interval
       Variable       Estimate     Std. Err.     Lower Conf. Limit   Upper Conf. Limit
     Background         0            *                *                   *
        Beta(1)           0          *                *                   *
        Beta(2)     9.10658e-007     *                *                   *

* - Indicates that this value is not calculated.

                        Analysis of Deviance Table

        Model      Log(likelihood)  # Param's  Deviance  Test d.f.   P-value
      Full model        -20.2482         4
     Fitted model       -20.5594         1      0.622507      3          0.8913
    Reduced model       -30.3072         1        20.118      3       0.0001604

          AIC:          43.1189

 Log-likelihood Constant             18.41952407526928

                                  Goodness  of  Fit
                                                                    Scaled
     Dose     Est._Prob.    Expected    Observed     Size       Residual
   ---------------------------------------------------------------------
    0.0000     0.0000         0.000         0          50        0.000
   16.0000     0.0002         0.012         0          50       -0.108
   81.0000     0.0060         0.292         0          49       -0.542
  398.0000     0.1343         6.717         7          50        0.118

 Chi^2 = 0.32      d.f. = 3        P-value = 0.9564


   Benchmark Dose Computation

Specified effect =           0.1
Risk Type        =      Extra risk
Confidence level =          0.95
             BMD =       340.143
            BMDL =       255.307
            BMDU =        481.19

Taken together, (255.307, 481.19 ) is a 90% two-sided confidence interval for the BMD
```

```
(Male rat liver adenomas and carcinomas or nasal cavity tumors)
**** Start of combined BMD and BMDL Calculations.****

  Combined Log-Likelihood                    -75.545958033937922

  Combined Log-likelihood Constant            67.712203159172617


   Benchmark Dose Computation

Specified effect =           0.1
Risk Type        =      Extra risk
Confidence level =          0.95
             BMD =         71.116
            BMDL =        41.9581
```

```
=================================================================
         MS_COMBO. (Version: 1.0;  Date: 07/06/2007)
         Input Data File: MLV12PR2.(d)
         Gnuplot Plotting File:  MLV12PR2.plt
                                          Wed Apr 23 15:01:06 2008
=================================================================
Male Rat Liver Carcinomas or Adenomas AND Peritonial Mesothelioma Degree 1&2, Tbl D-27
~~~~~~~~~~~~~~~~~~~~~~~~~~~~~~~~~~~~~~~~~~~~~~~~~~~~~~~~~~~~~~~~~
   The form of the probability function is:

   P[response] = background + (1-background)*[1-EXP(-beta1*dose^1-beta2*dose^2)]

   The parameter betas are restricted to be positive

   Dependent variable = PERITON
   Independent variable = DOSE

 Total number of observations = 4
 Total number of records with missing values = 0
 Total number of parameters in model = 3
 Total number of specified parameters = 0
 Degree of polynomial = 2
 Maximum number of iterations = 250
 Relative Function Convergence has been set to: 1e-008
 Parameter Convergence has been set to: 1e-008

                  Default Initial Parameter Values
                     Background =     0.035746
                        Beta(1) =  0.000579165
                        Beta(2) = 3.49814e-006
           Asymptotic Correlation Matrix of Parameter Estimates

             Background      Beta(1)      Beta(2)
Background            1        -0.66         0.59
   Beta(1)        -0.66            1        -0.98
   Beta(2)         0.59        -0.98            1

                                Parameter Estimates

                                                     95.0% Wald Confidence Interval
       Variable     Estimate      Std. Err.     Lower Conf. Limit   Upper Conf. Limit
     Background     0.0365244         *                *                   *
        Beta(1)     0.00053631        *                *                   *
        Beta(2)     3.60862e-006      *                *                   *

* - Indicates that this value is not calculated.
```

Analysis of Deviance Table

Model	Log(likelihood)	# Param's	Deviance	Test d.f.	P-value
Full model	-67.2386	4			
Fitted model	-67.2683	3	0.0595644	1	0.8072
Reduced model	-95.5731	1	56.6691	3	<.0001

AIC: 140.537

Log-likelihood Constant 60.799215762920063

Goodness of Fit

Dose	Est._Prob.	Expected	Observed	Size	Scaled Residual
0.0000	0.0365	1.826	2	50	0.131
16.0000	0.0456	2.282	2	50	-0.191
81.0000	0.0991	4.854	5	49	0.070
398.0000	0.5606	28.029	28	50	-0.008

Chi^2 = 0.06 d.f. = 1 P-value = 0.8088

Benchmark Dose Computation

Specified effect = 0.1
Risk Type = Extra risk
Confidence level = 0.95
BMD = 112.02
BMDL = 51.0435
BMDU = 171.695

Taken together, (51.0435, 171.695) is a 90% two-sided confidence interval for the BMD

(Male rat liver adenomas and carcinomas or peritoneal mesotheliomas)
**** Start of combined BMD and BMDL Calculations.****

Combined Log-Likelihood -122.25487850925802

Combined Log-likelihood Constant 110.09189484682341

Benchmark Dose Computation
Specified effect = 0.1
Risk Type = Extra risk
Confidence level = 0.95
BMD = 51.1199
BMDL = 28.5793

(Male rat peritoneal mesotheliomas or nasal cavity tumors)
**** Start of combined BMD and BMDL Calculations.****

Combined Log-Likelihood -87.827775784366935

Combined Log-likelihood Constant 79.21873983818935

Benchmark Dose Computation
Specified effect = 0.1
Risk Type = Extra risk
Confidence level = 0.95
BMD = 104.476
BMDL = 49.9353

Table D-18. Calculation of HED values for additional studies reporting the incidence of liver and nasal cavity tumors in rats and mice exposed to 1,4-dioxane in the drinking water for 2 years

Source	Species/strain/gender	Animal BW (g) TWA[a]	Animal dose (mg/kg-day)	HED (mg/kg-day)[c]
Kociba et al., 1974	Sherman rats, male and female combined	325	14	3.7
		325	121	32
		285[b]	1307	330
NCI, 1978	Male Osborne-Mendel rats	470	240	69
		470	530	152
	Female Osborne-Mendel rats	310	350	90
		310	640	165
	Male $B6C3F_1$ mice	32	720	105
		32	830	121
	Female $B6C3F_1$ mice	30	380	55
		30	860	124

[a]TWA BWs were determined from the BW curve provided for control animals unless otherwise indicated.
[b]BWs of high dose male and female rats were significantly lower than controls throughout the study. TWA represents the mean of TWA for male and females (calculated separately from growth curves).
[c]HEDs are calculated as HED = (animal dose) × (animal BW/human BW)$^{1/4}$.

Table D-19. Summary of BMD modeling estimates and CSF values associated with liver and nasal tumor incidence data resulting from chronic oral exposure to 1,4-dioxane in rats and mice

Source	Species/strain/gender	$BMD_{10\ HED}$ (mg/kg-day)	$BMDL_{10\ HED}$ (mg/kg-day)
Liver tumors			
Kociba et al., 1974	Sherman rats, male and female combined[a]	238.9	148.4
NCI, 1978	Female Osborne-Mendel rats[b]	30.19	21.44
	Male $B6C3F_1$ mice[c]	51.68	18.40
	Female $B6C3F_1$ mice[c]	23.47	9.87
Nasal cavity tumors			
Kociba et al., 1974	Sherman rats, male and female combined[d]	880.8	387.8
NCI, 1978	Male Osborne-Mendel rats[d]	18.75	13.85
	Female Osborne-Mendel rats[d]	36.90	25.57

[a]Incidence of hepatocellular carcinoma
[b]Incidence of hepatocellular adenoma
[c]Incidence of hepatocellular adenoma or carcinoma
[d]Incidence of nasal squamous cell carcinoma

D.8. BMD MODELING RESULTS FROM ADDITIONAL CHRONIC BIOASSAYS (NCI, 1978; KOCIBA ET AL., 1974)

D.8.1. Hepatocellular Carcinoma and Nasal Squamous Cell Carcinoma (Kociba et al., 1974)

The incidence data for hepatocellular carcinoma and nasal squamous cell carcinoma are presented in Table D-20. As assessed by the χ^2 goodness-of-fit statistic, all degree MS polynomial models (betas restricted $\geq$ 0) provided adequate fit (χ^2 $p > 0.1$) to the data for the incidence of hepatocellular carcinoma and nasal squamous cell carcinoma (Table D-21). The one-degree model was the lowest degree polynomial that provided an adequate fit to the data (Figures D-13 and D-14). The predicted $BMD_{10\ HED}$ and $BMDL_{10\ HED}$ values are also presented in Table D-21.

Table D-20. Incidence of hepatocellular carcinoma and nasal squamous cell carcinoma in male and female Sherman rats (combined) treated with 1,4-dioxane in the drinking water for 2 years

HED (mg/kg-day) (average of male and female dose)	Incidence of hepatocellular carcinoma[a]	Incidence of nasal squamous cell carcinoma[a]
0	1/106[b]	0/106[c]
3.7	0/110	0/110
32	1/106	0/106
330	10/66[d]	3/66[d]

[a]Rats surviving until 12 months on study.
[b]$p < 0.001$; positive dose-related trend (Cochran-Armitage test).
[c]$p < 0.01$; positive dose-related trend (Cochran-Armitage test).
[d]$p < 0.001$; Fisher's Exact test.

Source: Kociba et al. (1974).

Table D-21. Goodness-of-fit statistics and $BMD_{10\ HED}$ and $BMDL_{10\ HED}$ from multistage models fit to incidence data for hepatocellular carcinoma and nasal tumors in male and female Sherman rats (combined) exposed to 1,4-dioxane in the drinking water for 2 years

Polynomial Degree	χ^2 *p*-value[a]	AIC	$BMD_{10\ HED}$ (mg/kg-day)	$BMDL_{10\ HED}$ (mg/kg-day)
Hepatocellular carcinoma				
3	0.31	86.28	263.56	161.11
2	0.31	86.29	263.56	161.11
1[b]	0.37	85.20	238.92	148.35
Nasal squamous cell carcinoma				
3	1.00	26.42	433.59	329.84
2	1.00	26.50	500.51	332.09
1[b]	0.91	27.39	880.84	387.79

[a]Values < 0.1 fail to meet conventional goodness-of-fit criteria.
[b]Lowest degree polynomial with adequate fit.

Source: Kociba et al. (1974).

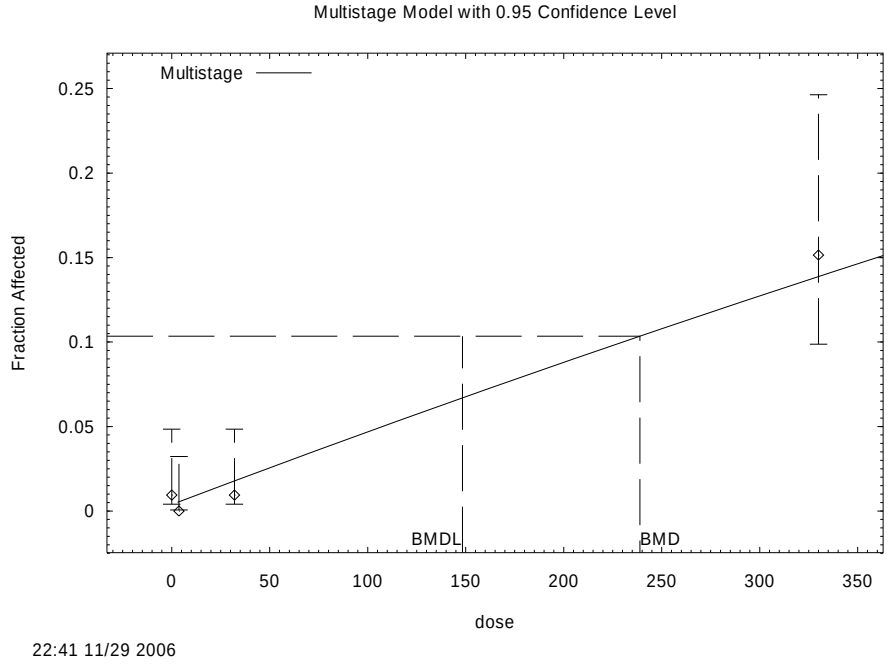

Source: Kociba et al. (1974).

Figure D-13. BMD multistage model (1-degree polynomial) of the incidence of hepatocellular carcinoma in male and female Sherman rats exposed to 1,4-dioxane in drinking water.

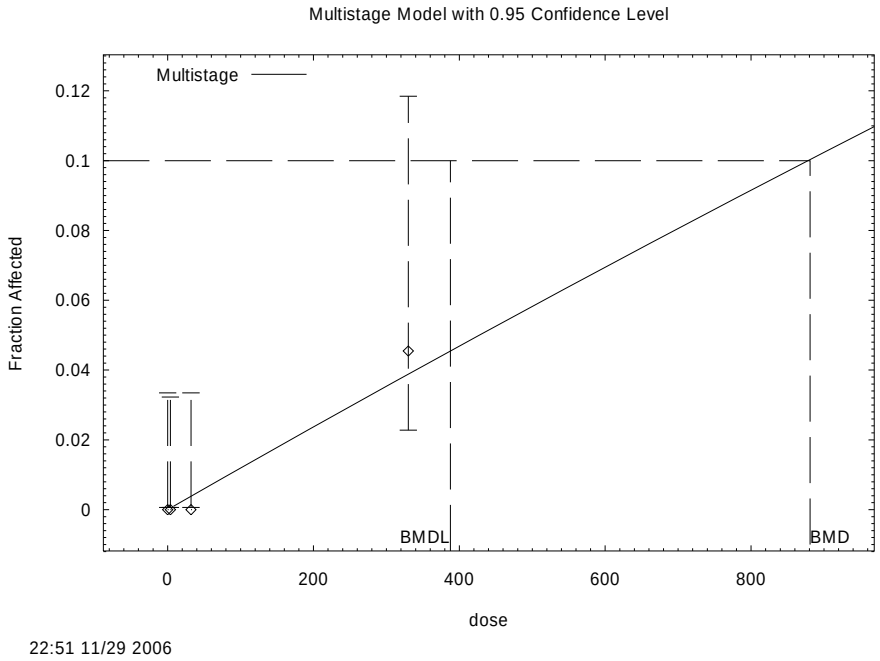

Source: Kociba et al. (1974).

Figure D-14. BMD multistage model (1-degree polynomial) of the incidence of nasal squamous cell carcinoma in male and female Sherman rats exposed to 1,4-dioxane in drinking water.

D.8.2. Nasal Cavity Squamous Cell Carcinoma and Liver Hepatocellular Adenoma in Osborne-Mendel Rats (NCI, 1978)

The incidence data for hepatocellular adenoma (female rats) and nasal squamous cell carcinoma (male and female rats) are presented in Table D-22. The one-degree multistage model (betas restricted $\geq$ 0) adequately fit both the male and female rat nasal squamous cell carcinoma data (Figures D-15 to D-5). The predicted $BMD_{10\ HED}$ and $BMDL_{10\ HED}$ values are presented in Table D-23.

Table D-22. Incidence of nasal cavity squamous cell carcinoma and liver hepatocellular adenoma in Osborne-Mendel rats exposed to 1,4-dioxane in the drinking water

Male rat HED (mg/kg-day)[a]			
	0	**69[b]**	**152**
Nasal cavity squamous cell carcinoma	0/33[c]	12/26[d]	16/33[d]
Female rat HED (mg/kg-day)[a]			
	0	**90**	**165**
Nasal cavity squamous cell carcinoma	0/34[c]	10/30[d]	8/29[d]
Hepatocellular adenoma	0/31[c]	10/30[d]	11/29[d]

[a]Tumor incidence values were adjusted for mortality (animals surviving to 52 weeks, presented in text of NCI, 1978).
[b]Group not included in statistical analysis by NCI (1978) because the dose group was started a year earlier without appropriate controls.
[c]$p \leq 0.001$; positive dose-related trend (Cochran-Armitage test).
[d]$p \leq 0.001$; Fisher's Exact test.

Source: NCI (1978).

Table D-23. Goodness-of-fit statistics and $BMD_{10\ HED}$ and $BMDL_{10\ HED}$ from multistage models fit to incidence data for hepatocellular adenoma and nasal tumors in male and female Osborne-Mendel rats exposed to 1,4-dioxane in the drinking water for 2 years

Degree polynomial	χ^2 *p*-value[a]	AIC	$BMD_{10\ HED}$ (mg/kg-day)	$BMDL_{10\ HED}$ (mg/kg-day)
Males				
Nasal cavity squamous cell carcinoma				
1[b]	0.18	86.88	18.75	13.85
Females				
Nasal cavity squamous cell carcinoma				
1[b]	0.20	77.40	36.90	25.57
Hepatocellular adenoma				
1[b]	0.60	79.69	30.19	21.44

[a]Values <0.1 fail to meet conventional goodness-of-fit criteria.
[b]Lowest degree polynomial with adequate fit.

Source: NCI (1978).

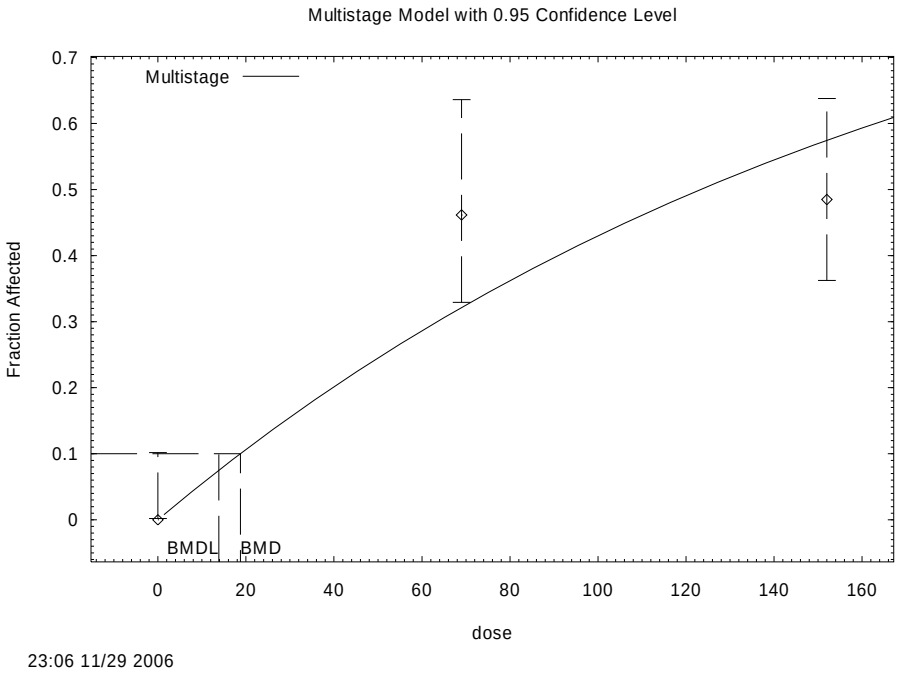

Source: NCI (1978).

Figure D-15. BMD multistage model (1-degree polynomial) of the incidence of nasal squamous cell carcinoma in male Osborne-Mendel rats exposed to 1,4-dioxane in drinking water.

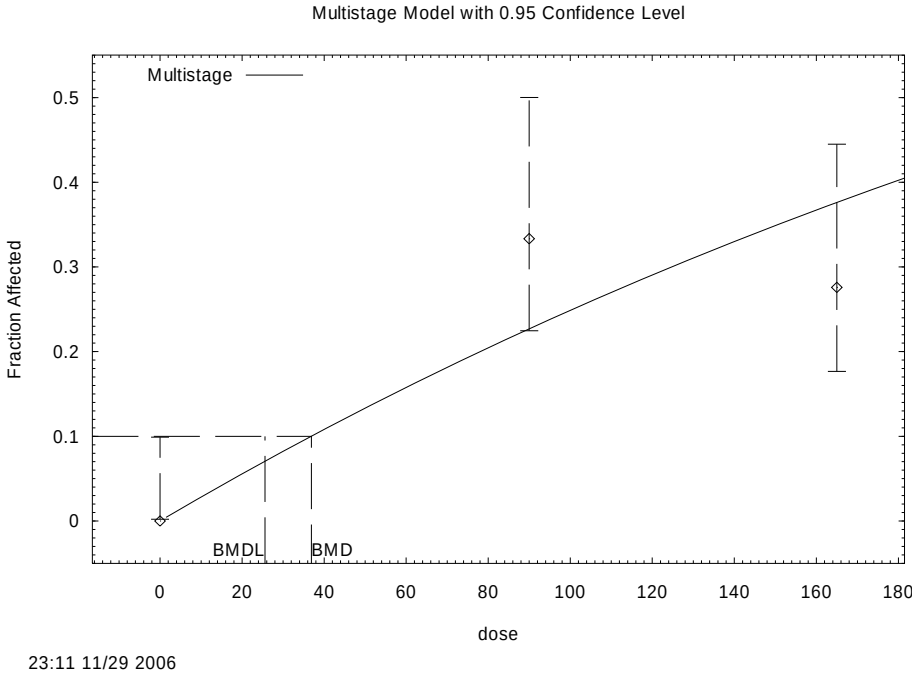

Source: NCI (1978).

Figure D-16. BMD multistage model (1-degree polynomial) of the incidence of nasal squamous cell carcinoma in female Osborne-Mendel rats exposed to 1,4-dioxane in drinking water.

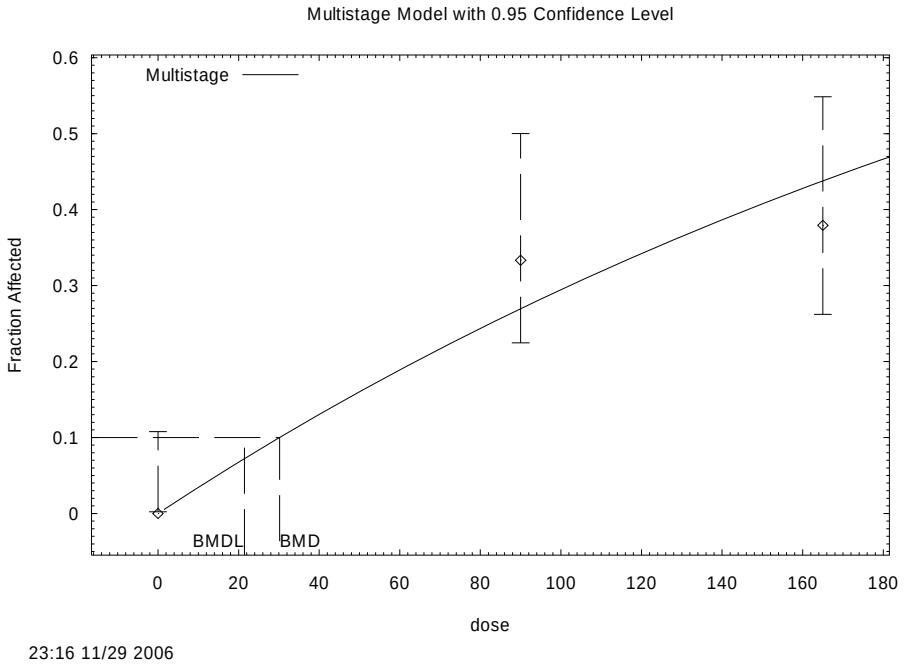

Source: NCI (1978).

Figure D-17. BMD multistage model (1-degree polynomial) of the incidence of hepatocellular adenoma in female Osborne-Mendel rats exposed to 1,4-dioxane in drinking water.

D.8.3. Hepatocellular Adenoma or Carcinoma in B6C3F$_1$ Mice (NCI, 1978)

The incidence data for hepatocellular adenoma or carcinoma in male and female mice are presented in Table D-24. As assessed by the χ^2 goodness-of-fit statistic, only the 2-degree polynomial models, provided adequate fit (χ^2 $p > 0.1$) to the data for the incidence of hepatocellular carcinoma in both male and female mice (Table D-25). The 2-degree polynomial model (betas restricted $\geq$ 0) was the lowest degree polynomial that provided an adequate fit to both the male and female mouse data (Figures D-18 and D-19). The predicted $BMD_{10\ HED}$ and $BMDL_{10\ HED}$ values are also presented in Table D-25.

Table D-24. Incidence of hepatocellular adenoma or carcinoma in B6C3F$_1$ mice exposed to 1,4-dioxane in drinking water

Male mouse HED (mg/kg-day)[a]			Female mouse HED (mg/kg-day)[a]		
0	105	121	0	55	124
8/49[b]	19/50[d]	28/47[c]	0/50[b]	21/48[c]	35/37[c]

[a]Tumor incidence values were not adjusted for mortality.
[b]$p < 0.001$, positive dose-related trend (Cochran-Armitage test).
[c]$p < 0.001$ by Fisher's Exact test pair-wise comparison with controls.
[d]$p = 0.014$.

Source: NCI (1978).

Table D-25. Goodness-of-fit statistics and BMD$_{10\ HED}$ and BMDL$_{10\ HED}$ values from multistage models fit to incidence data for hepatocellular adenoma or carcinoma in male and female B6C3F$_1$ mice exposed to 1,4-dioxane in the drinking water for 2 years

Degree polynomial	χ^2 *p*-value[a]	AIC	BMD$_{10\ HED}$ (mg/kg-day)	BMDL$_{10\ HED}$ (mg/kg-day)
Males				
2[b]	0.16	179.49	51.68	18.40
1	0.08	180.62	23.96	17.11
Females				
2[b]	1.00	85.35	23.47	9.87
1	0.05	90.05	7.10	5.61

[a]Values < 0.1 fail to meet conventional goodness-of-fit criteria.
[b]Lowest degree polynomial with adequate fit.

Source: NCI (1978).

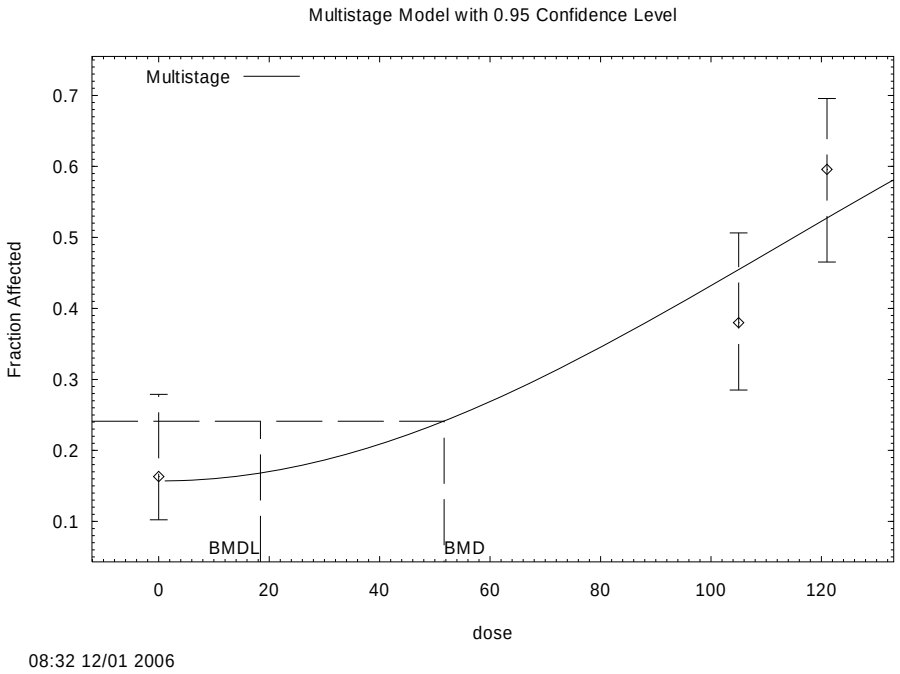

Source: NCI (1978).

Figure D-18. BMD multistage model (2-degree polynomial) of the incidence of hepatocellular adenoma in male B6C3F$_1$ mice exposed to 1,4-dioxane in drinking water.

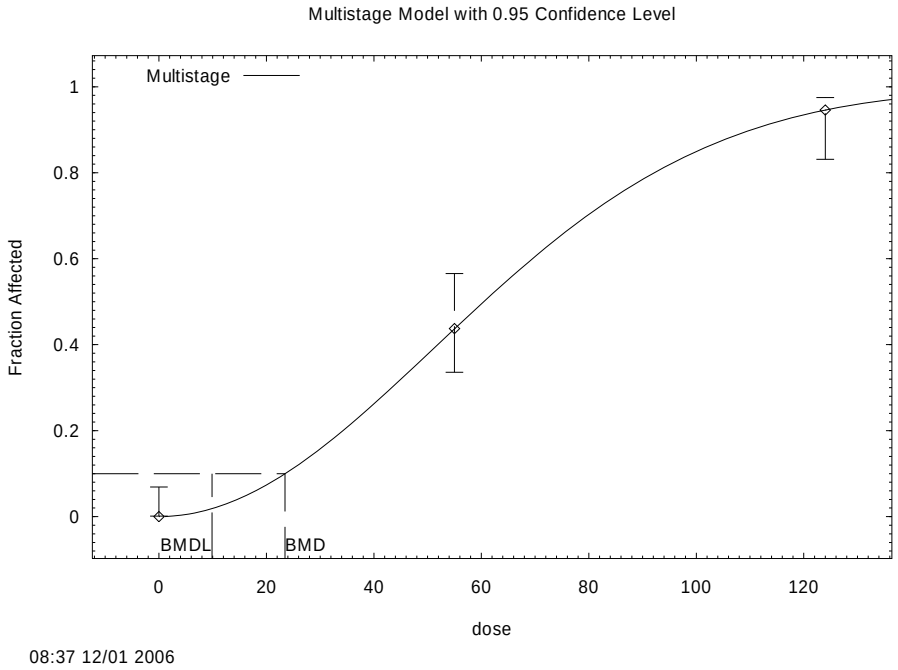

Source: NCI (1978).

Figure D-19. BMD multistage model (2-degree polynomial) of the incidence of hepatocellular adenoma in female B6C3F$_1$ mice exposed to 1,4-dioxane in drinking water.